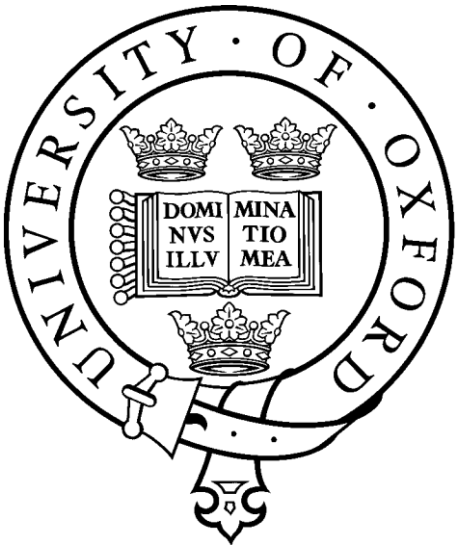
The interplay between hypoxia signalling and hepatitis B virus replication



James Michael Harris

Magdalen College

University of Oxford

Professor Jane A McKeating & Professor Adrian L Harris

A thesis submitted for the degree of

Doctor of Philosophy in Clinical Medicine

Nuffield Department of Medicine

Michaelmas Term 2021

This thesis is submitted in loving memory of

James Stephen Charlton

13th November 1995 – 26th January 2022

Abstract

Viral replication is influenced by the host cell microenvironment, and local oxygen tension is a major factor that shapes the intracellular landscape. Hepatitis B virus (HBV) replicates in the liver which harbours a naturally low oxygen environment. However, *in vitro* culture systems apply atmospheric oxygen conditions, and so our understanding of the role of oxygen sensitive factors in the viral life cycle is limited.

We uncover evidence of hypoxic signalling in the HBV infected liver that associates with the inflammatory status of this chronic disease. We develop simple PCR assays to determine the source of HBV RNAs and ascribe patterns of viral transcription. Investigating the interplay between the hepatic inflammasome and viral transcription identified 24 host factors that positively associate with HBV transcriptional activity. Culturing HBV infected hepatoma cells under low oxygen uncovered a new role for hypoxia inducible factors (HIFs) in the viral life cycle. Our studies demonstrate that HIFs bind an evolutionarily conserved hypoxic response element in the basal core promoter *in vitro* and *in vivo*, which drives the synthesis of pre-genomic RNA and potentiates particle genesis. HIFs are not the only regulators of the cellular response to low oxygen, and we expand our observation to show that hypoxic inhibition of histone lysine demethylase 4 (KDM4) also promotes transcription from episomal and integrated HBV genomes. We show that KDM4 is a major orchestrator of host gene expression and this defines host susceptibility to HBV infection.

Identifying roles for oxygen sensors in the HBV life cycle suggests that this pathogen has evolved to exploit the hypoxic signalling pathways in the liver. This study highlights the importance of understanding the pathways which are active in physiological oxygen tensions when considering virus-host interactions, and provides innovative routes to therapeutically target HBV.

Acknowledgements

I would like to take this opportunity to thank the many people who have helped me to produce this thesis and complete my studies. I'd like to thank Professor Jane McKeating for her ongoing supervision, guidance, and tutelage spanning both my undergraduate and post-graduate degrees. I would also like to thank Professor Adrian Harris for his supervision, and his readiness to provide us with invaluable guidance, support, and reagents whenever called upon. I would like to thank Dr Peter Balfe, for first sowing the seed of research science in my mind in a lecture theatre in 2014, thank you for all that you have taught me.

To Dr Peter Wing and Dr Andrea Magri, thank you for tolerating me for the last 4 years, and for making me laugh on a daily basis. Without you two this experience would not have been so enjoyable and successful. I would like to thank all members of the McKeating group, past and present, for being willing to help, answering my many questions, and always being around for coffee and cake. To Claudia, Rory, Alan, Helene, Mirjam, Olivia, Senko, Donall and Vale – thank you. I would also like to acknowledge the contributions of many collaborators that I have had the pleasure of working with on exciting projects; long may our fruitful relationships last. My thanks are extended to the Nuffield Department of Medicine, and Magdalen College for their support throughout my studies.

To my parents Rachel and Dave, my Grandparents Annette and Michael, my sister Amy, and her partner Graeme – thank you for your continued support. Thank you all for everything that you do and have done for me, and for helping me to become the person I am today.

To my better half, Ellie. Thank you for sticking by me, albeit not geographically. Thank you for providing me with countless hours behind the wheel; travelling between Oxford and Birmingham, Harpenden, Davenham and Pontefract. Congratulations on surviving a national lockdown with me, despite then fleeing to Alabama for 6 months of respite. I would also like to thank the rest of the Copsey family: Pam, Dave, and Beth.

To my dearest friend George Picker, thank you for the hours of uncontrollable laughter; I hope they continue for many years. To David Grainger, for the last 7 years of beer, kebabs and science – thank you, it has been a pleasure. I would also like to extend my sincere thanks to the Flowers Band, Gloucester, for 4 years of wonderful music making, opportunities, and countless memorable experiences.

Statement of originality

I declare that the work presented within this thesis entitled ‘The interplay between hypoxia signalling and hepatitis B virus replication’ is my own. Contributions made by collaborators have been clearly acknowledged. I have not submitted this thesis, in whole, or in part for any other degree or qualification at the University of Oxford or elsewhere.

Table of Contents

ABSTRACT 3
ACKNOWLEDGEMENTS 4
STATEMENT OF ORIGINALITY 5
TABLE OF CONTENTS 6
LIST OF FIGURES 9
LIST OF TABLES 10
LIST OF COMMON ABBREVIATIONS 11

CHAPTER 1: INTRODUCTION 12

1.1: The liver 12
1.1.1: Liver physiology and structure 12

1.2: Hepatitis B Virus 19
1.2.1: Prevalence and epidemiology 19
1.2.2: HBV natural history 24
1.2.3: Vaccines and drugs 29
1.2.4: Host immune responses 32
1.2.5: Liver cancer 37
1.2.6: HBV genotypes 40
1.2.7: Life cycle of HBV 44
HBV transcription and translation 45
Entry 53
cccDNA genesis 55
Two templates for transcription 60
Transcriptional regulation and activation 62
Epigenetic regulation 71
HBV assembly and egress 74
1.2.8: HBV model systems 79
in vitro 79
in vivo 86

1.3: The cellular response to hypoxia 90
1.3.1: 2-Oxoglutarate dependent dioxygenases 94
1.3.2: Prolyl hydroxylases and HIF signalling 98
1.3.3: Inflammation and HIFs 105
1.3.4: Chromatin 107
1.3.5: Histone lysine demethylases 109
1.3.6: Oxygen sensitive epigenetic modifiers 112
1.3.7: Chromatin and hypoxia 115

1.4: HBV and hypoxia 118

1.5: Aims 123

CHAPTER 2: MATERIALS AND METHODS 124
2.1: Chemicals and reagents 124
2.2: Tissue culture 125

2.3: Plasmid transfections 126
2.4: Nucleic acid extraction 128
2.5: RT-qPCR 132
2.6: Cellular protein extraction 135
2.7: Western blotting: lysate preparation and immunoblotting 136
2.8: HBV E and S antigen ELISA 137
2.9: Luciferase assays 138
2.11: HBV Infection 142
2.12: Flow cytometry: determining cell cycle phase 144
2:13: Human liver biopsy samples 145
2.14: Bioinformatic analysis 146
2.15: Statistics 152
2.16: Data deposition 152
2.17: Sequence-based reagents 153
2.18: Antibodies 156

CHAPTER 3: HYPOXIC GENE EXPRESSION IN CHRONIC HEPATITIS B INFECTION 157
3.1: Introduction 157
3.2: Host gene expression in the CHB liver 159
3.3: A naturally hypoxic microenvironment 162
3.4: Hypoxic gene expression in a CHB cohort 167
3.5: A qPCR to detect HBV transcripts 171
3.6: Ascribing transcript patterns to *in vitro* and *in vivo* systems 175
3.7: Determining the source of HBV transcripts 181
3.8: Integrant derived transcripts and antigen 185
3.9: An immune gene signature associating with HBV replication 188
3.10: Summary 192

CHAPTER 4: A ROLE FOR HIF IN HBV LIFE CYCLE 196
4.1: Introduction 196
4.2: HREs are evolutionarily conserved in the hepadnaviruses 198
4.3: Requirement for a DMSO free system 201
4.4: Hypoxia arrests hepatocyte cell cycle 204
4.5: Low oxygen potentiates HBV replication 207
4.6: Lipid transfection of overlength genomes 210
4.7: HBV-HRE mutant constructs 213
4.8: Shearing HBV DNA 216
4.9: Assessing HBV transcription factor interactions 220
4.10: HIFs bind HBV DNA 224
4.11: HBV-HIF complexes exist *in vivo* 227
4.12: Hypoxia selectively activates the BCP 232
4.13: Hypoxic regulation of HBV host factors 235

CHAPTER 5: HISTONE LYSINE DEMETHYLASE 4 AS A HBV RESTRICTION FACTOR 243
5.1: Introduction 243
5.2: Host and viral transcriptional responses to low oxygen 245

5.3: A role for KDM4 in HBV transcription 249
5.4: The interplay between HIF signalling and KDM4 activity 254
5.5: Episomal and integrated genomes are sensitive to KDM4 inhibition 258
5.6: KDM4 inhibition promotes particle genesis 262
5.7: KDM4 and the hepatocellular transcriptome 267
5.8: KDM4 is inhibited in the CHB liver 271
5.9: Summary 275

CHAPTER 6: DISCUSSION AND FUTURE WORK 280
CHAPTER 7: PUBLICATIONS 297
CHAPTER 8: BIBLIOGRAPHY 300

List of Figures

Figure 1.1: The liver lobule 14
Figure 1.2: Metabolic zonation 18
Figure 1.3: Geographical distribution of HBV infection 23
Figure 1.4: HBV and host parameters for EASL classification 27
Figure 1.5: Viral and host parameters in the natural history of HBV 28
Figure 1.6: The molecular life cycle of HBV 44
Figure 1.7: Viral genomes 46
Figure 1.8: Viral ORFs 47
Figure 1.9: HBV RNAs 51
Figure 1.10: HBV proteins 52
Figure 1.11: cccDNA genesis 57
Figure 1.12: HBV transcription factors 63
Figure 1.13: HBV particles 78
Figure 1.14: HBV1.3 genome 82
Figure 1.15: Oxygen tension in human organs 92
Figure 1.16: 2-Oxoglutarate dependent dioxygenases 96
Figure 1.17: 2-Oxoglutarate dependent dioxygenase functions 97
Figure 1.18: HIF-PHD signalling axis 100
Figure 1.19: HIF regulated cellular processes 102
Figure 1.20: HIF structure 104
Figure 1.21: Epigenetic readers and writers 111
Figure 3.1: Host gene expression in the CHB liver 161
Figure 3.2: A natural hypoxic microenvironment 165
Figure 3.2: Hypoxic gene expression in a CHB cohort 170
Figure 3.4: A qPCR to detect HBV transcripts 173
Figure 3.5: Ascribing HBV transcript patterns to in vitro and in vivo systems 179
Figure 3.6: Determining the source of HBV transcripts 183
Figure 3.7: Integrant derived transcript and antigen 187
Figure 3.8: An immune gene signature associating with HBV replication 190
Figure 4.1: HREs are evolutionarily conserved in the hepadnaviruses 200
Figure 4.2: Requirement for a DMSO free system 203
Figure 4.3: Hypoxia arrests hepatocyte cell cycle 206
Figure 4.4: Low oxygen potentiates HBV replication 209
Figure 4.5: Lipid transfection of overlength genomes 212
Figure 4.6: HBV-HRE mutant constructs 215
Figure 4.7: Shearing HBV DNA 218
Figure 4.8: Assessing HBV and transcription factor interactions 222
Figure 4.9: HIFs bind HBV DNA 226
Figure 4.10: HBV-HIF complexes exist in vivo 230
Figure 4.11: Hypoxia selectively activates the BCP 234
Figure 4.12: Hypoxic regulation of HBV host factors 237
Figure 5.1: Host and viral transcriptional responses to low oxygen 247
Figure 5.2: A role for KDM4 in HBV transcription 252
Figure 5.3: The interplay between HIF signalling and KDM4 activity 257
Figure 5.4: KDM4 regulation of integrated and episomal genomes 260
Figure 5.5: KDM4 inhibition promotes particle genesis 265
Figure 5.6: KDM4 regulation of host cell processes 269
Figure 5.7: KDM4 is inhibited in the CHB liver 273
Figure 6.1: Suggested model 295

List of Tables

Table 1.1: HBV incidence 21
Table 1.2: HBV endemicity 23
Table 1.3: EASL stratification criteria 27
Table 1.4: Mechanisms of HCC development 39
Table 1.5: Geographical distribution of HBV genotypes 41
Table 1.6: HBV in vivo systems 89
Table 1.7: bHLH transcription factors 100
Table 1.8: Human viruses and hypoxia 121
Table 2.1: Chemicals and reagents 124
Table 2.2: Kits 124
Table 2.3: Drugs and compounds 125
Table 2.4: Cell lines 125
Table 2.5: Culture media 126
Table 2.6: Transfection conditions 127
Table 2.7: Transfection mixes 127
Table 2.8: cDNA synthesis 132
Table 2.9: SYBR green qPCR 133
Table 2.10: T5 exonuclease 133
Table 2.11: cccDNA qPCR 134
Table 2.12: Extracellular rcDNA quantification 135
Table 2.13: Data deposition 152
Table 2.14: qPCR primer sequences 153
Table 2.15: ChIP PCR primer sequences 154
Table 2.16: Plasmids and constructs 155
Table 2.17: siRNAs 155
Table 2.18: Antibodies 156

List of Common Abbreviations

Common Abbreviations	
Ag	Antigen
ALT	Alanine aminotransferase
APAS	Alternative polyadenylation signal
BCP	Basal core promoter
cccDNA	Covalently closed circular DNA
CDK	Cyclin dependent kinase
CHB	Chronic hepatitis B
CHC	Chronic hepatitis C
ChIP	Chromatin immunoprecipitation
DMSO	Dimethyl sulphoxide
dslDNA	Double stranded linear DNA
EASL	European association for study of the liver
ed-RNA	Episome derived RNA
ENCH	Hepatitis B Virus E antigen negative chronic hepatitis
ENCI	Hepatitis B Virus E antigen negative chronic infection
EnhI	Enhancer I
EnhII	Enhancer II
ETV	Entecavir
FACs	Fluoresence associated cell sorting
GSEA	Gene set enrichment analysis
Gt	Genotype
HBc	Hepatitis B virus Core protein
HBe	Hepatitis B virus E antigen
HBs	Hepatitis B virus S antigen
HBV	Hepatitis B virus
HBx	Hepatitis B virus X protein
HCC	Hepatocellular carcinoma
HCV	Hepatitis C virus
HIF	Hypoxia inducible factor
HNF	Hepatocyte nuclear Factor
HRE	Hypoxic responsive element
id-RNA	Integrant dervied RNA
iDNA	Integrated HBV DNA
KDM	Histone lysine demethylase
K_m	Michaelis constant
Luc	Luciferase
MOI	Multiplicity of infection
MSigDB	Molecular signatures database
NTCP	Sodium taurocholate co-transporting polypeptide
ORF	Open reading frame
PAS	Polyadenylation signal
pC/pg	pre-Core/pre-genomic
PCR	Polymerase chain reaction
PHD	Prolyl hydroxylase
PHH	Primary human hepatocyte
PI	Propidium iodide
Pol	Polymerase
PTM	Post translational modification
rcDNA	Relaxed circular DNA
ROS	Reactive oxygen species
RT	Reverse transcriptase
SAMHD1	SAM and HD domain containing deoxynucleoside triphosphate triphosphohydrolase 1
VHL	Von hippel lindau
VLP	Virus-like particle
2-OG	2-oxoglutarate
2-OGDD	2-oxoglutarate dependent dioxygenase

Chapter 1: Introduction

1.1: The liver

The liver is the largest solid organ of the body and is highly specialised to carry out a vast and diverse range of roles, particularly in the metabolism of glucose and glycogen, lipids, cholesterol, and bile acids (Adeva-Andany et al., 2016; Chiang, 2013; Han et al., 2016; Sato et al., 2018). The liver is also responsible for the detoxification of the blood, and as such is implicated in the xenobiotic response, the detection and neutralisation of pathogenic organisms, and the metabolism and processing of many drug components and alcohol (Krebs et al., 1969; Kubes and Jenne, 2018; Natsoulis et al., 2008). Whilst the liver is fundamental for life, it is also the primary site of infection for hepatotropic pathogens; the most notable are a family of 5 different viruses named hepatitis A-E. They have distinct genomes and exhibit vastly different replicative life cycles, with widespread variation in their clinical characteristics, manifestation and outcomes (Valenzuela, 1990).

1.1.1: Liver physiology and structure

The mammalian liver is highly organised, and the cells of the liver form functional zones referred to as lobules. These are roughly hexagonal shaped structures, which are formed around the central hepatic vein with the portal triads (comprised of the hepatic portal vein, branches of the hepatic artery, and the bile duct) defining the outer perimeter. The most abundant cells of the liver are the hepatocytes, polarised epithelial cells which are essential to the many roles of the organ. The hepatocytes constitute around 80% of total liver mass, and are

fundamental in establishing the cellular architecture, which is key to organ function (Kholodenko and Yarygin, 2017). The hepatocytes are precisely arranged in distinct rows only 1 or 2 cells thick, to form chord like structures that are known as trabeculae (**Figure 1.1**) (Treyer and Musch, 2013). These are adjacent to rows of liver sinusoidal epithelium which form a structure for blood flow that differs from a classical capillary bed. The sinusoidal epithelial cells do not form tight junctions, and so maximise the contact between hepatocytes and the blood allowing efficient exchange of the blood content via fenestrations (Trefts et al., 2017).

Cholangiocytes are the second most dominant hepatic cell type, and their main function is providing the epithelium for the bile ducts, to allow the transport of products from the gall bladder which are essential for bile acid metabolism (Tabibian et al., 2013).

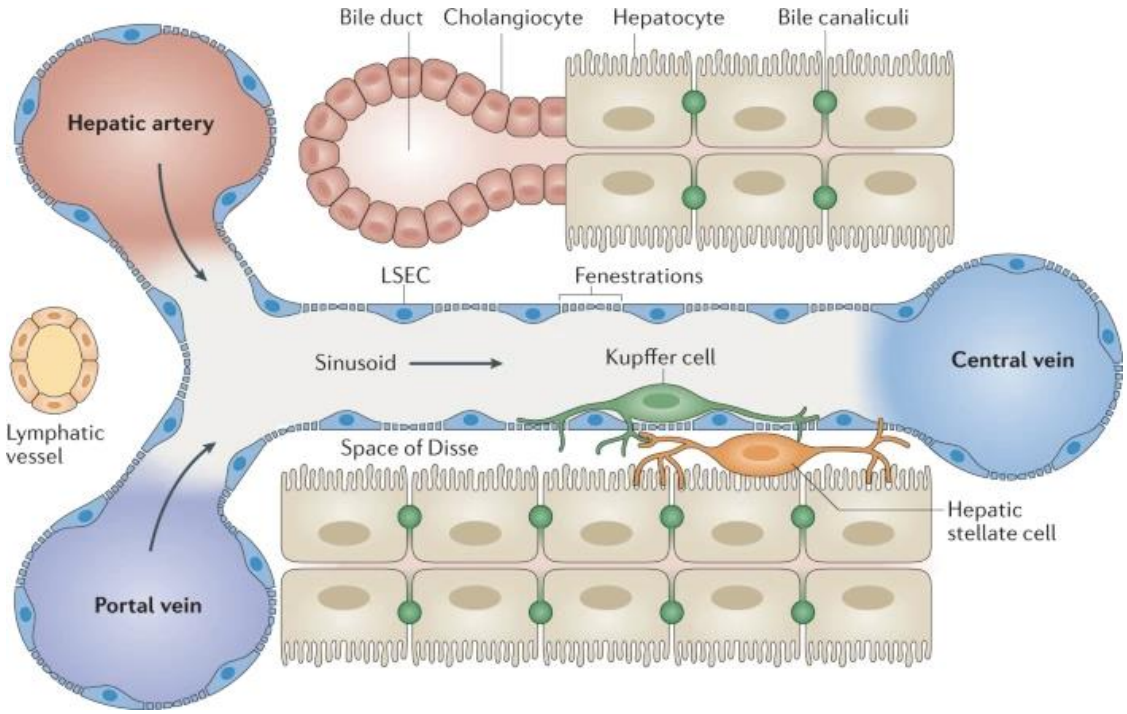


Figure 1.1: The liver lobule

A schematic diagram to show the architecture of the liver lobule, the repeated unit that forms the functional core of the liver. Figure taken from (Iannacone and Guidotti, 2021).

The immune functions of the liver are largely regulated by the liver resident macrophages known as Kupffer cells, which represent between 80-90% of all hepatic resident immune cells (Bilzer et al., 2006). They act in a sentinel surveillance capacity, and monitor the content of the blood for pathogenic substances or toxins, which are likely to arrive from the gut via portal vein circulation (Dixon et al., 2013). Kupffer cells are not the only immune cells of the liver, hepatic stellate cells (HSCs) constitute around 10% of all liver resident immune cells (Wake, 1971). The small cavity between the sinusoidal epithelium and the hepatocytes is known as the perisinusoidal space, or the space of Disse (Han et al., 2001). This gap is home to many cell types but the dominant cells are the stem cell-like stellate cells, and infiltrating natural killer cells which patrol the sinusoids on the hunt for virally infected hepatocytes (Haussinger and Kordes, 2019). In a healthy liver, HSCs are largely quiescent and act as a reservoir for vitamin A, but they remain highly sensitive to activation by liver injury, where they transdifferentiate into myofibroblasts (Moreira, 2007). These cells are a highly proliferative, inflammatory cell type which are characterised by enhanced production of extra-cellular matrix (Puche et al., 2013).

Blood arrives at the liver from two sources: the hepatic artery which delivers oxygen rich blood directly from the aorta, and the hepatic portal vein delivers nutrient rich blood from the gastro-intestinal tract (Kholodenko and Yarygin, 2017). Blood from both sources mixes in the sinusoids, and flows across the lobule towards the central hepatic vein for drainage, delivering nutrients and oxygen to the adjacent parenchyma. The hepatocytes metabolise oxygen and nutrients from the blood, and return waste products to be removed from the liver via the central hepatic vein. As such, the blood which enters the liver at the peripheral triad has a

different composition to the blood in the central vein. This results in distinct zonation of the lobules, which are fundamental for proper liver function (Trefts et al., 2017). Roughly, the lobule can be divided into 3 zones, with zone 1 being the periportal region, 2 as the mid-zone, and 3 as the area immediately surrounding the central vein (**Figure 1.2**) (Halpern et al., 2017; Kietzmann, 2017). This process also generates a natural oxygen gradient across the lobules, whereby cells in zone 1 are likely to experience an oxygen tension of around 8% O_2, whereas the pericentral cells will experience a much lower oxygen concentration of approximately 4% (Gebhardt et al., 2007; Jungermann and Kietzmann, 2000; Wilson et al., 2014b).

The differential metabolic functions across the radial axis of the lobule associates with the oxygen gradient. For example, the pericentral cells in zone 3 preferentially execute bile acid synthesis, glycolysis and xenobiotic metabolism, as these consume less energy. In contrast, the highly oxygenated cells in zone 1 are specialised in protein secretion and gluconeogenesis due to the high oxygen demand of these processes (Gebhardt and Matz-Soja, 2014; Halpern et al., 2017). The sinusoids have also been compared with a production line, whereby bi-products and metabolites are released from cells in zone one, and utilised by cells downstream in zones two or three. This is evident in the periportal production of glucose, and its subsequent uptake in the pericentral region (Manco and Itzkovitz, 2021). Another example of this is the urea cycle, where the peripherally located hepatocytes detoxify ammonia using the conversion of glutamine into glutamate, and glutamate is secreted by these cells back into the sinusoid. The pericentral cells then recycle the excess glutamate and convert it back into glutamine thus rebalancing the amino acid content of the lobule (Godoy et al., 2013) (**Figure 1.2**).

There are limitations to the studies on liver zonation, as the liver of mice and humans differ in their zonation patterns and a recent study employed signal cell RNA-sequencing to assess differential gene expression across the liver of mice (Halpern et al., 2017). This study from Halpern and colleagues identified that over 50% of the hepatic transcriptome was regulated by spatial location and position of cells on the radial axis. Additionally, our collaborators in Strasbourg have recently published a liver atlas, whereby the gene expression profiles of all liver cells have been characterised, but this does not address their spatial location (Aizarani et al., 2019; Juhling et al., 2021). Similarly, MacParland et al. employed single-cell sequencing and flow cytometry to divide the liver into 20 discreet populations of resident cells to map the human hepatic immune environment (MacParland et al., 2018).

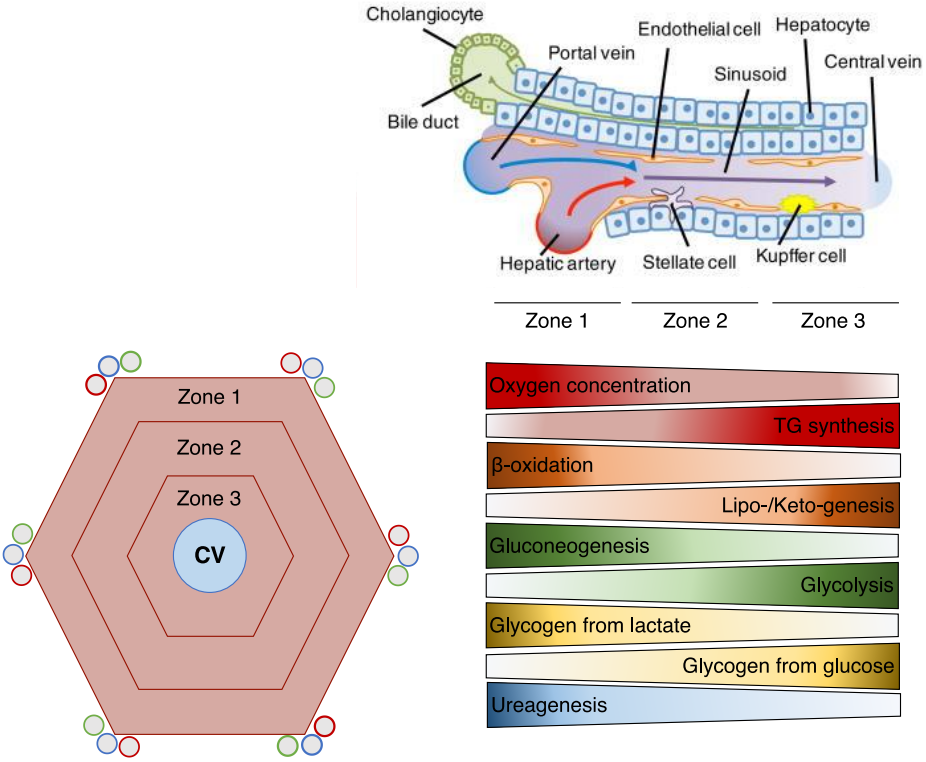


Figure 1.2: Metabolic zonation

A cartoon to show the metabolic zonation of the liver lobule. Exemplar metabolic process are shown, with differential activity depicted by colour intensity and arrow size. Diagram adapted from (Trefts et al., 2017).

1.2: Hepatitis B Virus

1.2.1: Prevalence and epidemiology

Hepatitis B Virus (HBV) is one of the most prevalent infectious diseases worldwide. Up to 350 million individuals are infected globally, with 1.5 million new cases every year resulting in between 0.5 and 1.2 million deaths annually (Lavanchy, 2004; Lee, 1997; Mahoney, 1999; World Health Organisation, 2021). HBV often leads to chronic disease (chronic hepatitis B, CHB) whereby viral infection is life long and progressive. Up to 40% of patients develop cirrhosis, with viral infection carrying a 10-25% life time risk of hepatocellular carcinoma (HCC) development (Crissien and Frenette, 2014; El-Serag, 2012; Lok, 2002; Ringelhan et al., 2017). It is estimated that over 2 billion people worldwide show evidence of active or past infection with HBV, which accounts for over 20% of the global populace (World Health Organisation, 2021).

HBV infection can be acute, and spontaneous clearance through immune control of the virus can be achieved in the first year of infection. This occurs in more than 90% of infected adults, with only around 5% of infections progressing to chronicity. However, once in the chronic phases around 30% of patients will develop cirrhosis and, likely, HCC. The rates of CHB are much greater when infection occurs in infants below the age of 6, and up to 90% of these will develop chronic infections (Schweitzer et al., 2015). The most frequent route of transmission of HBV is vertical, whereby the mother is infected and the virus transmits perinatally to the child during development (Ghendon, 1987). When a mother is serologically positive for both viral antigens, transmission rates can be as high as 90% (Hou et al., 2005; Kwon and Lee, 2011). Vertical transmission can

occur via 3 routes: when in gestation the virus can transmit across the placenta (*in utero*); during delivery of the child; or throughout post-natal care and breast feeding (Hou et al., 2005; Kwon and Lee, 2011; Petrova and Kamburov, 2010; Stevens et al., 1975).

Whilst blood is the most common vehicle for transmission, saliva and semen have been implicated as viable routes for spread (Bancroft et al., 1977; Scott et al., 1980). It is therefore no surprise that second to vertical transmission is horizontal transmission, whereby an individual becomes infected through contact with infected blood, largely via parenteral or percutaneous routes (Hou et al., 2005). Risk factors for horizontal transmission are wide spread and include many situations where one may be exposed to HBV positive blood. Intravenous drug use, dialysis, blood transfusions or surgery, and tattoos and piercings account for many cases, and prolonged use of needles increases the likelihood of encountering the virus (Fabrizi et al., 2008; Jafari et al., 2012). However, this puts those administering health care such as nurses, dentists and doctors, as well as laboratory technicians and police officers amongst those at the highest risk (Dahiya et al., 2015; Welch et al., 1988).

Global distribution of HBV is variable, with endemicity being categorised as low, intermediate or high (**Table 1.1**) (Margolis et al., 1991). High endemicity is generally associated with the developing world where populations are large. Studies suggest that at least 8% of the populations of South East Asia, sub-Saharan Africa and the Amazon are chronically infected with the virus. Epidemiological studies use the Hepatitis B surface antigen (HBsAg) as the parameter to indicate infection. Here, the disease burden is highly prevalent

amongst children, many of whom are asymptomatic, however in the adult population liver disease and HCC rates are high (Abdel-Hady and Kelly, 2013; Alter, 2003). Epidemiological studies suggest that the greatest tool to combat these rates is childhood vaccination, and previous reports have not only shown a marked reduction in prevalence of population HBsAg, but also in the onset of HCC (Chang et al., 2009; Plymoth et al., 2009; Zoulim and Durantel, 2015). In the UK, a hepatitis B virus containing vaccine is administered to all new born babies as part of the 6-in-1 vaccine (McCormack, 2013).

Prevalence	Incidence	Geographic area	Age at infection	Possible routes of transmission
Low	<2%	North America, Western Europe	Early adulthood	Sexual, percutaneous, others
Intermediate	2 - 8%	Mediterranean, Eastern Europe	Childhood	Horizontal
High	>8%	East Asia, Africa	Birth, toddler stage, preschool	Perinatal, horizontal

Table 1.1: HBV incidence

A table summarising the incidence of HBV infection by geographical location, and the most common routes of transmission. Figure adapted from (Nguyen et al., 2020).

Infection in young children and adolescents is frequent in Southern and Eastern Europe, Japan, the Middle East, and regions of South America, where endemicity is intermediate. Between 10-60% of the population have encountered the virus in their lifetime, and 2-7% are chronically infected. If infected in young adult life there is a high chance that the immune system will bring the virus under control and it will be cleared (Chou et al., 2015). These acute infections are common in intermediate level countries, but the level of infection in the population is maintained by those who were infected during infancy (Hou et al., 2005; Toukan, 1990).

High endemicity is commonly associated with the developing world, and in contrast, there is low endemicity in the developed Western World. In North America, Australia, and Northern and Western Europe only around 5-7% of the population is infected, and even fewer progress to become chronic carriers, with the rate of CHB being as low as 0.5-2% (McQuillan et al., 1989). In these countries, the majority of infected individuals encounter the virus as young adults, and usually fall into one of the high risk groups, such as intravenous drug users, dialysis or transfusion patients, or homosexual males (Hou et al., 2005; Polaris Observatory, 2018; Schreeder et al., 1982). This information is summarised in (**Figure 1.3** and **Table 1.2**).

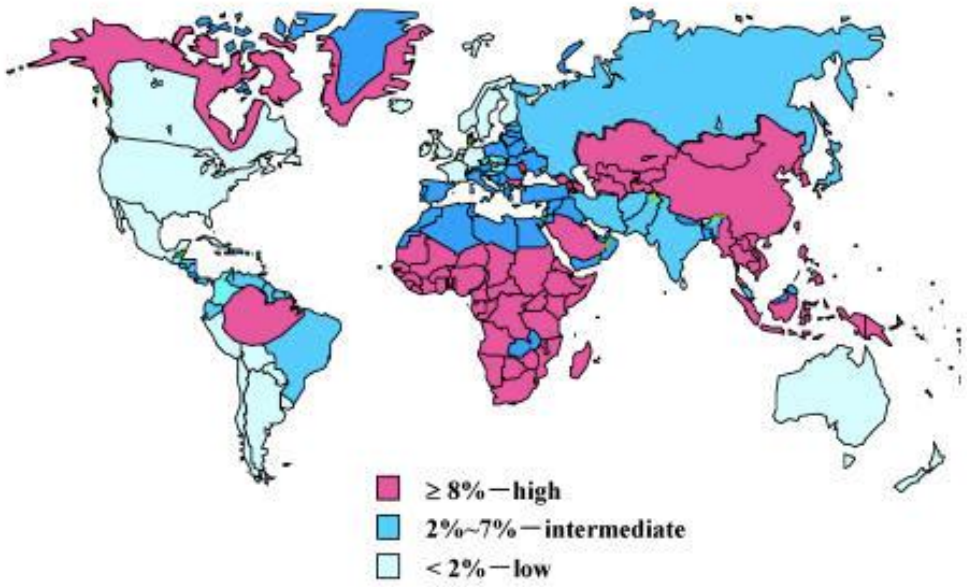


Figure 1.3: Geographical distribution of HBV infection

A world map coloured by incidence of HBV infection, using HBsAg as the indicator of positivity. Figure taken from (Hou et al., 2005).

Characteristic	Endemicity of infection (%)		
	Low	Intermediate	High
Chronic infection prevalence	0.5-2.0	2.0-7.0	≥8.0
Past infection prevalence	5.0-7.0	10.0-60.0	70.0-95.0
Perinatal infection	Rare (<10)	Uncommon (10-60)	Common (>20)
Early childhood infection	Rare (<10)	Common (10-60)	Very common (>60)
Adolescent/adult infection	Very common (70-90)	Common (20-50)	Uncommon (10-20)

Table 1.2: HBV endemicity

A table to summarise the characteristics of HBV cases categorised by levels of endemicity. Table adapted from (Hou et al., 2005)

1.2.2: HBV natural history

CHB disease state was previously categorised into 4 groups, known as immune tolerant, immune active, inactive carrier and reactivation, however this was revised by the European Society for the Study of the Liver (EASL) in 2017 to more accurately describe the replicative status of the virus, and the physiological state of the host (**Figure 1.4**, **Table 1.3**, and **Figure 1.5**) (Belongia et al., 2008; EASL, 2017). The revised nomenclature separates the disease into 5 distinct stages, where progression between them is not strictly linear, nor will a patient experience all of the stages throughout their infection. Abbreviations for each of the 5 phases were defined by Zhang et al. in 2019 (Zhang et al., 2019).

Phase (I) HBeAg-positive chronic infection (EPCI) was previously referred to as the immune tolerant phase. Here, hepatitis B e antigen (HBeAg) is readily detectable in serum, with high levels of peripheral HBV DNA, indicative of active viral replication, but with normal (<40IU/L) peripheral Alanine Aminotransferase (ALT). ALT is routinely used as a peripheral marker of liver inflammation, but strictly is only released from hepatocytes when their membranes are compromised and damaged (McGill, 2016). When studying immunohistochemical images of liver tissue in this stage of disease, there is little evidence of necro-inflammatory conditions or fibrosis, but there is often a high frequency of HBV integration sites and clonal expansion of infected hepatocytes (Mason et al., 2016). Spontaneous clearance of the virus is unlikely in this phase, and patients are highly infectious due to their elevated HBV DNA burden.

Phase (II) HBeAg-positive chronic hepatitis (EPCH) was previously referred to as immune reactive HBeAg positive, and this represents the stage of CHB

where outcome is perhaps at its most variable. It is characterised by high serum HBeAg and concomitantly high levels of HBV DNA indicative of highly active viral replication. As such, there is elevated ALT in the periphery, which is indicative of either moderate or severe inflammation and necrosis of the liver (Fateen et al., 2012). Patients often present with rapid progression of fibrosis, and this is more commonly noticed in subjects who are infected during adulthood (EASL, 2012). From here, many patients achieve seroconversion and enter Phase III, however it is important to note that progression between phases is not a certainty, and patients may fail to control viral replication and enter Phase IV for many years (EASL, 2017).

Phase (III) HBeAg-negative chronic infection (ENCI) was formerly labelled as ‘inactive carrier’ and represents the largest group of HBV positive patients (Sharma et al., 2005). This phase is characterised by high levels of antibodies directed against HBeAg in the serum, with low peripheral HBV DNA and little evidence of liver inflammation as determined by ALT (EASL, 2017). Largely, liver biopsies from this stage return normal histological results with little to no necroinflammation, and minor incidences of fibrosis and, as such, patients have low risk of progression to cirrhosis or HCC (Lok et al., 2001a; Lok et al., 2001b). From this phase between 1-3% of cases may spontaneously resolve, resulting in HBsAg loss or seroconversion (EASL, 2012).

Phase (IV) HBeAg-negative chronic hepatitis (ENCH) is characterised by the absence of HBeAg and high prevalence of anti-HBeAg antibodies, in addition to fluctuating HBV DNA levels which are proportionally lower than quantifications from patients in EPCI or EPCH (EASL, 2012). The peaks in HBV DNA are

matched with flares and peaks in ALT, consistent with a hepatitis phenotype, and necroinflammation visible in liver histology (EASL, 2017). The low levels of HBeAg expression is thought to be attributable to higher prevalence of HBV integrants which are unable to produce HBeAg, and a less abundant or active cccDNA pool. In this phase of disease, spontaneous remission rates remain low (EASL, 2012).

Phase (V) HBsAg negative, or 'occult HBV infection' is characterised by the absence of both HBs and anti-HBs in the periphery, and detectable antibodies to HBcAg. Patients in this phase usually have normal levels of ALT, and undetectable HBV DNA. If HBsAg loss occurs before the onset of cirrhosis then there is little chance that a patient will develop cirrhosis, however HCC does remain a risk (EASL, 2017). It is paramount to note that reactivation is possible in instances of immunosuppression. All patients irrespective of their disease classification, are at risk of developing liver cirrhosis and subsequent progression to hepatocellular carcinoma, even when subjects have undergone long term anti-viral treatment (EASL, 2012; Varbobitis and Papatheodoridis, 2016).

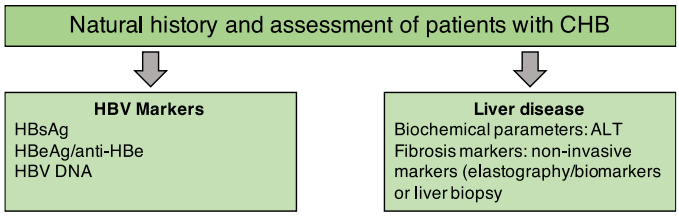


Figure 1.4: HBV and host parameters for EASL classification

A diagram to show the HBV and host parameters used to categorise patients by disease stage. Figure adapted from (EASL, 2017).

	HBeAg Positive		HBeAg Negative	
	Chronic Infection EPCI	Chronic Hepatitis EPCH	Chronic Infection ENCI	Chronic Hepatitis ENCH
HBsAg	High	High/intermediate	Low	Intermediate
HBeAg	Positive	Positive	Negative	Negative
HBV DNA	$>10^7$ IU/mL	10^4-10^7 IU/mL	<2,000 IU/mL	>2,000 IU/mL
ALT	Normal	Elevated	Normal	Elevated
Liver disease	None/minimal	Moderate/severe	None	Moderate/severe
Old terminology	Immune tolerant	Immune reactive HBeAg positive	Inactive carrier	HBeAg negative chronic hepatitis

Table 1.3: EASL stratification criteria

A table detailing the criteria by which patients are sorted into EASL disease stages, with expected clinical parameters listed. Table adapted from (EASL, 2017)

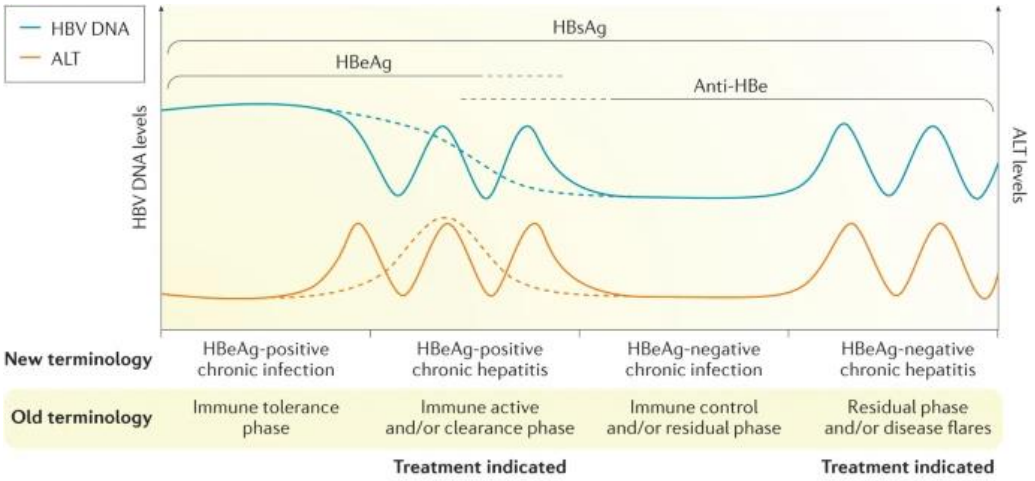


Figure 1.5: Viral and host parameters in the natural history of HBV

The relationship between viral and host parameters across the natural history of HBV infection. Figure taken from (Yuen et al., 2018)

1.2.3: Vaccines and drugs

Currently, there is no curative therapy available for chronic HBV, however drugs are available which work to limit viral replication and reduce the incidence of disease progression to cirrhotic states and liver cancer. There is also a prophylactic vaccine available which has worked to reduce the endemicity of the disease in the developed world, however it offers nothing to patients who are already infected, and does little to tackle the issue of vertical transmission in countries with high disease burden. It is safe to say that, in the absence of curative therapy, preventative measures offer the best solution; for example routine blood-screening of high risk individuals, or the implementation of protection during sexual intercourse. The importance of the prophylactic vaccine was made clear by the World Health Organisation (WHO) over 30 years ago, when all countries were encouraged to incorporate the prophylactic HBV vaccine into their national inoculation programmes (Kane, 1996).

The very first HBV vaccine was developed in 1969 by Blumberg and Millman, where a heat treated form of HBV was delivered to patients (Das et al., 2019). Since then, a new vaccine has been developed whereby an immune response is generated in response to recombinant HBsAg that is expressed in yeast lines or Chinese hamster ovary cells, and vaccines are delivered in a 3 dose routine of day 0, then 1 and 6 months after that (Leroux-Roels, 2015). The response to vaccine can be tested using serology and patients determined to have a low response may need to receive a booster vaccine. It is common place in the developed world to offer health care workers, laboratory research scientists and police officers HBV vaccines, due to increased occupational hazard, and

increased probability of exposure to the pathogen (Ryan and Aamoth, 1984). Patients in receipt of liver transplants are also encouraged to be immunised to prevent infection of the replacement organ. As is the case with many vaccines, there are a number of patients who will not respond to vaccination, and an individual is considered a non-responder if their anti-HBs serum titre is lower than 10 IU/L after the vaccine schedule (Caimi et al., 1995). Many factors can influence the probability of response such as age, body mass, gender and immunodeficiency (Leroux-Roels et al., 2001; Zannolli and Morgese, 1997). The vaccine is largely effective in responders, and Chang et al. demonstrated that with vaccination the incidence of HBV could be reduced from 0.7 per 100,000 patients to 0.57 per 100,000 in young children aged 6-14 (Chang et al., 1997).

According to the Hepatitis B Virus Foundation, there are over 50 new agents currently in clinical trials to combat HBV (Hepatitis B Foundation, Drug Watch, 2022). A functional cure for HBV is likely to come in the form of a small molecule that silences cccDNA and renders it transcriptionally inactive and, indeed many of the therapies currently used aim to reduce viral replication and lower viral load. It is of note that disease state is usually determined by the amount of peripheral HBs antigen, and much of this could be the product of transcriptionally active integrated genomes (Honer Zu Siederdissen and Cornberg, 2014; Ning et al., 2019). Peripheral HBV DNA or HBc/e antigen would instead offer an insight into the transcriptional activity of cccDNA. Hepatitis C virus (HCV) offers an experimental paradigm for HBV, where following the discovery of the virus, *in vitro* culture systems were developed, and a series of directly acting antiviral agents against several of the viral proteins followed (Holmes et al., 2019; Houghton, 2009; Lindenbach et al., 2005). This has not yet happened for HBV, and the

ongoing replication from low levels of cccDNA provides the biggest hurdle. As it stands, the current treatments recommended by the WHO are the nucleos(t)ide analogues (NA), entecavir (ETV) and tenofovir disoproxil fumarate (TDF). These are orally administered once daily as a pill and require no advanced storage systems, meaning these stand to penetrate the developing world much more readily than vaccination.

ETV is a guanosine analogue, and inhibits reverse transcription of the viral genome by being incorporated into the viral DNA. As it prevents the synthesis of new viral genomes, ETV has been shown to reduce viral load and maintain normal ALT levels in patients over a 5 year course of therapy. TDF was originally used as an anti-HIV treatment and, as both viruses are reliant on a reverse transcriptase stage in their life cycle, the drug was repurposed and used to reduce viral replication in CHB patients. Patients can be treated with both TDF and ETV in combination to prevent the emergence of drug resistant viruses, although the incidence of such mutants is already extremely low (Colonno et al., 2006). Routinely, patients are treated with NAs and pegylated-interferon (Peg-IFN), an immunomodulatory compound responsible for stimulating the host innate and adaptive immune response, which enhances the process of HBeAg seroconversion (Zhang et al., 2018). In turn, the antiviral properties of the NA therapy also enhances the immunologic response to pegylated-interferon (Tan et al., 2014). The current Peg-IFN treatment could result in the loss of HBsAg in a subset of patients, however previous studies have demonstrated highly variable success rates when treating diverse viral genotypes (Kim et al., 2011a; Kramvis, 2014). NA treatment neither directly targets the cccDNA, nor does it often achieve a state of immune control which means treatment is lifelong, and patient

compliance over many years may call success rates into question (Ning et al., 2019; Petersen et al., 2016). Many of the candidate drugs for HBV were originally developed to treat HIV-1, and one of the prime examples is lamivudine, a nucleoside reverse transcriptase inhibitor (NRTI) which was approved for HIV-1 treatment in 1995 and then HBV in 1998 (Quercia et al., 2018). However, the one pill per day regime required for lamivudine treatment lead to the occurrence of a resistance mutation in the polymerase gene which rendered the NRTI defunct. The YMDD mutant in the polymerase was found in all patients who had lamivudine resistant HBV, with between 65-70% of patients developing this within 5 years of the start of treatment (Li et al., 2005; Liaw, 2005). Whilst lamivudine treatment greatly accelerated the acquisition of this mutation, it has also been found in patients who were not on treatment at the time, suggesting that this mutation can also occur stochastically (Huang et al., 2005; Matsuda et al., 2004).

1.2.4: Host immune responses

Whilst the clinical phases of disease are well characterised, the EASL classification attempts to assess the status of the host inflammatory response using ALT as a surrogate marker. However, this does not accurately describe the interplay between the host immune response and viral replication, and the immune pathways controlling viral replication are not well defined. These limitations are likely reflective of a lack of peripheral biomarkers for liver inflammation and disease, and many studies are reliant on studying liver tissue for markers of viral replication and intra-hepatic immune activity (Lebosse et al., 2017; Meier et al., 2021; Suslov et al., 2021). HBV has gained a reputation for being a ‘stealth virus’, however previous studies have identified relationships between the virus and both

innate and adaptive arms of the immune system. Our understanding of the immune control of HBV has been limited by the rarity of patients recruited in early pre-symptomatic stages, poor *in vitro* infection systems in primary cells, and the high costs associated with animal studies and mouse models (Bertoletti et al., 2010; Dandri et al., 2001; Gripon et al., 2002; Roggendorf and Tolle, 1995).

Innate immune control

HBV is recognised to evade and suppress innate immune recognition, which results in a dampened anti-viral response in CHB (Lebosse et al., 2017; Ma et al., 2018; Wu et al., 2009). As such, in humans infected with HBV there is little evidence of pro-inflammatory cytokine expression in the early phases of infection, especially compared with patients infected with HCV or HIV (Bertoletti and Ferrari, 2012; Stacey et al., 2009). Interferons have been implicated in the life cycle of many viruses, and can be used for the treatment of HBV. Interferons have been shown to reduce cccDNA transcriptional output by perturbing the acetylation pattern of viral-associated histones and recruitment of co-repressors (Belloni et al., 2012; Tropberger et al., 2015). However, a study from Dunn et al. noted a lack of interferon expression in a cohort of patients with acute HBV infection, which was confirmed in a chimpanzee model where infection failed to induce interferon stimulated gene expression (Dunn et al., 2009; Wieland et al., 2004). This is in direct contrast to animals infected with HCV, where innate response genes are rapidly upregulated in response to infection, indicating that despite the same tropism and target organ, these pathogens co-opt different strategies to persist in their host (reviewed in (Bertoletti and Ferrari, 2012; Su et al., 2002)). *In vitro* it has

been demonstrated that HBV DNA can be detected by the innate immune system, as a study from Lucifora and colleagues identified that infection of differentiated HepaRG cells induced interferon-β expression (Lucifora et al., 2010). It has been suggested that the nature of cccDNA enables HBV to avoid innate immune recognition, as it is stable in the nuclei of infected cells, and new genomes are protected by the nucleocapsid whilst travelling across the cytoplasm during egress (Bertoletti and Ferrari, 2012; Wieland and Chisari, 2005). However, Kaposi's sarcoma herpesvirus (KSHV) also replicates via episomal copies of the DNA genome, and immune interferon-16 (IFI-16) has been identified as an innate nuclear DNA sensor, highlighting possible implications for HBV virology (Kerur et al., 2011).

However, there is a current debate as to whether HBV evades the immune system, or whether it actively and directly supresses innate sensing mechanisms (Bertoletti and Ferrari, 2012). For example, *in vitro* experiments have shown that the HBV polymerase is able to disrupt intracellular interferon-β induction through inhibiting signalling from interferon regulatory factor (IRF), toll-like receptor (TLR) -3, and RIG-1 (Wang and Ryu, 2010; Yu et al., 2010b). As discussed in *Ubiquitous transcription factors,* nuclear factor-κB (NF-κB) is a transcription factor known to repress HBV, with implications in the regulation of both the innate and adaptive immune system (Aggarwal, 2004). The viral polymerase has been shown to disrupt NF-κB signalling and downstream interferon-β production (Liu et al., 2014). Similarly, studies from Kumar et al. and Wang et al. showed that HBV could perturb IRF3 signalling, however they attributed this to the activity of the HBx protein (Kumar et al., 2011; Wang et al., 2010). Additional studies reported that HBx perturbs interferon signalling through interactions with RIG-1 and inhibition of

mitochondrial antiviral signalling (MAVS) protein (Kumar et al., 2011; Wang et al., 2010). An alternative mechanism for suppression of interferon signalling is that HBx can affect STAT-methylation, and thereby inhibits the downstream induction of interferon stimulated genes (Christen et al., 2007; Yu et al., 2010b). It is also possible that secreted HBs and HBe antigens can dampen the TLR response, by perturbing the surface expression of TLR-2 (Visvanathan et al., 2007; Wang and Ryu, 2010; Wu et al., 2009). Furthermore, these secreted antigens have been reported to induce IL-10, an immunosuppressive cytokine which reduces natural killer cell activity, perhaps rationalising why HBV persistently produces both of these proteins in large quantities (Frelin et al., 2009; Peppa et al., 2010).

In short, there are a number of mechanisms acting in the arms race between virus and host, and there is still much to learn about the intricate relationship between HBV replication and the innate immune response. Further understanding of the host response to virus, and viral evasion mechanisms will inform the design of future anti-viral therapies.

Adaptive immune response

Given the persistent nature of HBV infection it is not surprising that there is dynamic interplay between the adaptive immune response and virally infected hepatocytes. From between 4-7 weeks post initial infection, it is possible to detect HBV-specific CD4- and CD8- cell mediated responses in a chimpanzee model (Fisicaro et al., 2009; Webster et al., 2000). In these early stages HBV-specific T cell responses are largely driven by Th1 cells and can be sufficient to clear infection, displaying higher efficiency than responses seen in the later chronic

phases of disease (Bertoletti and Ferrari, 2003; Bertoletti et al., 2010; Rehermann and Nascimbeni, 2005; Tan et al., 2015; Wieland and Chisari, 2005). The initial quiescence and 'slow' viral replication may not stimulate T cells to undergo activation and subsequent expansion (Webster et al., 2000; Whalley et al., 2001). As discussed in the *HBV natural history,* many infections are self-limiting and spontaneously cleared, with a previous report noting a 90% reduction in peripheral HBV DNA within 3 weeks of the peak of replication (Guidotti et al., 1999). This clearance happens before histological evidence of liver damage, suggesting that the virus is cleared through non-cytopathic mechanisms, such as the production of interferon-γ and tumour necrosis factor- α (TNF-α) secreted by CD8+ T cells (Bertoletti and Ferrari, 2012; Guidotti and Chisari, 2006; Guidotti et al., 1999). In contrast, HBV-specific cytotoxic T lymphocytes (CTLs) are recruited to infected cells through cytokine signalling, and CXCL-9 and CXCL-10 are released to facilitate the activity of antigen presenting cells (Iannacone et al., 2005; Iannacone et al., 2007; Lee et al., 2013; Sitia et al., 2004).

During immune control of infection, there is an increase in CD127+ T memory cells with a decrease in programmed death-1 (PD-1) expression on HBV-CD8+ cells (Boettler et al., 2006; Boni et al., 2007). Chronic infection is characterised by exhausted CD8+ T cell responses, where during the peak of disease most HBV-CD8+ cells are activated but unable to proliferate, possibly due to IL-10 mediated suppression (Dunn et al., 2009; Sandalova et al., 2010). As shown in *Figure 1.5* levels of ALT and peripheral HBV DNA are usually inversely proportional. Previous studies identified that T cell activity follows the same trend, whereby intrahepatic T cell function peaks when viraemia is low (Boni et al., 2007; Fisicaro et al., 2010; Maini et al., 2000; Webster et al., 2004). Whilst the

mechanisms underlying HBV-CTL tolerance are not fully understood, it is thought that this is due to continuous viral antigen expression, as liver resident antigen presenting cells could be expressing HBV epitopes for prolonged periods of time (Bertolino et al., 1998; Bowen et al., 2004; Crispe, 2011; Schildberg et al., 2011). Additional mechanisms such as CD3ζ-chain down-regulation, T-cell apoptosis, or inflammatory mediated changes to hepatic metabolism may also affect anti-HBV T cell activity (Das et al., 2008; Yang et al., 2010).

1.2.5: Liver cancer

Liver cancer is a generic term that refers to a heterogenous mix of cancer types that originate from one of the many different cell types in the liver. Liver cancer is the sixth most commonly diagnosed cancer worldwide, and is ranked fourth in terms of mortality (Bray et al., 2018). In 2018 alone, 841,000 cases of liver cancer were diagnosed, and over 782,000 individuals died. It is estimated that these numbers will only increase, and that by 2025 there will be 1,000,000 diagnoses of liver cancer per annum (Lozano et al., 2012). The incidence of liver cancer varies geographically due to the global distribution of risk factors (Kulik and El-Serag, 2019). In Europe around 5.1 people per 100,000 are diagnosed with liver cancer, whereas it is over three times more prevalent in Asian populations with 17.7 incidences per 100,000 (Ferlay et al., 2019). Of all primary liver cancers, HCC is the most common and accounts for more than 75% of all diagnoses, with intrahepatic cholangiocarcinoma representing the next most common and around 15% of the total burden (Petrick and McGlynn, 2019). HCC has a 5 year survival of only 19%, and this highlights the need for new treatment strategies and

preventative measures for the disease (Bray et al., 2018; Islami et al., 2017). The prevalence of HCC is over 3 fold higher in men than women, and is most frequently found in the presence of liver disease or cirrhosis, but over 60% of all HCC cases are caused by viral hepatitis (de Martel et al., 2015; Yang et al., 2014; Yang et al., 2011). Chronic infection with hepatitis B or C virus drives HCC, and it has been estimated that HBV is responsible for between 50 and 80% of all HCC cases worldwide, with HCV infection driving between 1 in 10 and 1 in 4 incidences (Anthony, 2001; Block et al., 2003; Global Burden of Disease Liver Cancer et al., 2017).

The precise molecular link between HBV infection and HCC is not fully understood, and has been attributed to direct and indirect pathways. It is often theorised that integration of the viral genome is the main driver, particularly when viral gene expression falls under the transcriptional regulation of a host oncogene (**Table 1.4**) (Peneau et al., 2021; Tu et al., 2017; Zhao et al., 2016). The viral accessory protein HBx is frequently labelled as an oncoprotein, and its expression has been implicated in regulating many of the pathways which associate with the hallmarks of cancer. HBx has been shown to bind p53 and transform cells to a more actively proliferating state, through compromising cell cycle regulatory checkpoints (Gearhart and Bouchard, 2011; Truant et al., 1995; Wang et al., 1994). Equally, HBx has been linked to differential expression of growth-control genes, many of which are commonly associated with a wide range of cancer types such as ERK, Ras, MAPK and Raf (Nijhara et al., 2001; Tarn et al., 2001). Alternatively HCC could develop due to differential gene expression in cells that are infected with HBV, and these transcriptome wide changes result in aberrant and inappropriate gene expression, and the subsequent onset of tumorigenesis.

As reviewed by Levrero and Zucman-Rossi (Levrero and Zucman-Rossi, 2016), the mechanisms of differential gene expression are widespread and involve epigenetic reprogramming through histone modification and the hypo-methylation of DNA, and may result in an increase in plasticity of HBV infected cells (Arzumanyan et al., 2011; Calvisi et al., 2007; Fujimoto et al., 2012). It is interesting to note that both prophylactic vaccination in young adults, and treatment using nucleos(t)ide analogue therapy have both been shown to reduce the rate of progression to HCC (Chang et al., 2009; Wong et al., 2013). It goes without saying that our understanding of the progression from CHB to HCC needs to be increased, to offer a wider range of tools to provide better outcomes for patients.

Direct	Indirect	HBx Protein
Integration of HBV DNA into chromsomes	Inflammation and regeneration associated with CHB	HBx transcriptional activation
Integration within or near functional cellular genes	Via cirrhosis associated with CHB	Activation of Ras-Raf-MAPK pathway
		Interaction with p53
		Truncated HBsAg product transactivation

Table 1.4: Mechanisms of HCC development

A table showing putative mechanisms for HCC development as a result of HBV infection adapted from (Blum and Moradpour, 2002).

1.2.6: HBV genotypes

Based on nucleotide sequence divergence, HBV has been classified into 8 genotypes (Gt) labelled A-H (Kramvis et al., 2005). There has been speculation that both genotypes I and J have also been identified, although this is still somewhat controversial within the field and not yet widely accepted, summarised in (**Table 1.5**) (Tatematsu et al., 2009; Yu et al., 2010a). In order to qualify as a distinct genotype there must be at least 7.5% variability in the genome, and further intra-genotype variability has resulted in the classification of genomes into sub genotypes, where variation is between 4 and 7.5% (Kramvis, 2014; Kramvis and Kew, 2005). The diverse genotypes broadly cause the same symptoms of disease, but show distinct geographical distribution with GtD and E representing the majority of cases in the Western World (Kramvis et al., 2005). GtA is also found in Europe, but is more frequent in circulation in the Americas and Africa, and its distribution is largely attributed to the progression of the slave trade (Kramvis and Paraskevis, 2013). GtB and C are both prevalent in Asia, and GtF and H can be more commonly found in both Southern and Central America (Kramvis and Paraskevis, 2013). The distribution of HBV genotypes is accredited almost entirely to immigration and the movement of people, for example GtI has spread from Vietnam to Canada, and since colonisation more recently to France (Colson et al., 2009; Osiowy et al., 2010).

Genotype	Global Distribution
A	Sub-Saharan Africa, India, northern Europe, Western Africa, Gambia, Nigeria
B	Japan, East Asia, Taiwan, China, Indonesia, Vietnam, Philippines, Alaska, northern Canada, Greenland
C	Taiwan, China, South Korea, Japan, Southeast Asia, Australia, Philippines, Vietnam, Indonesia
D	Africa, Europe, Mediterranean countries, India, Indonesia, Australia
E	Western and central Africa, Saudi Arabia
F	Central and South America
G	France, Germany, United States
H	Central America
I	Vietnam and Laos
J	Japan

Table 1.5: Geographical distribution of HBV genotypes

A table to summarise the geographical distribution of HBV genotypes. Table adapted from (Nguyen et al., 2020)

Due to the distribution patterns of the various genotypes, many comparative studies have been performed to understand the contribution of genotype to the natural history of infection, as well as the response to antiviral therapies (Kao, 2002; Liaw et al., 2010; McMahon, 2009). Patients infected with GtE show higher levels of HBeAg positivity than those infected with GtD, and are more likely to have a higher viral load. HBeAg is essential for the progression from acute disease to chronicity and, whilst HBeAg is not essential for viral replication, studies have identified HBeAg as an immune tolerogen and an essential factor in establishing viral persistence (Chen et al., 2005; Cote et al., 2000; Hadziyannis and Vassilopoulos, 2001; Yousif et al., 2013). These studies have noted genotype and sub-genotype specific minutia when it comes to the onset and progression of disease. For example infection with Gt A1, B2-4, C, F1 or D show increased complications, higher incidence of cirrhosis and more common progression to HCC than A2, B1, and B5 (McMahon, 2009). Generally speaking, GtC is more commonly associated with early risks of inflammation and onset of fibrosis, cirrhosis and subsequent HCC, suggesting a more aggressive phenotype (Araujo et al., 2011). In contrast, GtH is associated with occult HBV infection, with low viral loads and a minimal risk of HCC development (Panduro et al., 2013).

It is tempting to draw comparisons between clinical disease and genotype specific phenotypes in *in vitro* model systems, where stark differences in replication capacity, efficiency and transcript patterns have been observed (Sozzi et al., 2016). For example, recent studies have identified a low replication capacity *in vitro* for GtH, which as previously stated results in low viral load in patients (Sozzi et al., 2018). However, without comprehensive comparative studies, this is little more than speculation. To that end, the majority of cell culture models,

including chronically infected immortalised cell lines, support replication from a genotype D virus, of the D3 sub-genotype. Since the advent of cell culture systems, *de novo* infection of hepatoma lines is considered to be the gold standard model system, however many studies are still reliant on lipid transfection of overlength HBV genomes (HBV1.1, HBV1.3) and often use plasmid constructs encoding HBV of other genotypes (Lim et al., 2021).

1.2.7: Life cycle of HBV

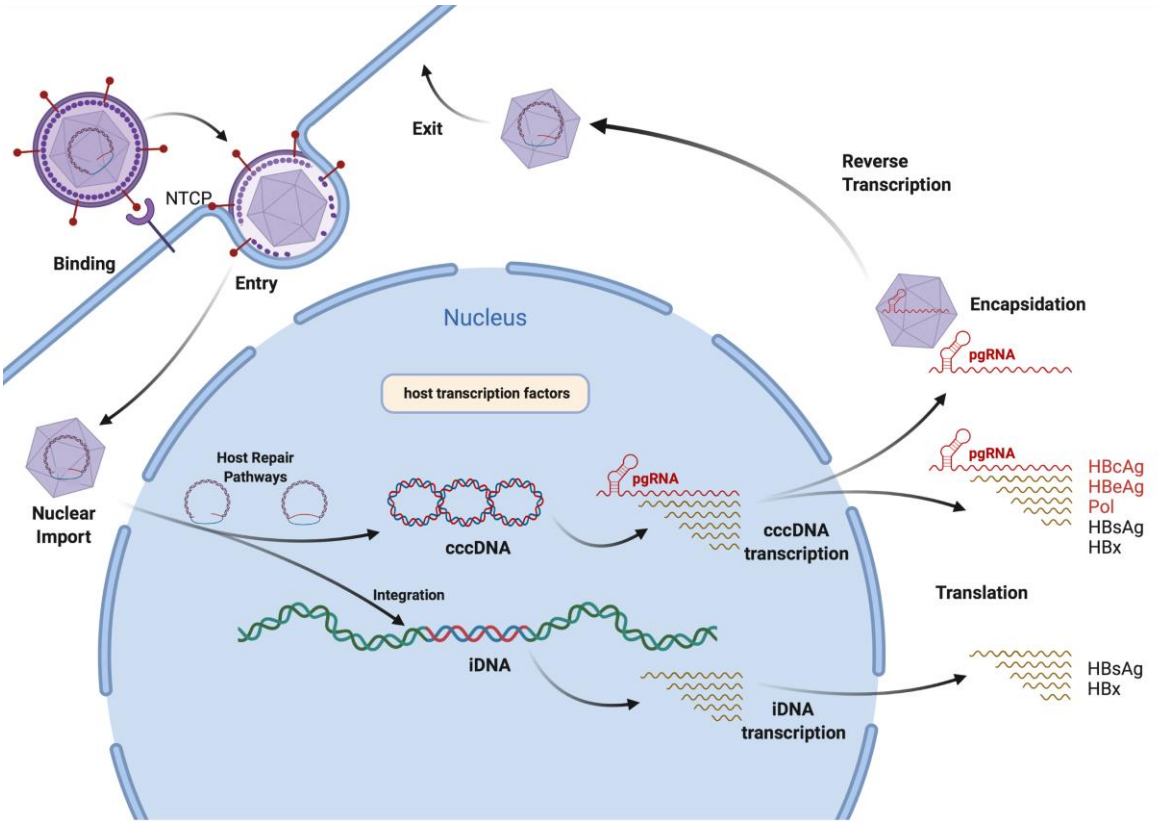


Figure 1.6: The molecular life cycle of HBV

A cartoon showing the key stages in the life cycle of HBV. Each of these stages are discussed at length below. *With thanks to Dr Peter Balfe and Professor Jane McKeating for providing this cartoon.*

HBV transcription and translation

At only 3.2kb in length, the viral genome is one of the shortest amongst all human viruses, and is the smallest DNA virus known to infect humans (**Figure 1.7**). The episomal cccDNA forms the template for total viral replication, whereby the genome consists of 4 overlapping open reading frames, which encode 7 viral proteins from 5 major RNA transcripts. Transcription of the viral RNAs are under the regulation of 4 promoters, the basal core promoter (BCP), PreS1 Promoter, PreS2 promoter, and X promoter, and also 2 enhancer (Enh) elements known as EnhI and EnhII (Hong et al., 2017; Ni et al., 2014) (**Figure 1.8**).

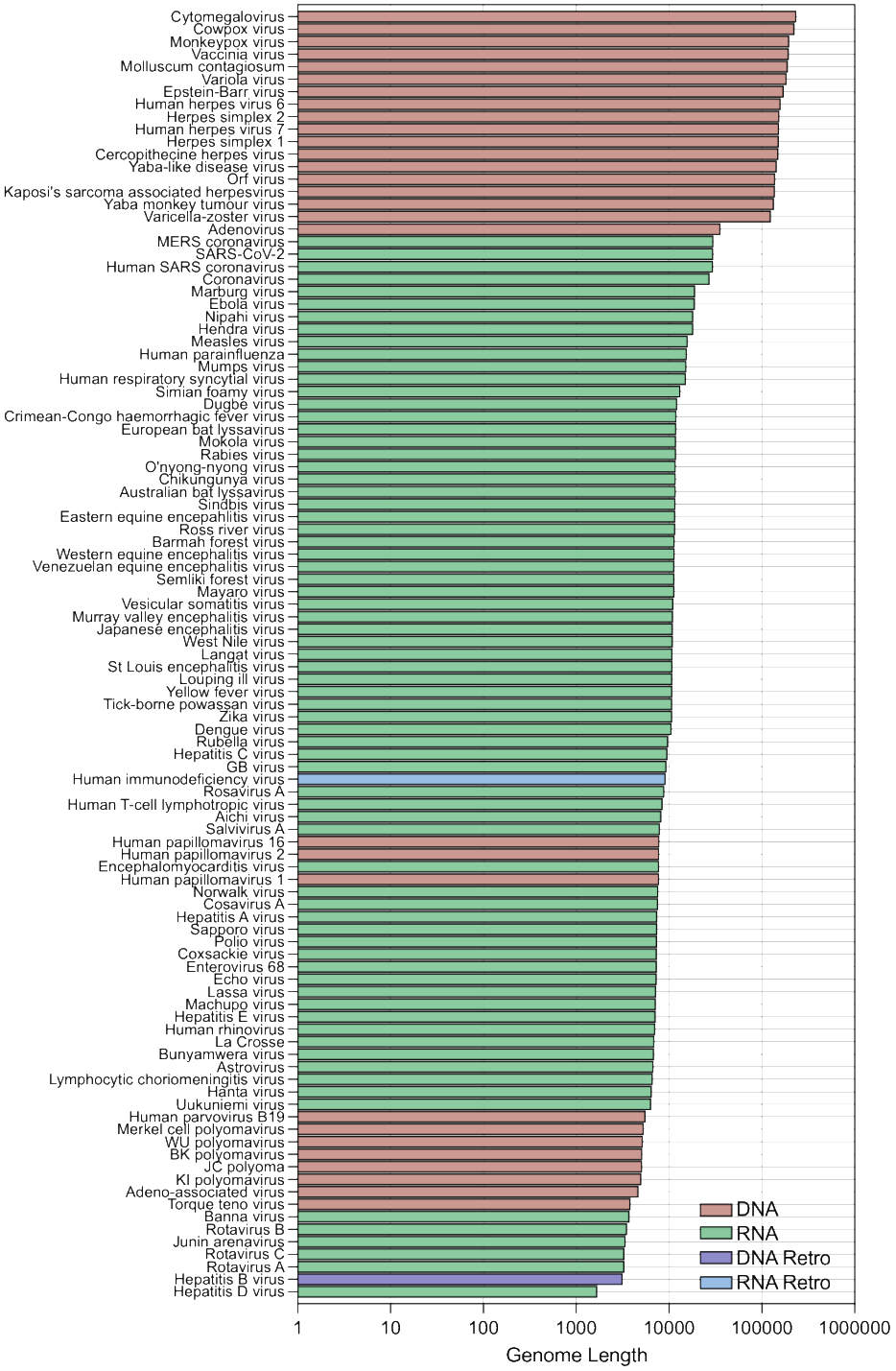


Figure 1.7: Viral genomes

A diagram to show the length of the genomes of a panel of human viruses. Examples are ranked by genome size (in nucleotides), and coloured by the nature of the genomic material. Human viruses accessed from ViralZone database, accession numbers are provided in Chapter 2.14 (Hulo et al., 2011).

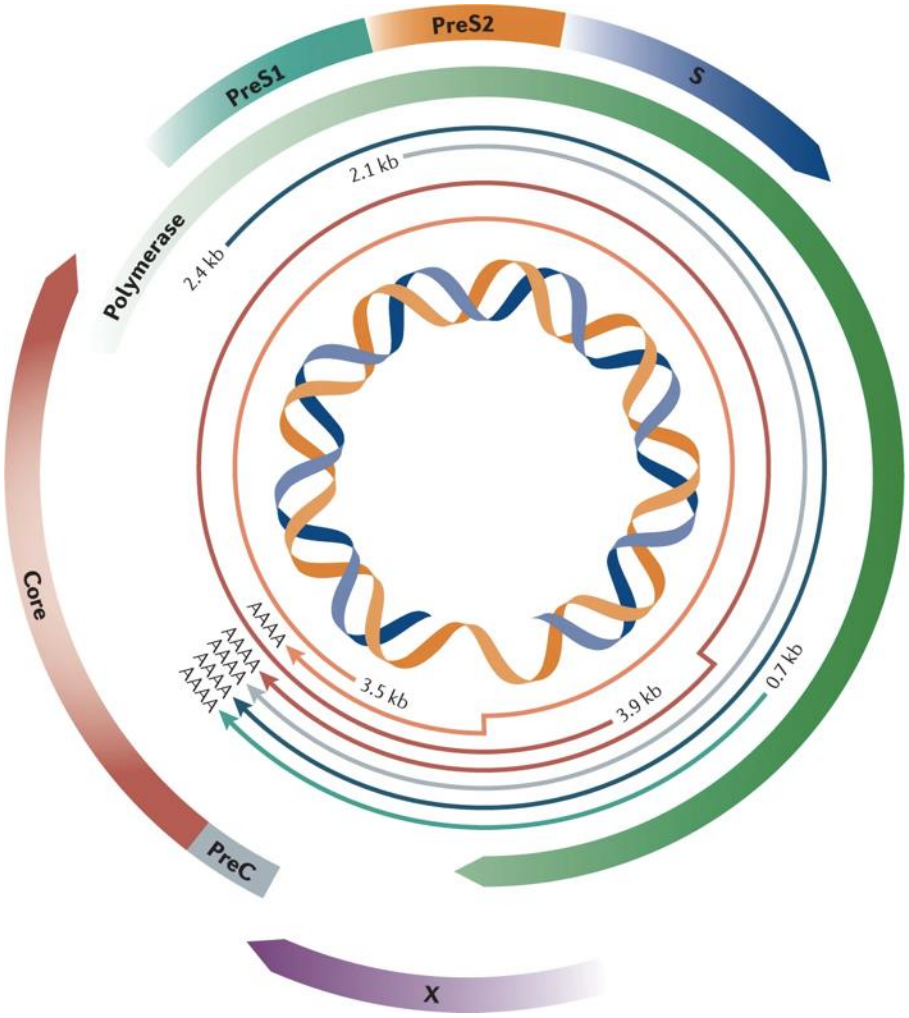


Figure 1.8: Viral ORFs

A cartoon to show the overlapping reading frames and protein coding regions of the circular viral genome (Iannacone and Guidotti, 2021).

The BCP is directed by EnhI and regulates transcription of the 3.5kb pre-core (pC) and pre-genomic (pg) RNAs, which are driven from the same open reading frame, but utilise an alternative start codon, some 30 nucleotides apart (Hu and Siddiqui, 1991). The pC RNA can be translated to form Hepatitis B e Antigen (HBeAg), and the pgRNA serves as the genomic template for new progeny virus, as well as the core (HBc) antigen. The 3.5kb fragment also encodes the HBV polymerase (Pol) although this is read from an independent open reading frame. It is important to note that HBV Pol is an RNA-dependent DNA-polymerase, or a reverse transcriptase, and is therefore independent of RNA Pol II, the factor that is required for transcription of the viral RNAs (Hong et al., 2017; Jeong et al., 1996; Rall et al., 1983). The PreS1 promoter drives the transcription of the 2.4kb PreS1 mRNA which is translated to form the largest of the viral glycoproteins (HBs-L), where the PreS2 promoter initiates transcription of the 2.1kb RNA, or PreS2, which can be translated into either medium or small glycoproteins (HBs-M, or HBs-S) (Heermann et al., 1984). Both PreS1 and PreS2 promoters are under the regulation of EnhII, which largely overlaps the BCP, but regulates transcription of the glycoproteins downstream (Yuh and Ting, 1990). It is worth noting that the glycoproteins are encoded by the same open reading frame (ORF) but rely on initiation of translation from 3 alternative ATG start codons in the same frame (**Figure 1.9**).

HBx mRNAs encode the multi-functional viral accessory protein, which is deemed to be essential for HBV replication (Lucifora et al., 2011). The 0.7kb transcript is driven from its own promoter, and leads to the production of the 154aa X protein (**Figure 1.10**). X is implicated in many host cell pathways, although the experimental design and model systems used are often contentious (Guerrieri et

al., 2017). Typically, Northern Blotting is used to evaluate the abundance of viral RNAs, however probing these membranes for HBx can be challenging without using over-expression constructs (Ko et al., 2018; Stadelmayer et al., 2020). Many studies investigating the role of HBx in regulating host pathways rely on over expression systems, or genetically manipulated HepaRG cells with tetracycline inducible HBx expression (D'Arienzo et al., 2021b; Lucifora et al., 2011). Whilst *in vitro* infection systems for HBV remain relatively inefficient, the exogenous X alternatives offer some insight into protein function, but their conclusions should be taken with caution (Slagle et al., 2015).

As well as positive regulatory elements in the genome, the virus also encodes a negative regulatory element (NRE) which overlaps the EnhII region adjacent to the BCP, and represses BCP activity and viral replication (Sun et al., 2001). In addition to the major viral RNAs, HBV transcribes several spliced RNAs derived from both the pC reading frame, and the HBx reading frame. Recent sequencing based approaches have characterised the spliced variants of the pC/pgRNA, and identified Sp1 as the major spliced transcript which is translated to a truncated protein, HBSP (Duriez et al., 2017). Using an Illumina sequencing platform Lim et al. identified 16 spliced forms of the pC/pg RNA, and previous reports have described associations between spliced RNAs and HCC development, as well as the immune response or the response to interferon (Bayliss et al., 2013; Chen et al., 2015; Duriez et al., 2017; Lim et al., 2021). Equally, studies have identified spliced and truncated forms of HBx, and these have been implicated in HCC development, cellular reprogramming and metabolism (Al-Anazi et al., 2018; Ng et al., 2016; Sze et al., 2013; Zhang et al., 2021).

Due to the overlapping ORFs and compact genome structure, over 60% of the viral genome encodes multiple functional proteins in at least one ORF (McNaughton et al., 2019; Osiowy et al., 2006). The ORF for the viral polymerase completely overlaps the S ORF, and it has been suggested that this provides a major constraint to viral evolution (Mizokami et al., 1997). A synonymous (or silent) mutation in the polymerase reading frame could result in a non-synonymous change in the S ORF (Cento et al., 2013). As such it has been noted that the overlapping regions show much lower rates of variability than the regions encoding a single protein (Li et al., 2017; Torres et al., 2013). Cento and colleagues identified 70% nucleotide conservation in the region where pol and S overlap, compared with a 41% conservation in the non-overlapping region (Cento et al., 2013). This is referred to as suppression of synonymous site variability.

Based on nucleotide sequence divergence HBV can be separated into 8-10 distinct genotypes (discussed in depth in *Chapter 1.2.6*)(Kramvis, 2014; Kramvis *et al.*, 2005; Kramvis and Kew, 2005). Due to the overlapping nature of the viral genome, and conservation of the polymerase and surface open reading frames, much of this genetic variability is found in the pre-core and core regions. McNaughton et al. summarised the location of genotype defining mutations, and identified most variability in the HBc and BCP regions, with some genotypes exhibiting deletions in preS1 (McNaughton et al., 2019). The polymerase and S-encoding regions of the genome are largely conserved between genotypes, which is to be expected, as they are the primary targets of the antiviral therapies and antibody responses respectively (Cento et al., 2013; Kramvis and Kew, 2005; Lok and McMahon, 2009).

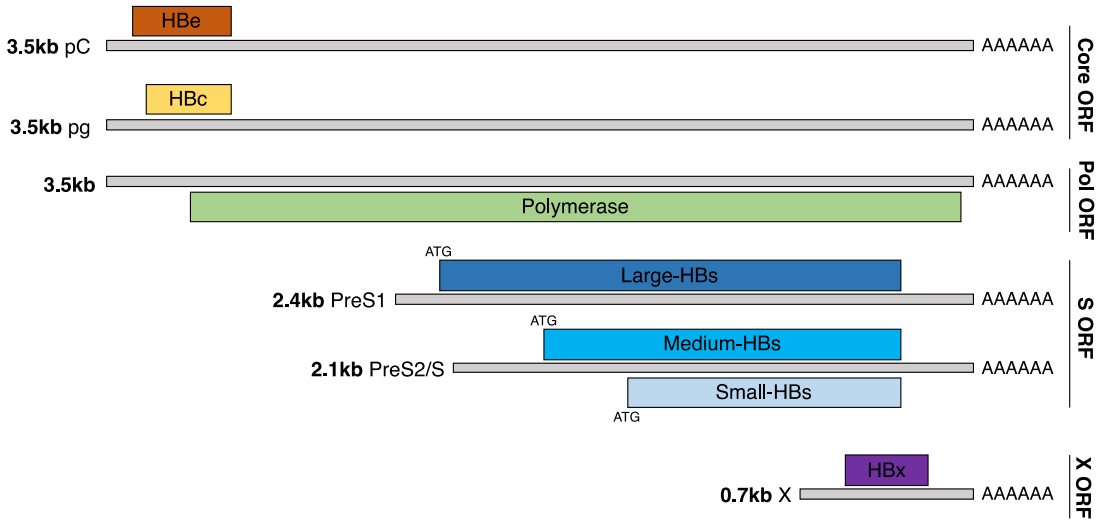


Figure 1.9: HBV RNAs

A schematic diagram to show the major HBV RNAs and the protein products encoded by each of the HBV ORFs. Surface antigens are encoded in the same ORF, starting at independent start codons, denoted by ATG. AAAAAA represents the poly-adenylation sequence. Figure adapted from (Tsukuda and Watashi, 2020).

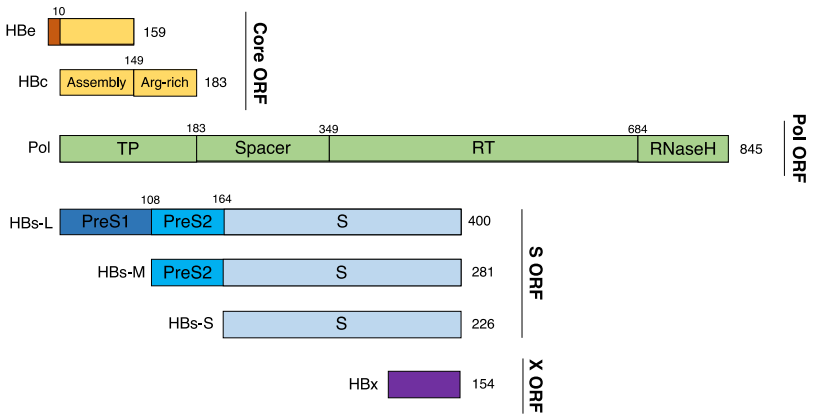


Figure 1.10: HBV proteins

A cartoon to show the 7 viral proteins, and their key features with amino acid positions listed. Cartoon adapted from (Tsukuda and Watashi, 2020).

Entry

HBV exclusively infects hepatocytes, and the first stage in its infectious life cycle is entry (**Figure 1.6**). Hepatocytes express heparin-sulphate proteoglycans (HSPGs) on their membrane which form low affinity interactions with the viral capsid (Leistner et al., 2008; Schulze et al., 2007; Verrier et al., 2016). This initial, non-specific interaction is essential in the entry process, and inhibitors of HSPGs such as suramin, a polysulphonated napthylurea, have been shown to inhibit HBV entry (Leistner et al., 2008). Interestingly, HSPGs are implicated in the entry process of several viruses, including herpes simplex virus (HSV), human papilloma virus (HPV) and also dengue virus (DENV) (Chen et al., 1997; Shieh et al., 1992; Surviladze et al., 2015). Once the capsid is associated with the cell membrane, the virus enters the cell through an endocytosis-dependent mechanism, which is the result of highly specific interactions between the HBV PreS1 surface glycoprotein and the bile acid transporter, sodium taurocholate co-transporting polypeptide (NTCP) (Herrscher et al., 2020; Huang et al., 2012a; Zhang et al., 2016b). NTCP is exclusively expressed on the basolateral-surface of hepatocytes and it is believed that this is a major determinant of tropism, as it forms high affinity interactions with amino acids 2-48 of the viral PreS1 (Ni et al., 2014; Yan et al., 2012). Even before the discovery that NTCP was fundamental for HBV entry, it was well documented that this 46 amino acid fragment of PreS1 was essential for virus-receptor interactions (Barrera et al., 2005). It was noted that NTCP was also highly expressed in both primary human hepatocytes (PHHs) and differentiated HepaRG cells in cell culture, and exogenous NTCP expression in other hepatoma lines rendered cells permissive of HBV entry (Ni et al., 2014; Yan

et al., 2012). To extend this observation, Muller and colleagues studied the role of NTCP in mediating cross-species transmission by cloning 11 NTCP isoforms from New World and Old World primates into HepG2 and HEK293T cells (Muller et al., 2018). This study revealed that the 158G residue of NTCP was sufficient to discriminate between the susceptible New World great apes and humans, and the non-susceptible Old World monkeys. These essential findings have contributed to the development of PreS1 analogues as pharmacological entry inhibitors, such as myrcludex B (Glebe et al., 2005; Lempp and Urban, 2014).

Hepatitis D Virus (HDV) does not encode its own envelope glycoproteins and instead hijacks and utilises the HBV Pres1 peptides. As such HDV also enters hepatocytes via NTCP, and its entry is indeed inhibited by PreS1 agonists (Yan et al., 2012). Around 1 in 20 patients infected with HBV are coinfected with HDV, and this is associated with poor prognosis and advanced disease progression. Many patients exhibiting HBV/HDV coinfection show progression to cirrhosis, liver failure and HCC within 5-10 years (Urban et al., 2021). Interestingly, disease progression can be differentially impacted depending on whether HBV/HDV infection occurs via simultaneous co-infection, or through superinfection of a HBV-positive patient (Negro, 2014). Simultaneous co-infection often results in acute hepatitis and rapid clearance of both viruses, whereas superinfection exacerbates the existing HBV induced liver damage and drives a state of chronic hepatitis (Sagnelli et al., 2021).

Since the discovery of NTCP as the major cellular receptor for HBV in 2012, the membrane bound epidermal growth factor receptor (EGFR) has also been reported to be a mediator of HBV internalisation, in events proceeding binding with NTCP (Iwamoto et al., 2020; Iwamoto et al., 2019). The mechanism by which the capsid traffics to the nucleus post entry still remains largely unknown.

However studies have identified that the cellular microtubule network is utilised for transport, and nuclear entry is executed in an importin-dependent manner through the nuclear pore complex (Kann et al., 1999; Rabe et al., 2006; Rabe et al., 2003).

cccDNA genesis

Before any viral RNAs can be transcribed, the incoming encapsidated genome must be repaired. The partially double stranded relaxed circular DNA (rcDNA) must be converted into a complete and replication competent episomal structure, referred to as covalently closed circular DNA (cccDNA). Upon repair the viral genome closely resembles authentic host cell chromatin, as it associates with host nucleosomes and forms a classic ‘string of pearls’ structure (Bock et al., 1994). The cccDNA forms a mini-chromosome where viral proteins, such as HBc, and host histones, with all of their associated post-translational modifications, can regulate the activity of this template (Bock et al., 2001; Tang et al., 2019). The formation of cccDNA is fundamental in the replicative life cycle of the virus, as cccDNA is capable of transcribing all of the viral RNAs, including the pre-genomic RNA (pgRNA) which is the template for progeny viral genomes. Despite the importance of this stage in the life cycle, until recently it has not been well understood, with multiple repair mechanisms suggested and debated at length. The work of Wei and Ploss has been paramount in understanding the mechanism by which the cccDNA is formed from rcDNA, and their studies have investigated the fundamental steps and host factors in facilitating the repair (Wei and Ploss, 2020; 2021a). Over time, the field has been restricted by the availability of model systems to study HBV *in vitro*, and has largely been reliant on studying the repair of the closely related Duck-HBV (Gong et al., 2001; Radziwill et al., 1988).

However, the recent advent of biochemical and cell-free assays for DNA repair has allowed the mystery of cccDNA genesis to be unravelled (**Figure 1.11**) (Wei and Ploss, 2021b).

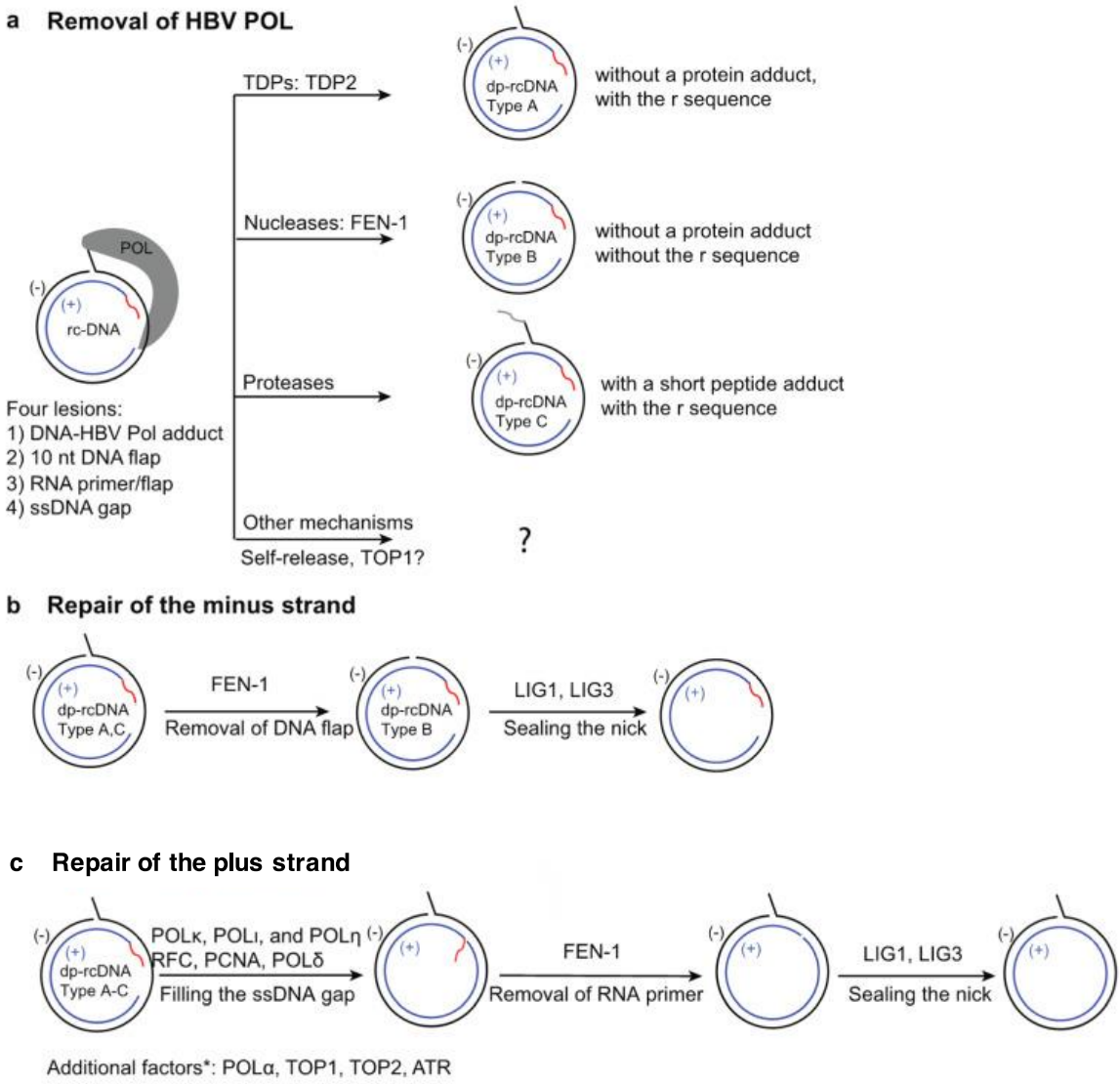


Figure 1.11: cccDNA genesis

A series of diagrams to show the key stages and host factors in the process of cccDNA repair. Each of these stages and the role of the relevant host factors are discussed below. Figure taken from (Wei and Ploss, 2021b).

dp-rcDNA is a recombinant, de-proteinated (dp) form of the viral genome, used by Wei and Ploss in their *in vitro* biochemical studies.

There are four major hurdles to overcome in the repair process, starting with (1) the removal of the HBV polymerase from the incoming rcDNA; (2) the *r* terminal redundancy sequence constituting the DNA flap; (3) a 5'-capped RNA primer for repair; and (4) a repair of a single-stranded DNA lesion on the positive strand (Wei and Ploss, 2021b). All of which need to be resolved before the genome is competent to serve as the transcriptional template and drive infection. By employing a biochemical assay using a recombinant rcDNA, which is almost identical to authentic viral rcDNA, the 5 host factors responsible for the repair have been elucidated. Proliferating cell nuclear antigen (PCNA), replication factor C complex (RFC), DNA polymerase delta (POLδ), flap endonuclease 1 (FEN-1) and DNA ligase 1 (LIG1) have been identified as the essential factors to convert rcDNA to cccDNA *in vitro*. The first stage is the removal of the covalently bound viral polymerase, which is catalysed by FEN-1. Whilst FEN-1 is deemed to be an essential factor in cccDNA repair, it may also cause inefficient cccDNA genesis in cell culture models (Kitamura et al., 2018). The nuclease activity of FEN-1 is greatly restricted in the presence of the polymerase, and has restricted access to the 5' end of the redundancy flap. As such, other cellular factors like TDP2 may first be recruited to cleave the covalent bond which tethers Pol to the genome (**Figure 1.11a**) (Kawale and Povirk, 2018; Koniger et al., 2014).

Whilst the viral polymerase blocks the repair of both strands of the genome, the repair of the minus strand is also dependent on the removal of the 10nt redundancy sequence, which exists to prevent frame shifts and deleterious truncations. FEN-1 begins the repair of the negative strand by generating a single nucleotide nick at the 5' end of the flap, which allows subsequent ligation to the 3' end facilitated by LIG-1 (Wei and Ploss, 2021a). Following this the positive strand

lesion, which resembles a single strand DNA break not dissimilar from an Okazaki fragment, must be repaired. However the repair is inhibited by the 18bp RNA primer which sits across the positive strand and covers 7 nucleotides of the lesion, leaving the remaining 11 as a RNA flap. The mechanism underlying the removal of this primer is not yet fully understood although this would appear to be the natural substrate of FEN-1 (**Figure 1.11b**) (Murante et al., 1996). However both HBV Pol and host cell RNAseH encode the relevant RNAse activity which could catalyse the removal of the primer (Hyjek et al., 2019; Tavis and Lomonosova, 2015).

Finally, following the removal of the RNA primer the positive strand is synthesised and requires PCNA, RFC and Polδ. The 3' end of the positive strand is equivalent to a primer, and is recognised by the RFC complex to load the homotrimer clamp PCNA ring onto the rcDNA (Majka and Burgers, 2004; Yao and O'Donnell, 2012). Together, PCNA-Polδ serve to complete the synthesis of the positive strand, and turn the RNA primer into another flap. FEN-1 is once again recruited to cleave this flap, which results in a simple nick that DNA ligases can then repair with ease (**Figure 1.11c**). This complex repair process is fundamental in the viral life cycle, yet is carried out almost entirely by host cell factors. The nucleus is the exclusive site of cccDNA genesis, due to the coincidence of host factor expression and the site-specific release of inbound rcDNA from the viral capsid (Wei and Ploss, 2021a). This is a clear demonstration of the parasitic nature of a virus.

Two templates for transcription

The major output from an infected hepatocyte is progeny virus, where the viral pgRNA is reverse transcribed in the nucleocapsid to form the rcDNA genome. These are either secreted as new infectious virions, or undergo capsid reimport where they can maintain the cellular cccDNA pool (Ko et al., 2018; Lythgoe et al., 2021). The nuclear cccDNA reservoir is the major determinant of viral replication and can be depleted due to dilution during cell division, or natural degradation. However, during reverse transcription (RT) a double stranded linear intermediate of the viral DNA (dslDNA) can form. This occurs in instances where the RNA primer does not translocate, and instead aberrant RT begins from direct repeat (DR)-1 (Tu et al., 2017). Unlike HIV-1, integration is not an essential stage in the viral life cycle (**Figure 1.6**, iDNA), and the dslDNA formation is erroneous. However, it has been suggested that there is evolutionary pressure behind its formation. *In vitro,* around 30% of capsids contain dslDNA, and mutagenesis of the genome proximal to DR2 can increase the frequency of dslDNA containing capsids (Haines and Loeb, 2007; Lee et al., 2004). These dslDNA-containing capsids can be secreted as virions, or re-imported and translocate to the nucleus in a manner comparable to authentic rcDNA, and form redundant cccDNA due to a 16bp insertion (Yang and Summers, 1998). Although it is labelled as redundant cccDNA it is still transcriptionally active, and constitutes up to 20% of the cccDNA species in woodchuck models (Yang et al., 1996). It has also been suggested that the 16bp adduct can be excised, and the redundant cccDNA can be repaired to authentic cccDNA via a homologous-recombination like mechanism (Yang and Summers, 1998). Alternatively, once in the nucleus the dslDNA can integrate into the host cell genome, and whilst this only happens in one in every 100,000-

1,000,000 infected cells they are extremely clinically significant (Summers et al., 2003; Yang and Summers, 1999).

The site of genomic integration is random and, except in the context of HCC, HBV genomes can be seen spread randomly throughout the human chromosome (Sung et al., 2012; Zhao et al., 2016). The mechanism behind integration is still not known, and it could be introduced through canonical or alternative non-homologous end joining (NHEJ) (Mladenov et al., 2016). Integration can be considered a replicative dead-end for the virus, as the linearization process affects the expression of the viral open reading frames with the exception of HBsAg. Whilst its ability to express PreS1/2 RNAs remains unchanged, the pathways regulating their expression differ (Tu et al., 2017). The integration process does not result in the loss or truncation of the coding region for polymerase, HBe or HBc Ag, but instead detaches them from their upstream promoter (Edman et al., 1980; Twist et al., 1981). There is evidence of chimeric reads containing the HBe/c coding fragments *in vitro*, but this is driven from host promoters upstream of the integration site (Lee et al., 1999).

In the natural history of HBV infection integration is associated with early infection; with integrants detected in children as young as 5 months, who were infected congenitally (Edman et al., 1980; Scotto et al., 1983; Yaginuma et al., 1987). Integrated genomes are the main source of HBsAg transcripts in the CHB liver during the HBeAg negative stage of disease, with high frequencies of HBs positive hepatocytes (Mason et al., 2016; Meier et al., 2021; Tu et al., 2017). HBsAg is a potent immune tolerogen, and can bind anti-HBs specific antibodies leading to the eventual exhaustion and depletion of HBs-specific T cells (Cornberg et al., 2017; Hadziyannis and Papatheodoridis, 2006). The first isolated integrant

was identified in samples derived from patient HCC sections, and therefore it was easy to speculate that this was the driver behind the onset of tumorigenesis (Brechot et al., 1980; Koshy et al., 1981). Whilst there is a noted enrichment in specific integration sites in HCC, such as insertion of HBV DNA into the TERT and MLL4 genes, the mechanisms behind HBV induced HCC are still not well understood (Dong et al., 2015; Jang et al., 2021; Sze et al., 2021).

Transcriptional regulation and activation

As a DNA virus, the viral genome is able to interact with host transcription factors (TFs) and despite the parsimonious nature of HBV it encodes binding motifs for many TFs. Furthermore, despite encoding its own polymerase HBV replication is dependent on host RNA polymerase II (Rall *et al.*, 1983). The viral polymerase is a reverse transcriptase, essential for the conversion of pgRNA to rcDNA genomes in the capsid. As well as binding host factors, the HBc protein binds HBV cccDNA, and association between HBc and CpG islands has been shown to mediate HBV replication (Guo et al., 2011). Whilst bioinformatic sequence analysis approaches have been widely used, the presence of the target motif does not always indicate functional activity, or guarantee TF binding. Many studies have relied on electrophoretic mobility shift assays (EMSA) to ascertain whether factors bind the viral genome, however with the constant improvement in experimental methods and HBV model systems, ChIP-PCR and ChIP-seq are now frequently employed to study this (Buckwold et al., 1997; Guerrieri et al., 2017; Pollicino et al., 2006; Raney et al., 1995; Wing et al., 2021; Zheng et al., 2004). The factors previously reported to regulate the viral promoters and enhancers are depicted in (**Figure 1.12**).

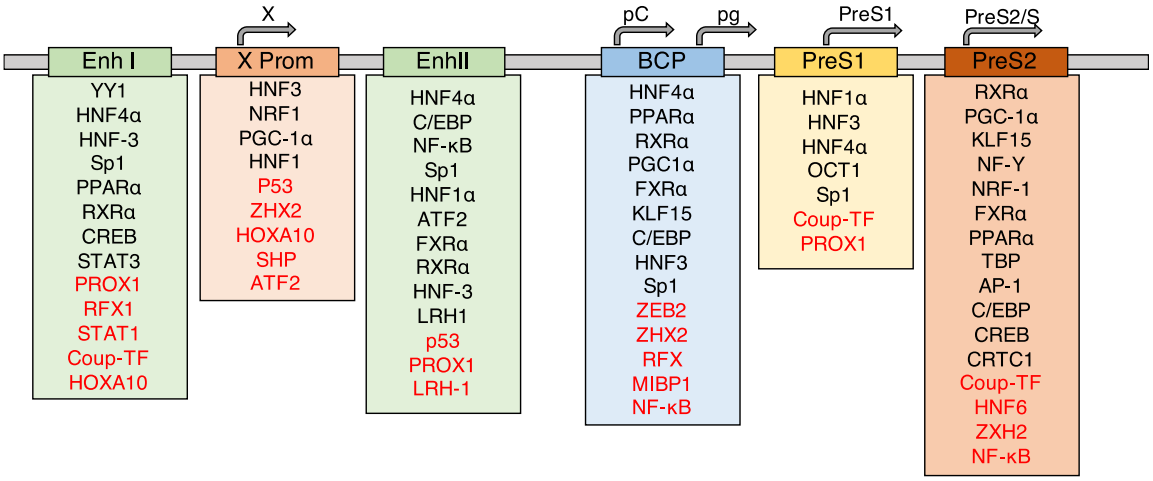


Figure 1.12: HBV transcription factors

A schematic diagram showing host TFs that have been reported as activators or repressors of HBV transcription. Factors are listed under the region of the genome where associations have been reported, and are coloured to denote their function: activators in black, and repressors in red. Cartoon adapted from (Turton et al., 2020).

The viral genome encodes four independent promoters, and 2 additional enhancer regions which regulate viral gene expression. The viral enhancers operate in a manner that is indistinguishable from eukaryotic genes, whereby they recruit transcription factors or co-activators to stimulate the activity of distal promoters. Typically, they are also decorated with activatory histone marks such as H3K4me3 and H3K27ac (reviewed in (Arnold et al., 2019)). Interestingly, in the human genome enhancers can be found thousands of nucleotides upstream of the target promoter, however HBV encodes 2 in its compact 3.2kb genome. Many studies have investigated the relationship between host transcription factors and the promoter and enhancer regions of the virus, which are explored and discussed below.

Hepatocyte specific factors

As the liver is the exclusive site for HBV replication, it is not surprising that HBV has been shown to interact with hepatic TFs to support its life cycle. As such, perhaps the most studied host TFs in the context of HBV replication are the hepatocyte nuclear factors (HNF). These are a family of liver enriched factors, with roles in metabolism, inflammation and embryogenesis, and have been implicated in the replicative life cycle of the virus (Chen et al., 2020; Odom et al., 2004; Sund et al., 2000; Wolfrum and Stoffel, 2006). HNF1α can associate with DNA through the POU domain, and interacts with the viral PreS1 promoter, although other studies have suggested that it could also bind HBx promoter, the BCP and EnhII (Li et al., 2002; Wang et al., 1998). Despite interacting with multiple regulatory elements of the genome, its role in mediating viral replication is not overly clear, as *in vivo* studies have demonstrated complete HBV replication in its absence, as well as a role for inhibition of NF-κB signalling – a pathway essential for the virus (Bar-Yishay et al., 2011; Lin et al., 2017). HNF3 is also implicated in the viral life cycle and data suggest that it may have a role in unwinding the cccDNA to allow other transcription factors to access binding elements (Cirillo et al., 2002). The protein associates with EnhI and II, as well as the PreS1 promoter (Chen et al., 1994; Li et al., 1995; Raney et al., 1995). HNF4α is another positive regulator of HBV replication, and like its other family members associates with EnhI, EnhII as well as both the BCP and PreS1 promoter (Cho et al., 2013; Long et al., 2009; Zheng et al., 2004). Previously defined experiments have silenced HNF4α using siRNA and observed noteworthy downregulation of pC/pgRNA, however due to the wide reaching roles in regulation of hepatic metabolism the cells suffered impaired glucose metabolism and growth (Babeu and Boudreau, 2014; He et al.,

2012). Interestingly, researchers have also observed elevated HNF4α expression in response to HBV infection, perhaps suggesting a virally mediated positive feedback loop whereby the virus hijacks the host to enhance its own replication (Xia et al., 2018). In contrast, HNF6 has been shown to be a negative regulator of HBV transcription; it interacts with the PreS2 promoter, and has been shown to downregulate transcripts when over expressed (Hao et al., 2015).

The Farsenoid X receptor α (FXRα) is activated by bile acids, and akin to the HNF family is a key regulator of liver metabolism and regeneration (Claudel et al., 2005; Pineda Torra et al., 2003). FXRα binds the BCP and EnhII site when in complex with the retinoid x receptor α (RXRα), eliciting a positive transcriptional response (Mouzannar et al., 2019; Ramiere et al., 2008). RXRα largely regulates transcription by interacting with other factors such as the Peroxisome Proliferator-Activated receptor α (PPARα) where it binds EnhI, BCP and S promoters (Chandra et al., 2008), but can also interact with PGC-1α and COUP-TF (Chandra et al., 2008; Kliewer et al., 1992). The Zinc Finger and Homeoboxes 2 (ZHX2) is a potent repressor of host cell transcription and a tumour suppressor, and is a negative regulator of HBV replication, restricting the activity of the BCP, X and PreS2 promoters (Kawata et al., 2003; Xu et al., 2018). The liver receptor homolog 1 (LRH-1) has roles in regulating hepatic hormone responses and development, and directly binds EnhII to activate transcription. Like many of these nuclear factors, it often works in partnership with another transcription factor in complex, and has shown a synergistic activatory capacity with HNF1 (Cai et al., 2003). The PPARα has wide reaching effects on hepatic metabolism by regulating gluconeogenesis, fatty acid and lipid metabolism (Pawlak et al., 2015), and works in partnership with the FXRα to stimulate HBV transcription through interactions

with the BCP, EnhI and PreS1 and 2 promoters (Huan et al., 1995; Raney et al., 2001). Finally, Kruppel-like factor 15 (KLF15) is associated with adipogenesis and glucose uptake, but has demonstrated binding efficiency for the BCP and PreS1 promoter (Takeuchi et al., 2016; Xu et al., 2004). It is worth noting that many of these studies identified the presence of a binding motif in promoter or enhancer regions, and gained a positive result using EMSA. However they have not mapped TF binding through ChIP-seq, and simply note an association between viral DNA and the factor of interest.

Ubiquitous transcription factors

Given the close resemblance of the viral DNA to the host chromosome, it also interacts with more generic host TFs, in addition to the previously listed specific hepatic regulators. NF-κB is a host DNA binding protein that regulates both the innate and the adaptive immune response with implications in positive and negative transcriptional regulation (Hayden et al., 2006). NF-κB signalling can be activated by oxidative stress in response to pathogens, as well as in response to DNA damage, both of which are pathways associated with HBV infection (Taniguchi and Karin, 2018). Upon induction NF-κB can bind the promoter region of inflammatory associated genes and regulate their transcription (Xiao and Ghosh, 2005). NF-κB is widely acknowledged as a negative regulator of HBV transcription, and *in vitro* studies have elucidated a feedback loop between NF-κB and HBx induced oxidative stress, with potential roles in the onset of HCC (Lim et al., 2013; Pan et al., 2011; Wilson et al., 2011). Specificity protein 1 (Sp1) is a cellular transcription factor which functions to regulate many cellular processes

such as angiogenesis and cell cycle, but has been well characterised as a key regulator of HBV transcription (Grinstein et al., 2002). Sp1 has been shown to regulate the BCP, both PreS1 and 2 promoters as well as EnhII, although this was largely achieved by using HBV DNA fragments or reporter constructs (Raney et al., 1992; Raney et al., 1990). Mutagenesis of the cognate binding motif encoded on HBV plasmids revealed a dual role for Sp1 as it resulted in decreased pC RNAs, but potentiated both S and X RNAs, thus revealing a direct regulatory role for Sp1 (Li and Ou, 2001; Quasdorff and Protzer, 2010). This suggests that Sp1 could perhaps influence transcription of PreS1/2 RNAs from integrated copies of the viral genome. Tumour protein 53 (TP53) is a fundamental cellular factor, referred to as the guardian of the genome. p53 is a potent tumour suppressor gene with roles spanning almost every cell function with critical implications in cancer and hypoxia biology (Lane, 1992; Zhou et al., 2015; Zilfou and Lowe, 2009). P53 forms a homo-tetramer to bind DNA, and has been shown to inhibit HBV transcription, particularly in reducing HBx mRNAs (Truant et al., 1995). In turn, HBx expression has been shown to alter the transcriptional activity of p53, and can upregulate other HBV positive regulators such as Sp1 as a result (Chan et al., 2016).

Nuclear Transcription factor Y (NF-Y) is a positive regulator of HBV; binding the S promotor and initiating transcription (Lu and Yen, 1996). Ordinarily, NF-Y regulates host processes such as proliferation and cell cycle, but also regulates the shuttling of proteins for efflux, perhaps a mechanistic insight into the relationship between NF-Y and HBsAg expression (Benatti et al., 2011; Yoshida et al., 2000). The role of CCAAT enhancer binding protein family (C/EBP) is not so clear cut, as it can have both positive and negative impacts on viral replication.

C/EBP regulates liver metabolism and hormone signalling but interacts with the EnhII, reportedly facilitated by interactions with HBx. C/EBP binding activity is indirectly proportional to replication, where high binding results in inhibition (Lopez-Cabrera et al., 1990; 1991; Takiguchi, 1998). However, it has been shown to positively regulate S transcription through binding the PreS1 promoter (Bock et al., 1999). Similarly, the role of the cAMP response element binding transcription factor (CREB) is not fully understood, and in different model systems has been identified to both activate and repress transcription. One study showed that CREB facilitates the binding of co-activatory proteins to the S promoters, increasing their expression, which resulted in CREB being labelled as an essential factor for replication (Kim et al., 2008). However CRTC1, which CREB recruits to the viral genome, has also been shown to inhibit HBV replication in cell culture (Tang et al., 2014). Chicken Ovalbumin Upstream Promoter Transcription Factor (COUP-TF) is also a cellular factor essential for liver hormone signalling, interacting with liver enriched transcription factors such as RXRα, and is a negative regulator of HBV replication (Butler and Parker, 1995; Fischer et al., 2006). COUP-TF binds EnhI, and represses the activity of the BCP and PreS1 promoter, resulting in a reduction of HBV RNAs (Li et al., 2016c).

Some of the host factors implicated in HBV replication have no inherent DNA binding ability, and can act as co-factors to other HBV-binding TFs. One such example of this is the small heterodimer partner (SHP). SHP can be described as an orphan receptor with roles spanning bile acid synthesis and innate immune signalling, which dimerises with HNF4α to repress HBV replication, despite the positive role of HNF4α (Hao et al., 2020; Miao et al., 2009; Oropeza et al., 2008). Viral proteins can also act as co-factors to host TFs. HBx has been

shown to complex with Transcription Factor IIB (TFIIB), and upregulate expression of all viral RNAs and activate viral replication by recruiting RNA Polymerase II (Lin et al., 1997). The Octamer binding protein (Oct1) is a positive regulator of HBV replication with the capability of interacting with HBx (Antunović et al., 1993). Oct1 has been shown to activate the PreS1 promoter and work in conjunction with HNF1 *in vitro* (Zhou and Yen, 1991). Nuclear respiratory factor 1 (NRF1) is another factor that is not essential for HBV replication, but mediates the recruitment of PGC-1α to the genome to activate transcription, as well as demonstrating binding capacity on the HBx promoter (Hossain et al., 2009; Tokusumi et al., 2004). Zinc-Finger E-Box binding homeobox 2 (ZEB2) is a cellular factor shown *in vitro* to inhibit HBV transcription in both HepAD38 and HepG2.2.15 models (He et al., 2016).

Previous studies have observed that Regulatory factor box 1 (RFX1) inhibits HBV replication. RFX1 regulates cell proliferation and the immune response, but elicits its effect on HBV through its interaction with the c-Myc associated protein MIBP1 (Stein et al., 2008). In non-hepatic cells RFX1 has no impact on the virus, suggesting that it acts a co-factor with a hepatocyte specific partner capable of interacting with the BCP and EnhI (Buckwold et al., 1997; Reith et al., 1994). Similarly, the homeobox A1 (HOXA10) is an inhibitor of HBV replication, and has been shown to bind EnhI and the X promoter in a panel of routinely used HBV model systems *in vitro* (Yang et al., 2019). HOXA10 has been implicated in perturbation of STAT mediated transcription, where STAT3 is a potent activatory factor for the virus and HOXA10 competes for binding to EnhI (Yang et al., 2019). Both STAT1 and STAT3 have roles to play in regulating HBV replication, with both factors forming part of the JAK/STAT signalling cascade and

influence the immune response through the interferon pathway (Majoros et al., 2017). STAT1 binds EnhI and X promoter regions to inhibit HBV, however HBx has evolved to antagonise its repression by preventing interferon activation (Yang et al., 2016). In contrast, STAT3 activates HBV replication through interactions with HNF3, and subsequent production of IL-6, a potent activator of HBV replication (Belloni et al., 2012; Jiang and Tang, 2010). Activator protein 1 (AP-1) is also under the regulation of the Jak signalling pathway, but can dimerise with many well characterised transcription factors such as JUN, FOS and MAF (Halazonetis et al., 1988). AP-1 is a positive regulator of HBV and is able to activate the PreS2 promoter (Lauer et al., 1994).

Prospero-related homeobox protein 1 (PROX1) is a noted regulator of circadian rhythm, a pathway known to regulate HBV replication. PROX1 forms a complex with LRH-1 to suppress the activity of EnhI/II and the PreS1 promoter (Qin et al., 2004). Previously defined experiments have also shown that PROX1 can interfere with the positive mediators HNF1α and Sp1 (Audette et al., 2016). TATA Box Protein (TBP) is a well-known ubiquitous transcription factor, and it interacts with the TATA like sequences in the PreS2 promoter to enhance replication (Bogomolski-Yahalom et al., 1997; Nikolov et al., 1996). Ying Yang 1 (YY1) has binding affinity to the CGCCATNTT motif adjacent to DR1, and was hypothesised to have a role in regulating integration events, however, it is believed that YY1 elicits its effect indirectly, and mediates alternative pathways (Belloni et al., 2012; Shang et al., 2015). Finally, Activating Transcription factor 2 (ATF2) is a cellular factor with roles in the DNA damage response. It can competitively bind with AP-1 to repress EnhI and subsequently reduce the abundance of HBx encoding viral RNAs (Bhoumik et al., 2005; Choi et al., 1997).

Epigenetic regulation

HBV replication is primarily determined by the size of the cccDNA reservoir, as despite integrated genomes being transcriptionally active, they are unable to produce new progeny genomes (Urban et al., 2010). cccDNA resembles host chromatin and its transcriptional activity is determined by epigenetic regulation such as DNA methylation and acetylation or methylation of lysine residues on host histone (Bock et al., 1994; Bock et al., 2001; Pollicino et al., 2006). Despite HBV being a small DNA virus, the mechanisms which regulate the viral epigenome are broadly applicable to other, larger DNA viruses, which are also chromatinised in the host cell such as HPV, Epstein Barr Virus (EBV) and KSHV (Favre et al., 1977; Jenkins et al., 2000; Shin et al., 2014; Stunkel and Bernard, 1999). In the case of HPV it is believed that histone modification regulates the expression of the viral RNAs temporally, controlling differential viral gene expression throughout the life cycle (del Mar Pena and Laimins, 2001; Wooldridge and Laimins, 2008). The overlapping genome of HBV, and distinct promoter driven transcription highlights the importance of understanding its epigenetic regulation when aiming to develop new anti-viral therapies.

Recent studies have characterised the HBV epigenome by performing ChIP-sequencing to study the association of HBV with specific lysine residues on histone 3 and 4 (H3, H4) (Tropberger et al., 2015). Tropberger et al. demonstrated that regions of the viral genome which are more heavily decorated with post translational modifications were a major determinant of cccDNA activity (Tropberger et al., 2015). Host transcriptional activation is largely determined by the presence of 4 different histone marks; trimethylation (me3) of H3K4 and H3K27, and acetylation (ac) of H3K27 and H3K122 (Creyghton et al., 2010;

Santos-Rosa et al., 2002; Tropberger et al., 2015; Tropberger et al., 2013). Of these, H3K4me3, H3K27ac and H3K122ac are usually found at the transcription start site (TSS), or in the enhancer region of actively transcribed host genes. H3K36me3 is also a marker of transcriptional activation although this is found in the 3' end of the gene body, and its role is not fully understood (Chantalat et al., 2011). Interestingly, the viral BCP and EnhII regions appeared to be devoid of the activatory histone marks, however the TSS for the pC/pgRNAs were rich in the expression of the 3 post translational modifications responsible for activation (Tropberger et al., 2015). Tropberger and colleagues showed that activatory histone marks outnumbered repressive marks, such as H3K9me3 which is fundamental for gene expression regulation in the host, but almost entirely undetectable on the virus (Beisel and Paro, 2011; Flecken et al., 2019; Tropberger et al., 2015).

The cellular epigenome is plastic, and gene expression patterns need to be flexible so that a cell to adapt to changes in the micro-environment such as metabolism, immune responses and oxygen; the viral epigenome is no different (Lu and Thompson, 2012). It is known that inflammation is a primary determinant of viral replication, although the pathways defining this are not well understood. Inflammation can drive epigenetic silencing of gene expression via accumulation of H3K9me3 repressive marks, perhaps regulated by NF-κB. NF-κB signalling can have wide-reaching effects, as despite regulating the silencing of some genes it can promote the transcription of others by driving histone acetylation through CBP/p300 (Villagra et al., 2010). Inhibition of histone de-acetylases (HDACs) resulted in an increase of H4ac marks on the viral genome and increased viral transcription (Gong et al., 2011). In contrast, the viral epigenome is sensitive to the

effects of interferon alpha (IFNα), as it has been shown to modulate the acetylation patterns of histone and subsequent recruitment of STAT1 and STAT2 to the cccDNA, thus repressing cccDNA driven transcription (Belloni et al., 2012). The antiviral activity of IL-6 *in vitro* was attributed to the reduced interaction between the liver specific transcription factors, HNF4α and HNF1α, and cccDNA which resulted in reduced histone acetylation and concomitant decrease in pC/pgRNA levels (Palumbo et al., 2015). Recently, studies have demonstrated that long term treatment with nucleoside analogues causes a switch to a repressive histone state. Patients under telbivudine treatment, who had low pC/pgRNA levels, showed an enrichment in H3K9me3 marks on the cccDNA, which are associated with transcriptional repression (Lebosse et al., 2020).

Histone modification is just one mechanism by which viral replication is determined. Methylation of DNA also regulates transcription, and the advent of bisulphite free sequencing methods will inevitably facilitate advances in our understanding (Liu et al., 2020c; Liu et al., 2019). At least 6 CpG (3 conventional) islands have been identified in the HBV genome, with CpG-1 located at the start of PreS1, CpG-2 spans EnhI and X-prom, and CpG-3 is found at the start codon of Pol (Zhang et al., 2013). Studies on CHB liver biopsies discovered that CpG-1 and -2 were heavily methylated, and this was associated with decreased expression of both HBs and HBe antigens (Guo et al., 2009; Vivekanandan et al., 2008a; Vivekanandan et al., 2008b). In contrast, Kim et al. did not find the same association between methylation density and HBs expression in a HBV+ cirrhotic cohort. Instead they noted that increased methylation correlated with lower virion production, subsequently lower viral load and decreased cccDNA transcriptional output (Kim et al., 2011b). Recently in collaboration with Professor Chunxiao

Song, we investigated HBV DNA methylation patterns and found that cccDNA was not methylated at early time points post *de novo* infection, whereas the integrated copies in Huh1 cells showed heavy methylation patterns especially in the CpG islands (Liu et al., 2020c). DNA methylation can also regulate the binding of CCTC-binding factor (CTCF), which is well known to regulate oncogene expression in HPV, and has recently been identified as a putative restriction factor for HBV (D'Arienzo et al., 2021a; Nanavaty et al., 2020; Paris et al., 2015; Pentland et al., 2018). This demonstrates that the viral epigenome is essential in mediating the interaction between virus and host, as well as regulating the activity of cccDNA and integrated genomes. The factors responsible for epigenetic regulation are discussed at length in *Chapter 1.3.4.*

HBV assembly and egress

Following transcription and translation of the viral RNAs to form the 7 viral proteins and the pgRNA, all of the necessary components are available to form the viral capsid, package the genome and egress from the infected hepatocyte. The encapsidation process occurs in the cytosol of infected hepatocytes and requires HBc, polymerase and the pgRNA. The icosahedral capsid is formed from either 90 or 120 homodimers of individual core molecules, and thus the synthesis of viral proteins must be tightly regulated to ensure that the ratio of HBc to Pol molecules is conducive to capsid formation (Diab et al., 2018; Patel et al., 2017; Venkatakrishnan and Zlotnick, 2016; Zheng et al., 2019). The viral polymerase interacts with the 5’ epsilon stem loop, a 60 nucleotide bulged-stem loop with a UGU sequence, of the pgRNA through its terminal peptide (TP) domain. This

forms a ribonucleoprotein complex which includes the genome that must be incorporated into the capsid for the genesis of infectious particles (Flodell et al., 2002; Li et al., 2020; Ryu et al., 2010). It is documented that the covalent bond of the 5' epsilon loop and the Pol prevents the association of the pgRNA with the ribosomes, ensuring that the genome is preserved and ready for encapsidation (Ryu et al., 2008). Whilst pC/pgRNAs are the only transcripts to encode a 5' epsilon structure, all of the transcripts, due to their overlapping nature and conserved 3' end, contain a 3' epsilon loop (Imam et al., 2018; Seeger and Mason, 2000). These loops regulate RNA stability and are the sites of epigenetic modification via one of the most prominent epitranscriptomic pathways, N6-methyladenosine (m6A) RNA methylation (Wang et al., 2014). The 5' epsilon stem loop of the pgRNA contains the packaging signal, which drives the association of the pgRNA with the viral polymerase, forming a ribonucleoprotein complex to facilitate the genesis of the rcDNA genome (Bartenschlager and Schaller, 1992). In the context of HBV, it has been demonstrated that differential methylation of the RNAs can determine their fate and whether pgRNA is translated or associates with polymerase to form the new genome (Kim et al., 2021; Kim and Siddiqui, 2021; Wang et al., 2014).

Host cell chaperone proteins are hijacked by the virus; the polymerase recruits heat shock proteins (Hsp) 90 and 40, as well as heat stress cognate 70 (Hsc70) to facilitate the encapsidation process, with RNA-binding motif protein (RBM24) involved in the final stage (Hu and Seeger, 1996; Prange et al., 1999). Pol is essential for the conversion of pgRNA to rcDNA, the stable form of the viral genome. Pol initiates reverse transcription by using itself as a protein primer and the 5' epsilon loop as a template (Jones et al., 2012). It is during the process of

DNA synthesis that the capsid matures. It is believed that successful RT and formation of rcDNA alters the turgidity of the nucleocapsid and this serves as the signal for envelopment with the surface antigens (Tzlil et al., 2003). The viral surface antigens are translated from preS1/S2 mRNAs, and are integrated into the membrane of the endoplasmic reticulum (ER), which is regulated by the first and second transmembrane domain of S (Eble et al., 1987; Wounderlich and Bruss, 1996)). The large surface antigen is post-translationally translocated to the lumen of the ER, where the first transmembrane domain anchors the protein to the ER membrane. This looping allows the capsid interaction site to be presented in the cytosol, whereby the small and large glycoproteins can associate with the capsid, and envelope the virion (Bruss, 1997; Poisson et al., 1997). Finally, the virion is able to bud with the host membrane once the envelope proteins have associated with the particle. It is, however, essential to note that not all particles are signalled to egress, and some rcDNA containing particles are re-imported to the nucleus whereby the genome is released and used to amplify the nuclear cccDNA reservoir (Lythgoe et al., 2021; Urban et al., 2010).

Many of the early studies on the capsid recycling mechanisms used duck-HBV, where this process occurs much more frequently. Nonetheless, capsid reimport is essential to sustain cccDNA transcription and persistent infection (Kock et al., 2010; Wu et al., 1990). The secretion of complete virions is dependent on the cellular multivesicular body-associated endosomal sorting complex required for transport (ESCRT), a multi-protein complex involving gamma-2-adaptin, CHMP3/4, Vsp4, Nedd4 and α-taxilin (Lambert et al., 2007; Stieler and Prange, 2014). Lambert et al. suggested that the virions leave the cell via an exosomal pathway, which was in agreement with earlier observations that outbound particles

associate with the membranes of late stage endosomes (Lambert *et al.*, 2007; Roingeard and Sureau, 1998).

This process is by no means error free, and frequently the capsid can form without packaging the genome, thus ‘empty’ or genome-free particles can be secreted from the cells (**Figure 1.13**) (Luckenbaugh et al., 2015; Ning et al., 2011). Their true function remains unclear, however they may have a role in antagonising the host immune response. Despite their recent discovery, these particles are not rare, and can be found to outnumber complete virions, known as Dane particles, in a ratio of 100:1. Equally, it is possible that the polymerase does not covalently bind the pgRNA 5’ epsilon stem loop, and as such only pgRNA is packaged into the virion, although these are a minor sub-species of viral particles and Dane particles outnumber these in a range of 1,000:1 (Rokuhara et al., 2006; van Bommel et al., 2015; Wang et al., 2016). Other subviral particles (SVP) exist which do not contain any genetic material, and are either spherical or filamentous and consist almost entirely of the viral glycoproteins. Notably, these HBs-containing SVPs are abundant in the blood of CHB patients and allowed the field to discover HBV before the characterisation of the viral genome (Blumberg, 1977; Movsisyan et al., 2016). The spherical SVPs largely consist of HBs-S glycoprotein and leave the cell through the host endoplasmic reticulum secretory pathway, whereas the filamentous SVPs also contain the large epitope and rely on the same ESCRT-dependent egress pathway as authentic particles. Interestingly, SVPs which do not contain genome leave cells via an alternative route that is independent of ESCRT, but instead use the host factors Alix and HGS for egress (Jiang et al., 2015; Patient et al., 2009; Patient et al., 2007; Watanabe et al., 2007). The HBs-rich SVPs are of high clinical significance and the persistent

expression of HBs is responsible for the continuous stimulation of HBs-specific antibodies and T-cells, and their subsequent exhaustion and depletion (Ye et al., 2015).

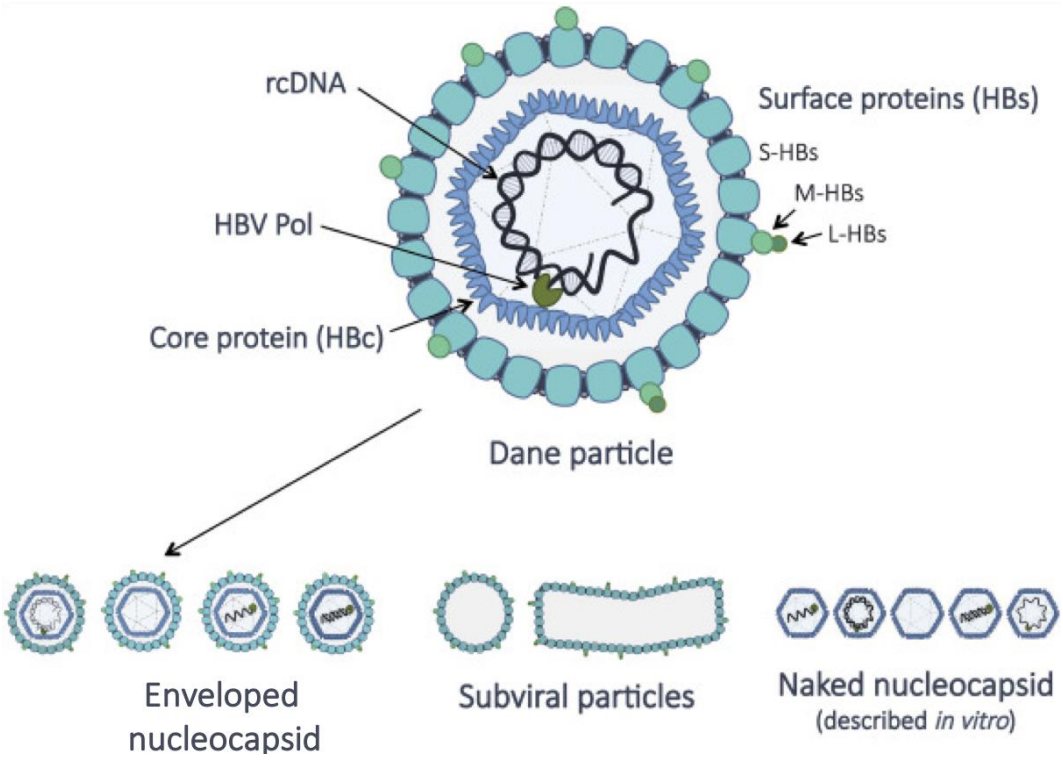


Figure 1.13: HBV particles

A cartoon to show a competent Dane particle (top), compared with alternative SVPs. Figure taken from (Tsukuda and Watashi, 2020).

There is also evidence to suggest that not only viral proteins are packaged into the virion, as host restriction factors APOBEC3G and DDX3 have been found in the viral nucleocapsid (Nguyen and Hu, 2008; Wang et al., 2009). APOBEC3G is a member of the apolipoprotein B mRNA editing enzyme catalytic polypeptide-like (APOBEC), which is well known to be a potent RNA editing enzyme. APOBECs have implications in infectious disease and cancer, as they are capable of inducing genomic instability through cytidine deamination, the process of C>U transitional changes in RNA (Vieira and Soares, 2013; Wang et al., 2009). APOBEC3 members have been studied in the context of HBV and are believed to restrict the virus by inducing hypermutation in the rcDNA genome, and therefore rendering the cccDNA functionally impaired (Kock and Blum, 2008). This is not dissimilar from the way in which APOBECs work as a restriction factor against HIV-1, where cytidine deamination also occurs in the nucleocapsid (Sheehy et al., 2002). Other studies have also identified that APOBEC3 family members are capable of acting on the cccDNA to induce mutations that lead to subsequent degradation (Lucifora et al., 2014).

1.2.8: HBV model systems

in vitro

Producer cell lines

HBV 'producer cell' lines were developed in order to circumvent the requirement to deliver the viral genome by *de novo* infection or lipid transfection. The first example of these was engineered in 1987, when a tandem repeat of 2 copies of the viral genome was integrated into the genome of a HepG2 cell, resulting in the commonly used HepG2.2.15 line (Sells et al., 1987). Ordinarily,

linearization of the genome would cause the 3.5kb pC/pg RNA reading frame to be incomplete, however the tandem repeat completes the reading frame and allows for constitutive expression of all major viral RNAs and antigen production (D'Arienzo et al., 2021b; Sells et al., 1988). Due to the intracellular recycling pathway, HepG2.2.15 cells will also transcribe viral RNAs from authentic cccDNA in addition to the integrated genomes. Similarly, the routinely used HepAD38 cells were developed in 1997 to generate an inducible HBV producer line. In these cells, viral gene expression is driven from a 1.1 times overlength HBV genome which is regulated by a tetracycline inducible CMV promoter (Ladner et al., 1997). Compared with the HepG2.2.15 models, the HepAD38 cells exhibit more robust virion production, as well as increased levels of cccDNA (Ladner et al., 1997; Sun and Nassal, 2006). The second generation of HepAD38, known as HepDE19, cells were developed where the 5'-ATG site of the 1.1x genome was mutated, such that HBeAg can only be expressed from re-imported cccDNA, providing a system to study cccDNA genesis and transcription (Cai et al., 2012; Guo et al., 2007).

As these producer cell lines were engineered in a HepG2 hepatoma cell background, their application to studying HCC is limited, but their immortalised nature means that they can be cultured for long periods (Xu et al., 2021). This makes them well suited to the production of viral stocks, testing anti-viral agents and compounds, and also in co-culture systems to assess the effects of viral-specific immune-cells on HBV replication (Ding et al., 2008; Li et al., 2007b; Liu et al., 2015). Whilst these all allow for the production of infectious viral particles, and provide a useful tool for studying viral transcription and protein synthesis, they do

not model the early stages in the viral life cycle as entry and cccDNA formation is bypassed (Chakraborty et al., 2020; D'Arienzo et al., 2021b; Ko et al., 2018).

More recently, given the importance of cccDNA in the viral life cycle, a producer cell line that supports HBV replication from episomal DNA in the absence of viral integrants was developed. The HepG2-pEpi cells express a HBV1.3 genome encoded in a vector which is resistant to integration, and under geneticin selection (Lucifora et al., 2014). These HepG2-pEpi cells have been used to assess host transcription factor binding in the context of circadian control, CTCF regulation and hypoxic signalling in HBV in chromatin immunoprecipitation assays (D'Arienzo et al., 2021a; Wing et al., 2021; Zhuang et al., 2021).

HBV DNA constructs

Until the discovery of NTCP as the essential receptor for HBV entry, *de novo* infection of cells *in vitro* was challenging. In order to bypass the inefficient and rate limiting stages of cccDNA genesis, overlength HBV genomes can be delivered by lipid transfection (Chakraborty et al., 2020). Human hepatoma cell lines such as HepG2 and Huh7 cells are easy to transfect, and the advent of high efficiency reagents for cell culture made this an ideal model system to study post-entry events in the life cycle (Li et al., 2013a; Lim et al., 2021; Sozzi et al., 2018; Sozzi et al., 2016). In order to complete the ORF for the pC and pg RNAs the viral genome must be overlength, and plasmid constructs generally encode either a 1.1- or a 1.3- times linear genome (**Figure 1.14**) (He et al., 2016; Li et al., 2016b; Sun et al., 2020). Transfection allows for the delivery of high quantities of HBV DNA into the cells, and replication is driven from authentic viral promoters through

interactions with host transcription factors. However, as this circumvents entry events, non-hepatic cell lines are also capable of supporting replication from these constructs, and studies have used easily transfectable cells such as HEK293Ts to study replication (Yang et al., 2020; Zhou et al., 2021). Whilst transfection efficiency and gene expression may be high in these alternative systems, data must be analysed with caution due to their non-hepatic nature, and their expression of hepatocyte specific factors will be low and limiting (Junker et al., 1987; Tang and McLachlan, 2001; Yang et al., 2020). It would also be interesting to consider the application of these constructs to study epigenetic regulation of viral gene expression, as the non-viral plasmid backbone is likely to impact chromatinization and association with host histone (Kamiya et al., 2013; Riu et al., 2007).

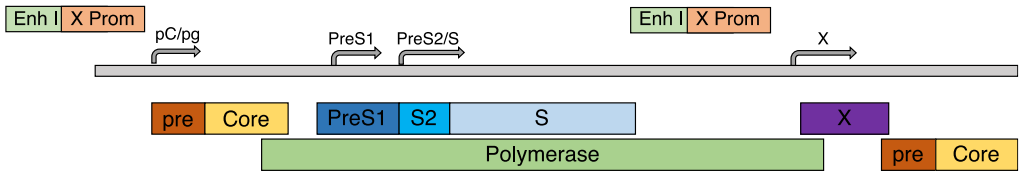


Figure 1.14: HBV1.3 genome

A cartoon to show the genome structure of a 1.3-times overlength HBV construct.

Even since the discovery of NTCP as the fundamental receptor for HBV entry, lipid transfection has not been entirely replaced by *de novo* infection systems, and many studies are reliant on HBV1.3 constructs to assess HBV gene expression (Lim et al., 2021; Sozzi et al., 2018). Adenoviral-vectors encoding a HBV1.3 genome (Ad-HBV-GFP) have also been developed to allow the efficient delivery of highly transcriptionally active HBV DNA into cells (Huang et al., 2012b). This system again uses an overlength HBV genome, expressed from an adenovirus engineered to encode a GFP reporter (Huang et al., 2012b). The virus is produced from transfection of non-hepatic cells such as HEK293Ts, and encapsidated Ad-HBV-GFP constructs are harvested from the extra-cellular media (Wing et al., 2019).

In order to bypass particle entry and maintain high levels of DNA input whilst maintaining an exclusively viral backbone, HBV-minicircles (mcHBV) were developed. This technology utilises a circularised HBV1.0 construct which is delivered into the cells by lipid transfection, and viral replication is driven from authentic viral promoters (Guo et al., 2016; Li et al., 2016a). Due to the circular nature of the mcHBV it is not dissimilar from a plasmid transfection, however it does not require an overlength genome to complete all of the ORFs to transcribe all of the major RNAs (D'Arienzo et al., 2021a; Yan et al., 2017). These constructs enabled the introduction of reporter constructs, such as gaussia luciferase, into the mcHBV which are under the control of authentic promoters (Murphy et al., 2016). This results in cheaper and quicker experimental read outs for promoter activity, rather than relying on labour intensive RNA extraction and qPCR analysis.

HBV promoter constructs are widely used in HBV *in vitro* studies, where a reporter gene such as renilla, firefly or gaussia luciferase are under the

transcriptional regulation of a viral promoter or enhancer region. These are quick assays that rely on transfection of the construct into hepatoma cell lines, and can be used to assess the impact of any given condition on promoter activity. As previously noted, these assays have their limitations in that they are not authentic infection systems and carry a large amount of non-viral DNA in their backbone, but they are quick, cheap and informative assays to perform (Wing et al., 2021; Zhuang et al., 2021).

de novo infection

Whilst there are many other model and reporter systems available to study HBV *in vitro,* the *de novo* infection of hepatocytes remains the gold standard method for studying HBV. HepG2.2.15 or HepAD38 cells are used to produce infectious virus, which can either be concentrated via precipitation in polyethylamine glycol (PEG), or selectively purified using a heparin column (Ko et al., 2018; Wettengel et al., 2021). There are several options for cell lines to be used, all of which support HBV infection and the full viral life cycle, however they also all have their limitations and caveats.

Primary human hepatocytes (PHH) arguably represent the most physiologically representative culture system, showing infection efficiency as high as 90% as well as supporting infection from HBV+ patient sera (Galle et al., 1994; Ortega-Prieto et al., 2018; Schulze-Bergkamen et al., 2003; Winer et al., 2017). They express NTCP and all of the required hepatocyte-specific factors to support high level viral replication, however, due to their finite nature they are expensive and show high levels of donor-variability (Konig et al., 2014; Zeilinger et al., 2016). As primary cells they require a cocktail of growth factors and additives to the

culture media to maintain their differentiated status, but previous reports have noted that PHH retro-differentiate *in vitro*, which limits their application in long term culture systems (Elaut et al., 2006; Heslop et al., 2017).

One alternative to primary human hepatocytes are HepaRG cells, a bi-potent liver progenitor stem cell capable of differentiating into either hepatocytes or biliary epithelial cells. As such, they preserve the functional properties of hepatocytes and support the entire HBV life cycle (Antherieu et al., 2010; Gripon et al., 2002; Ni and Urban, 2017). They are challenging to culture, and require strictly regulated conditions for differentiation over a 4 week period. Once differentiated into hepatocytes and epithelial cells they support around 25% infection efficiency, which is notably lower than PHHs and comparable to more simple human hepatoma lines (reviewed in (Witt-Kehati et al., 2016)). Perhaps the most wide spread and accessible model system are hepatoma cell lines engineered to express NTCP. HepG2 cells are a prime example of this, and many clonal lines are routinely used across the HBV research community. These cells offer easy and simple handling, without the requirement for complicated culture conditions and expression of NTCP facilitates HBV entry and allows for completion of the viral life cycle (Yan et al., 2013; Yan et al., 2012). However they are largely recalcitrant to patient derived sera, and require high titre virus to establish infection (Xu et al., 2021). There is limited evidence for viral spread, and infection efficiency is comparatively lower, up to around 50% (Iwamoto et al., 2014). In order to improve the efficiency of infection, HepG2 cells are differentiated with dimethyl-sulfoxide (DMSO) in the culture media, which also arrests cell cycle in order to maintain the cccDNA reservoir (Paran et al., 2001).

More recently, reporter viruses have been developed to facilitate quicker and lower cost assays to measure HBV replication. Previous studies used a HBV genome engineered to express a reporter gene, such as green or red fluorescent proteins or secreted gaussia luciferase, in place of the viral polymerase (Protzer et al., 1999; Untergasser et al., 2006). These viruses undergo a single cycle of replication, in that they enter cells via NTCP and form cccDNA but as they lack the polymerase they cannot convert pgRNA to rcDNA. This means they are excellent systems to study cccDNA formation and viral transcription, but their applications to study particle genesis or egress are limited.

in vivo

The development of suitable mouse models for HBV replication has improved our understanding of the replicative life cycle and there are now several models to study post entry events. The HBV transgenic mice (HBVtg) have been widely used to study viral replication *in vivo.* The first versions of HBVtg did not encode the full viral genome, but encoded the ORFs to express HBs , HBc, HBe and HBx Ag, and provided a useful tool to study the immune response, antiviral agents and HCC development (Chisari et al., 1985; Guidotti et al., 1994; Kim et al., 1991; Milich et al., 1990). However, this meant they could not be used to study replication *per se*, until eventually an overlength HBV1.3 genome was introduced as integrant into the mouse chromosome (Guidotti et al., 1995; Ortega-Prieto et al., 2019). As previously discussed the overlength genome allows for the transcription of all viral RNAs and these animals showed robust production of viral antigens and infectious viral particles (Li et al., 2013a; Luo et al., 2020). However,

all viral gene expression occurs from the integrated transgene and not authentic cccDNA. Despite this, this model offers an *in vivo* approach for screening pharmacological agents, and also allows for the delivery of siRNAs to transiently silence factors and assess their role in the viral lifecycle (Ebert et al., 2011; Wing et al., 2021).

As previously discussed, murine hepatocytes are not capable of supporting cccDNA formation even when engineered to overexpress NTCP. As such, it was important to establish a mouse model that would support the complete life cycle including cccDNA formation (Allweiss and Dandri, 2016; Scheer and Wilson, 2016). The humanised liver chimeric mice represent the state-of-the-art method for studying HBV *in vivo*. These mice are immunodeficient, with no adaptive immune system and are fumarylacetoacetate negative (*Fah -/-*), NOD *rag1*$^{-/-}$*, il2ry*$^{-/-}$, and referred to as FNRG-NOD mice (Wolff, 1997; Yang et al., 2002). As a result, these mice can develop chimeric livers where human hepatocytes are delivered via intra-splenic injection and proliferate in the murine liver (reviewed in (Ortega-Prieto et al., 2019)). Whilst there is a large percentage of murine hepatocytes and exclusively murine parenchyma, the human hepatocytes are distributed throughout the organ. As the endogenous murine cells are recalcitrant to HBV due to the absence of NTCP, when these animals are infected only the engrafted human hepatocytes support HBV entry and cccDNA genesis (Cui et al., 2015). Alternatively, liver chimeric mice have also been generated in a Alb-urokinase type plasminogen activator (uPA) knockout line, and whilst the genetic background is different, their functionality remains largely unchanged (Dandri et al., 2001). These mice have been widely used to study the efficacy of anti-viral agents, and more recently for the study of transcription factor binding in the

context of circadian and hypoxic regulation of HBV transcription (Bissig et al., 2010; Wing et al., 2021; Zhuang et al., 2021).

Aside from laboratory and cell culture models, both woodchuck and duck strains of HBV (WHV and DHBV respectively) have been reported (**Table 1.6**). They provide attractive models for testing antiviral agents and vaccine candidates as the animals are immuno-competent and support cccDNA formation (Cote et al., 2000; Mason, 2015; Menne and Cote, 2007; Roggendorf et al., 2007; Schultz et al., 2004; Wang et al., 2011). WHV shares many steps in its replicative life cycle with HBV and infected animals display high incidence of chronic hepatitis and HCC (Guo et al., 2018; Summers et al., 1978). In contrast, DHBV shows diverse replication between duck species and methods of inoculation (Guo et al., 2018). These animal models have their limitations in that they are not entirely representative of human HBV, for example, DHBV cccDNA levels remain unchanged following either ETV treatment or resolution of infection ((Reaiche et al., 2010), reviewed in (Guo et al., 2018)).

	 HBV-transgenic mouse	 Liver-chimeric mouse	 Duck	 Woodchuck	 Human
HBV entry	No	Yes	DHBV only	WHBV only	Yes
cccDNA formation	No	Yes	Yes	Yes	Yes
Dane particle secretion	Yes	Yes	Yes	Yes	Yes
Cure?	No	Yes	Yes	Yes	Yes
Susceptible to patient isolates	No	Yes	No	No	Yes
Type of infection	Chronic	Chronic	Chronic	Chronic	Acute/chronic
Immune responses	No	No	Yes	Yes	Yes
Host background	Mouse	Human	Duck	Woodchuck	Human
Reagent availability	Excellent	Excellent	Poor	Poor	Excellent
Ease of use	Easy	Advanced	Easy	Easy	N/A

Table 1.6: HBV *in vivo* systems

A table to summarise the main properties of a panel of *in vivo* methods to study the HBV life cycle. Table adapted from (Ortega-Prieto et al., 2019).

1.3: The cellular response to hypoxia

Throughout the course of human evolution, cells have evolved to survive by adapting to subtleties in the microenvironment such as changes in pH, infection by a micro-organism, and the presence of oxygen. Oxygen is essential for life itself, and cells must be able to rapidly respond to changes in oxygen availability to maintain oxidative metabolism and tissue homeostasis (Walmsley et al., 2004). The term hypoxia itself can be somewhat confusing, as clinically this refers to a state of oxygen deprivation on a systemic level, usually as a consequence of hypoxaemia - reduced oxygen saturation of haemoglobin. As such, hypoxia can be observed on an organism level, such as when experiencing reduced oxygen in high altitude environments (for reviews see (Kenneth and Rocha, 2008; Rocha, 2007)). For the purposes of this study the term 'hypoxia' is used to describe a state in which oxygen is limited, either through reduced blood supply or increased metabolic demands, to maintain homeostasis (Kaelin and Ratcliffe, 2008; Sarkar et al., 2017). This can be observed on an organ, tissue or cellular level and can also be referred to as local oxygen, whereby the arterial blood supply to each organ is specific, and the 3D structure and microarchitecture of the tissue will also influence the precise oxygen and nutrient delivery on a cell by cell basis (**Figure 1.15**) (Carreau et al., 2011). This is particularly relevant in the context of the liver where, as we have discussed in C*hapter 1.1.1*, the blood supply, sinusoid structure and cell arrangement facilitates the formation of an oxygen gradient (Halpern et al., 2017; Kietzmann, 2017; Wilson et al., 2014b). The importance of cellular oxygen sensing cannot be understated and in acknowledgement of the magnitude of the research carried out Sir Peter Ratcliffe, Greg L. Semenza and William Kaelin were awarded the 2019 Nobel Prize in Physiology or Medicine

(Oxygen Sensing: After the Nobel, 2020). The main focus of their work was identifying a role for, and the mechanism behind the regulation of, hypoxia inducible factor (HIF). HIF is considered to be the master regulator of the cellular response to hypoxia and will be discussed in detail in *Chapter 1.3.2*.

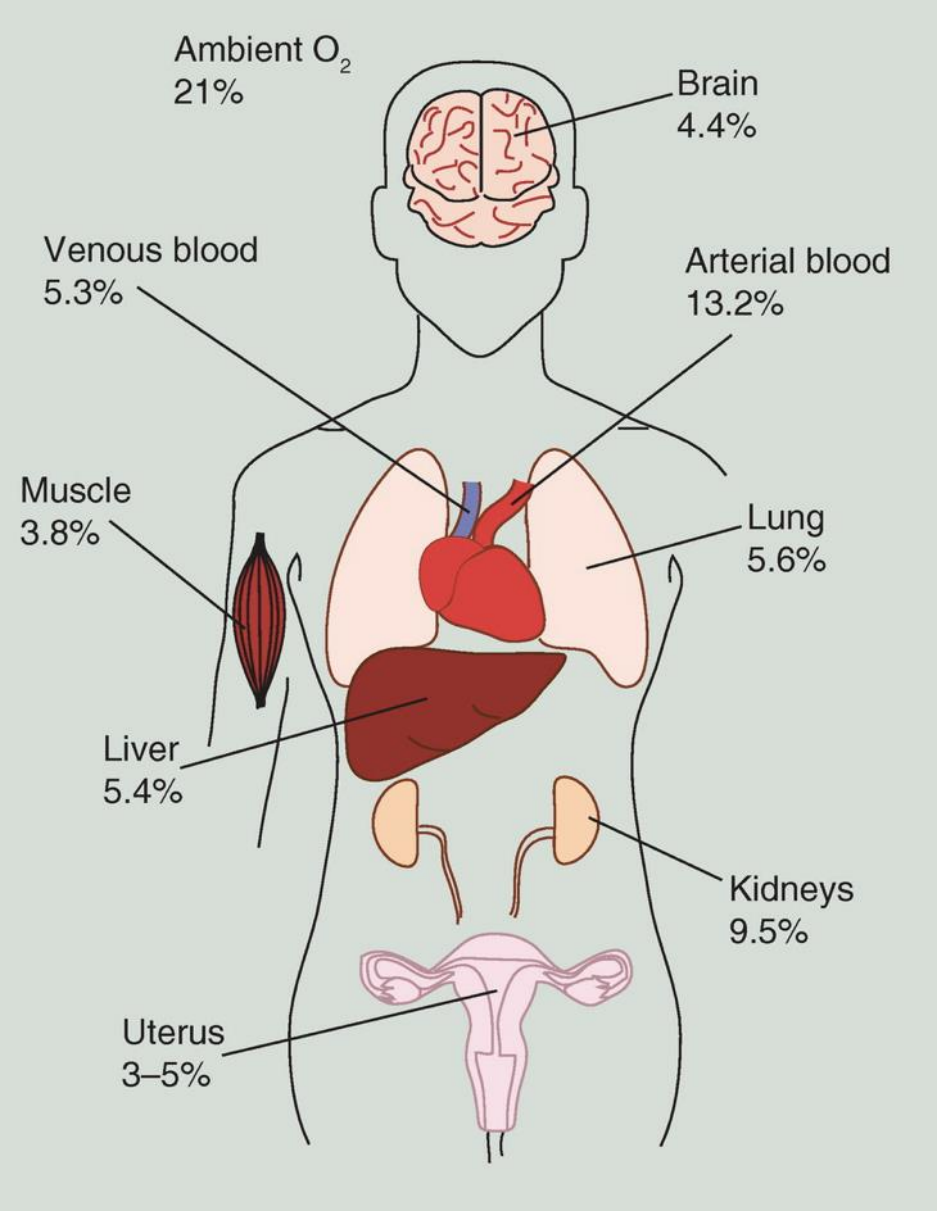


Figure 1.15: Oxygen tension in human organs

A figure to show the relative oxygen tension in different organs of the body. Figure taken from (Hancock et al., 2015).

Whilst it is now understood that hypoxia signalling regulates many host pathways, the importance of the cellular oxygen response was first realised in the context of erythropoiesis, and that erythropoietin (EPO) was hypoxic regulated (Ratcliffe et al., 1990; Semenza et al., 1991). This seminal work was the basis of the aforementioned Nobel Prize award. Hypoxia is a key regulator of tissue growth, whereby many angiogenic genes such as vascular endothelial growth factor (VEGF) are upregulated in response to decreased oxygen availability, in order to increase the development of new blood vessels proportionally to increased cell numbers (Kindrick and Mole, 2020). Oxygen is a major determinant of cellular metabolism where cells must reduce mitochondrial oxygen consumption and lower rates of oxidative phosphorylation, and reduce their oxygen independent ATP producing pathways. Hypoxia upregulates the expression of many of the genes required for glycolysis, such as the glucose transporters and hexokinase (Goda and Kanai, 2012).

The tri-carboxylic acid (TCA) cycle is also fundamental in the genesis of 2-oxoglutarate (2-OG), which is an essential co-factor for many oxygen sensitive transcriptional regulators which are discussed at length below. The degree of hypoxia, determined by oxygen tension and duration of exposure, is a major determinant of the shift in metabolism whereby many genes involved in glycolysis are upregulated in acute hypoxia, and ATP genesis and fatty-acid desaturation are both inhibited in low oxygen conditions (Eales et al., 2016). Similarly, there are explicit links between hypoxia, the immune response and immune cell function whereby increased metabolic demands in areas of infection or inflammation drive a decrease in local oxygen availability, altering gene expression profiles of the neighbouring cells and infiltrating immune cells (Taylor and Colgan, 2017).

Hypoxia is also a hallmark of a diverse range of cancer types, where it is believed to be the driver of a necrotic core of many solid tumours (Leek et al., 1999; Wykoff et al., 2001). HCC is no exception, and due to abnormal vasculature development and uncontrolled cell proliferation, hypoxia is a common phenotype in the intra-tumour regions of patients with HCC (Chen and Lou, 2017; Jain, 2005). As with other tumour types, such as melanoma and breast cancer, hypoxia contributes to several biological processes in HCC, and is believed to drive a more aggressive tumour and may even contribute to the resistance to chemo- and immuno-therapy (Chouaib et al., 2017; Crowder et al., 2014; Dratkiewicz et al., 2021; Kasper et al., 2005).

1.3.1: 2-Oxoglutarate dependent dioxygenases

Transcriptional responses to hypoxia must be dynamic and adjustable, and therefore a super-family of enzymes known as the 2-oxoglutarate dependent dioxygenases (2-OGDDs) have evolved to regulate gene expression at every level to allow cells to respond to hypoxia (**Figure 1.16** and **Figure 1.17**) (Losman et al., 2020; Nakashima et al., 2021). The 2-OGDDs are a family of between 60 and 80 enzymes which require iron, the TCA intermediate 2-OG, and molecular oxygen to function, and thus sit at the interface between oxygen sensing, metabolism and epigenetic modification (Schofield and Zhang, 1999). This superfamily are phylogenetically related, but each have distinct roles and specific molecular targets and substrates to facilitate their function. These enzymes are responsible for regulating the expression of genes essential for cellular adaptation to and survival in hypoxia, and as such many can be considered as oxygen sensors.

Whilst all of these enzymes require molecular oxygen to function, the signalling cascade and interplay is governed by their unique K_m values for O_2. This means that whilst some enzymes may lose function in moderate oxygen tensions, others are capable of operating in almost anoxic conditions (Hancock et al., 2015). The family can broadly be divided into 6 functional subsets, the collagen hydroxylases, the nucleic acid hydroxylases and demethylases, the protein hydroxylases, the histone lysine demethylases, small-molecule hydroxylases, and the prolyl hydroxylases (Johansson et al., 2014).

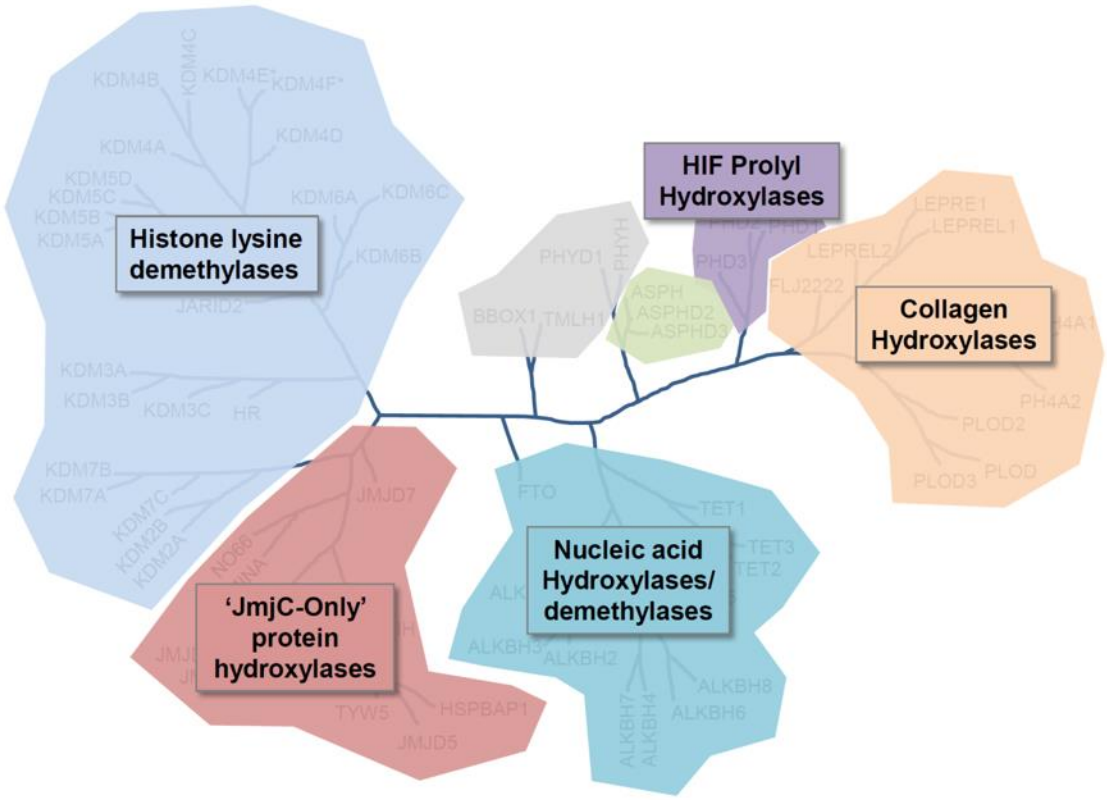


Figure 1.16: 2-Oxoglutarate dependent dioxygenases

A phylogenetic tree of the closely related 2-oxoglutarate dependent dioxygenases, grouped into their sub-families based on molecular function. *Figure courtesy of Dr Mathew Coleman, University of Birmingham.*

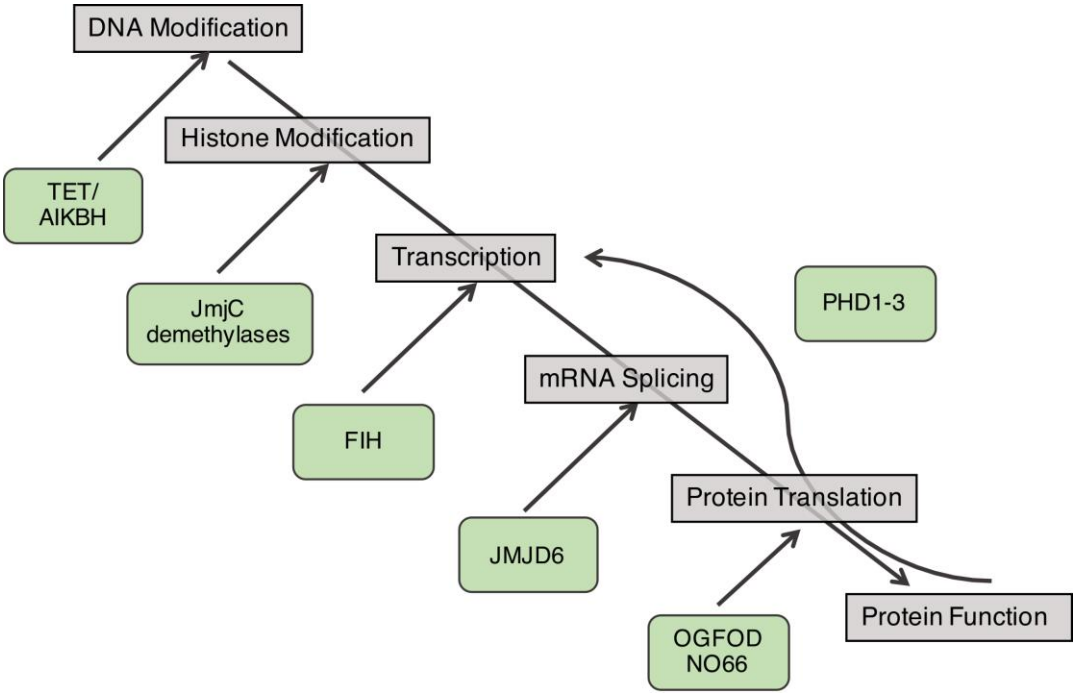


Figure 1.17: 2-Oxoglutarate dependent dioxygenase functions

A schematic diagram to show the regulatory capacity of the 2-OGDDs. *Adapted from a figure presented by Professor Chris Pugh, University of Oxford.*

1.3.2: Prolyl hydroxylases and HIF signalling

Perhaps the best studied aspect of the hypoxia signalling pathway is the activity of HIF-1α, which is a cellular transcription factor under the control of the 2-OG dependent prolyl hydroxylases (PHDs). There are 3 PHD enzymes, referred to as PHD1, 2 and 3, or alternatively EGLN2, 1, and 3 respectively (Epstein et al., 2001). They regulate HIF-1α stability through post translational hydroxylation of specific proline residues, p402 and p564, in the LXXLAP motif of the oxygen dependent degradation domain of the protein (Masson et al., 2001). HIF-1α is constitutively expressed at the RNA transcript level, and shows little evidence of hypoxia mediated differential transcription. They are continuously translated and degraded with a half-life of around 5 minutes, but their post translational modification by PHDs is highly oxygen sensitive (Kallio et al., 1997; Salceda and Caro, 1997). When oxygen is abundant, PHDs hydroxylate HIF-1α subunits and recruit the von Hippel-Lindau (VHL) E3 ubiquitin ligase complex which ubiquitinates HIF-1α and targets it for degradation at the proteasome (**Figure 1.18**) (Ivan et al., 2001; Jaakkola et al., 2001). In contrast, when oxygen is limited, PHD activity is perturbed and HIF-1α subunits remain un-hydroxylated and escape VHL-mediated degradation. As the PHDs require molecular oxygen to function they can act as an intracellular oxygen sensing mechanism providing a direct link between oxygen availability and HIF stabilisation (Schofield and Ratcliffe, 2004). As is the case with all the 2-OGDDs their absolute requirement for molecular oxygen is the foundation of the sensing mechanism of this superfamily of enzymes, and the K_m for each factor determines the severity of hypoxia the enzyme can tolerate and still retain function. As such, biochemical and *in vitro* assays have been performed to study the K_m of these factors to investigate the

precise sequence of events as oxygen tension declines. The PHDs have a relatively high $K_m(O_2)$ 250 μM, or around 8% oxygen, although this is tissue and cell type specific (Ehrismann et al., 2007; Hirsila et al., 2003; Kietzmann, 2017). This is much higher than many of the other 2-OGDDs, such as the histone lysine demethylases, or the collagen hydroxylases meaning that they are amongst the first members of the 2-OGDD family to be inhibited under hypoxia (reviewed in (Kindrick and Mole, 2020)). As a result, HIFs can be stabilised long before many of the oxygen sensitive epigenetic modifications occur. HIF-α subunits are members of the basic helix-loop-helix (bHLH) superfamily of transcription factors, which dimerise via the HLH domain to act as a transcriptional complex and bind DNA (Semenza, 2001b). It is worth noting that several of these factors are fundamental for the host circadian rhythm, which has recently been implicated in the regulation of HBV (**Table 1.7**) (Zhuang et al., 2021). The HIF-α subunits are capable of dimerising with the bHLH-PAS containing subunits, where the PAS denotes an auxiliary dimerization interface named after the first 3 proteins discovered to encode this domain, PER, ARNT and SIM (Crews and Fan, 1999). The dimers must be composed of both a class I and a class II subunit. Class I subunits are the aryl hydrocarbon receptor nuclear translocator 1 (ARNT1) which is also known as HIF-1β, ARNT2, ARNT3 (or BMAL1) or MOP9. The class II subunits are HIF-1α, HIF-2α (EPAS1), HIF-3α, the aryl hydrocarbon receptor (AhR), CLOCK, NPAS1-2 and SIM1-2 (Hogenesch et al., 2000; Semenza, 2000). HIF-1β is constitutively expressed and is considered as the universal subunit for hypoxia signalling as it is the dimerization partner of all of the HIFα isoforms (Semenza, 2001a).

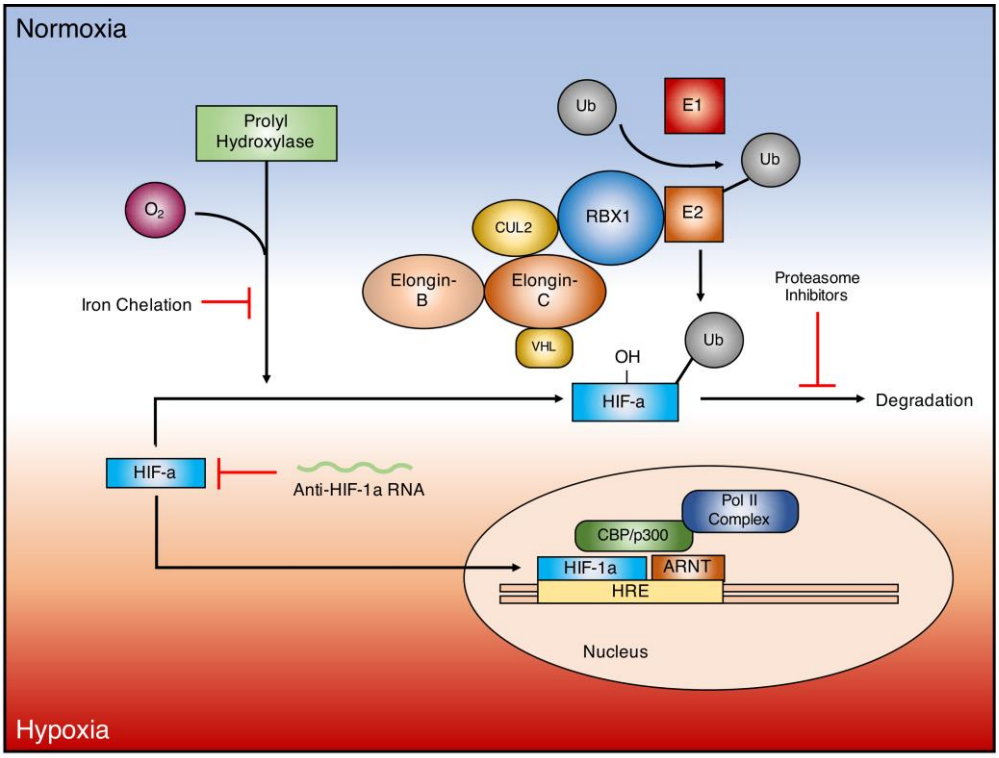


Figure 1.18: HIF-PHD signalling axis

A cartoon to show the HIF-PHD signalling axis, and the regulation of HIF stabilisation in hypoxia. Figure adapted from (Harris, 2002).

Group A	Group B	Group C	Group D	Group E	Group F
MyoD	MAX	AhR	EMC	HEY1	EBF1
Myf5	C-Myc	BMAL-1		HEY2	
Beta2/NeuroD1	N-Myc	CLOCK			
Tal1	TCF4	HIF			
Neurogenins		NPAS1			
		NPAS3			
		MOP5			

Table 1.7: bHLH transcription factors

A table showing members and classification of the bHLH transcription factor family. Examples taken from (Ledent et al., 2002).

When oxygen is limited, stable HIFα subunits translocate to the nucleus where they dimerise with HIF-1β, and bind to host DNA at well-defined RCGTGC motifs, known as a Hypoxic Response Elements (HRE) (Wenger et al., 2005). The HIF- α/β heterodimer recruits the CBP/p300 complex as a co-activator and associates with RNA Pol II to drive transcription of essential genes (**Figure 1.18**) (Arany et al., 1996). The HRE motif is usually found in the promoter or enhancer region of responsive genes, and is present in great abundance in the human genome, occurring more than 1,000,000 times (Kindrick and Mole, 2020; Roche et al., 2016), however far fewer functionally active HREs have been identified *in vitro* (Dmitriev and Papkovsky, 2015). The genes regulated by HIF are wide spread, and hypoxia is implicated in regulating a plethora of host cell processes (**Figure 1.19**). The presence of the motif alone is not sufficient to determine a gene as a HIF target gene; the cellular epigenome will regulate the DNA accessibility and in turn control HIF activity, which goes someway in defining the cell type specific nature of the hypoxic transcriptome (Encode Project Consortium, 2012). Hypoxic regulation of epigenetic modification and chromatin accessibility will be addressed further below. There is also a positive feedback loop for PHD activity, whereby persistent hypoxia drives HIF-mediated upregulation of PHD2 and 3 expression and subsequent hydroxylation and degradation of HIF-1α. This process is called desensitisation and is an anti-necrotic pathway, demonstrating the importance of PHDs in tailoring the host cell response to both acute and chronic hypoxia (Ginouves et al., 2008).

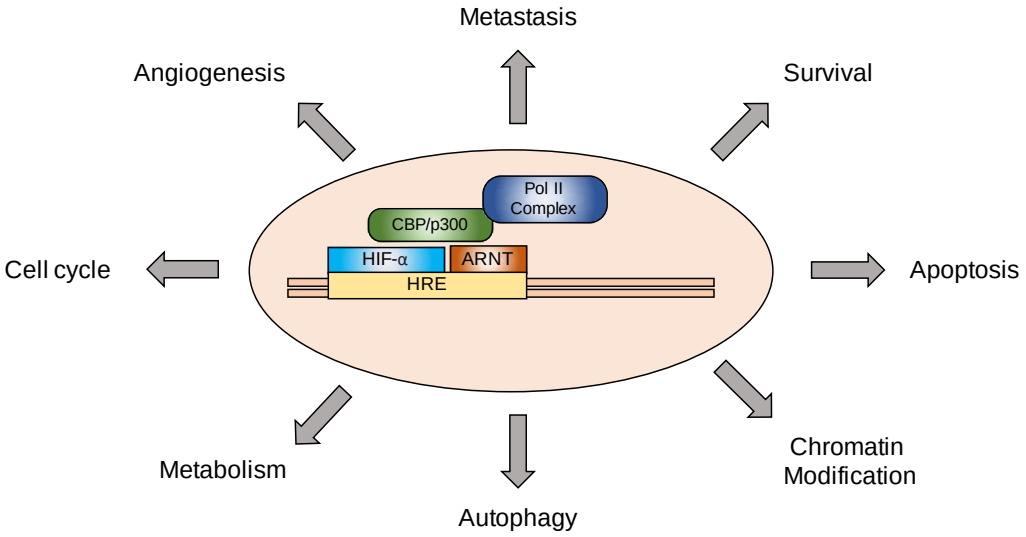


Figure 1.19: HIF regulated cellular processes

A figure to show the wide reaching effects of HIF signalling on cell physiology. Figure adapted from (Batie and Rocha, 2020)

Whilst HIF-1α and HIF-2α share a high degree of structural homology they show distinct patterns of expression, both in terms of tissue-specificity and the timing of their hypoxic induction (Holmquist-Mengelbier et al., 2006; Stiehl et al., 2012; Tian et al., 1997; Wiesener et al., 2003). As such, it has been suggested that they play a unique and distinct role in regulating the hypoxic response, and also show differential activity in disease. In VHL-defective renal cancer both HIF isoforms are constitutively active due to faults in the degradation pathway, and it is thought that HIF-2α promotes oncogenesis, and in direct opposition HIF-1α stimulates tumour suppressive pathways (Raval et al., 2005). There are reports suggesting they act via a different mechanism of action, despite encoding the conserved DNA binding domain and dimerization site (Choudhry et al., 2014; Hu et al., 2003; Schodel et al., 2011; Takeda et al., 2010). HIF-1α binds to responsive

promoters closer to the transcriptional start site than HIF-2α which binds much further upstream. This is likely regulated by the epigenetic landscape of the promoter which governs the ability of transcription factors to associate with DNA (Dmitriev and Papkovsky, 2015; Dobrynin et al., 2017). However, it has been suggested that the accessibility of HRE motifs to HIFs does not alter in response to hypoxia, and that instead the promoter of hypoxia inducible genes are already primed and in a state awaiting HIF binding (Smythies et al., 2019). This suggests that HIFs are not pioneer transcription factors, and rapidly induce gene expression by associating with already 'open' chromatin, decorated with activatory histone marks such as methylation of H3K4 and H3K27ac (Ebert and Bunn, 1998; Kindrick and Mole, 2020). It is thought that the methylation status of the promoter may be a major determinant of whether a gene binds HIF-1α or -2α, with HIF-1α associating more closely with H3K4me3 bound promoters, and HIF-2α preferentially binding sites with H3K4me1 marks (Dobrynin et al., 2017). For this reason, chromatin conformation and accessibility is of paramount importance as HIFs elicit their transcriptional regulation via direct binding to the genome at HREs (Batie et al., 2018). A study from Smythies and colleagues demonstrated that whilst some genes are exclusively regulated by one HIF-α isoform, others have shown dual regulation by both HIF-1α and -2α subunits (Smythies et al., 2019). In such instances, it is not entirely clear as to how the dual regulation operates, or whether this is driven by cell type specificity or if other factors such as duration of hypoxia, or HIF mRNA stability are responsible (Bartoszewski et al., 2019; Smythies et al., 2019).

Whilst the role of HIF-1α and -2α are well studied, the role of HIF-3α is somewhat less well defined. HIF-3α shares highly conserved structural similarity

with the -1α and -2α isoforms encoding the bHLH and PAS domains, but it does not possess the C-terminal domains (C-TAD) which are required for transactivation (Hara et al., 2001) (**Figure 1.20**). However, it is believed that HIF-3α may have a role to play in the regulation of genes involved in both glucose metabolism and adipogenesis, but it is unclear whether it carries out its activity truly independently of HIF-1α (Hatanaka et al., 2009; Heidbreder et al., 2007).

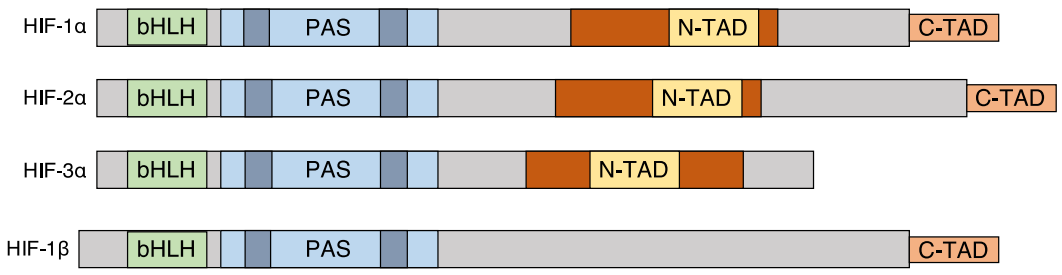


Figure 1.20: HIF structure

A cartoon to show the structural homology and key domains of the HIF isoforms. Figure adapted from (Schofield and Ratcliffe, 2004).

1.3.3: Inflammation and HIFs

As well as stabilisation via the PHD-VHL pathway, reactive oxygen species (ROS) have been implicated in HIF signalling through both direct and indirect mechanisms. Indirectly ROS, such as hydrogen peroxide, increase the synthesis of TNF-α or IL-1β, which are inflammatory mediators with the capacity to induce HIF-1α mRNA transcription and protein expression (Haddad, 2002; Westra et al., 2007). TNF-α induction of HIF is dependent on the activity of NF-κB, which has also been shown to increase HIF-1α protein stability independently of RNA transcription (Jung et al., 2003a; Zhou et al., 2003). Interestingly, IL-1β can influence HIF stability by activating NF-κB signalling and inhibiting VHL-mediated HIF degradation (Jung et al., 2003b). In addition, transforming growth factor-β (TGF-β) was reported to inhibit PHD2 expression via SMAD signalling, and to prevent HIF degradation (McMahon et al., 2006). This forms an intricate link between the immune system and HIF signalling, whereby inflammatory mediators can regulate HIF expression, which can in turn modulate the transcriptome of immune cells. Of course in the context of infection, inflammatory mediators and immune cells are more abundant (Palazon et al., 2014).

Mammalian target of rapamycin (mTOR) and oestrogen have been implicated in the regulation of HIF signalling. HIF-1α encodes a mTOR signalling (TOS) motif in the N terminus, which is essential for the interaction between HIF-1α and the regulatory associated protein of mTOR (Raptor). Deletion of the TOS has been shown to inhibit HIF function by preventing p300/CBP binding in hypoxia (Land and Tee, 2007). mTOR is an essential regulator of angiogenesis which, as previously discussed, is a well-studied hypoxic mediated pathway. mTOR complex 1 regulates the hypoxic response by maintaining HIF-1α transcript levels via

STAT3 activation, and its inhibition has been shown to suppress HIF-1α and to reduce vascular endothelial growth factors (Dodd et al., 2015). mTOR signalling is linked to the hypoxic tumour environment where the kinase function of mTOR is inhibited, and drives a hypoxic-tolerant and progressive tumour environment (Wouters and Koritzinsky, 2008). Due to the angiogenic pathways regulated by mTOR, rapamycin is a drug candidate to inhibit angiogenesis in hypoxic tumours, although it is important to note that rapamycin does not alter HIF-1α expression and regulates its function independent of VHL activity (Land and Tee, 2007).

Oestrogen signalling is also implicated in the HIF-response and drives sex dependent changes in HIF signalling cascade. The oestrogen receptor-α (ERα) directly regulates the transcription of HIF-1α, and in turn, HIF-1α regulates the expression of many other ERα target genes (Yang et al., 2015). Studies have shown that female rats are less sensitive to chronic intermittent hypoxia than male animals, indicative of an inhibitory role for oestrogen in regulating the HIF response (Fuady et al., 2016; Hinojosa-Laborde and Mifflin, 2005). As such, when female rats underwent an ovariectomy, they became equally as responsive as male rats to hypoxia (Rubin et al., 2020). A study in the context of invasive breast cancer revealed that oestrogen preferentially downregulated HIF-2α rather than HIF-1α, perhaps consistent with the presence of an oestrogen-E2 response element (ERE) in the intron of EPAS1 suggesting transcriptional co-repression by the ERα (Fuady et al., 2016).

1.3.4: Chromatin

Chromatin is arguably the most complexed and dynamic molecular structure in the cell, and is a network of DNA which associates both directly and indirectly with protein and RNA (van Steensel, 2011). The major component of chromatin is the nucleosome, which is a 147bp region of DNA that is wrapped around a histone octamer, with 20-50bp of 'linker' DNA connecting adjacent nucleosomes; giving the chromatin structure the classic 'beads on a string' appearance (Kornberg, 1974). The histone octamer is a highly conserved structure consisting of two copies of each of the four core histones (H), H2A, H2B, H3 and H4, arranged as a dimer of tetramers of H3/H4 and H2A/H2B (Woodcock and Ghosh, 2010). H1 was identified as a linker histone which associates with the linker DNA, and ultimately provides the scaffolding to form a chromosome (Luger et al., 2012). Broadly speaking chromatin is in one of 2 states, either 'open' or 'closed' known as euchromatin and heterochromatin respectively (Li et al., 2007a). Heterochromatin and its closed status are commonly associated with transcriptionally silenced gene loci, whereby transcription factors cannot access the tightly bound DNA, whereas euchromatin is more open, less tightly associated with the histone and readily accessible to host transcription complexes (Batie et al., 2018). As previously discussed, transcription factors such as HIFs must be able to access the target region of the genome and as such chromatin conformation is a major determinant of gene expression.

The structure of the chromatin is directly regulated by post translational modifications of histone, and the 2 major pathways implicated are methylation and acetylation. Typically lysyl residues 4, 9, 27, 36 and 79 of H3 are the most common post-translationally modified sites which determine gene expression by

modifying accessibility and chromatin compaction (Benveniste et al., 2014; Hancock et al., 2015). Methylation of lysine residues can be in mono (me1), di- (me2), or tri- (me3) forms, and this can determine activation status. H3K9me2/me3 and H3K27me3 sites are most commonly associated with transcriptional repression, and have been implicated in tissue specific gene expression (Saksouk et al., 2015). H3K9me3 is primarily found in the promoter regions of silenced genes where it can cross talk with the DNA methylation machinery to regulate the maintenance and formation of heterochromatin (Du et al., 2015). H3K27me3 represses gene expression in regions of open chromatin by recruiting polycomb repressive complexes to the promoters (Czermin et al., 2002). In contrast, H3K4me3 is found to be ubiquitously expressed at the 5' end of actively transcribing nucleosome bound gene loci, often closely associated with RNA Pol II (Barski et al., 2007; Zhang et al., 2009). However its role in the induction of gene expression is not fully understood, as discussed by Howe et al. (Howe et al., 2017). This debate may stem from the observation that H3K4me3 can co-localise with H3K27me3 at promoter regions and these sites are referred to as bivalent (Voigt et al., 2013). As well as histone modification, chromatin looping can define transcription, as it allows distal components of DNA to be brought together allowing interactions between multiple gene promoters and transcriptional complexes (Kadauke and Blobel, 2009). This is perhaps the mechanism by which some genes are upregulated in hypoxia but do not encode HRE motifs in their promoter (Schodel et al., 2011). One of the major regulators of chromatin looping is CTCF, a recently identified HBV restriction factor, which stabilises chromatin loops with cohesin to create epigenetic boundaries between transcriptionally

active and inactive regions of chromatin (D'Arienzo et al., 2021a; Rowley and Corces, 2018).

1.3.5: Histone lysine demethylases

The Jumonji-C (JmjC) histone lysine demethylases (KDMs) are epigenetic regulators that catalyse the removal of methyl groups from specific lysyl residues on histone tails, using Fe(II) and 2-OG as substrates (Tsukada et al., 2006). This group of 32 enzymes all encode a JmjC domain, and are separated into subgroups (KDM2-8) based on their structural homology and their unique binding domains determine their specific lysine target (reviewed in (Kindrick and Mole, 2020; Shmakova et al., 2014)) (**Figure 1.21**). The common double stranded β helix domain is responsible for the initiation of hydroxylation, which forms a hemiaminal (a compound with both a hydroxyl and amine group attached to the same carbon atom) which fragments to generate a demethylated lysine product and formaldehyde (Costa et al., 2003).

Their relationship with molecular oxygen is two-fold, primarily they are 2-OGDDs and therefore require oxygen to function, and secondly, many of the KDMs have been identified as HIF target genes, whereby their expression is increased when oxygen is depleted. Several studies have identified which KDMs are hypoxia inducible using transcriptomic and motif scanning analysis. As such, KDM2A-B, KDM3A-B, KDM4B-D, KDM5A-D, KDM6A-B, KDM8, JARID2 and PHF8 have all previously demonstrated hypoxic induction *in vitro* (for all references, see Table 1 of review by Melvin and Rocha, (Melvin and Rocha, 2012)). As well as being hypoxia inducible, further mechanistic studies have identified KDM3A, KDM4B-C, KDM5C, and KDM6B as direct HIF-1α target genes (Lee et al., 2014; Niu et al., 2012; Pollard et al., 2008). Increased expression of

the KDM proteins may form a feedback mechanism to maintain enzymatic activity when oxygen is depleted, in a manner comparable to that of PHD2 and 3 (Batie and Rocha, 2020).

Due to the oxygen dependency of these fundamental epigenetic regulators, studies have begun to investigate the impact of hypoxia on chromatin status, as a result of oxygen mediated inhibition of KDM activity. A recent study by Chakraborty et al. identified for the first time that KDM6A (also known as UTX) is an oxygen sensor and regulator of cell fate, which works independently of the HIF-PHD axis. KDM6A was shown to be inhibited in hypoxia and as such prevented the demethylation of its cognate mark H3K27me3, resulting in a blockade to cellular differentiation (Chakraborty et al., 2019). Similarly, another study from Batie et al. revealed that KDM5A was a novel oxygen sensor, and observed that modification of many lysyl residues occurred before HIF-1α was stabilised. They also showed that depletion of KDM5A modulated the cellular sensitivity to low oxygen with oxygen-mediated transcriptomic changes occurring at 15%, rather than 10% O_2 (Batie et al., 2019). Equally, chromatin status has been shown to regulate the HIF signalling pathway, as KDM4A regulates the abundance of H3K9me3 on the HIF-1α locus. Thus when KDM4A is inhibited in hypoxia, the repressive histone mark accumulates and results in decreased HIF-1α mRNA and concomitant reduction in HIF expression (Dobrynin et al., 2017).

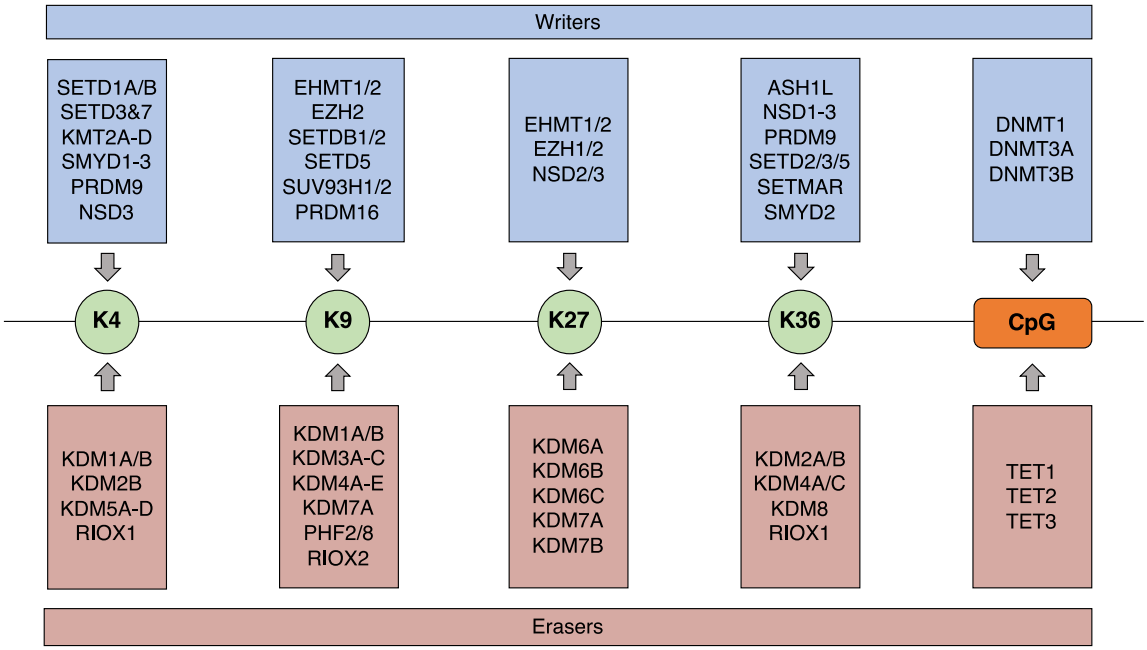


Figure 1.21: Epigenetic readers and writers

A cartoon to show the enzymes responsible for the post-translational modification of key histone residues and CpG islands. Figure adapted from (Kindrick and Mole, 2020)

KDMs are considered to be epigenetic ‘erasers’, but ‘writers’ also exist; however in the context of histone modification this is not a property of the 2-OGDDs. Nonetheless, histone methylation is not entirely independent of low oxygen signalling. SET1B, also known as SETD1B, is a major histone methyltransferase for both H3K4 and H3K9 residues, meaning that it can regulate both activation and repression of gene expression (**Figure 1.21**) (Lee et al., 2007; Torrano et al., 2019). SETB1 is recruited by HIF to facilitate the rapid activation of HIF target genes involved in angiogenic processes, in response to hypoxia (Ortmann et al., 2021).

1.3.6: Oxygen sensitive epigenetic modifiers

The protein hydroxylases, or the JmjC oxygenases, are closely related to the KDMs as they also contain the JmjC domain, however these specifically catalyse the oxidation of protein or tRNA to yield a hydroxylated product (Markolovic et al., 2016). There is some controversy within the field as to whether a true distinction between the KDMs and the JmjC enzymes can be made. The best studied JmjC member is the asparagine hydroxylase, factor inhibiting HIF (FIH). FIH likely contributes to this controversy as it encodes a double stranded β barrel structure, just as the KDMs do, although despite containing a JmjC domain, FIH has no demethylase activity (Hangasky et al., 2013). FIH does not regulate HIF transcription but instead, when oxygen is abundant, hydroxylates N803 on HIF-1α subunits causing steric inhibition of its ability to interact with p300/CBP, and thus inhibits the HIF signalling cascade (Schofield and Ratcliffe, 2004). In contrast, in hypoxia FIH is inhibited and therefore the asparagine residue remains un-hydroxylated, HIF-1α is stabilised and able to translocate to the nucleus and activate gene expression in complex with HIF-1β and p300/CBP (Semenza, 2012). FIH is functional at very low oxygen tensions ($K_m(O_2)$ 90 mM), compared with PHD2 ($K_m(O_2)$ 250 mM), which suggests that there is interplay between PHD- and FIH- regulation of HIF stability and that both factors may regulate when HIF is activated and then degraded (Tarhonskaya et al., 2015). As well as being an essential regulator of HIF signalling, it is believed that FIH may have roles in the regulation of cell metabolism, however it is challenging to dissect the HIF-independent role of FIH due to the intricate relationship between the two factors (Scholz et al., 2016; Zhang et al., 2010).

The collagen hydroxylases are fundamental in the post translational modification of collagen, which is the most abundant protein in the human body and constitutes the major component of connective tissue, bone and extra-cellular matrix (Shoulders and Raines, 2009). It is an extremely strong protein which increases its tensile strength by forming a triple-helix of interweaving polypeptide chains, and the presence of 4-hydroxyproline is essential in regulating the conformational structure of the triple helices (Berg and Prockop, 1973). Therefore the collagen hydroxylases are essential in regulating collagen structure, and reorganising the extra-cellular matrix in response to external stimuli.

As well as acting on protein targets, the 2-OGDDs can act on nucleic acids and can regulate the methylation of both DNA and RNA, which are fundamental modifications in the regulation of eukaryotic gene expression. One of the most abundant epigenetic modifications of DNA is 5-methylcytosine, which is found to be highly expressed at CpG islands (Ooi et al., 2009), and considered a major repressor of gene expression, via inhibition of transcription factor binding (reviewed in (Luo et al., 2018)). The identification of a further modification, 5-hydroxymethylcytosine (5hmC) led to the discovery that the 2-OGDDs ten-eleven translocation (TET) family were responsible for the conversion of 5mC to 5hmC (**Figure 1.21**) (Kriaucionis and Heintz, 2009; Tahiliani et al., 2009). The conversion of 5mC to 5hmC is the beginning of the demethylation process and as such can be considered as a pathway by which gene expression is reactivated, however it is complex, and not fully understood. 5hmC can undergo cytidine deamination to form 5-hydroxymethyluracil, and TETs regulate successive oxidation to formylated- (5fC) then carboxylated- (5caC) cytosine, which can be excised from the genome, triggering aspects of the DNA repair pathways (He et al., 2011;

Pfeifer et al., 2013; Rusmintratip and Sowers, 2000). As previously discussed, the K_m value for molecular oxygen determines a factors ability to retain function in hypoxia, and the activity of TETs is evidently paramount as they have an extremely low K_m for oxygen and can retain function in almost anoxic conditions. TET1 and TET2 have been shown to be active at oxygen tensions as low as 0.31% and 0.5% (K_m O_2 approximately 30 μM) (reviewed in (Kindrick and Mole, 2020; Laukka et al., 2016; Thienpont et al., 2016)).

In the same sub-family as the TET enzymes are the AlkB proteins, which are fundamental DNA repair enzymes responsible for the removal of alkyl adducts through an oxidative pathway, hence their dependence on molecular oxygen to function. There are 9 AlkB homologues in mammalian cells, named ALKBH1-8 and FTO which cover a wide range of modifications to either DNA or RNA. ALKBH1 can function as a demethylase of mitochondrial DNA, ALKBH2 and 3 are nuclear DNA repair enzymes, and ALKBH8 is a methylator of tRNA (Chen et al., 2010; Fu et al., 2010; Westbye et al., 2008). FTO and ALKBH5 act on N6-methyladenosine modified RNAs to determine RNA half-life, stability and translatability (Thalhammer et al., 2011). The role of the remaining family members remains to be fully understood, although ALKBH4 has been shown to demethylate actin subunits, ALKBH7 is a potential regulator of alkylation mediated necrosis, whilst the role of ALKBH6 is yet to be discovered (Fedeles et al., 2015; Fu et al., 2013; Li et al., 2013b).

The remaining small molecule hydroxylase sub-families of the 2-OGDDs are somewhat less well studied, however their reliance on molecular oxygen is well defined. Generally speaking, they play an essential role in the post translational modification of metabolic intermediates. For example PHYH is an

important regulator of phytanoic acid degradation, and BBOX1 and TMLH1 are involved in carnitine synthesis (Leung et al., 2010; McDonough et al., 2005). Interestingly, a previous study has shown that anti-aspartate beta-hydroxylase domain-containing protein 2, ASPHD2, was shown to be upregulated in the perivascular and necrotic regions of glioblastoma, perhaps suggesting a role for this 2-OGDD in this hypoxic tumour niche (Seidel et al., 2010).

1.3.7: Chromatin and hypoxia

Given the oxygen dependency of the machinery regulating histone methylation, acetylation and DNA methylation, the study of chromatin structure in hypoxic conditions is an emerging field. However, there is still much to be learned about the status and compaction of chromatin in low oxygen, and the implications for gene expression (Batie et al., 2018). The ATP-dependent chromatin remodellers are responsible for changing chromatin structure, and act by modulating protein-DNA contacts and catalysing the removal of nucleosomes from gene loci (Melvin and Rocha, 2012).

Perhaps the best studied of these factors is the Switch/Sucrose Fermentable (SW1/SNF), an evolutionary conserved multi-subunit complex essential for transcriptional activation, although repressive roles have also been identified (Melvin and Rocha, 2012; Mohrmann and Verrijzer, 2005; Simone, 2006). SW1/SNF complexes utilise one of two catalytic subunits: either SW1/SNF regulated, matrix associated, actin dependent regulator of chromatin subfamily A, member 4 (BRG1), a factor essential for embryonic development, or SW1/SNF regulated, matrix associated, actin dependent regulator of chromatin subfamily A,

member 2 (BRM). Components of the SW1/SNF complex have been found to be aberrantly expressed or mutated in several cancers, however their role in hypoxia is yet to be fully understood (Bultman et al., 2000; Melvin and Rocha, 2012; Wilson and Roberts, 2011). Interestingly, a previous study identified SW1/SNF to regulate HIF expression by recruiting BRG1 to its promoter as well as being essential for hypoxic induced cell cycle arrest (Kenneth et al., 2009). Furthermore, there is a connection between BRG1 and vascularisation, whereby BRG1 knockout mice showed defective angiogenesis, and both BRG1 and BRM have been implicated in the regulation of EPO induction (Griffin et al., 2008; Kenneth et al., 2009; Wang et al., 2004).

Imitation Switch (ISW1) is another ATP-dependent chromatin remodeller, with roles in DNA replication and repair, transcriptional regulation, and modification of chromatin structure (Kim et al., 2011c). Importantly, ISW1 has been found to regulate several aspects of the host response to hypoxia; ISW1 depletion enhances HIF activity without altering expression levels, regulates the expression of FIH mRNA, and reduces autophagy (Kim et al., 2011c). The INO80 family of chromatin remodellers are characterised by their split ATPase domain, and are fundamental in host cell processes such as DNA repair and transcriptional regulation, however our understanding of their role in hypoxia signalling is limited. INO80 complexes involve the Reptin protein, which has been shown to repress the expression of a subset of HIF-1α target genes when methylated (Grigoletto et al., 2011; Lee et al., 2010). The final subset of ATP-dependent factors are the CHD chromodomain remodellers, but their function and regulation are not well studied. As such, there has been no comprehensive investigations into their role in

oxygen dependent chromatin regulation (Batie et al., 2018; Melvin and Rocha, 2012; Yap and Zhou, 2011).

Whilst there have been several studies assessing the impact of hypoxia on histone modification and transcriptional regulation, there have been comparatively fewer investigating the effect on chromatin status. In 2015, Kirmes et al. cultured cardiomyocytes in low oxygen conditions and used Single Molecule Localisation Microscopy (SMLM) and *in situ* DNA digestion to reveal that hypoxia caused rapid compaction of chromatin (Kirmes et al., 2015). They also demonstrated that chromatin plasticity was oxygen dependent, as reoxygenation reversed the changes in chromatin structure (Kirmes et al., 2015). The compact nature of heterochromatin renders the host DNA refractory to digestion by mononucleases (Thomson et al., 2010). A study from Dutta et al. cultured A431 cancer cells in 0.1% oxygen for 48 hours, then treated with mononuclease, and found that the hypoxic cultured cells were less sensitive to digestion, suggesting that hypoxia increased the abundance of heterochromatin (Dutta et al., 2014b). Furthermore, they employed proteomics and identified that expression of Heterochromatin Protein 1 Binding Protein 3 (HP1BP3), a factor responsible for heterochromatin maintenance, was elevated in hypoxia (Dutta et al., 2014a; Dutta et al., 2014b). A recent study from Wang et al. investigated the impact of cardiac hypoxia on chromatin accessibility, and employed a dual approach of ATAC-seq and RNA-seq to study chromatin structure and gene expression respectively (Wang et al., 2020). They found that differential gene expression associated with more ‘open’ chromatin status on the gene loci, and noted that some genes took longer to restore basal levels following reoxygenation. They attributed this to the duration of time required to restore usual chromatin structure and conformation. As previously

discussed, chromatin looping is an important mechanism in establishing transcriptional boundaries and bringing distal sequence regions together to regulate gene expression (Kadauke and Blobel, 2009; Mora et al., 2016). A study from Smythies and colleagues studied the distribution and functionality of HRE motifs in the human genome, and their results suggest that HIF induction does not alter chromosome looping, however this assumption is based only on HRE motifs and so further analyses with other transcription factors would be required (Batie et al., 2018; Smythies et al., 2019). The conformation of chromatin adjacent to HRE motifs was also studied by Disatham et al, and they found an enrichment of motifs in open areas of chromatin consistent with a role for rapid induction of gene expression in hypoxia (Disatham et al., 2021). In short, there is emerging evidence to suggest that hypoxia can alter the physical status of chromatin, and the future application of sequencing technologies and high resolution imaging will increase our understanding (Batie et al., 2018; Batie et al., 2019; Chakraborty et al., 2019).

1.4: HBV and hypoxia

Having discussed the molecular life cycle of HBV and the cellular response to hypoxia at length, it is important to address what is known about the interplay between both topics. The naturally hypoxic microenvironment of the liver presents a niche for both HIF and non-HIF mediated pathways to influence the life cycle of HBV, and indeed other hepatotropic viruses. As an obligate intracellular parasite, HBV is dependent on host cell factors for entry, the repair of the rcDNA genome to form the cccDNA episome, host transcription factors for replication, and export processes for egress. This means that hypoxia has the potential to impact on the

life cycle of the virus at every stage, and our work will focus on transcription and replication.

Whilst roles for HIF and hypoxia signalling have been elucidated in the life cycle of many human viruses (summarised in **Table 1.8**), until our work there had been no comprehensive study to understand the interactions between HIFs and HBV (reviewed in (Liu et al., 2020a; Wing et al., 2021)). This could perhaps be reflective of the limited availability of appropriate model systems to study these two complicated pathways. As discussed in *Chapter 1.2.8***,** HBV model systems are still in their infancy, and equally, the *in vitro* systems used to study hypoxia biology have their limitations. The gold standard method for hypoxic culture is to use a hypoxic workstation, a glove box style incubator whereby the whole experimental procedure can be performed in hypoxic conditions (Fry et al., 2017; Hancock et al., 2017; Smythies et al., 2019; Wing et al., 2021). However, in the absence of such technology, pharmacological agents are available to activate and inhibit various aspects of the oxygen signalling pathways. One could suggest, that until recently most studies on hypoxia have focussed on the PHD-HIF signalling axis, and the importance of other 2-OGDDs is only starting to be realised. As such, many studies use pharmacological agents to stabilise HIFs in otherwise normoxic conditions, and are often referred to as hypoxic mimetics. Dimethyloxalylglycine (DMOG) is a 2-OG analogue routinely used to stabilise HIFs (Jaakkola et al., 2001). As a 2-OG analogue, DMOG will have inhibitory effects on the enzymatic function of all 2-OGDDs, and as such will have a much wider impact on cellular physiology than stabilising HIFs alone (Hopkinson et al., 2013; Thinnes et al., 2014). HIFs can also be induced using cobalt chloride ($CoCl_2$), as the Co^{2+} ion is able to compete with Fe^{2+} and bind to the PHD enzymes, rendering them

functionally inactive (Nag and Resnick, 2017; Triantafyllou et al., 2006). This prevents HIFs from being hydroxylated and allows them to elicit their transcriptional response, although the precise mechanism of action and true impact on the host cell is difficult to unpick (Triantafyllou et al., 2006). In contrast FG-4592, or roxadustat, is a selective inhibitor to the PHD enzymes and therefore stabilises HIFs specifically with limited impact on other members of the 2-OGDDs. FG-4592 is therefore is our preferred pharmacological agent to study HIF signalling, and has been used in clinical practise to induce polycythemia and to treat renal anaemia (Provenzano et al., 2016; Schley et al., 2019).

Virus	Tropism	Influence of hypoxia	Citations
Dengue Virus DENV RNA	Immune Cells	Hypoxia enhances antobody-dependent infection of THP1 cells and monocytes. DENV infection activated HRE-luciferase activity in a Huh7 cell, but no experiments to assess HIF levels A pro-viral role for HIFs in regulating DENV RNA replication and translation DENV is sensitive to KDM4 inhibition in a Huh7 background	Gan et al. 2017 Frakolaki et al. 2018 Frakolaki et al. 2018 Magri et al. unpublished
Epstein Barr Vrius EBV DNA	Immune Cells	HIF-1a binds HRE in the latent-lytic switch BZLF1 gene to promote EBV transcription EBV-LMP1 increases HIF-1a expression by promoting PHD1/3 degredation by Siah E3 ubiquitin ligase LMP1 blockade increases the senstivity of nasopharyngeal cancers to radiotherapy by downregulating HIF-1a and VEGFA	Kraus et al. 2020 Kraus et al. 2017 Kondo et al. 2006 Yang et al. 2015
Hepatitis C Virus HCV RNA	Liver	Low oxygen enhances HCV replication, through HIF dependent and independent mechanisms Hypoxic regulated autotaxin is essential for HCV replication Entry receptor SR-B1 is a HIF target gene, increased HCV entry in hypoxia KDM4 is a potent regulator of HCV RNA replication FTO regulates m6A methylation of HCV RNAs	Vassilaki et al. 2013 Wilson et al. 2012 Farquhar et al. 2017 Internal, unpublished Magri et al. unpublished Gokhale et al. 2016
Human Immunodeficiency Virus Type 1 HIV-1 RNA	Immune Cells	HIV-1 replication is restricted by hypoxia HIF-2a binds a HRE motif in the LTR to repress activity HIV-Vpr can generate ROS to stabilise HIFs during immune activation	Charles et al. 2009 Zhuang et al. 2020 Duette et al. 2018 Deshmane et al. 2009
Human Papilloma Virus HPV DNA	Skin and Epidermis	HPV16 integration associates with HIF-1a expression HPV16 and 18 encoded E6 and E7 stabilise HIF-1a and induce VEGFA and IL-8 expression HPV stabilises HIF through E6-inhibition of HIF-VHL interaction; E2 inducing ROS through mitochondrial interactions; E6 and E7 inducing HIF-2a through LKB1	Kim et al. 2007 Li et al. 2011 Guo et al. 2014 Lai et al. 2013 Shao et al. 2017
Human T-lymphotropic Virus Type 1 HTLV-1 RNA	Immune Cells	Hypoxia enchances HTLV-1 reactivation from latency, via a HIF independent mechanism HTLV-1 Tax protein induces HIF-1a protein expression and stability	Kulkarni et al. 2017 Muhleisen et al. 2014
Infleunza A Virus IAV RNA	Respiratory Tract	IAV H1N1 replicates to a higher titre in HIF-1a knockout mouse HIF-1a promotes the expression of pro-inflammatory cytokines and regulate alveolar epithelial cell differentiation following IAV infection IAV leads to acute lung injury which activates hypoxia signalling and HIF-1a stability	Zhao et al. 2020 Sinha et al. 2011 Zampell et al. 2012 Xi et al. 2017 Zhao et al. 2020
Kaposi's Sarcoma Associated Herpesvirus KSHV DNA	Skin and Epidermis	Encodes functional HRE motifs in promoters of late stage and lytic genes, responsive to HIF-1a and -2a KSHV tumours are highly vascular, and it is thought that virus-mediated HIF signalling may promote VEGFA expression KSHV-IRF3 can bind to HIF-1a and prevent its degradation High overlap of KSHV-induced and HIF-target genes	Haque et al. 2003 Nishimura et al. 2017 Sodhi et al. 2000 Shin et al. 2008 Viollet et al. 2017
SARS-Coronavirus-2 SARS-CoV-2 RNA	Respiratory Tract	Hypoxia and HIF-1a both reduce ACE2 surface receptor expression Post-entrance stages are also oxygen sensitive and hypoxia restrcits SARS-CoV-2 RNA replication SARS-CoV-2 infection of monocytes induces ROS generation at the mitochondria and stabilises HIF-1a	Wing et al. 2021 Wing et al. 2021 Codo et al. 2020

Table 1.8: Human viruses and hypoxia

A table to summarise the role of HIFs or hypoxia in the life cycle of human viruses, as reviewed by (Liu et al., 2020a)

The vast majority of studies on HBV *in vitro* have been performed at atmospheric oxygen tensions of 18% O_2, and so the role of hypoxic regulated transcription factors and epigenetic modifiers are likely to have been overlooked. There are, however, a number of studies which have explored hypoxic regulation of host factors, and the impact of HBV infection on the hypoxic response. A recent study from Hallez et al. reported that host deoxyribonuclease 1 (DNASE1) was hypoxic regulated and could facilitate the degradation of the rcDNA genome and promote the secretion of empty virions (Hallez et al., 2019). Hallez and colleagues used DMOG and $CoCl_2$, as well as 3% oxygen to stimulate HIF signalling in cells either transfected with HBV1.3 genomes or infected with authentic virus (Hallez et al., 2019). There are also reports that the HBx protein is able to directly interact with HIF-1α and lead to its stabilisation and transcriptional activation. Studies from Yoo et al. showed that HBx prevented HIF degradation via inhibition of the interaction between HIF-1α and the VHL complex. Additionally, HBx was shown to induce HIF RNA transcripts and protein through MTA1 and HDAC perturbation of HIF acetylation (Yoo et al., 2008; Yoo et al., 2003). Yoo et al. also demonstrated, by transfection of HBx plasmids with functional domain deletions, that the C-terminus of HBx could enhance the transactivation function of HIF-1α (Yoo et al., 2004). In contrast, a study from our group assessed the interaction between HBV and HIF, and we did not observe HIF protein stabilisation or downstream induction of HIF target genes in response to HBV infection in state-of-the-art *in vitro* and *in vivo* models (Liu et al., 2020b).

1.5: Aims

We hypothesised that the hypoxic environment of the liver would influence the activity of oxygen sensitive transcriptional regulators, and we sought to investigate their role in orchestrating the hepatocellular transcriptome and the HBV life cycle. As a DNA virus HBV has the potential to directly bind HIF isoforms, and we wanted to understand the interactions between HBV and HIFs *in vitro* and *in vivo.* Finally, the hypoxic response is governed by HIF-dependent and -independent regulators, and we explored the non-HIF regulators of HBV replication.

Objective 1: Investigate the contribution of oxygen signalling in the CHB liver

- Employ bio-informatic analysis to investigate HIF signalling *in vitro* and *in vivo*
- Develop a qPCR assay to ascribe relative viral transcript patterns, and understand the contribution of both cccDNA and HBV integrants in HBV infection
- Investigate HBV transcript patterns in a CHB cohort, and the role of inflammation in promoting viral replication in the HBeAg negative phase of disease

Objective 2: Understand the role of HIFs in the life cycle of HBV

- Characterise the hepatoma response to hypoxia *in vitro*
- Investigate the impact of hypoxia on HBV model systems
- Optimise ChIP assays for HBV DNA, and assess whether HIFs can bind the viral genome

Objective 3: Explore HIF-independent, oxygen sensitive regulation of HBV

- Investigate the contribution of other 2-OGDDs to the HBV life cycle
- Understand the interplay between HIF signalling and KDM-mediated epigenetic modification
- Explore the role of oxygen tension in determining cellular sensitivity to 2-OGDD inhibition

Chapter 2: Materials and Methods

2.1: Chemicals and reagents

Table 2.1: Chemicals and reagents

Chemical/Reagent	Supplier	Product Code
2-Propanol	Sigma	34863
Ammonium Persulfate	Sigma	A3678-25G
Bovine Serum Albumin	Sigma	A7906-100G
Chloroform	Sigma	366927
cOmplete protease inhibitor	Roche	1169749001
DharmaFECT 4 Transfection Reagent	Horizon	T-2004-03
Dimethylsulphoxide (DMSO)	Santa-Cruz	Sc-202581
Ethanol	Sigma	32221-2.5-m
Ethylenediaminetetraacetic acid (EDTA)	Invitrogen	AM 9260G
Formaldehyde	Sigma	F8775-500mL
Fugene6	Promega	E2691
Glycine	Sigma	G8898-1KG
IGEPAL CA-630	Sigma	18896-100mL
Methanol	Sigma	32213-2.5l-m
Passive Lysis Buffer	Promega	E1941
Pepsin	Sigma	77160-25G
Phenol:Chloroform:Isoamyl Alcohol	Sigma	P3803-400mL
Polyethylene glycol 8000 (PEG)	Fisher	10407773
Polyethylenimine (PEI) 25kD linear	Polyscience	29366-100
Propidium Iodide	Invitrogen	F10797
Proteinase K	Invitrogen	AM2546
RNAse A	Fisher	EN0531
Sodium acetate buffer	Sigma	S7899-100mL
Sodium Azide	Sigma	S2002
Sodium chloride	SLS	31434-1KG-R-D
Sodium Deoxycholate	Sigma	L7026-100mL
Sodium dodecyl sulphate (SDS)	Fisher	10265153
Sodium hydrogen carbonate	Sigma	S6297-250G
SuperSignal West Dura Extended Duration Substrate	Thermo Scientific	34076
Tris-EDTA Buffer Solution	Sigma	93283-100mL
Triton x-100	Sigma	T8787-100mL
Trizma base	Sigma	T6066-1KG
Trizol	Thermofisher	15596026
Trypan Blue	Sigma	T8154-100mL
Tween 20	Sigma	P7949-100mL

Table 2.2: Kits

Kits	Supplier	Product Code
AllPrep DNA/RNA	Qiagen	80204
GenElute HP Plasmid Midiprep Kit	Sigma	NA0200-1KT
PCR Purification	Qiagen	28004
Pierce BCA protein assay kit	Fisher	23227
QiaAmp MinElute Virus Spin Kit	Qiagen	57704
QIAprep Spin Miniprep Kit	Qiagen	27104
RNeasy Mini Kit	Qiagen	74106

Table 2.3: Drugs and compounds

Kits	Supplier	Product Code
Bromodeoxyuridine	Sigma	B5002
CPI-455	MedChemExpress	HY-100421
DMOG	Merck	400091-50MG
FG-4592	MedChemExpress	HY-13426
GSK-J4	MedChemExpress	HY-15648B
JIB-04	MedChemExpress	HY-13953
QC6352	MedChemExpress	HY-104048

2.2: Tissue culture

Table 2.4: Cell lines

Cell Line	Description	Source
HepAD38	HepG2-derived cell line supporting HBV replication from integrated overlength genomes, episomal cccDNA and random integration events.	Professor Ulrike Protzer, TUM
HepG2	Human hepatoma cell line, HCC origin	ATCC
HepG2-NTCP	HepG2 stably transfected with a lentiviral vector encoding NTCP	Professor Stephan Urban, TUM
HepG2-pEpi	HepG2 expressing an episomal vector encoding an overlength HBV genome and G418 resistance gene	Professor Ulrike Protzer, TUM
HepG2-rHBV-GLuc	HepG2 expressing a reporter strain of HBV, encoding a Gaussia luciferase in place of the Pol, with Pol provided in Trans	Professor Ulrike Protzer, TUM
HepG2.2.15	HepG2 harbouring 2 tandem repeats of HBV linearized genome	Professor Ulrike Protzer, TUM

Culture conditions

Hepatoma cell lines were cultured in fully supplemented DMEM containing 10% FBS, Penicillin-Streptomycin, and non-essential amino acids. Cells were cultured on collagen coated plasticware. HepG2-pEpi cells were cultured in the presence of geneticin (500 µl/µg) for routine passage, and antibiotics removed for assays (Lucifora et al., 2014). All cell lines were maintained at 37^{o}C, 5% CO_2 in a standard cell culture incubator (New Brunswick).

Table 2.5: Culture media

Culture Media	Supplier	Product Code
Collagen, from calf skin	Sigma	C8919-20mL
DMEM, high glucose, GlutaMAX	Gibco	31966047
Fetal Bovine Serum, heat inactivated	Gibco	10500064
Geneticin	Life Technology	10131019
MEM-Non essential amino acids (100X)	Gibco	11140050
Opti-MEM	Thermofisher	31985070
Penicillin-Streptomycin (10,000 U/mL)	Gibco	15140122

Hypoxic culture

Hypoxic incubations were performed for the specified durations in an atmosphere-regulated In Vivo2 400 Hypoxia Workstation (Ruskinn Technology) set to 37^{o}C, 5% CO_2 and 1-3% O_2 balanced with N_2, for uninfected containment level 2 materials. For HBV infected cultures, hypoxic incubation was carried out in a Galaxy 48R incubator (New Brunswick), at the indicated oxygen tensions and durations.

2.3: Plasmid transfections

Plasmid transfections in this study were performed using a reverse transfection protocol to maximise the transfection efficiency and DNA uptake. Typically, transfection mixes were set up in 10% of the final culture volume. Plasmid DNA was diluted in OPTIMEM, and Polyethylenimine (PEI) 25 kD linear (Polysciences) added at a 1 µl/µg ratio, typically at a 4:1 dilution to minimise cytotoxicity, although this ratio is cell type dependent. After vortexing, the transfection mix was incubated at room temperature for 30 minutes, before being directly added to the correct number of trypsinised cells previously resuspended in complete DMEM. This mixture was then directly seeded into required well format and left overnight to recover before proceeding with experimental protocol. pRL-

SV40 was used as a control for transfection efficiency at ratio of 1:8 with construct of interest.

Table 2.6: Transfection conditions

Culture Format	Cell Number	Reaction Volume
96 well plate	10,000	100 µL
24 well plate	50,000	500 µL
12 well plate	100,000	1 mL
6 well plate	300,000	2 mL
10cm dish	2,000,000	7 mL
15cm dish	4,500,000	15 mL

Table 2.7: Transfection mixes

Culture Format	OPTIMEM	DNA	PEI (3/4:1)
96 well plate	10 µL	100 nG	0.3 – 0.4 µL
24 well plate	50 µL	500 nG	1.5 – 2.0 µL
12 well plate	100 µL	1 µG	3.0 – 4.0 µL
6 well plate	200 µL	3 µG	9.0 – 12.0 µL
10cm dish	700 µL	7-8 µG	24.0 – 32.0 µL
15cm dish	1500 µL	11-12 µG	36.0 – 48.0 µL

siRNA transfection

To maximise transfection efficiency, cells were transfected with siRNAs while in suspension and seeded directly. HepG2-NTCP cells were trypsinised and counted before mixing with 50 nM of siRNA to gene of interest or a scramble control, and DharmaFECT4 transfection reagent. Cells were seeded and allowed to recover for 16 hours, with a media change to reduce cytotoxicity after 4 hours. Cells were then infected with HBV and treated as indicated. siRNA are tabulated in *Sequence-based reagents.*

2.4: Nucleic acid extraction

RNeasy

All RNA extractions were carried out using the RNeasy kit (Qiagen), according to the manufacturer's instructions. Briefly, cells were lysed in 350 µl of RLT lysis buffer, and stored at -80°C until extraction. Lysates were mixed with 1 volume of 70% ethanol, followed by a wash with buffer RW1. At this point, samples were treated with DNAse (RNAse-free DNase set, Qiagen) for 30 minutes at room temperature, to remove any DNA contaminant. This was routinely used to minimise contamination of HBV RNAs with cccDNA or rcDNA carryover. In the instance of plasmid transfections or human biopsy samples, where the level of DNA is comparatively higher or a complete DNA removal is required, a more rigorous digestion with TURBO DNase was performed (see *TURBO-DNase* below). Following digestion, samples were washed twice in RPE buffer, and the optional spin in a dry collection tube was carried out in all instances. Samples were typically eluted in 30 µl of nuclease free water.

AllPrep

Where paired RNA and DNA was required from the same biological replicate, for example to quantify both HBV DNA and RNA transcripts, the AllPrep kit from Qiagen was used according to the manufacturer's instruction. Cultures were lysed in 350 µl of RLT+ lysis buffer and could be stored at -80°C until extraction. Lysates were passed through the DNA column, and flow through precipitated in 1 volume of 70% ethanol, before adding to the RNA column.

RNA samples were then processed as described above in *RNeasy.* DNA columns were stored on ice or at 4°C, whilst RNA extraction was taking place. DNA columns were washed with both AW1 and AW2, before elution of DNA in 30 µl of elution buffer.

QIAamp MinElute virus spin kit

To determine titre of HBV in genome equivalents, QIAamp MinElute Virus Spin Kit was used following manufacturer's instructions. Briefly, PEG precipitated virus was diluted 1:10 in 0.9% NaCl to give a volume of 200 µl, before mixing with 25 µl of QIAGEN Protease, and 200 µl of Buffer AL (supplemented with 28 µg/ml of carrier RNA). Samples were incubated at 56°C for 15 minutes, at which point samples are inactivated sufficiently to remove from CL3. 250 µl of absolute ethanol was added to samples and incubated for 5 minutes at room temperature, before transferring the reaction to the QIAamp MinElute column. Samples were washed in 500 µl of AW1 and AW2, with all centrifugation steps at 6,000 x *g* for 2 minutes, and a clean collection tube for each spin. Finally, samples were washed on column with 100% ethanol, before thorough drying with a secondary spin, and heating at 56°C for 3 minutes. Typically, DNA was eluted in 35 µl of buffer AVE following incubation and a 2 minute centrifugation at full speed.

MinElute PCR purification kit

For the extraction of DNA products post-PCR, or as a final clean-up following Chromatin Immunoprecipitation (ChIP) protocol, Qiagen MinElute PCR purification kit was used, as per the manufacturer's instructions. 5 volumes of Buffer PB was added to the PCR reaction and the entire volume transferred to a MinElute DNA column. Samples were centrifuged for 2 minutes at 17,900 x *g*.

Flow through was discarded and columns washed with 750 µl of Buffer PE through centrifugation at 8,000 x *g*. Residual ethanol was removed by centrifugation at 16,000 x *g* for 1 minute. DNA was eluted in 10-20 µl of elution buffer, and stored at -20°C .

Trizol

When extracting RNA from tissue, it was preferable to extract using Trizol to maximise yield. Tissue was lysed in 500 µl of Trizol and homogenised through 25 gauge needles. At this point lysates were stored at -80°C until extraction. For extraction, 100 µl of chloroform was added to the homogenates, and tubes inverted several times. Samples were left for 5 minutes to allow the interphase to form before centrifugation at 16,000 x *g* for 15 minutes at 4°C. The aqueous phase was transferred into a clean eppendorf, and RNA precipitated through the addition of isopropanol in a 1:1 ratio followed by incubation at room temperature for 10 minutes. Samples were then centrifuged for 15 minutes at 4°C at 16,000 x *g*. Supernatants were carefully aspirated and discarded, leaving a clear pellet in the tube, which was washed in 75% ethanol, and span at 12,000 x *g* for 5 minutes. Supernatants were discarded, pellets allowed to air dry and heated at 55°C for 5 mins before resuspension in 35 µl of DEPC water. RNAs extracted from tissues were also subjected to TURBO DNase digestion, as described below.

Phenol:Chloroform

As well as using the above column based extraction methods for DNA isolation, phenol:chloroform extraction was also used for nucleic acid extraction in this study. Samples were lysed in 500 µl of SDS lysis buffer and added to 1 volume of phenol:chloroform, mixed well and centrifuged for 15 minutes at 12,000

x *g*, at 4°C. Supernatant was aspirated with caution to not take any of the protein interphase and transferred to a new tube and 2 µl tRNA; 1/10V 3M NaAc; and 2 volumes of 100% ethanol were added, then left at -20°C overnight to precipitate. Following precipitation, lysates were centrifuged for 15 minutes, 12,000 x *g* at 4°C, and supernatants discarded. As carrier RNA was used, a small white pellet was visible at the bottom of the tube. DNA pellets were washed in 75% ethanol, and allowed to air dry well, before resuspension in 30 µl of elution buffer.

TURBO DNase

Due to the lack of intron splicing in the HBV genome, primers designed to amplify target viral RNAs will also amplify the DNA template, hence DNAse digestion is routinely used to remove any DNA contaminant. As lipid transfection of plasmid delivers a bolus of DNA into the cells, standard on-column extraction is too gentle to remove this quantity of DNA carry-over. In order to overcome this, TURBO DNA-free kit (Thermofisher) was used for HBV1.3 transfection experiments, following the manufacturers protocol. Reactions were carried out in 50 µl with up to 2 µg of input RNA, and 2 units (1 µl) of TURBO DNase reagent. Samples were incubated at 37°C for 30 minutes, before inactivating the DNase with 0.1 volumes (5 µl) of resuspended DNase Inactivation buffer at room temperature with regular agitation. Samples were then centrifuged at 10,000 x *g* for 90 seconds, supernatant aspirated, and pellets discarded. RNA was then re-quantified, and reverse transcribed for gene expression analysis by qPCR. TURBO DNase digestion was also applied to clinical biopsy samples due to their limited and valuable nature.

2.5: RT-qPCR

Reverse transcription: cDNA synthesis

Following RNA extraction and DNase digestion, RNA was quantified by Nanodrop (Nanodrop 3000) or by using the LVis plate and Clariostar Plate Reader (BMG). Typically, 0.25-1 µg of RNA was reverse transcribed in a 20 µl cDNA synthesis reaction, using cDNA synthesis kit (PCR Biosystems), consisting of random hexamers and oligodT, in a peqSTAR thermal cycler (VWR). Where concentrations of RNA were too low to achieve at least 0.25 µg of input material, sample input was adjusted to use the maximum concentration in 15 µl, so that reverse transcription was carried out on equal quantities across all samples. cDNA was stored at -20^{o}C for stability.

Table 2.8: cDNA synthesis

Master Mix: 1 Reaction	
cDNA synthesis buffer	5 μL
Reverse transcriptase	0.5 μL
Template	250-1000 nG
ddH2O	Up to 15 μL
Total reaction volume	20 μL

Real-Time PCR

SYBR green protocol

Following cDNA synthesis, samples were diluted at least 1:2 to allow quantification of a panel of genes per experiment, typically the 20 µl sample was made up to 50 µl before qPCR as described below. Reactions were carried out using SyGreen Blue Mix (PCR BioSystems).

Table 2.9: SYBR green qPCR

Master Mix: 1 Reaction	
2X SYBR Green Buffer	5 μL
ddH2O	2.5 μL
Primers (F:R Stock)	0.5 μL
Template	2 μL
Total reaction volume	10 μL

All real-time PCRs were carried out on a LightCycler 96 (Roche) using the following amplification protocol: 2 minutes at 95ºC, followed by 45 cycles of 5 seconds at 95°C and 30 seconds at 60°C, followed by sample dissociation melt peak. Melting curves were analysed following every qPCR to ensure amplification of the target sequence was specific.

cccDNA quantification

In order to quantify cccDNA, residual HBV rcDNA must be destroyed, as they will both be detected by qPCR amplification. Due to the complete double stranded structure of cccDNA, it is resistant to T5 exonuclease treatment. However, as rcDNA is partially double stranded, it will be destroyed by T5 treatment, allowing the specific quantification of cccDNA copies.

Table 2.10: T5 exonuclease

Master Mix: 1 Reaction	
Input DNA	8μL
T5 Exonuclease	0.5μL
ddH2O	0.5μL
Buffer	1μL

Cellular DNA was treated with T5 exonuclease for 30 minutes at 37°C; following incubation the reaction was diluted at least 1:4 before qPCR

quantification. Samples without T5 digestion were diluted in an exact replicate of the digestion, but in the absence of T5. These samples were essential for the quantification of the prion protein (PrP) gene, used as sample normaliser. Reactions were carried out using SyGreen Blue Mix (PCR BioSystems) using the following amplification protocol: 5 minutes at 95ºC, followed by 50 cycles of 15 seconds at 95ºC, 5 seconds at 60ºC, 45 seconds at 45ºC and 2 seconds at 88ºC, followed by a melting profile.

Table 2.11: cccDNA qPCR

Master Mix: 1 Reaction	
2X SYBR Green Buffer	5 μL
ddH2O	0.5 μL
Primers (F:R Stock)	0.5 μL
Template	4 μL
Total reaction volume	10 μL

Extracellular rcDNA quantification

Supernatants of cells infected or transduced with HBV genomes were treated with DNaseI (ThermoFisher) at 37°C for 30 minutes supplemented with EDTA, to digest any DNA not protected by the viral nucleocapsid. Following this, samples were mixed 1:1 with ecDNA lysis buffer (0.1 M Tris-HCl, 50 mM KCl, 0.25% Triton X-100, and 40% glycerol), then a final heat inactivation stage of 10 minutes at 65°C. Samples were then diluted 1:2 in nuclease free water, before qPCR analysis using HBV4 primer sets. PCR amplification protocol: 2 minutes at 95ºC, followed by 45 cycles of 5 seconds at 95ºC, and 30 seconds at 65ºC, followed by high resolution melting profile.

Table 2.12: Extracellular rcDNA quantification

Master Mix: 1 Reaction	
Input DNA	4 μL
2x SYBR Green	10 μL
ddH2O	5.5 μL
HBV4 Primers (F/R)	0.5 μL
Total reaction volume	20 μL

2.6: Cellular protein extraction

Protein lysates

In order to extract protein for western blotting, samples were routinely lysed in either RIPA (20 mM Tris pH 7.5; 2 mM EDTA; 150 mM NaCl; 1% IGEPAL + Protease inhibitor) or Urea (8 M urea; 150 mM NaCl; 20 mM Tris pH7.5; 0.5 M β-mercaptoethanol) lysis buffer. Supernatants were aspirated, and cells washed twice in PBS. Lysis buffers were added directly to the cell surface and incubated for 5 minutes, before scraping and transfer of lysates to 1.5 ml tubes for storage at -20°C.

Acetone precipitation of protein

During the isolation of RNA using on column methods, it is possible to also extract protein from these samples using biproducts that would ordinarily be disposed of. Following RLT lysis and precipitation in 70% ethanol, the column flow through was added to at least 2 volumes of ice-cold acetone. Protein precipitates were incubated on ice, or at -20°C for 30 minutes. Samples were then centrifuged at >16,000 x *g* for 30 minutes. Protein pellets were washed once in ice cold 100% ethanol and span for a further 10 minutes. Supernatant was aspirated, and the pellet allowed to dry, before resuspension in an appropriate lysis buffer.

2.7: Western blotting: lysate preparation and immunoblotting

Protein concentration in cellular lysates was determined by Bicinchoninic acid assay (BCA), whereby 5µl of lysate was mixed with 95 µl of Pierce reagent and incubated for 60 minutes. Following colorimetric development, absorbance was measured at 592 nm using Clariostar (BMG) and protein concentration was determined by interpolation from a standard curve of known concentrations of albumin. Lysates were sonicated for 2 minutes, 30s on/off, high (Diagenode), then mixed with 4x Laemmli sample buffer (Tris-HCL pH 8, 0.0625 M; 2% SDS; 10% glycerol, 5% 2-mercapto ethanol and bromophenol blue). Samples were boiled for 10 minutes at 95°C, then rested on ice for 10 minutes before loading equal concentrations of each sample. Proteins were resolved on an 8-12% polyacrylamide gel (based on target protein size), then transferred to a methanol activated PVDF membrane (Amersham). Following transfer, membranes were blocked in PBST (PBS; 0.1% Tween), 5% skimmed milk (Sigma), and incubated overnight in primary antibody at 4°C. Membranes were washed thrice in PBST and incubated at room temperature with appropriate HRP-conjugated secondary antibodies diluted in blocking solution. Proteins bands were detected using Pierce SuperSignal West Pico chemiluminescent substrate kit (Thermofisher) and images collected with a G-Box mini (Syngene). Where densitometric quantification was performed, band intensity was adjusted to host housekeeping gene (β-Actin) using ImageJ (Schneider et al., 2012).

2.8: HBV E and S antigen ELISA

Supernatants were taken from HBV infected cells, typically 200 µl, which would allow for quantification of both HBe and HBs antigens (HBe-, HBs- Ag), as well as quantification of viral DNA. Supernatants were clarified by centrifugation to pellet any cellular debris, as a freeze-thaw cycle would result in cell lysis and subsequent release of viral proteins.

HBe and HBs Ag were quantified using the chemi-luminescent ELISA assay (AutoBio, China) as per the manufacturer's instructions. 50 µl of clarified supernatant or standards were mixed with 50 µl of HRP-enzyme conjugate and incubated for 30 minutes at 37°C. Wells were aspirated and washed 6 times in 200 µl of ELISA wash buffer, taking care not to scratch the surface of the well with the tip. Following the final wash, wells were incubated with a 1:1 mixture of development substrates A&B (AutoBio, China) and left at room temperature for 10 minutes. Luminescence was then read on an BMG Omega plate reader, and viral antigen expression enumerated by interpolation from a standard curve. In the instance of clinical samples, HBsAg was quantified from the plasma using the integrated LIASION-XL Murex HBsAg Quant chemiluminescence system (DiaSorin).

2.9: Luciferase assays

Intracellular renilla or firefly reporter constructs

HepG2-NTCP cells were transfected using Fugene-6 (Promega) with pRL-SV40 construct as described in *Transfections* and transferred to their relevant experimental conditions. Cells were then lysed in 100 µl of passive lysis buffer (Promega), and luciferase activity quantified using Luciferase Assay kit (Promega), with readings taken on a Centro LB960 Microluminometer.

Extracellular gaussia luciferase

rHBV-GLuc, an HBV reporter virus encoding secreted gaussia luciferase was generated as previously reported (Wing et al., 2019). HepG2-NTCP cells were infected with rHBV-GLuc for 6 hours then cultured for 72 hours in either 18% or 1% oxygen. Supernatants were harvested, and mixed 1:1 with 500 µg/ml Coelenterazine (PJK, Germany) in PBS, and luciferase activity read on a FluoSTAR Omega plate reader (BMG).

2.10: Chromatin immunoprecipitation

Cell preparation, fixation and harvesting

Cell culture

1 x 10^7 HepG2-pEpi cells were seeded per 15cm culture dish, keeping a volume of 20 ml of culture media, in the absence of G418. Cells were left over night, to achieve around 75% confluence at time of treatment. After the duration of the treatment, cells were checked to ensure that cell density and viability did not significantly differ between conditions, as this would have adverse effects on the level of input material. Cells were fixed and crosslinked with 1% formaldehyde (prepared in 20 ml culture media) and incubated on ice for 10 minutes with frequent gentle rocking. Cells were then quenched with Glycine (1 M in PBS) at a final concentration of 125 mM (2.5 ml of stock per 20 ml of culture media) and incubated for 10 minutes at room temperature with frequent gentle rocking. Media was aspirated, and cells were washed twice in ice cold PBS. Cells were then scraped using a rubber cell scraper into 5 ml of ice-cold PBS, and cell suspensions transferred to 15 ml falcon tubes. Suspensions were pelleted at 800 rpm, for 10 minutes at 4^{o}C. Supernatants were discarded and cell pellets resuspended and lysed in SDS Lysis buffer (1% SDS; 10 mM EDTA; 50 mM Tris pH 8.1) supplemented with 2x complete protease inhibitor cocktail (40 µl per 960 µl of buffer). At this point, the lysates are stable and can be stored at -80^{o}C until needed (Wing et al., 2021).

Tissue

To extract chromatin from snap frozen liver samples, small sections of tissue were taken, thawed, and homogenised in DMEM containing 1% formaldehyde. A motorised tissue homogeniser was used, to ensure thorough disruption of the tissue. Lysates were then quenched with Glycine (1M in PBS) at a final concentration of 125 mM and incubated for 10 minutes at room temperature with frequent gentle rocking. Suspensions were centrifuged at 1,500 rpm for 4 minutes, and washed twice in ice cold PBS. Supernatants were discarded, and cell pellets resuspended and lysed in SDS Lysis buffer (1% SDS; 10 mM EDTA; 50 mM Tris pH 8.1) supplemented with 2x complete protease inhibitor cocktail (40 µl per 960 µl of buffer) (Wing et al., 2021).

Sonication

Lysates were diluted 1:1 with ChIP dilution buffer (0.01% SDS; 1.1% triton X-100; 1.2 mM EDTA; 16.7 mM Tris pH 8.1; 167 mM NaCl), prior to sonication. Lysates were transferred to Diagenode bio-ruptor falcon tubes, and then sonicated: 15s on, 15s off, High, for up to 30 minutes, in a Diagenode waterbath sonicator. Sonicated lysates were transferred to 1.5 ml Eppendorf tubes and centrifuged at 13,000 rpm for 10 minutes, at 4^{o}C. If the supernatant remained cloudy, centrifugation was be repeated. Once cleared, a 2% input control was taken and stored at -20^{o}C (Smythies et al., 2019).

Pre-clear and immunoprecipitation

For pre-clear and immunoprecipitation, proteinase A agarose beads were washed twice in 800 µl of ChIP dilution buffer (5 minutes on an over-end rotator, at

4ºC followed by centrifugation at 2,000 rpm for 3 minutes, 4ºC). 40 µl of beads per condition were used for pre-clear. Samples were transferred to 15 ml falcon tubes, diluted 1 in 6 with ChIP dilution buffer, and washed Protein A Agarose beads (Millipore, 16-156) were added. Samples were incubated on an over-end rotator for 1 hour at 4ºC, followed by centrifugation at 1,000 rpm for 5 minutes, 4ºC. Supernatants were transferred to new falcon tubes for immunoprecipitation with 3-5 µg of antibodies of interest or irrelevant IgG control.

Pull-down, washing and elution

90 µl of washed bead slurry was added to the immunoprecipitate and incubated at 4ºC for 90 minutes on an over-end rotator. Samples were centrifuged at 380 x *g* for 8 minutes at 4ºC to harvest the beads. Supernatants were discarded, and beads transferred to 1.5 ml Eppendorf tubes in 800 µl of low salt wash buffer (0.1% SDS; 1% Triton X-100; 2 mM EDTA; 20 mM Tris pH 8.1; 150 mM NaCl), and then pelleted at 2,000 rpm for 3 minutes at 4ºC. Supernatants were discarded without disruption of the pellet and resuspended in high salt wash buffer (0.1% SDS, 1% Triton X-100; 2 mM EDTA; 20 mM Tris pH 8.1; 500 mM NaCl), then pelleted as above. Beads were washed in 800 µl lithium chloride wash buffer (1% Igepal; 1 mM EDTA; 10 mM Tris pH 8.1; 250 mM LiCl; 1% sodium deoxycholate), and pelleted as above. Beads were then washed twice in TE wash buffer (10mM Tris pH 8.0; 1mM EDTA) and centrifuged after each wash. Finally, to elute the DNA complexes from the beads 240 µl of elution buffer (0.1 M sodium hydrogen carbonate, 1% SDS) was added, then incubated on a heated shaker (1400rpm, room temperature for 15 minutes) and then centrifuged at 2,000rpm for 3 minutes. Supernatants were transferred to a new Eppendorf tube, and beads discarded. 240 µl of elution buffer was added to the 2% input controls.

Reversal of cross-linking and proteinase K digestion

Eluates were supplemented with 12.5 µl of 4 M NaCl, and incubated overnight on a heated shaker at 65ºC, 1400 rpm. Following decrosslinking, eluates were cooled and treated with 2 µl of 20 mg/ml proteinase K for 4 hours at 45ºC, 1400 rpm. Digested eluates were then treated with 1 µl RNaseA and incubated on a heated shaker, 1400 rpm, 37ºC for 30 minutes. Samples were then cleaned up using Qiagen MinElute PCR Purification Columns (*See Nucleic Acid Extraction*). Inputs and immunoprecipitates were diluted 1 in 4, and transcription factor binding assessed by qPCR.

2.11: HBV Infection

Routinely, 2.5 x 10^4 HepG2-NTCP cells/cm^2 were seeded in a collagen-coated 24 well plate and left overnight to adhere. Media was replaced and cells were inoculated with HBV MOI 300 and 4% PEG for 6 hours (NB: MOI is expressed as genome equivalent per cell; GE/cell). Following inoculation, cells were thoroughly washed thrice in PBS, and experimental media added. At this point drug treatments could be applied, and this has been referred to throughout as post infection.

Generation of HBV stocks

Ordinarily, HBV was purified from HepAD38 cells and the infectious titre measured following heparin column purification (Ko et al., 2018). For small scale experiments, such as assessing the infectivity of virus generated in specific experimental conditions, a revised protocol was adopted. Typically, HepAD38 cells

were treated for up to six days, with supernatant collection and media replenishment at 3d and 6d post treatment. Supernatants were stored at 4°C for short term storage but kept at -80°C long term. Virus was PEG precipitated in a final concentration of 8% PEG, overnight at 4°C, before centrifugation at 4,000 x *g* for 1 hour in a 4°C centrifuge. Supernatants were discarded and pellets resuspended in 250 µl DMEM. Viral DNA levels were then quantified following extraction with QIAamp MinElute Virus Spin kit, as described above. Viral titre was determined by qPCR using HBV rcDNA primer pair, and copy number interpolated from a standard curve.

Ad-HBV-GFP transduction

Ad-HBV-GFP stocks were produced as previously reported. Infectious virus was harvested from the extracellular media of HEK-293T cells transduced with an adenoviral vector encoding a 1.3-times overlength HBV genome and GFP reporter (Sprinzl et al., 2001). HepG2-NTCP cells were seeded at standard seeding density of 2.5 x 10^4 cells/cm^2 before transduction with Ad-HBV-GFP (a 1.3x HBV genome, encoded in an adenoviral vector) at an MOI of 20 focus forming units (ffu)/cell. Cells were inoculated for 2 hours, before thorough washing with PBS, and subsequent application of experimental conditions. Typically, extracellular HBV DNA was analysed by qPCR as described above, and cells were lysed for protein or nucleic acid detection.

Generation of Vpx-Viral like particles

HEK-293T cells were plated in poly-L-lysine coated 10cm dishes 24 hours pre-transfection at around 80% confluency. Cells were transfected with 2 µg of SIV3+ (Vpx+) or SIV4+ (Vpx-), with 2 µg of VSVg envelope plasmid using

Fugene6 in a 1:3 ratio. Cells were left overnight before a media change, then supernatants were harvested and filtered at 48 and 72 hours post transfection. Filtered supernatants were aliquoted and stored at -80°C (Hrecka et al., 2011; Laguette et al., 2011; Wing et al., 2019).

2.12: Flow cytometry: determining cell cycle phase

Harvesting and fixation

HepG2-NTCP cells were seeded at low density (5 x 10^4 cells/cm^2) which would provide around 90% confluence at the end of the treatment, so to avoid contact inhibition interfering with cell cycle progression. Typically, cells were allowed to adhere overnight, then media changed and treatment applied for the duration as indicated in the appropriate figure.

At the end of the treatment protocol, cells were treated with 10 µM bromodeoxyuridine (BrdU) (Sigma) and incubated for 30 minutes at 37^{o}C maintaining the treatment conditions of the experiment. Cells were then trypsinised, pelleted at 1,200 rpm for 5 minutes and washed in PBS. Supernatants were aspirated and cells were fixed in 1 ml of ice cold 70% ethanol, whilst gently vortexing. At this stage samples were stable and could be stored at 4^{o}C until ready to stain and analyse.

Staining and sample preparation

Samples were pelleted at 1,200 rpm for 5 minutes, supernatant aspirated, then incubated in pre-warmed pepsin solution (1 mg/ml Pepsin; 30 mM HCl) for 30 minutes at 37^{o}C with frequent shaking. Samples were then pelleted at a higher speed to pellet nuclei, 4,000 rpm for 4 minutes. After this step, samples did not

appear as a distinct pellet but form a white halo shape in the bottom of the FACs tubes. Pepsin solution was aspirated, and pellets were disrupted and incubated for 15 minutes in 2 M HCl. Samples were then washed twice in PBS, with centrifugation at 4,000 rpm for 5 minutes. Supernatants were discarded, and samples were blocked for 30 minutes at room temperature (blocking solution: 0.5% BSA; PBST). Samples were pelleted and incubated in staining solution (1:10 dilution of anti-BrdU-488 antibody) for 30 minutes, at room temperature, wrapped in foil to preserve the fluorophore. Finally, samples were incubated in 300 µl of propidium iodide/RNAseA solution (Thermofisher) for 30 minutes at room temperature, before acquisition on CyAn (Beckman Coulter) (Davenne et al., 2020; Wing et al., 2021).

2:13: Human liver biopsy samples

Liver biopsy samples from chronic HBV infected patients (n=26) or non-infected subjects (n=8) were collected with informed consent, under the ethical committee approval (CE90/19). A small fragment of the biopsy specimen was allowed to be used for research purposes, beyond the requirements for complete pathological examination, in conjunction with anonymized demographic and clinical data. Samples were stored in RNAlater at -80^{o}C or fixed in 10% buffered formalin. Paraffin embedded sections were stained with haematoxylin and eosin, Masson's trichrome and silver impregnation. Pathological examination was performed, and samples were scored and graded as determined by the Ishak criteria (Ishak et al., 1995). IHC for viral proteins were performed using a BENCHMARK XT staining system (Ventana Medical Systems) using specific monoclonal antibodies against HBsAg (Santa Cruz) or HBcAg (Leica Biosystems).

With thanks to collaborators at the University of Piedmont for provision of liver biopsy samples and clinical data.

Human liver chimeric mice

FNRG-NOD mice were housed and bred at the INSERM U1110 animal facility (regional agreement n°E-67-482-7) and fed 2-(2-nitro-4-trifluoromethylbenzoyl)-1,3-cyclohexanedione (NTBC) in their drinking water at 16 mg/l. Once six weeks old, mice were transduced with urokinase-like plasminogen encoded in an adenoviral vector ($1.5x10^9$ pfu), and NTBC treatment reduced to 8 mg/l. 48 hours later, animals with transplanted with 10^6 cryopreserved PHHs (Life technologies) intrasplenically and fed 0.8 mg/l NTBC. Dosage of NTBC was reduced every two days following transplantation to 0.4 mg/l, 0.2 mg/L then withdrawn completely. 8 weeks post transplantation, efficiency of engraftment was determined by measuring human albumin levels by ELISA (Bethyl). Mice with sufficient engraftment were infected with 10^9 HBV genome equivalents derived from HepG2.2.15 supernatants. Four weeks post infection animals were sacrificed and liver samples snap frozen for qPCR and ChIP analysis (Liu et al., 2020b; Zhuang et al., 2021).

2.14: Bioinformatic analysis

RNA-Sequencing

RNAs were extracted using RNeasy kit as described above, including on-column DNAse digestion. RNA integrity was assessed using RNA Screen tape and TapeStation (Agilent), and concentration calculated by Nanodrop (ThermoFisher). 2 µg of high integrity RNA (RIN>8) was sent to Novogene (UK)

for poly-A-enriched RNA-sequencing, using 300bp pair end reads on an Illumina sequencing platform.

Alignment, mapping and differential expression analysis

300bp fragments were aligned to the human reference genome (GRCh38/hg38, GCA_000001405.05) using HISAT2 algorithm to map to introns, exons and intergenic regions. Intergenic reads can usually be attributed to poor annotation of the referent genome and do not constitute more than 2% of reads in any of our samples. Once reads were mapped to genes, CPM was calculated to adjust to the library size, and differential expression was performed using a DESEQ2 package in R (Love et al., 2014). Differentially expressed genes were classed as significant based upon a $\log_2$FC of +/- 1, and an adjusted p-value (Benjamini-Hochberg) of less than 0.05. Following host gene mapping by Novogene, we used STAR aligner (Dobin et al., 2013) to map reads to the HBV genome, genotype D (ayw strain), and generated BAM files to assess splice junctions in Salmon (Patro et al., 2017). Viral reads were aligned to the HBV pgRNA ORF, as per a recent study by Lim et al. (Lim et al., 2021).

Gene set enrichment analysis

Gene Set Enrichment Analysis (GSEA) was carried out in GSEA_4.1.0 (Subramanian et al., 2007), using gene sets of interest and Hallmark gene sets obtained from the Molecular Signatures Database (MSigDB) or from internal RNA-sequencing data (Edgar et al., 2002; Liberzon et al., 2015; Liberzon et al., 2011). 1000 permutations and phenotype grouping were ran as standard, with genes

sorted according to the t-Test function. Exploratory FDR of 0.25 was used as a threshold for statistical significance. Data sets explored are documented under *Data Deposition*.

Pathway analysis

Further to using the Hallmarks gene set from MSigDB, the PantherDB was used to test for over-representation of genes of interest in previously documented Gene Ontology: Biological Processes (Mi et al., 2021). Testing was performed using a Fishers Exact test, and p-values adjusted using Bonferroni method. Redundancy was accounted for by using REVIGO (Supek et al., 2011), with medium output and further refined for pathways were at least 50% of the genes of interest were present.

nCounter

Gene expression was quantified using nCounter technology (NanoString) (Eastel et al., 2019). 50 ng of RNA derived from human biopsy samples were incubated with a probe set mapping to 249 human inflammatory transcripts and a panel of 30 custom genes, at 65^{o}C for 16 hours. Samples were then diluted in DEPC-water and loaded into cartridges, and fluorescence detected using nCounter (Nanostring) (Eastel et al., 2019). Gene expression values were adjusted to the geometric mean expression of a panel of 6 housekeeping genes (CLTC, GAPDH, GUSB, HPRT1, PGK1, TUBB) using the nSolver program.

Single cell expression analysis

Single cell expression TSNE plots were generated as previously described (Aizarani et al., 2019; Juhling et al., 2021). Plotexpmap function in RaceID3

package for R was employed to create overlay log_2-transformed expression of inflammatory gene signature.

Human and non-human Hepadnaviridae phylogeny

Referent genome sequences for a diverse panel of *hepadnaviridae* were obtained from the HBV database (Hayer et al., 2013) and NCBI, then interrogated for the HRE (RCGTGC) motif (Wenger et al., 2005). A neighbour-joining phylogenetic tree (Saitou and Nei, 1987; Wing et al., 2021) was constructed from the following sequencing: Snow goose; NC_005950.1, Duck; NC_001344.1, Sheldgoose; NC_005890.1 and Ross's goose; NC_005888.1. Heron; NC_001486.1, Tinamou; NC_035210.1 and Parrot; NC_016561.1. Tibetan frog; NC_030446.1, White sucker fish; NC_027922.1 and Bluegill fish; NC_030445.1. Tent-making bat; NC_024445.1, Horseshoe bat; NC_024444.1, Roundleaf bat; NC_024443.1 and Long-fingered bat; NC_020881.1. Woolly monkey; NC_028129.1 and Capuchin Monkey; KY703886. Woodchuck; M19183.1 and Ground squirrel; NC_001484.1. Orangutan; F193863, Gorilla; FJ798097 and Chimpanzee; FJ798098. Human: Genotype (Gt) A; EU054331, X02763, Gt B; AB219428, D00331 Gt C; GQ924620, GQ358158, Gt D; AF121240, FJ904433, Gt E; AB106564, AY738145, Gt F; AY090458, X75658, Gt G; AB064313, AF160501 and Gt H; AY090454, FJ356716.

Human viruses genome analysis

Using the ViralZone Database (Hulo *et al.*, 2011), we accessed a list of all viruses known to infect humans. We interrogated NCBI to obtain the length of the viral genomes (bp), as well as the nature of the nucleic acid. Genome sequences were accessed from NCBI, under the following accession numbers. Hepatitis D

virus (NC_001653); Hepatitis B virus (NC_003977); Rotavirus A (NC_110507); Rotavirus C (NC_007547); Junin arenavirus (NC_005080); Rotavirus B (NC_007548); Banna virus (NC_004217); Torque teno virus (NC_002076); Adeno-associated virus (NC_001401); KI polyomavirus (NC_009238); JC polyoma (NC_001699); BK polyomavirus (NC_1538); WU polyomavirus (NC_009539); Merkel cell polyomavirus (NC_010277); Human parvovirus B19 (NC_000883); Uukuniemi virus (NC_005220); Hantaan virus (NC_00522); Lymphocytic choriomeningitis virus (NC_004294); Astrovirus (NC_001943); Bunyamwera virus (NC_001926); Le Crosse (NC_004109); Human rhinovirus (NC_001617); Hepatitis E virus (NC_001434); Machupo virus (NC_005078); Lassa virus (NC_004296); Echo virus (NC_001897); Enterovirus 68 (NC_001430); Coxsackie virus (NC_001612); Polio virus (NC_002058); Sapporo virus (NC_006554); Hepatitis A virus (NC_001489); Cosavirus A (NC_012800); Norwalk virus (NC_001959); Human papillomavirus 1 (NC_001356); Encephalomyocarditis virus (NC_001479); Human papillomavirus 2 (NC_001352); Human papillomavirus 16 (NC_001526); Salvivirus A (NC_012957); Aichi virus (NC_001918); Human T-cell lymphotropic virus (NC_001436); Rosavirus A (NC_024070); Human immunodeficiency virus (NC_001802); GB virus (NC_001710); Hepatitis C virus (NC_004102); Rubella virus (NC_001545); Dengue virus (NC_001477); Zika virus (NC_012532); Tick-borne powassan virus (NC_003687); Yellow fever virus (NC_002031); Louping ill virus (NC_001809); St Louis encephalitis virus (NC_007580); Langat virus (NC_003690); West Nile virus (NC_001563); Japanese encephalitis virus (NC_001437); Murray valley encephalitis virus (NC_000943); Vesicular somatitis virus (NC_001560); Mayaro virus (NC_003417); Semliki forest virus (NC_003215); Venezuelan equine encephalitis virus

(NC_001449); Western equine encephalitis virus (NC_003908); Barmah forest virus (NC_001786); Ross river virus (NC_001544); Eastern equine encepahlitis virus (NC_003899); Sindbis virus (NC_001547); Australian bat lyssavirus (NC_003243); Chikungunya virus (NC_004162); O'nyong-nyong virus (NC_005576); Rabies virus (NC_001542); Mokola virus (NC_006429); European bat lyssavirus (NC_009527); Crimean-Congo haemorrhagic fever virus (NC_005300); Dugbe virus (NC_004157); Simian foamy virus (NC_001364); Human respiratory syncytial virus (NC_001781); Mumps virus (NC_002200); Human parainfluenza (NC_003461); Measles virus (NC_001498); Hendra virus (NC_001906); Nipahi virus (NC_0027728); Ebola virus (NC_002459); Marburg virus (NC_001608); Coronavirus (NC_002645); Human SARS coronavirus (NC_004718); SARS-CoV-2 (NC_045512.2); MERS coronavirus (NC_019843); Adenovirus (NC_001405); Varicella-zoster virus (NC_001348); Yaba monkey tumour virus (NC_005179); Kaposi's sarcoma (KS)-associated herpesvirus (NC_009333); Orf virus (NC_006439); Yaba-like disease virus (NC_002642); Cercopithecine herpes virus (NC_006560); Herpes simplex 1 (NC_001806); Human herpes virus 7 (NC_001716); Herpes simplex 2 (NC_001798); Human herpes virus 6 (NC_001664); Epstein-Barr virus (NC_007605); Variola virus (NC_001611); Molluscum contagiosum (NC_001731); Vaccinia virus (NC_006998); Monkeypox virus (NC_003310); Cowpox virus (NC_003663); Cytomegalovirus (NC_006273.2).

2.15: Statistics

All plots were generated in GraphPad Prism version 9 unless stated otherwise. Statistical tests were carried out using inbuilt analysis features of prism, and the tests used are indicated in each figure legend. Data are plotted as mean and SD, unless stated otherwise. Throughout: * indicates p <0.05; ** p<0.01; *** p<0.001 and **** p<0.0001.

2.16: Data deposition

Table 2.13: Data deposition

Dataset	Type	Accession ID	Reference
HepG2 0.5% Oxygen	RNA-Seq	GSE120886	Smythies et al. 2019
HepG2 0.5% Oxygen	HIF ChIP-Seq	GSE120885	Smythies et al. 2019
HepG2-NTCP (O2 and QC6352)	RNA-Seq	GSE186279	
Human Hepatoma Lines	RNA-Seq		Chakraborty et al. 2020
CHB Cohort	Affymetrix	GSE83148	Zhou et al. 2017
CHB Pirisi Cohort	nCounter	GSE169110	
CHC Cohort	Affymetrix	GSE14323	Mas et al. 2009
TMT Proteomics	PRIDE	PXD020086	Wing et al. 2021
HBV (O2, FG-4592, QC6352)	RNA-Seq	GSE186178	

2.17: Sequence-based reagents

Table 2.14: qPCR primer sequences

qPCR primer sequences		
B2M	Forward	CTACACTGAATTCACCCCCACTG
	Reverse	ACCTCCATGATGCTGCTTACATG
ACTB	Forward	CCAACCGCGAGAAGATGA
	Reverse	CCAGAGGCGTACAGGGATAG
RPLP0	Forward	GCAATGTTGCCAGTGTCTG
	Reverse	GCCTTGACCTTTTCAGCAA
T1	Forward	GGGGAACTAATGACTCTAGCTACC
	Reverse	TTTAGGCCCATATTAGTGTTGACA
T2	Forward	CAAGGTAGGAGCTGGAGCATTC
	Reverse	GAGGCAGGAGGCGGATTTG
T3	Forward	CTCCAGTTCAGGAACAGTAAACCC
	Reverse	AGGAATCCTGATGTGATGTTCTCC
T4	Forward	ACGGGGCGCACCTCTCTTTA
	Reverse	GTGAAGCGAAGTGCACACGG
T5	Forward	TTTCACCTCTGCCTAATCATCTCT
	Reverse	CTTTATAAGGGTCAATGTCCATGC
T1G	Forward	AGACCACCAAATGCCCCTATC
	Reverse	TTGAGATCTTCTGCGACGCG
rcDNA	Forward	GTTGCCCGTTTGTCCTCTAATTC
	Reverse	GGAGGGATACATAGAGGTTCCTTGA
cccDNA	Forward	GCCTATTGATTGGAAAGTATGT
	Reverse	AGCTGAGGCGGTATCTA
HBV4	Forward	TTTCACCTCTGCCTAATCATCTCT
	Reverse	CTTTATAAGGGTCGATG CCATGC
KDM4A	Forward	AGCTTGCTTAAAGGCTGACG
	Reverse	GAAGTTTCAGTGAGCGGGAG
KDM4B	Forward	ATCTTGACCATGTCCTTCCG
	Reverse	TCAACTGCGCAGAATCTACC
KDM4C	Forward	CTTTCCTGCAAGTGCACAAT
	Reverse	CCATGCTGGTTTTAATCATGG
KDM4D	Forward	GTGGGAGTGAAGAGCACACA
	Reverse	CAGTTACCCAGGAGAGCAGC
CA9	Forward	CTTGGAAGAAATCGCTGAGG
	Reverse	TGGAAGTAGCGGCTGAAGTC
NDRG1	Forward	TTTGATGTCCAGGAGCAGGA
	Reverse	ATGCCGATGTCATGGTAGGT
BNIP3	Forward	GCTCCCAGACACCACAAGAT
	Reverse	GAGAGTAGCTGTGCGCTTC
PrP	Forward	TGCTGGGAAGTGCCATGAG
	Reverse	CGGTGCATGTTTTCACGATAGTA
ACTB (Mouse)	Forward	CATTGCTGACAGGATGCAGAAGG
	Reverse	TGCTGGAAGGTGGACAGTGAGG

Table 2.15: ChIP PCR primer sequences

ChIP PCR primer sequences		
HepB1	Forward	GTCTGTGCCTTCTCATCTGCC
	Reverse	AGACCTTGGGCAATATTTGGTGG
HepB3	Forward	GGGGAGGAGATTAGGTTAAAGGTC
	Reverse	CAAGAGATGATTAGGCAGAGGTGA
cccDNA	Forward	CCGTGTGCACTTCGCTTCA
	Reverse	GCACAGCTTGGAGGCTTGA
CA9	Forward	TCTCGTTTCCAATGCACGTACAGC
	Reverse	AGTGACAGCAGCAGTTGCACAGT
NDRG1	Forward	TCCCTCCCAATCTCTCTCTTCTT
	Reverse	CACCATCAGCACAGCAAACTAC
BMAL1	Forward	TTGGGCACAGCGATTGGT
	Reverse	GTAAACAGGCACCTCCGTCC
yGlobin	Forward	GCCTTGACCAATAGCCTTGACA
	Reverse	GAAATGACCCATGGCGTCTG
APOB	Forward	GCATGTGAGGGTGAGGAAAT
	Reverse	GAGTCCAGCTGCAGTGATGA
RORE	Forward	TTACACACTCTATGGAAGGCGG
	Reverse	AAAGATTCTGCCCCATGCTGTA
HepB15	Forward	CTCCAGTTCAGGAACAGTAAACCC
	Reverse	AGGAATCCTGATGTGATGTTCTCC
HepB16	Reverse	CGGTAGTTCCCCCTAGAAAATTGA
HepB17	Reverse	CAGCAGGATGAAGAGGAAGATGAT
HepB18	Reverse	TTCCTTGAGCAGTAGTCATGCAG
HepB19	Reverse	TAGTAAACTGAGCCAGGAGAAACG
HepB20	Reverse	ACCCAAAGACAAAAGAAAATTGGT
HepB21	Reverse	AGGCCTGTTAATAGGAAGTTTTCT

Table 2.16: Plasmids and constructs

Plasmids and Source	
HBV1.3 Gt A1	A kind gift from Professor Peter Revill
HBV1.3 Gt A2	A kind gift from Professor Peter Revill
HBV1.3 Gt B1	A kind gift from Professor Peter Revill
HBV1.3 Gt B2	A kind gift from Professor Peter Revill
HBV1.3 Gt C1	A kind gift from Professor Peter Revill
HBV1.3 Gt C2	A kind gift from Professor Peter Revill
HBV1.3 Gt D3	A kind gift from Professor Peter Revill
HBV1.3 Gt E	A kind gift from Professor Peter Revill
HBV1.3 Gt Fic	A kind gift from Professor Peter Revill
HBV1.3 Gt H	A kind gift from Professor Peter Revill
D3_WT Mut_pUC57	A kind gift from Professor Peter Revill
H 1.3mer MUT_UC57	A kind gift from Professor Peter Revill
pRL-SV40	Promega E2231

Table 2.17: siRNAs

siRNA	Supplier	Product Code
HIF-1α	Ambion	4390824; s6539
HIF-2α	Ambion	4390824; s4700
KDM4A	Thermofisher	Duan et al. 2015
KDM4B	Thermofisher	Duan et al. 2015
KDM4C	Thermofisher	Duan et al. 2015
KDM4D	Thermofisher	Duan et al. 2015
Scramble	Ambion	4390824

2.18: Antibodies

Table 2.18: Antibodies

Antibody	Application	Supplier	Product Code
Alexa Flour 488 Mouse anti-BrdU	FACs	Biolegend	364105
Anti-HNF4α ChIP	ChIP	Abcam	Ab181604
Anti-RORA ChIP	ChIP	Sigma	SAB4502650
ECL anti-rabbit IgG, HRP linked whole antibody	Western Blot	GE Healthcare Life Sciences	NA934V
H3	Western Blot		
H3K27me3	Western Blot	Active Motif	
H3K4me3	Western Blot	Active Motif	
H3K9me3	Western Blot	Active Motif	
KDM4A	Western Blot		
Mouse anti- β-actin	Western Blot	Sigma	A5441
Mouse anti-HIF-1α	Western Blot	BD Transduction Labs	610959
Mouse anti-HIF-2α	Western Blot	Novus	NB100-132
Mouse-pAb to SAMHD1	Western Blot	Abcam	Ab67820
Polyclonal goat anti-mouse immunoglobulins HRP	Western Blot	Dako	P0447
Rabbit anti-HIF-1 β	ChIP	Novus	NB100-110
Rabbit anti-HIF-1 β (ARNT1)	Western Blot	Novus	NB100-110
Rabbit anti-HIF-1α ChIP	ChIP	A kind gift from Professor Peter Ratcliffe	
Rabbit anti-HIF-2α ChIP	ChIP	A kind gift from Professor Peter Ratcliffe	
Rabbit anti-Phospho SAMHD1 (Thr592)	Western Blot	CST	89930
Rabbit Serum	ChIP	Agilent	X090210-8

Chapter 3: Hypoxic gene expression in chronic hepatitis B infection

3.1: Introduction

The liver provides a naturally low oxygen environment for HBV to replicate in. The physiology of the liver generates a hypoxic gradient, and hepatocytes across the lobule experience different oxygen tensions that associates with distinct metabolic zonation and function (Aizarani et al., 2019; Halpern et al., 2017; Kietzmann, 2017; MacParland et al., 2018; Wilson et al., 2014b). There is a clear link between inflammation, immune responses and hypoxia signalling, and we sought to investigate the contribution of HIFs to the hepatic transcriptome in the context of HBV infection (Cramer et al., 2003; Imtiyaz and Simon, 2010; McMahon *et al.*, 2006; Zhou *et al.*, 2003).

In this chapter we investigate HIF gene expression in the CHB liver, and use a hepatocyte derived hypoxic gene signature to study the relationship between HIF signalling and inflammatory disease. We highlight the importance of understanding the hypoxic response in tissues and organs of interest, and note the limitations of previously published gene sets which originate from a diverse range of cell lines and conditions when performing pathway analyses (Liu et al., 2020b). We present a simple PCR based approach to quantify HBV transcript patterns and validate this in routinely used laboratory models (D'Arienzo et al., 2021b). We use this assay to study HBV transcript patterns in the HBeAg negative stage of CHB and developed primers to discriminate between episomal cccDNA and integrant derived viral RNAs. We employ nCounter Nanostring technology to

study the hepatic inflammasome, and identify a gene signature which associates with cccDNA transcriptional activity in HBeAg negative patients.

3.2: Host gene expression in the CHB liver

In order to study the interplay between hypoxia signalling, inflammation and HBV replication, we searched the Gene Expression Omnibus (GEO) for datasets from CHB cohorts which included non-viral infected subjects (Edgar et al., 2002). We identified a cohort of n=128 CHB patients where hepatic gene expression was quantified using an Affymetrix microarray (Zhou et al., 2017). Of these, n=122 had been diagnosed with HBV, whilst n=6 patients were not virally infected. Peripheral HBV DNA was defined as either low or high (low < 10^6 IU/mL, high >= 10^6 IU/mL), and both alanine aminotransferase (ALT) and aspartate aminotransferase (AST) values were classified as low (< 40 IU/mL) or high (>= 40 IU/mL). We excluded patients where HBV DNA had not been quantified, leaving a sample size of n=90 CHB patients (**Figure 3.1A**).

To define host pathways that were upregulated in the CHB patients (n=90) compared to the control subjects (n=6), we employed Gene Set Enrichment Analysis (GSEA) (Mootha et al., 2003; Subramanian et al., 2007; Subramanian et al., 2005). As there is a great deal of redundancy and overlap amongst commonly used pathway analysis platforms such as Gene Ontology, KEGG, and Reactome, we opted to utilise the hallmarks gene sets from the molecular signatures database (MSigDB) (Liberzon et al., 2015; Liberzon et al., 2011). The hallmarks were designed using an algorithm to minimise redundancy and maintain high confidence and specific gene sets to represent 50 common cellular processes (Liberzon et al., 2015). GSEA showed that 28 of 50 hallmarks were significantly upregulated in the CHB patients. Routinely, GSEA recommends using an exploratory false discovery rate (FDR) cut off of 0.25 (25%), however we opted to

increase the stringency of our analyses and used a statistical cut off of FDR < 0.1 (Subramanian et al., 2005). This analysis identified genes associated with 'allograft rejection' as the most significantly enriched in the CHB cohort; of note HIF-1α was recorded as a leading-edge gene in this pathway, contributing significantly to the core enrichment score. Amongst other hallmarks, we observed an enrichment of 'hypoxia' genes in the CHB liver, as well as genes associated with inflammatory signalling pathways such as TNF-α, NF-κB, and IFN-γ (**Figure 3.1B**) (Liu et al., 2020b). Since we noted an upregulation of the hypoxia hallmark in CHB, we searched the MSigDB using 'HIF' or 'Hypoxia' as key words to identify previously published or documented hypoxic gene signatures (Liberzon et al., 2015; Liberzon et al., 2011). This returned a panel of n=67 gene sets which originate from a diverse range of tissue and cancer types, and we observed a significant enrichment (FDR < 0.1) in nineteen gene sets in the CHB cohort (**Figure 3.1C**) (Liu et al., 2020b). In contrast, only 1 of the 67 hypoxic gene signatures was enriched in the non-viral patients. Collectively, these data suggest that CHB is associated with many host signalling pathways, particularly those associated with the inflammatory response. This could be linked to a hypoxic phenotype of the diseased liver *in vivo*, that warranted further investigation.

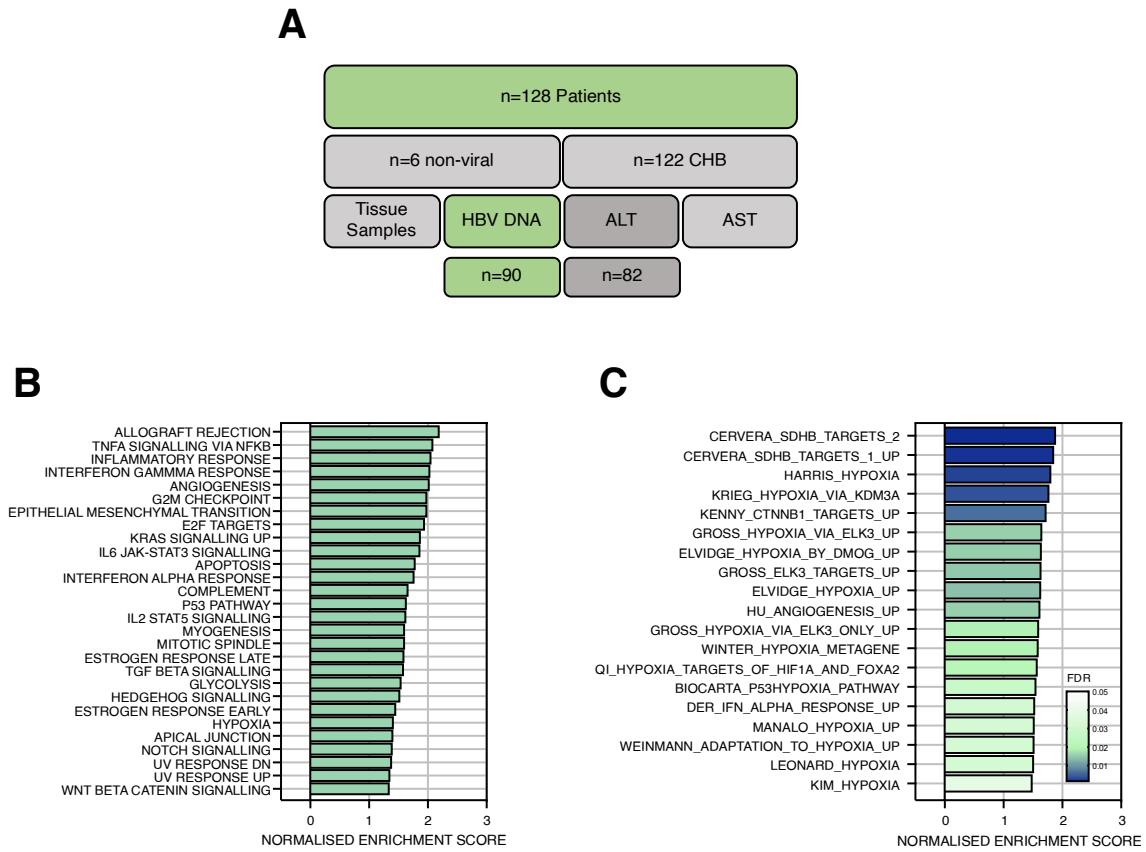


Figure 3.1: Host gene expression in the CHB liver

(A) A schematic diagram to describe the patient data sets from Zhou et al. where gene expression was quantified by Affymetrix microarray (Zhou et al., 2017). The study used material from n=122 CHB patients and n=6 uninfected patients, where they quantified peripheral HBV DNA, ALT and AST levels, as well as biopsy material for RNA preparation and transcriptomic analysis. Patients were only included in our analysis if HBV DNA had been recorded, leaving n=90 CHB patients. **(B)** Pathway analysis was performed using GSEA and the hallmarks gene set from MSigDB, between CHB patients (n=90) against non-viral subjects (n=6), revealing n=28 significantly upregulated (FDR<0.1) pathways in the diseased group. Gene sets are ranked by normalised enrichment score. **(C)** Hypoxic gene signatures were obtained from the MSigDB and their expression analysed in patients diagnosed with CHB, against non-viral subjects. 67 signatures were analysed, of which 19 were significantly upregulated in the diseased group above the uninfected group. Gene sets are ranked by normalised enrichment score, and coloured based on FDR.

3.3: A naturally hypoxic microenvironment

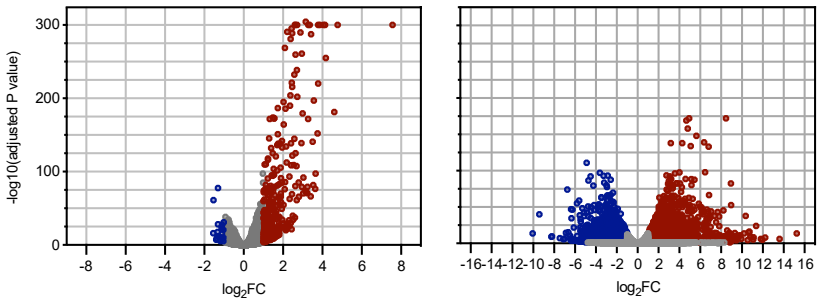
The cellular hypoxic response represents a complex interplay of many transcription factors, chromatin modifiers and epigenetic modulators (reviewed in (Kindrick and Mole, 2020)). HIFs are perhaps the best studied oxygen sensitive transcription factors, and are often labelled as the master regulator of the host cell response (Semenza, 1998). We therefore sought to understand whether there was evidence of HIF signalling in the CHB liver (**Figures 3.1A,B**). As HIF transcriptional responses are tissue and cell type specific, we sought to generate a hepatocyte specific gene signature, and analysed published RNA-sequencing data from HepG2 cells cultured at 0.5% oxygen for 16 hours (Batie and Rocha, 2020; Kindrick and Mole, 2020). These data were part of a study that investigated the differences in HIF-1α and HIF-2α driven transcriptional responses and therefore Smythies et al. opted to use a short term hypoxic culture conditions to focus on HIF signalling (Smythies et al., 2019). HIF transcriptional responses are generally associated with positive regulation of gene expression, and the volcano plot shows that upregulated genes outnumber the downregulated genes (**Figure 3.2A**, *left*). The acute hypoxic transcriptional footprint is thought to be attributable to HIFs, whereas persistent hypoxic culture will inhibit other 2-OGDDs, such as the chromatin modifying enzymes or DNA methylation machinery (Batie et al., 2019; Hancock et al., 2015; Majmundar et al., 2010). As such, we analysed the transcriptome of HepG2-NTCP cells cultured in 1% oxygen for 72 hours, and the difference in transcriptional response is stark, with the volcano plot showing a more even distribution of up- and down- regulated genes (**Figure 3.2A**, *right*).

We selected the 80 genes from the 0.5% oxygen cultured cells which show a log_2FC of at least 2, and FDR<0.05 as a putative hepatocyte specific HIF gene signature (**Figure 3.2B**). Smythies and colleagues performed parallel HIF-1α and HIF-2α ChIP-sequencing on matched samples, allowing us to assess the relative contribution of HIF-1α and -2α to our gene signature. We interrogated their data to see if any of the 80 genes showed binding of either or both HIF isoforms, as defined by a 1.5-fold enrichment over HIF-1β binding (Smythies et al., 2019). We noted that HIF-1α was more transcriptionally dominant, regulating 27 of the 80 genes, in contrast we only observed HIF-2α binding to n=12 genes. Of the eighty genes, only NDRG1 appeared to be co-regulated, showing significant binding of both HIF-1α and -2α upstream of the promoter region (**Figure 3.2C**). This means that under 50% of our hypoxic genes bound HIFs directly, suggesting a role for additional non-HIF pathways in regulating the acute hypoxic response.

We noted that the 'hypoxia' and 'HIF' signatures on the MSigDB were derived from a diverse range of tissues and cell lines. As none of the pathways used in our earlier analysis were exclusively hepatocyte derived, and it has been reported that hypoxia signalling is cell type specific and highly variable between different organs and tissues, we compared our 80 gene signature with the n=19 significantly enriched signatures in *Figure 3.1B* (Schodel et al., 2011; Smythies et al., 2019). It is worth noting that the two most significantly enriched gene sets used Hep3B human hepatoma cell lines in their analyses, however despite their hepatic origin they showed less than 1% conservation with our HepG2 derived signature. We observed a minimal overlap between the members of the 19 gene sets and our 80 gene signature, highlighting the need to use gene signatures from relevant

model systems when performing bioinformatic analyses (**Figure 3.2D**) (Encode Project Consortium, 2012).

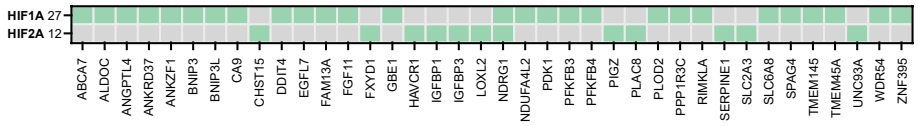
A



B

Rank	Gene Symbol	Gene Description	Rank	Gene Symbol	Gene Description
1	LOXL2	Lysyl oxidase like 2	41	ISM2	Isthmin 2
2	SMIM3	Small integral membrane protein 3	42	NDRG1	N-myc downstream regulated 1
3	LOC154761	Family with sequence similarity 115, member c pseudogene	43	SERPINE1	Serpin family e member 1
4	WDR54	Wd repeat domain 54	44	ESPN	Espin
5	DOK3	Docking protein 3	45	ADM	Adrenomedullin
6	HCAR3	Hydroxycarboxylic acid receptor 3	46	RNASET2	Ribonuclease t2
7	EHD2	Eh domain containing 2	47	FAM110C	Family with sequence similarity 110 member c
8	TNS1	Tensin 1	48	IGFBP3	Insulin like growth factor binding protein 3
9	HK1	Hexokinase 1	49	PDK1	Pyruvate dehydrogenase kinase 1
10	SLC2A3	Solute carrier family 2 member 3	50	PDGFB	Platelet derived growth factor subunit b
11	GYS1	Glycogen synthase 1	51	UNC93A	Protein unc-93 homolog a
12	PLAC8	Placenta specific 8	52	PPP2R2C	Protein phosphatase 2 regulatory subunit bgamma
13	IGFBP1	Insulin like growth factor binding protein 1	53	FAM13A	Family with sequence similarity 13 member a
14	FXYD1	Fxyd domain containing ion transport regulator 1	54	PLIN2	Perilipin 2
15	LSP1	Lymphocyte-specific protein 1	55	GBE1	Glycogen banching enzyme
16	SLC6A8	Solute carrier family 6 member 8	56	LCN15	Lipocalin 15
17	TFF1	Trefoil factor 1	57	ZNF395	Zinc finger protein 395
18	TUBB1	Tubulin beta 1 class vi	58	RAB42	Ras-related protein rab-42
19	RIMKLA	Ribosomal modification protein rimk like family member a	59	PGK1	Phosphoglycerate kinase 1
20	PFKFB3	6-phosphofructo-2-kinase/fructose-2,6-biphosphatase 3	60	PPP1R3C	Protein phosphatase 2 regulatory subunit 3c
21	CKB	Creatine kinase b	61	BNIP3L	Bcl2/adenovirus e1b 19kda protein-interacting protein 3-like
22	RASSF5	Ras association domain family member 5	62	ANKRD37	Ankyrin repeat domain 37
23	SLC51A	Solute carrier family 51 alpha subunit	63	ANKZF1	Ankyrin repeat and zinc finger domain containing 1
24	SPAG4	Sperm associated antigen 4	64	APOL1	Apolipoprotein l1
25	HAVCR1	Hepatitis a virus cellular receptor 1	65	DDIT4	Dna damage inducible transcript 4
26	ANGPTL4	Angiopoietin like 4	66	PNPLA7	Patatin-like phospholipase domain-containing protein 7
27	LOX	Lysyl oxidase	67	BNIP3	Bcl2 interacting protein 3
28	CA9	Carbonic anhydrase 9	68	RORA	Rar related orphan receptor a
29	IGLON5	Iglon family member 5	69	NDUFA4L2	Ndufa4 mitochondrial complex associated like 2
30	PFKFB4	6-phosphofructo-2-kinase/fructose-2,6-biphosphatase 4	70	PIGZ	Phosphatidylinositol glycan anchor biosynthesis class z
31	PLEKHA2	Pleckstrin homology domain containing a2	71	ABCA7	Atp binding cassette transporter a7
32	LOXL3	Lysyl oxidase like 3	72	HR	Protein hairless
33	CHST15	Carbohydrate (n-acetylgalactosamine 4-sulfate 6-o) sulfotransferase 15	73	EPO	Erythropoietin
34	TMCC1	Transmembrane and coiled-coil domain family 1	74	TMEM145	Transmembrane protein 145
35	BHLHE40	Basic helix-loop-helix family member e40	75	MIR210HG	Mir210 host gene
36	EGFL7	Egf like domain multiple 7	76	CITED2	Cbp/p300 interacting transactivator with glu/asp rich carboxy-terminal domain 2
37	EGLN3	Egl-9 family hypoxia inducible factor 3	77	PLOD2	Procollagen-lysine,2-oxoglutarate 5-dioxygenase 2
38	KCTD11	Potassium channel tetramerization domain containing 11	78	INHA	Inhibin alpha
39	FGF11	Fibroblast growth factor 11	79	BIRC7	Baculoviral iap repeat containing 7
40	TMEM45A	Transmembrane protein 45a	80	ALDOC	Aldolase, fructose-bisphosphate c

C



D

Upregulated Gene Signatures				
Rank	Signature	Size	Overlap	Origin
1	CERVERA SDHB TARGETS 2	111	1	Hep3B and HeLA Cells
2	CERVERA SDHB TARGETS 1 UP	113	2	Hep3B and HeLA Cells
3	HARRIS HYPOXIA	80	12	Pan-cancer
4	KRIEG HYPOXIA VIA KDM3A	50	2	Renal and colon carcinoma
5	KENNY CTNNB1 TARGETS UP	48	1	Breast and colon cancer
6	GROSS HYPOXIA VIA ELK3 UP	197	1	Skin endothelium
7	ELVIDGE HYPOXIA BY DMOG UP	130	26	Breast cancer cell line MCF7
8	GROSS ELK3 TARGETS UP	27	0	Skin endothelium
9	ELVIDGE HYPOXIA UP	164	29	Breast cancer cell line MCF7
10	HU ANGIOGENESIS UP	20	0	nSCLC
11	GROSS HYPOXIA VIA ELK3 ONLY UP	31	2	Skin endothelium
12	WINTER HYPOXIA METAGENE	232	25	Head and neck cancers
13	QI HYPOXIA TARGETS OF HIF1A AND FOXA2	30	3	Adeno and prostate carcinoma
14	BIOCARTA P53 HYPOXIA PATHWAY	20	1	Cardiovascular endothelium
15	DER IFN ALPHA RESPONSE UP	70	1	Fibroscarcoma
16	MANALO HYPOXIA UP	201	23	Pulmonary artery endothelium
17	WEINMANN ADAPTATION TO HYPOXIA UP	25	0	Hypoxia tolerant lung cancer cells
18	LEONARD HYPOXIA	42	10	Kidney tubule cells
19	KIM HYPOXIA	19	6	Fibroblasts

Figure 3.2: A naturally hypoxic microenvironment

(A) Volcano plots to show differential expression of the RNA transcriptome of HepG2 cells challenged with either 0.5% for 16 hours, as a model for acute hypoxia where HIF signalling should be at its most active (left), or HepG2-NTCP cells cultured in 1% oxygen for 72 hours to mimic a more chronic state (right) (Smythies et al., 2019). Differential expression analysis was performed using a DESeq2 package, and statistical significance was determined by a log_2FC of +/- 1 and an FDR q-value of <0.05 (Love et al., 2014). Significantly upregulated genes are coloured red, and down regulated genes in blue. **(B)** Using the acute hypoxic transcriptomic data, 80 genes were identified with a log2FC of >2.

These were highlighted as a putative hepatocyte specific hypoxic gene signature. **(C)** HIF-1α and HIF-2α ChIP-seq data was available from the same study and so RNA- and ChIP-seq data were cross referenced to assess the frequency of genes that were shown to be directly HIF regulated. Of the 80 genes, twenty seven showed binding of HIF-1α and twelve showed enriched HIF-2α at their promoter. **(D)** The origin and gene set size of the 19 significantly enriched signatures shown in *Figure 3.1C*. Overlap represents the number of genes in common between each signature and the gene signature identified in *Figure 3.2B*.

3.4: Hypoxic gene expression in a CHB cohort

In place of the previously published and variable hypoxic gene signatures from MSigDB, we used our hepatocyte derived gene signature to assess hypoxic gene expression in the CHB liver. We employed GSEA and used the Affymetrix microarray data from the Zhou et al. cohort, as per the analysis carried out in *Figure 3.1* (Subramanian et al., 2007; Subramanian et al., 2005; Zhou et al., 2017). Using the RNA transcriptome from biopsy samples derived from n=90 CHB patients and n=6 non-viral subjects, we observed a significant enrichment in hypoxic gene expression in the infected group (FDR=0.11) (**Figure 3.3A**) (Liu et al., 2020b).

CHB reflects a complex disease, where there is continuous attrition between the host immune system and viral replication, resulting in periods of active hepatitis which associate with an increase in both ALT and peripheral HBV DNA (Chang and Liaw, 2014; Liu et al., 2020b). To assess the association between viral replication and periods of active hepatitis, we grouped this cohort by peripheral ALT levels, and noted higher expression of our hypoxic gene signature in patients with elevated ALT (ALT>40 IU/mL (n=57)), compared to those with normal ALT (ALT<40 IU/mL (n=25)) (**Figure 3.3B**) (Liu et al., 2020b).

To ascertain whether increased hypoxic gene expression was a hallmark of inflammatory liver disease, we accessed Affymetrix microarray data from a cohort of patients infected with HCV (Mas et al., 2009). We compared the expression of our hepatocyte derived hypoxic gene signature between HCV patients (n=41) and uninfected subjects (n=19), and observed a significant enrichment of expression in the diseased group (**Figure 3.3C**) (Liu et al., 2020b). We compared the leading

edge genes from the GSEA from the HBV (n=30) and HCV (n=20) infected cases, and identified an overlap of 10 genes, however the majority of genes were unique to each cohort. Collectively these data show evidence of increased hypoxic gene expression with viral infection and inflammation, however it does not inform us mechanistically on cause or effect (Liu et al., 2020b).

Recently, an acute hypoxic transcriptome of primary human hepatocytes (PHH) cultured at 1% oxygen for 4 hours was published (Hettiarachchi et al., 2019). We analysed these published data set using our thresholds for differential expression ($log_2FC>2$, FDR<0.05), and this showed an upregulation of 113 genes. There are technical limitations to working with primary cells, and PHHs have been shown to retro-differentiate in cell culture, and require a cocktail of growth factors to maintain viability which may affect their response to hypoxia (Elaut et al., 2006; Heslop et al., 2017; Wing et al., 2021). In the context of stem cell differentiation, it has been suggested that hypoxic culture is able to halt the differentiation of adult stem and embryonic cells. This suggests that local oxygen could be a major determinant of differentiation status (reviewed in (Abdollahi et al., 2011; Hawkins et al., 2013)). It is challenging to speculate as to which of these cell backgrounds offers the closest representation of hepatocytes *in vivo*, given the immortalised hepatoma origin of HepG2-NTCP cells, and the *ex vivo* status of PHH. However, we were reassured to see an overlap of hypoxic regulated genes between PHH and HepG2 cells, and we assessed transcript levels of the 113 PHH derived genes in the CHB cohort (**Figure 3.3D**). Using GSEA we observed a positive upregulation in the infected patients, although this was above the threshold for statistical significance (**Figure 3.3E**) (Liu et al., 2020b).

Taken together, these data provide evidence of active hypoxic signalling in the diseased liver, although the precise sequence of events leading to HIF stabilisation and transcriptional activation remains unclear. As noted above, not all 80 genes were found to bind either HIF-1α or -2α in the study from Smythies et al. which could be reflective of a combination of other HIF-independent regulators, and the threshold and detection limit of ChIP-seq assays (Nakashima et al., 2021; Smythies et al., 2019). Whilst some studies have identified that viruses are capable of stabilising HIF, we did not observe this in our *in vitro* systems (reviewed in (Liu *et al.*, 2020a; Liu *et al.*, 2020b)). We therefore suggest that the inflammatory environment is likely to drive HIF signalling and that infiltration of immune cells, ROS and cytokine signalling offer potential explanations for the hypoxic phenotype (Imtiyaz and Simon, 2010; Liu et al., 2020b; Movafagh et al., 2015; Palazon et al., 2014; Zhou et al., 2003).

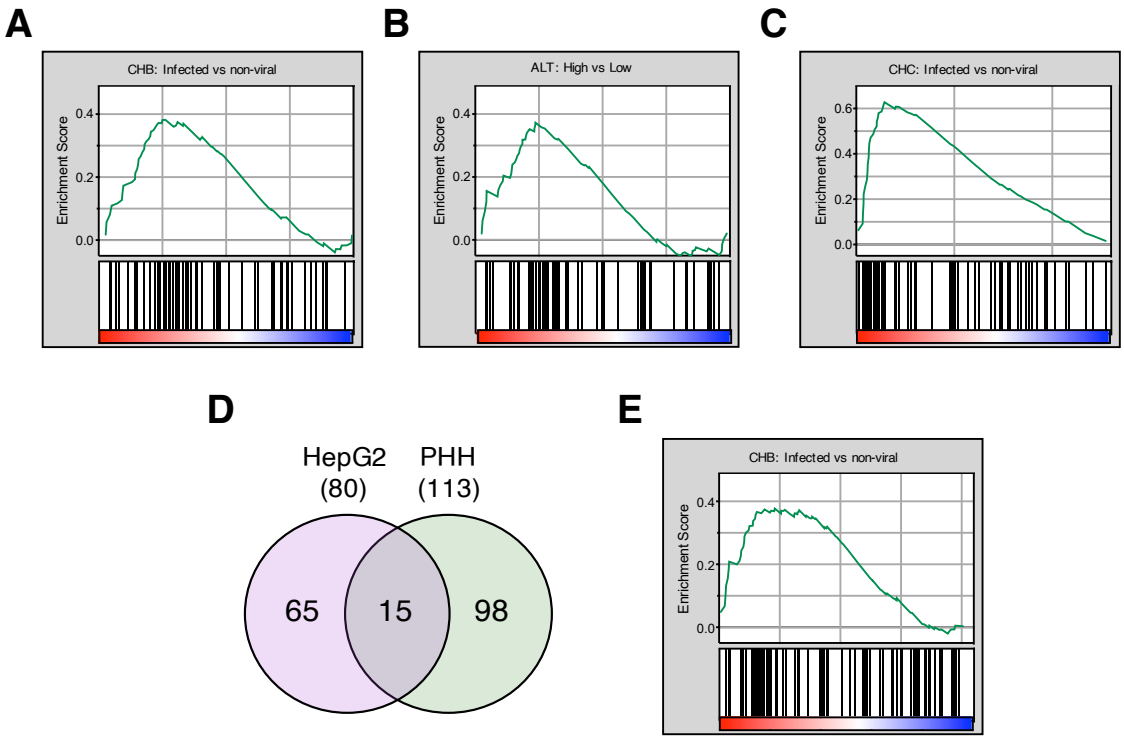


Figure 3.3: Hypoxic gene expression in a CHB cohort

(A) Gene set enrichment analysis showing enriched expression of the 80 hypoxic genes in chronically infected (n=90) above non-viral (n = 6) patients. Significant enrichment (FDR = 0.077) was observed in infected subjects. **(B)** Patients were grouped by peripheral levels of ALT, into low <40 IU/mL (n=25), or high >40 IU/mL (n=57) and enrichment of 80 genes analysed. Significant enrichment was found in patients with high ALT (FDR=0.11). **(C)** HepG2 derived hypoxic gene expression was assessed in a cohort of subjects with cirrhosis and HCV (n=41), above non-viral, non-cirrhotic subjects (n=19). Infected patients show significantly enriched expression of hypoxic genes (FDR=0.006). **(D)** A recent study published a hypoxic transcriptome of primary human hepatocytes, cultured under 1% oxygen for 4 hours (Hettiarachchi et al., 2019). 113 genes showed significant upregulation, and their overlap with our HepG2 gene signature is represented by a Venn diagram. **(E)** Gene set enrichment analysis shows enrichment of 113 PHH derived genes in the HBV infected (n = 82) above non-viral (n = 6) patients (FDR = 0.351).

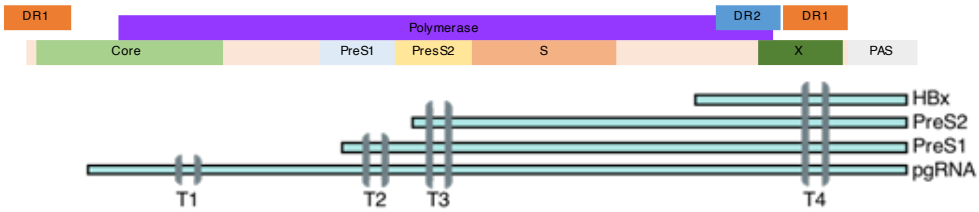
3.5: A qPCR to detect HBV transcripts

We were interested to understand the relative contribution of the major viral RNAs to the HBV transcriptome, and sought to explore differential viral promoter activity. Classically, the gold standard method for detecting HBV RNAs is the northern blot, but this is semi-quantitative at best and requires relatively large amounts of RNA, precluding its application to clinically derived samples (D'Arienzo et al., 2021b). To that end, collaboratively with Dr Andrea Magri and Dr Valentina D'Arienzo, we sought to develop a simple qPCR method to quantify the relative abundance of each of the HBV RNA transcripts. We designed a series of primer pairs (T1-T4) with short, comparable amplicon sizes (76-120bp) located in overlapping regions of the genome corresponding to each of the major viral RNAs (**Figure 3.4A**). Given the 30 nucleotide difference in the length of the pC and pg RNAs, we could not differentiate between the two RNA species, and label the amplicon as pC/pg to represent the sum of the two products. T1 targets the pC/pg transcripts; T2 the pC/pg and PreS1; T3 pC/pg, PreS1 and PreS2, and T4 amplifies all viral RNAs as it targets the common 3' end. Previous studies have identified as many as eighteen spliced forms of the pC/pgRNAs, with the most abundant being Sp1, and we believe our T1 primers will amplify all these spliced RNAs (**Figure 3.4B**) (D'Arienzo et al., 2021b; Duriez et al., 2017; Lim et al., 2021). Other groups have identified 3 major truncated forms of HBx RNA, and our T4 primer will amplify the 1-27 and 43-154 variants, but not the 61-154 product (Al-Anazi et al., 2018; Liu et al., 2008).

The majority of *in vitro* systems used for HBV research support viral replication from HBV GtD genomes. We designed primers to amplify a conserved

region in all of the documented GtD sequences recorded in the HBV database and show conservation across the binding sites (**Figure 3.4C**) (D'Arienzo et al., 2021b; Hayer et al., 2013). We interrogated the qPCR amplification profiles and checked for clean, distinct dissociation curves with each of the primer pairs. We noted well defined melting peaks for each of the 4 primers with T_m values of: T1 = 80°C; T2 = 88°C; T3 = 82°C; T4 = 86°C (**Figure 3.4D**) (D'Arienzo et al., 2021b). Finally, we assessed the amplification efficiency of the primer sets, by preparing a 10-fold serial dilution of HBV1.0 GtD DNA (**Figure 3.4E**). This revealed largely comparable amplification efficiencies, varying from 90-100% across the panel of primers, with a detection limit of around 50 copies/reaction, with a respective Ct value of approximately 31. Of course, this does not allow us to disregard the possibility of inter-assay variability, where variations in reverse transcription, qPCR replicates, and reagents could change the efficiency of the reaction on an assay-by-assay basis. However, we believe that consistent cycling conditions and utilisation of reliable and readily available reagents will minimise this, allowing us to apply our assay to a variety of *in vitro* and *in vivo* scenarios with some confidence (D'Arienzo et al., 2021b).

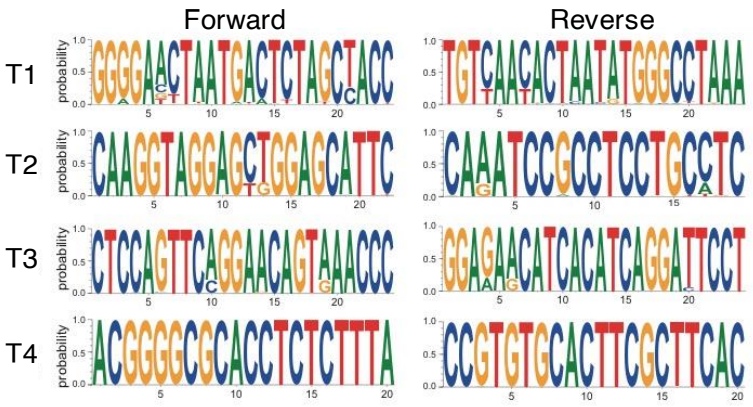
A



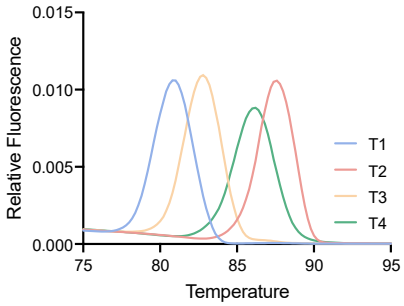
B

Primer name	Direction	Sequence	Location		Product length	Products amplified
T1	Forward	GGGGAACTAATGACTCTAGCTACC	2089	2112	101	pC/pg
	Reverse	TTTAGGCCCATATTAGTGTTGACA	2166	2189		
T2	Forward	CAAGGTAGGAGCTGGAGCATTC	2984	3005	120	pC/pg + PreS1
	Reverse	GAGGCAGGAGGCGGATTTG	3085	3103		
T3	Forward	CTCCAGTTCAGGAACAGTAAACCC	69	92	114	pC/pg + PreS1 + PreS2
	Reverse	AGGAATCCTGATGTGATGTTCTCC	159	182		
T4	Forward	ACGGGGCGCACCTCTTTA	1521	1540	76	pC/pg + PreS1 + PreS2 + X
	Reverse	GTGAAGCGAAGTGCACACGG	1577	1596		

C



D



E

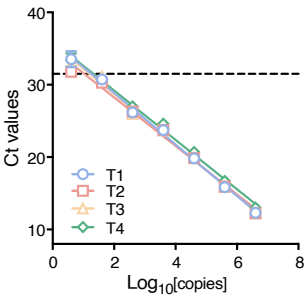


Figure 3.4: A qPCR to detect HBV transcripts

(A) A schematic diagram showing the HBV ayw genome with polyadenylation site (PAS), the DR1 and DR2 motifs, the four major viral transcripts and the locations of the open reading frames for core, Pol, PreS1, PreS2, S and X plotted. Underneath, the major transcripts and primer binding sites are illustrated. **(B)** A table to show primer design, amplicon length and product specificity of our 4 primer pairs, named T1-4. **(C)** Sequence symbol plots to show the alignment of the 4 primer pairs to HBV GtD sequences from the HBV

database (Hayer et al., 2013). **(D)** Melting profiles from qPCR reactions to show specificity of each of the primer pairs for single product amplification. **(E)** A serial dilution of HBV1.0 of known copy number was set up and amplified by qPCR with each of the primer pairs (T1-4). *Data produced in collaboration with Dr Andrea Magri and Dr Valentina D'Arienzo* (D'Arienzo et al., 2021b).

3.6: Ascribing transcript patterns to *in vitro* and *in vivo* systems

To validate our primer design and analysis pipeline on authentic HBV RNAs we used the well characterised HepG2.2.15 cell line. HepG2.2.15 support HBV GtD replication from 2 head-to-tail integrated copies of the genome as well as episomal cccDNA (Sells et al., 1987). It is important to note that in contrast to authentic HBV integrants, the HepG2.2.15 model can produce pC/pgRNAs as the tandem repeat completes the full length ORF (Ko et al., 2018; Sells et al., 1987). As described in *Materials and Methods*, all RNAs were treated with DNAse to remove any residual DNA carry-over. This is of particular importance when studying HBV, as unlike human RNAs there is no removal of introns, and the sequence of the DNA template perfectly replicates the RNA transcript. In order to perform a side by side comparison of the northern blot and our qPCR, we cultured HepG2.2.15 cells in the presence or absence of 2.5% DMSO for 72 hours. DMSO treatment is routinely used in HBV studies to limit cell division and maintain the cccDNA pool (D'Arienzo et al., 2021b; Ko et al., 2018; Villa et al., 1991). By northern blot, we noted that DMSO treated cells showed an approximate 16 fold increase in the 3.5kb transcripts and a more modest 5 fold increase in the 2.4/2.1kb species, when expressed relative to the ribosomal 28S and 16S RNAs (**Figure 3.5A**) (D'Arienzo et al., 2021b).

For our qPCR, we reverse transcribed between 0.25-1 µg of RNA using a cDNA synthesis kit consisting of oligo-dT and random hexamers (PCRBIO, UK). All amplification curves and melting peaks were assessed and quality checked before any further analysis. Due to the primer design and overlapping nature of the viral genome, each subsequent primer pair should amplify more material than

the previous, and amplify at a lower Ct value. We checked that Ct values for T1>T2>T3>T4 to assess amplification efficiency and interpolated copy number from a standard curve of known HBV copies. Using a simple subtractive method we ascribed transcript pattern whereby T1 copies = pC/pgRNA; T2-T1 copies = PreS1; T3-T2 copies = PreS2 and T4-T3 copies = HBx. All PCRs were carried out using a SYBR green qPCR kit (PCRBIO, UK) and performed on a LightCycler instrument (Roche) (D'Arienzo et al., 2021b).

Using the same samples as prepared for northern blot, we enumerated copies of each of the HBV RNA species by qPCR, and showed a significant increase in the relative abundance of both pC/pg RNAs and the PreS1 (2.4kb) transcript (**Figure 3.5B**). This suggests that our qPCR assay is sufficiently sensitive to note changes in transcript abundance, and provides comparable results to the current gold standard method. Whilst we achieved amplification with the T4 primer pair, after enumeration of copies we noted that RNAs encoding the HBx protein constituted a minor proportion of RNAs in this system, consistent with limited evidence of the presence of the 0.7kb transcript by northern blot (D'Arienzo et al., 2021b).

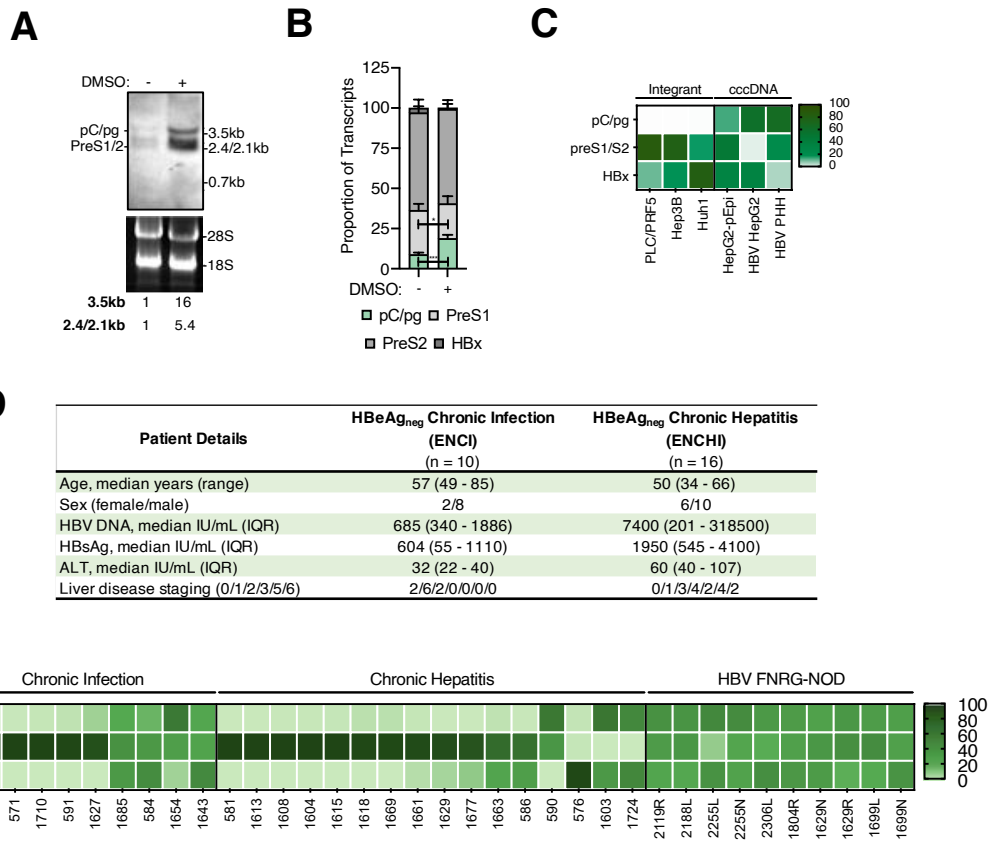
As discussed in the introductory *Chapter 1.2.7*, authentic HBV integrants are incapable of transcribing pC/pgRNA due to detachment of the BCP from the now linearized open reading frame. It was reassuring that the T1 primers failed to amplify a product from any of the integrant lines (PLC/PRF5, Hep3B or Huh1 cells) (Rivkina et al., 1988; Su et al., 1998). However we noted substantial representation of PreS1/2 and HBx RNAs in all 3 cell lines. A recent study from Ramirez et al. employed long read sequencing assess the transcriptional activity of these three integrant lines and reported that PreS1/2 were the major RNA

species, but did not detect any full length HBx transcripts (Ramirez et al., 2021). However, they cultured Hep3B and Huh1 cells for 9 and 10 days respectively, and claimed that HBx may be an early transcript and expression could decrease over time (Al-Anazi et al., 2018; Niu et al., 2017). In contrast, when screening RNAs derived from models supporting replication from episomal cccDNA (*de novo* infection of either HepG2-NTCP cells or PHH) or cccDNA-like genomes (HepG2-pEpi), we detected all of the viral RNAs with pC/pg and PreS1/2 RNAs constituting the major species in these models (**Figure 3.5C**) (D'Arienzo et al., 2021b; Lucifora et al., 2014). It is worth noting that the *de novo* infection samples were taken at an early time point (72h post infection) and integration events should be limited; perhaps only as frequent as 1 event per 10,000 cells (Tu et al., 2018).

Having validated our assay with several routinely used laboratory model systems, we were keen to explore whether there was any evidence of differential promoter usage or diverse transcript patterns in clinically derived material. Through a collaboration with Professor Mario Pirisi, we gained access to a cohort of CHB patients who were classified as either HBeAg negative chronic infection (ENCI) (n=10) or HBeAg negative chronic hepatitis (ENCH) (n=16), in accordance with EASL guidelines (EASL, 2017; Zhang et al., 2019). As well as receiving full clinical datasets with patient and viral parameters, we received a liver biopsy sample along with associated ethical approval to perform gene expression analysis (**Figure 3.5D**). RNAs were extracted from the tissue samples, integrity was assessed by TapeStation, and viral gene expression was quantified using our qPCR assay (D'Arienzo et al., 2021b). PreS1/2 RNAs were the most abundant RNA species in the majority of samples from this cohort, constituting over 95% of RNAs in 16/26 patients. However, we also detected pC/pgRNA transcripts which

suggests ongoing and active viral replication from cccDNA (**Figure 3.5E**). As a comparator we included RNAs from n=10 human liver chimeric mice, FNRG-NOD immune deficient mice that were engrafted with human hepatocytes and infected with HBV. Whilst murine hepatocytes are unable to support cccDNA, the human hepatocytes are replication competent and so these RNAs represent authentic viral RNAs derived from cccDNA in human cells *in vivo* (Budker et al., 1996; Yang et al., 2002). In these samples we observed comparable levels of pC/pg, PreS1/2 and HBx RNAs (**Figure 3.5E**).

These data show that our qPCR assay is sensitive and can be applied to both *in vitro* and *in vivo* settings. It also highlights that the patterns of HBV RNAs across routinely used model systems differ, and that PreS1/2 RNAs are the dominant RNA species in our CHB cohort. This is something that could perhaps be overlooked when pgRNA and total RNA are the only viral parameters detected (Hallez et al., 2019; Suslov et al., 2021). Finally, we see that in the HBeAg negative stage of disease HBV pC/pgRNAs are readily detectable, suggesting that some hepatocytes are supporting viral replication from cccDNA. However, the contribution of either episomal or integrated genomes to viral transcription in chronic disease is not well understood. Previous studies have identified a link between the inflammatory response and cccDNA transcriptional output, whereby flares in ALT occur in phase with peaks of viraemia and antigenemia (Chang and Liaw, 2014; Liaw and Chu, 2009; Liaw et al., 1983; Liaw et al., 1985).



Patient Details	$HBeAg_{neg}$ Chronic Infection (ENCI) (n = 10)	$HBeAg_{neg}$ Chronic Hepatitis (ENCHI) (n = 16)
Age, median years (range)	57 (49 - 85)	50 (34 - 66)
Sex (female/male)	2/8	6/10
HBV DNA, median IU/mL (IQR)	685 (340 - 1886)	7400 (201 - 318500)
HBsAg, median IU/mL (IQR)	604 (55 - 1110)	1950 (545 - 4100)
ALT, median IU/mL (IQR)	32 (22 - 40)	60 (40 - 107)
Liver disease staging (0/1/2/3/5/6)	2/6/2/0/0/0	0/1/3/4/2/4/2

Figure 3.5: Ascribing HBV transcript patterns to *in vitro* and *in vivo* systems

(A) Northern blot showing HBV RNA species from HepG2.2.15 cells treated with 2.5% DMSO for 72 hours, compared with undifferentiated cells. Ribosomal RNAs are shown below as internal loading controls, and relative abundance of viral RNAs was quantified by densitometry (Schneider et al., 2012). **(B)** Transcript patterns were quantified by qPCR, copy numbers were inferred from a standard curve, and plotted as percentage of total HBV RNAs. Data are representative of n=3 independent experiments, with Mann-Whitney U tests applied between conditions. **(C)** A heatmap to show the transcript patterns of routinely used HBV model systems, including hepatoma cells harbouring transcriptionally active integrants (PLC/PRF5, Hep3B and Huh1), or episomal genomes (HepG2-pEpi, or HepG2-NTCP and PHH infected with HBV). Data are representative of at least 2 independent experiments. **(D)** A table showing the clinical parameters of patients diagnosed with CHB, categorised according to EASL classification of ENCI or ENCH. **(E)** A heatmap showing the viral transcript patterns in our cohort of patients, grouped by ENCI (n=10) or ENCH (n=16), as well as in a group of HBV infected humanised liver chimeric mice (FNRG-NOD) (n=10). *Experiments and analysis designed and performed in*

collaboration with Dr Andrea Magri and Dr Valentina D'Arienzo (D'Arienzo et al., 2021b).

3.7: Determining the source of HBV transcripts

In collaboration with Dr Andrea Magri and Dr Valentina D'Arienzo, we sought to understand the relative contribution and activity of cccDNA and HBV integrants in our CHB patients. To that end, we designed additional primers to estimate cccDNA activity, and to be used in conjunction with our previously reported T4 primer pair. T4 targets the 3' end of all viral RNAs, and we used this to estimate total HBV RNA copies; the newly designed T5 primer target the repeated region between the 3' end of the linear genome (nt 1832, also referred to as DR1) and the polyadenylation site (nt 1917; PAS) (D'Arienzo et al., 2021b). The majority of integrant derived RNAs (id-RNAs) lack the usual PAS sequence and they utilise the alternative polyA site (APAS), therefore the T5 primers will only amplify RNAs that are derived from cccDNA (**Figure 3.6A**) (Lim et al., 2021; Meier et al., 2021).

When designing our 4 transcript PCR methodology we took great care to match the amplicon lengths and G:C content of our oligonucleotides to ensure that amplification efficiency was comparable between primer pairs (D'Arienzo et al., 2021b). We therefore tested T4 and T5 primer pairs side-by-side to ensure we could directly compare Ct values from both, without amplification efficiency limiting our interpretation. This was particularly important in the context of T5 as the repeated region is present at both the 5' and 3' ends of the pC/pgRNA transcript, and so it may overestimate the contribution of the cccDNA to the viral transcriptome (Flodell et al., 2002). We screened T4 and T5 primers against a 10-fold dilution series of HBV DNA, ayw strain GtD of known copies, assessed the dissociation curve and observed consistent amplification of a single product (**Figure 3.6B**). We also generated a standard curve from the serial dilutions, and

this resulted in two largely superimposable lines for T4 and T5, demonstrating comparable amplification efficiency (**Figure 3.6C**).

The difference in amplification between T4 and T5 represents the abundance of episomal (cccDNA) derived RNAs (ed-RNAs). $Log_{10}2^{(T4-T5)}$, or ed-RNA index, indicates the source of the majority of viral RNAs, such that a relatively large number indicates a high frequency of ed-RNAs, and a small number is indicative of more integrant derived RNAs (id-RNAs). To validate this approach, we screened RNAs derived from a variety of model systems reported to support replication from either integrated or episomal genomes. RNAs prepared from systems supporting cccDNA driven replication: HepG2-pEpi, *de novo* infected HepG2-NTCP and PHH, as well as the human liver chimeric mice showed amplification (Ct <31) with both primer sets and thus returned a high ed-RNA index. In contrast, RNAs prepared from the Huh1 and Hep3B cells failed to amplify with the T5 primers, but yielded Ct values within assay detection limits for T4, proving T5 primer specificity for PAS containing transcripts. As predicted, models supporting transcription from HBV integrants yield a much smaller ed-RNA index. (**Figure 3.6D**). As pC/pgRNAs can only be transcribed from cccDNA it was reassuring to note a significant association between ed-RNA index and pC/pgRNA levels in our patients. Furthermore, pC/pgRNA stratified patients by disease state with higher levels in ENCH than ENCI ($p<0.05$), but we did not observe any stratification by ed-RNA index (**Figure 3.6E**).

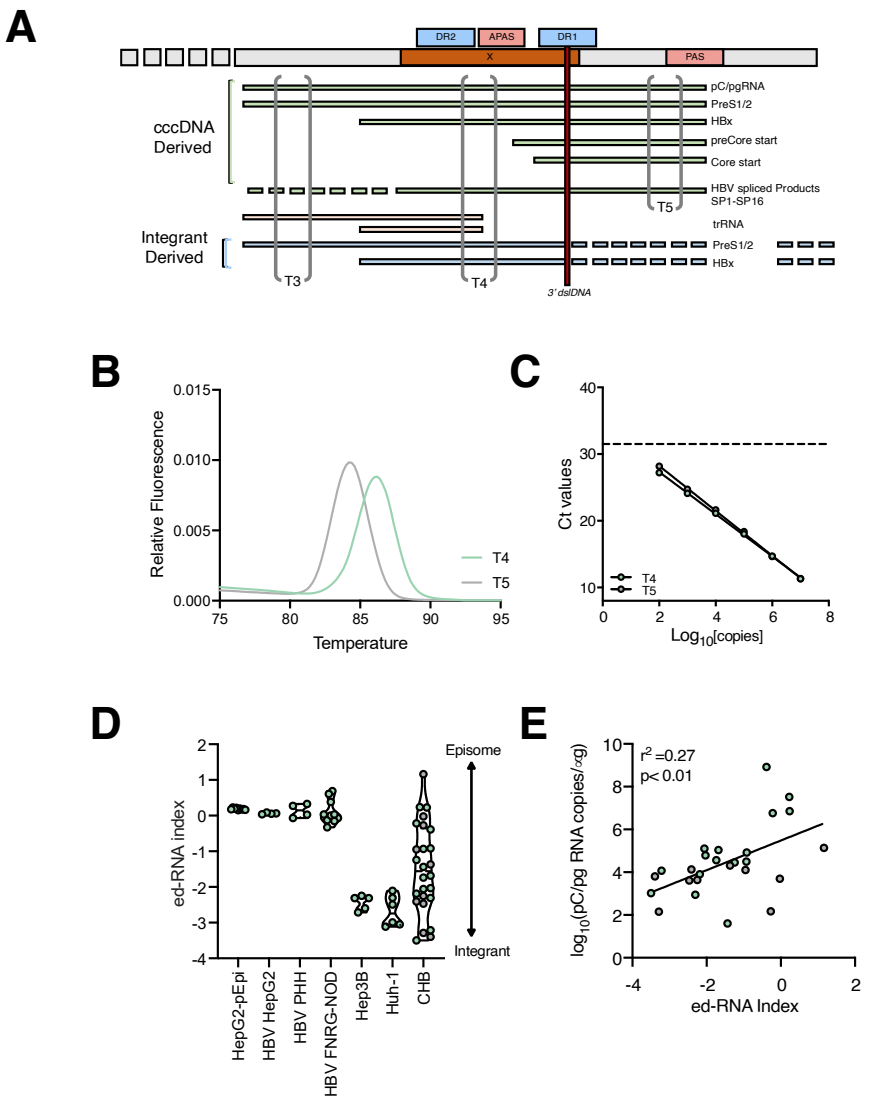


Figure 3.6: Determining the source of HBV transcripts

(A) A schematic diagram showing the 3' region of the viral genome and the terminals of the cccDNA and integrant derived RNAs. We show the X coding region, as well as the direct repeats DR1 and DR2, and the primary and alternative polyadenylation signals (PAS and APAS). Integrant derived RNAs terminate at the 3' end of the dslDNA genome (3'dslDNA), and use the APAS for transcription, and thus the T5 primer pair target a region beyond the 3'dslDNA and therefore exclusively amplify cccDNA derived RNAs. **(B)** qPCR product dissociation curves comparing our previously defined T4 primer pair with our new T5 primers, where they were screened against HBV 1.0 DNA of known copies. **(C)** T4 and T5 primers were screened against a dilution series of HBV 1.0 DNA of known copies and amplification efficiency calculated. **(D)** Using Ct values obtained from amplification with T4 and T5 we calculated the ed-RNA index, $Log_{10}2^{(T4-T5)}$. This was performed in model systems which support

replication from HBV episomes (HepG2-pEpi, n=4, *de novo* infection of HepG2-NTCP or PHH, n=4; FNRG-NOD mice (n=10)); integrants (Hep3B, Huh-1, n=6) and *o*ur CHB cohort (ENCI denoted in grey (n=10), ENCH denoted in green (n=16)). In all instances points are representative of values obtained from 2 technical duplicates. **(E)** Association between ed-RNA index and pC/pg RNA copies was assessed using Pearson's correlation coefficient, where symbols are colored as in (B). *Experiments and analyses carried out in collaboration with Dr Andrea Magri.*

3.8: Integrant derived transcripts and antigen

Having observed that PreS1/2 RNAs were the most abundant viral transcripts in our CHB cohort, we explored viral antigen immuno-stains from sequential liver sections that were examined by a pathologist. Immuno-stains were available for n=22 subjects, with seventeen patients staining for HBsAg (ENCI n=6/9, ENCH n=11/13) but only four patients stained positive for HBcAg, all of which were classified as ENCH. We observed a high frequency of hepatocytes expressing HBsAg, which localised in distinct clusters, possibly indicative of a clonal expansion of cells harbouring viral integrants (**Figure 3.7A**) (Mason et al., 2016; Mason et al., 2021; Tu et al., 2015). In stark contrast to this, in the samples that expressed HBcAg we noted the cells were sporadic and appeared as single isolated events. This raised an interesting question, why does a such a small population of cells appear to be capable of supporting cccDNA driven replication?

To investigate whether antigen expression associated with the high frequency of PreS1/2 RNAs, we correlated HBs positivity with PreS1/2 RNA copies. The immuno-stains were graded by the pathologist based on the frequency of HBsAg expressing cells: 0 – no positive cells, 1- less than 33% of cells are positive, 2- between 33% and 66% are positive, and 3- where more than 66% cells are positive. We identified an upwards trend towards significance where PreS1/2 RNA copies were proportional to HBsAg positivity, of note this did not associate with disease state (**Figure 3.7B**). In contrast, we observed no association or trend between HBsAg positivity and total hepatic HBV DNA copies, consistent with limited evidence that hepatocytes express both HBc and HBs antigens, highlighting the chimeric nature of the CHB liver (**Figure 3.7B**).

Recently, a study suggested that HBV integration events increase with the duration of infection, and we sought to explore the relationship between age and the abundance of id-RNAs in our cohort (Larsson et al., 2018). We stratified our patients by ed-RNA index, where patients with the highest levels of id-RNAs were in the lowest quartile (LQ), the 25-75% in the in MID group, and patients with the highest ed-RNA index in the upper quartile (UQ). We noted that patients with low ed-RNA levels were significantly older than the MID and UQ groups combined. This suggests that older patients show evidence of greater transcriptional activity of integrants than younger subjects (**Figure 3.7C**). It should be noted that our PCR does not detect HBV integration events, but instead their contribution to the viral transcriptome.

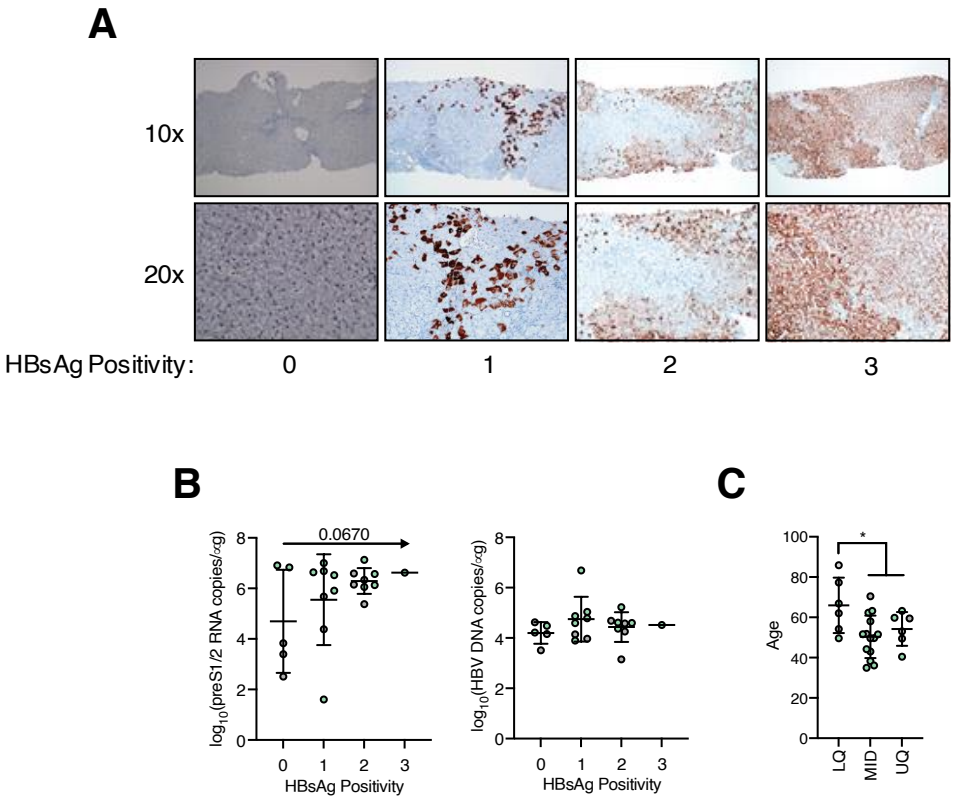


Figure 3.7: Integrant derived transcript and antigen

(**A**) HBsAg immune staining in liver biopsies. Samples were scored based on the frequency of HBsAg+ cells, where 0 is negative, 1 is less than 33%, 2 between 33-66% and 3 higher than 66%. Two magnifications shown: 10X (top) and 20X (bottom). (**B**) Association between HBs score and PreS1/S2 RNA (left) or total hepatic HBV DNA (right). Statistical significance was tested with ANOVA trend analysis. **(C)** Association between cccDNA transcriptional activity and age. Patients were groups into upper and lower quartiles, and mid- range values for ed-RNA index, based upon their deviation from the median value, LQ = 0-25%; MID 25-75%; and UQ – 75-100%. **(B-C)** Points are representative of the mean of 2 independent technical replicates, and coloured to denote ENCI (n=10, grey) and ENCH (n=16, green). *Analysis performed in collaboration with Dr Andrea Magri; Immuno-stains kindly sent by collaborators at University of Piedmont.*

3.9: An immune gene signature associating with HBV replication

As previously discussed, there is a well-documented association between hepatic inflammation and HBV replication, although the precise mechanism and pathways which regulate this are poorly understood (Chang and Liaw, 2014; Liaw and Chu, 2009; Liaw et al., 1983; Liaw et al., 1985). To understand the genes involved in the hepatic inflammasome we employed nCounter Nanostring technology to study the RNA transcripts of inflammatory genes (n=249) in our liver biopsy samples, in collaboration with Dr Andrea Magri (Eastel et al., 2019). Nanostring technology uses a fluorescent probe and oligonucleotide based approach to quantify gene expression, and requires as little as 50 ng of input RNA which means it is well suited for the study of clinical samples. We sought to understand which inflammatory mediators associated with HBV transcription, and began by identifying transcriptionally active genes in our cohort. Eighty seven gene transcripts were detected in all patients, of which 32 positively associated with pC/pgRNA, and 30 associated with viral RNAs amplified by the T5 primers (Spearman's rank correlation coefficient, FDR <0.05). In contrast, there was only 1 gene which associated with PreS1/2 transcripts, C1QB, and this was unique in that it did not associate with any other viral parameter (**Figure 3.8A**). To assess the relationship between viral replication and inflammation we used the subset of twenty four genes which associated with both pC/pgRNA levels and T5 amplification (**Figure 3.8A**). Interestingly, we noted that HIF-1α mRNA levels associated with cccDNA activity (1/T5 signal) and this is relevant given our later data showing that HIFs are positive regulators of HBV replication, but have limited impact on integrant derived PreS1/2 RNAs (discussed in *Chapter 4*) (Wing et al., 2021).

We assessed the expression of the 24-gene set in our CHB cohort categorising subjects as ENCH or ENCI, and not surprisingly noted higher levels in ENCH, consistent with increased inflammation during active hepatitis (**Figure 3.8B**) (EASL, 2017). Principal component analysis (PCA) showed that the expression of the 24 genes could partition patients based on disease classification (**Figure 3.8B**). Pathway analysis using Gene Ontology biological processes revealed an over representation of our 24 gene signature in pathways associated with defence response, the stress response and pathways pertaining to immune function (**Figure 3.8C**) (Ashburner et al., 2000; Mi et al., 2021; Supek et al., 2011). It is of course worth noting that there may be an intrinsic bias in this analysis as the genes all derive from an archived selection of immune regulated or regulatory genes. Our transcriptomic data is derived from a liver biopsy sample, and this means it will consist of a heterogenous mix of cell types. Whilst we expect that hepatocytes would represent the most abundant population, we cannot exclude the contribution of RNAs originating from Kupffer cells, endothelial cells, infiltrating immune cells, and other hepatic parenchymal cells. To better understand the cell types responsible for the expression of our 24 gene signature we analysed a single cell RNA-sequencing liver atlas which identified Kupffer and liver endothelial cells as the most dominant expressors of our gene signature (**Figure 3.8D**) (Aizarani et al., 2019; Juhling et al., 2021). In short, we believe that we have identified an inflammatory gene signature that associates with cccDNA activation and HBV replication in the HBeAg negative stage of disease.

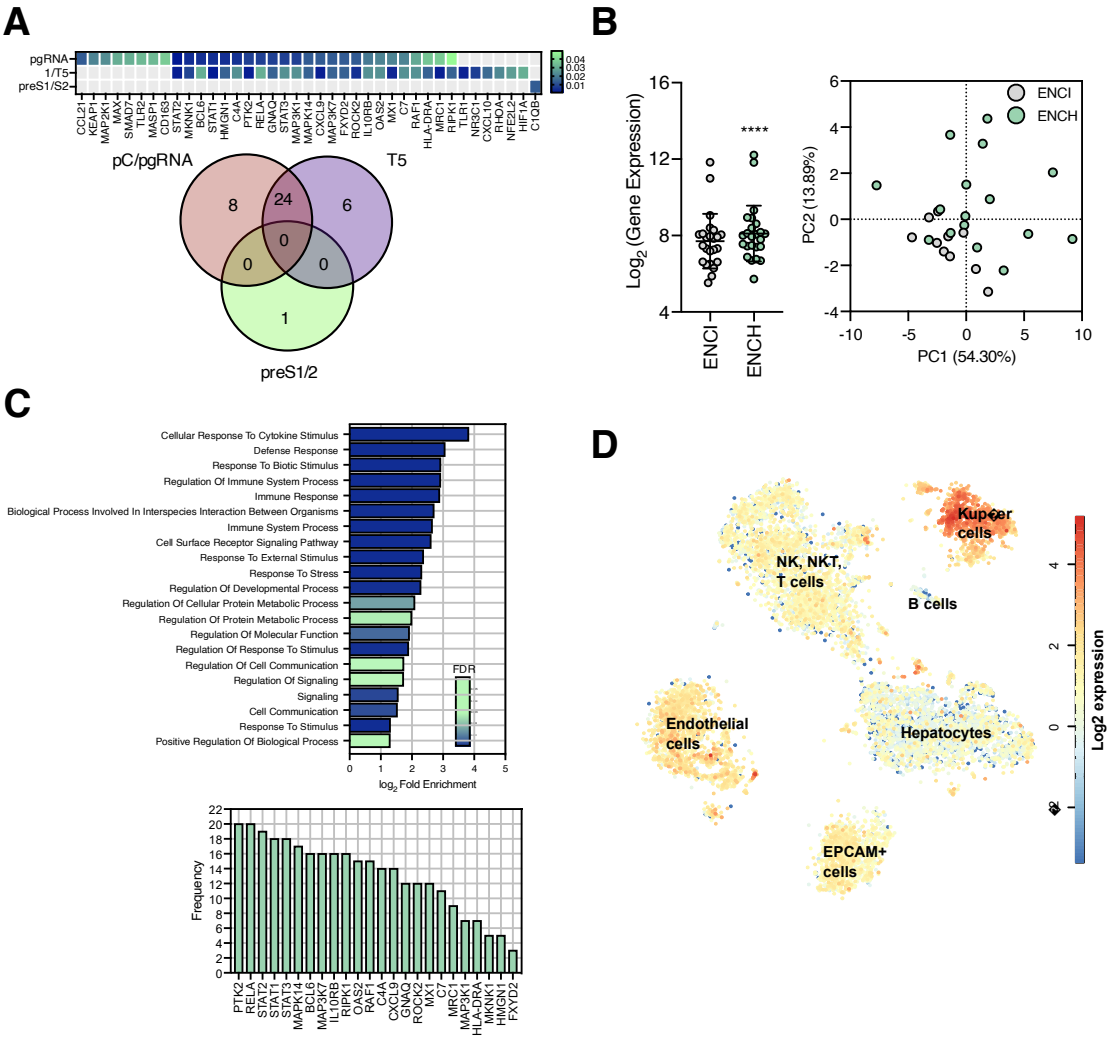


Figure 3.8: An immune gene signature associating with HBV replication

(A) Heatmap and Venn diagram depicting the q-value and number of inflammatory gene transcripts that positively associate with pC/pg, PreS1/S2 RNAs, or T5 from CHB biopsies and their overlap. Significance was estimated using Spearman's Rank Correlation Coefficient with p-values corrected for a 10% false discovery rate (FDR) using the two stage Benjamini-Krieger-Yekutieli method. **(B)** Expression of 24 genes in common between pC/pg RNA and T5 identified in (A) in patients grouped by ENCI or ENCH. Statistics tested by Wilcoxon signed-rank test, left. Principal component analysis (PCA) of the 24 genes in stratifies the patients according to their EASL disease staging (ENCI denoted in grey, ENCH in green). **(C)** Pathway analysis of enriched GO biological processes from PantherDB, GO redundancy was accounted for by collapsing by REVIGO (Mi et al., 2021; Supek et al., 2011). Pathways were selected based on FDR of 0.05, and where at least half of our gene set was represented. Frequency of genes in the 21 pathways presented below. (**D)** Cell type-specific expression of the 24 inflammatory genes in the human liver single

cell atlas, where data is presented as the mean of the log2-transformed values (Aizarani et al., 2019; Juhling et al., 2021). *Experiments and analyses carried out in collaboration with Dr Andrea Magri (Figure 3.9A,B); with thanks to Dr Frank Juhling and Prof Thomas Baumert for scRNA-seq data (Figure 3.9D).*

3.10: Summary

The aim of this results chapter was to gain a better understanding of the contribution of HIF to the diseased hepatic transcriptome. It became clear from the offset that it would be difficult to dissect the mechanism given the intricate interplay between hypoxia signalling and inflammation, and that the overarching conclusions would be limited by the caveat of: 'what came first' inflammation or HIFs? (Imtiyaz and Simon, 2010).

Primarily, we show evidence of hypoxic gene expression in the CHB liver by using GSEA and a series of archived gene sets from the MSigDB. This revealed that along with hypoxic genes, many host pathways and processes related to immune signalling and inflammatory pathways were enriched (**Figure 3.1A,B**) (Liu et al., 2020b). We noted that none of the hypoxic or HIF gene signatures recorded on MSigDB were of hepatic origin, and reflected transcriptomic data derived from a range of other carcinoma cell lines such as lung, breast and skin lines (**Figure 3.2D**) (Liberzon et al., 2011). We identified the need to develop a hepatocyte derived hypoxic gene signature, and used transcriptomic data from the human liver hepatoma line HepG2, the go-to model system for many HBV *in vitro* studies. We identified 80 genes that were upregulated in response to acute hypoxia and likely to be under the transcriptional regulation of HIFs (**Figure 3.2A-C**) (Kindrick and Mole, 2020; Liu et al., 2020b; Smythies et al., 2019).

We applied the new gene signature to a cohort of CHB patients and noted that HIF gene expression was enriched in the infected liver compared to non-viral infected samples (**Figure 3.3B**) (Liu et al., 2020b; Zhou et al., 2017). Additionally,

within the diseased subset, patients with elevated ALT, or higher liver inflammation showed a greater expression of HIF genes than those with normal ALT, suggesting an association between liver inflammation and HIF signalling (**Figure 3.3B**) (Cramer et al., 2003; Palazon et al., 2014). To further this, patients diagnosed with HCV and liver cirrhosis also showed enriched hypoxic gene activity over non-viral subjects, suggesting that this is likely a hallmark of inflammatory liver disease rather than a specific phenotype of CHB (**Figure 3.3C**) (Liu et al., 2020b; Mas et al., 2009; Wilson et al., 2014b).

To gain a greater understanding of viral replication, we sought to develop a qPCR assay that could determine viral transcript patterns and would be widely applicable to *in vitro* and *in vivo* studies. We designed a series of primers to amplify each HBV RNA cumulatively, and matched them for amplicon length and efficiency to allow direct comparison between the species, with a detection limit of around 50 copies per reaction (**Figure 3.4**) (D'Arienzo et al., 2021b). Our assay showed concordance with the gold standard Northern Blot, but required significantly less RNA input which meant it was applicable for use with clinical material. After screening the assay against several routinely used *in vitro* model systems, we applied it to patient samples with confidence (**Figure 3.5A-C**). We analysed HBV RNA transcript patterns in a cohort of CHB patients in the HBeAg negative stage of disease and observed that, in agreement with published literature, RNAs encoding the surface glycoproteins were the most abundant, constituting up to 95% of all viral RNAs (**Figure 3.5D,E**) (Meier et al., 2021; Suslov et al., 2021).

This led us to further develop our assay to distinguish between RNAs derived from integrated or episomal copies of the viral genome. We designed one

further primer pair located in the conventional polyA signal site, which is absent in most integrant derived RNA transcripts (**Figure 3.6A**). We used our primers to estimate the ed-RNA index, which represents the abundance of HBV RNAs that are derived from episomal viral genomes in a series of HBV model systems (**Figure 3.6D**). We observed a wide range of ed-RNA indices in our CHB cohort which suggested ongoing transcriptional activity of both integrants and episomes in the HBeAg- phases of CHB (**Figure 3.6D**). Interestingly, we also noted that the transcriptional activity of HBV genomic integrants increased with duration of infection (**Figure 3.7C**), however it is important to note that our assay does not detect individual integration events but simply the abundance of id-RNAs.

Having developed assays to study both the pattern (**Figure 3.4, 3.5**) and source (**Figure 3.6**) of viral transcription, we sought to investigate the link between hepatic inflammatory mediators and cccDNA activation (D'Arienzo et al., 2021b). We performed gene expression analysis using nCounter NanoString technology and assessed the RNA transcripts of 249 inflammatory genes (Eastel et al., 2019). We identified eighty seven transcripts present in all of our patients, of which a subset of 24 correlated with both pC/pgRNA levels and ed-RNA transcripts (**Figure 3.8A**). This gene set was able to stratify patients by disease staging, and was expressed at higher levels in patients with active hepatitis (**Figure 3.8B**). Using scRNA-seq we identified Kupffer and endothelial cells as the major expressors of these factors, highlighting an important role for the other liver cell types in regulation of viral transcription (**Figure 3.8D**) (Aizarani et al., 2019; Juhling et al., 2021).

In short, this chapter shows evidence of hypoxic signalling in the CHB liver, which may work alongside inflammatory pathways to regulate HBV replication. We

have developed assays to determine both the patterns and source of HBV transcripts, and these are widely accessible and applicable to HBV infected material from both *in vitro* and *in vivo* systems. We identify 24 host factors that could be regulating HBV cccDNA in the HBeAg negative phase of CHB, which are increasingly active in the chronic hepatitis stage in the natural history.

Chapter 4: A role for HIF in HBV life cycle

4.1: Introduction

Hypoxia and HIFs have been implicated in the life cycle of many viruses, and until our study no comprehensive work on the role for HIFs in HBV replication had been reported (Liu et al., 2020a; Wing et al., 2021). As discussed in *Chapter 1.3.2*, HIFs are some of the major transcriptional regulators under hypoxic conditions (Kindrick and Mole, 2020). When oxygen is abundant the prolyl-hydroxylase (PHD) enzymes are active, and they hydroxylate proline residues on newly synthesised HIF-1α or HIF-2α subunits, which targets them for poly-ubiquitination by the E3 ubiquitin ligase and their subsequent degradation (Ratcliffe et al., 1998). However when oxygen is limiting, the PHDs are inhibited and HIFs are not degraded and translocate to the nucleus, where they dimerise with HIF-1β and bind a canonical HRE in the promoter region of host genes, to activate their transcription (Ratcliffe et al., 1998; Semenza et al., 1996). HIFs regulate a myriad of host genes involved in a variety of cell processes such as metabolism, the immune response and angiogenesis (Cramer et al., 2003; Krock et al., 2011; Lum et al., 2007; Palazon et al., 2014). The majority of *in vitro* HBV studies will overlook the role of HIFs as they are performed at atmospheric oxygen levels of 18%; therefore we evaluated the impact of low oxygen culture and subsequent HIF signalling on HBV replication in a variety of model systems (Gan and Ooi, 2020; Keeley and Mann, 2019).

In the previous chapter we explored and discussed the contribution of HIFs to the diseased hepatic transcriptome (Liu et al., 2020b). We observed evidence of HIF signalling in CHB and sought to explore the impact of this pathway on HBV

replication. In this chapter we aim to define the hepatoma cell response to hypoxia and to explore the impact of HIF-signalling on HBV replication. Using bioinformatic analysis and molecular virology approaches, we identify a positive regulatory role for HIFs in the HBV life cycle. We optimise ChIP assays to assess transcription factor binding to HBV DNA, and explore the interplay between HIFs and HBV in both *in vitro* and *in vivo* model systems (Wing et al., 2021).

4.2: HREs are evolutionarily conserved in the hepadnaviruses

We hypothesised that HBV had evolved to bind HIFs to exploit the naturally hypoxic environment of the liver. As HBV replicates from a double stranded DNA copy of the genome, it is capable of interacting with host factors in a manner similar to host chromatin. In collaboration with Dr Peter Balfe we scanned 7,313 HBV genome sequences spanning all documented human genotypes and sub-genotypes, as well as ancient genome sequences derived from bronze age samples (Hayer et al., 2013; Muhlemann et al., 2018). To assess the evolutionary conservation of any putative binding factor motifs, we included genome sequences of primate, amphibian and avian viruses. We found 2 HRE motifs encoded in the HBV genome, one in the sense strand located in EnhI (nt 1236-1240), and an antisense element located between EnhI and EnhII (nt 1604-1599). These two motifs showed a high level of conservation and were present in all human genotypes with the exception of GtH, including ancient bronze age specimens, as well as sequences derived from higher primate and woodchuck hepadnaviruses (**Figure 4.1A**). However, the presence of a binding motif alone is not sufficient to claim functional activity, as many other factors such as chromatin conformation and DNA methylation can regulate accessibility and transcription factor binding (Kindrick and Mole, 2020; Stroud et al., 2011; Valinluck et al., 2004). The DNA must be sufficiently accessible to these transcription factors or complexes, to permit binding and subsequent transcriptional activation (Gusmao et al., 2016; Pique-Regi et al., 2011). There is ongoing research to combine motif scanning, ChIP/ChIP-seq assays, chromatin conformation and RNA transcriptomic data to understand the relationship between the presence of a motif, transcription

factor binding, and induction of gene expression (Karimzadeh and Hoffman, 2021).

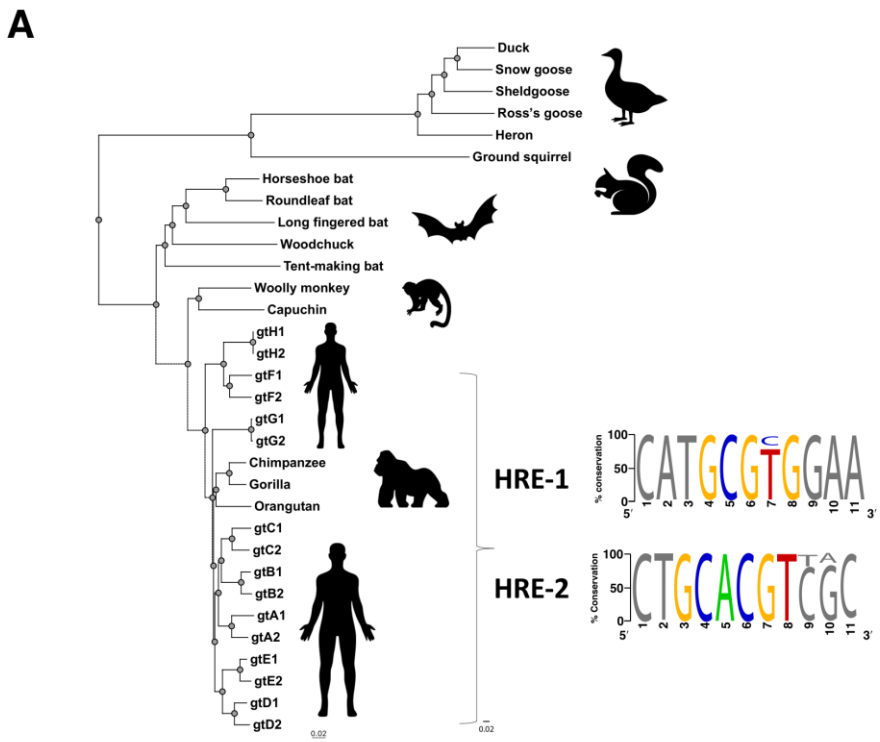


Figure 4.1: HREs are evolutionarily conserved in the hepadnaviruses

(A) Conservation of hypoxic responsive elements amongst hepadnavirus genomes of diverse lineages. 2 HRE motifs were identified in the genome, one at 1236-1240 and another in the antisense strand from position 1605-1599. RCGTGC motif was scanned in 7,313 genomes deposited on NCBI, including HBV genomes from bronze age specimens (Muhlemann et al., 2018). All human genotypes, with the exception of GtH, as well as woodchuck and higher primate derived viruses encode both HREs (Wing et al., 2021). *With thanks to Dr Peter Balfe for generating this figure.*

4.3: Requirement for a DMSO free system

DMSO is an aprotic solvent with pleiotropic effects on host cell gene expression, that is frequently used in HBV model systems as a cell cycle arresting agent to limit cell division and dilution of the cccDNA (Ko et al., 2018; Villa et al., 1991). Whilst low concentrations of DMSO are routinely used as controls for drug dilutions in cell biology, supplementing growth media with 2.5% DMSO is common place for HBV in vitro assays (Ko et al., 2018; Le et al., 2021). Given the wide-ranging effects of this solvent we sought to understand whether DMSO treatment altered hepatoma transcriptional response to low oxygen. In collaboration with Dr Nicholas Frampton, RNA was prepared from HepG2-NTCP cells that were untreated or cultured in 2.5% DMSO for 72 hours, then cultured in 18% or 1% oxygen for 24 hours. Gene expression was quantified using an SAB qPCR microarray that detected a panel (n=84) of hypoxic regulated gene transcripts. We screened this panel for genes identified to bind either HIF-1α or HIF-2α and showed that DMSO treatment blunted the hypoxic induction of both HIF-1α and HIF-2α regulated genes compared with untreated cells (**Figure 4.2A**) (Smythies et al., 2019; Wing et al., 2021).

We also analysed 37 hypoxic gene transcripts which were not previously identified as HIF targets. Reassuringly, fewer of these genes were upregulated in response to the low oxygen conditions, however we noticed that their induction was still blunted in the DMSO treated cells compared to the untreated controls (**Figure 4.2B**). It is worth noting that some of the hypoxic-regulated genes were downregulated in our hypoxic HepG2 cells, highlighting the conclusions from *Chapter 3*; the hypoxic response is cell type specific and this commercially

available micro-array may under-represent the HepG2 transcriptional response to low oxygen (Encode Project Consortium, 2012; Kindrick and Mole, 2020). To quantify the blunted hypoxic response, we performed a Wilcoxon paired rank test, and observed a dampening of the cellular response to hypoxia in the presence of DMSO (**Figure 4.2C**).

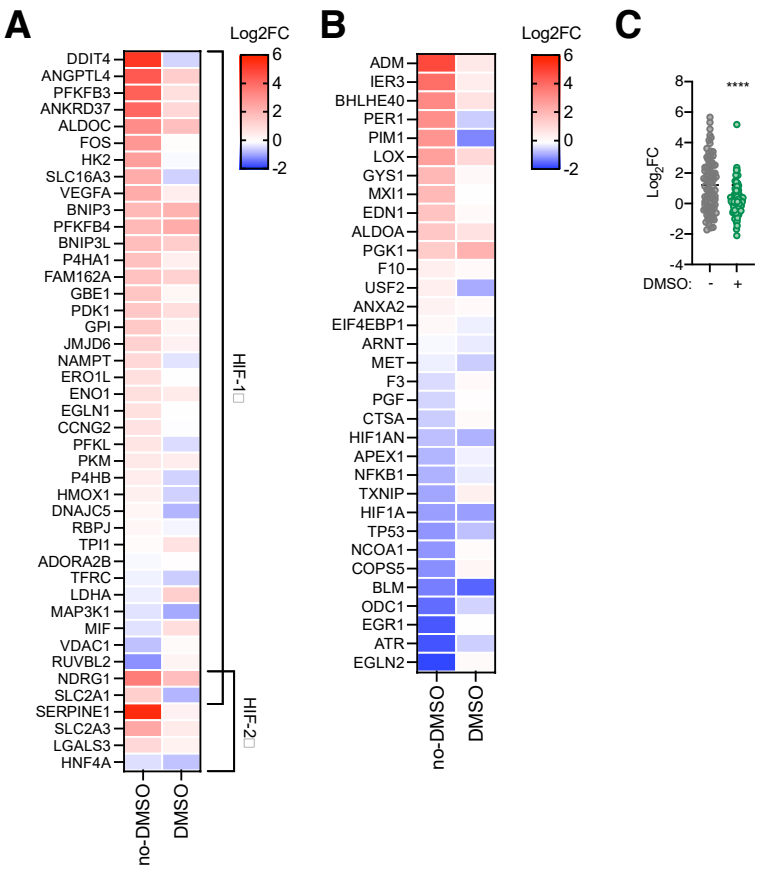


Figure 4.2: Requirement for a DMSO free system

(A) HepG2 cells were untreated or treated with 2.5% DMSO for 72 hours and cultured in either 18% or 1% oxygen for 24 hours. Cellular RNAs extracted, and screened for the expression of 84 hypoxic regulated genes by SAB micro-array, normalised to a panel of 6 house-keeping reference genes. Genes which show HIF-1α or HIF-2α binding by ChIP-seq are plotted in (A) (Smythies et al., 2019). **(B)** Hypoxic regulated genes which showed no evidence of direct HIF binding are plotted in order of fold change in no-DMSO treated cells (Wing et al., 2021). **(C)** Fold changes of hypoxic genes were compared between untreated or DMSO differentiated HepG2 cells. Statistics were analysed using a Wilcoxon paired sign rank test. *With thanks to Dr Nicholas Frampton for performing the qPCR assay.*

4.4: Hypoxia arrests hepatocyte cell cycle

As previously discussed, DMSO is routinely used in HBV *in vitro* studies to arrest cell proliferation to limit the loss of cccDNA during cell division ((Ko et al., 2018), reviewed in (Allweiss and Dandri, 2017)). For the purposes of this study, the terms arrest and synchronise refer to the mitotic cell cycle, rather than the host circadian cycle, which our group recently reported to be implicated in HBV replication (Zhuang et al., 2021). However, cell cycle and the circadian clock are intrinsically linked, with several checkpoint regulators identified to show rhythmic expression (Jiang et al., 2021)(reviewed in (Farshadi et al., 2020)) . For example, p21 is a critical inhibitor of cyclin dependent kinase-2 and is under the circadian regulation of REV-ERBα/β in the murine liver (Grechez-Cassiau et al., 2008). As such, it is likely that DMSO elicits pleotropic effects on many host regulatory pathways that are not limited to hypoxic signalling. A previous study from Goda et al. identified a role for HIF-1α in arresting cell cycle in response to hypoxia in embryonic fibroblasts and splenic B lymphocytes (Goda et al., 2003). We were interested to evaluate the effect of hypoxia on HepG2-NTCP cell cycle.

Many cell cycle studies rely on a simple 1 colour flow cytometry assay using a DNA dye such as 7-amino-actinomycin or propidium iodide. We opted to use a more sensitive 2 colour FACs panel that measured incorporation of the thymidine analogue, bromodeoxyuridine (BrdU), and propidium iodide (PI) as a DNA dye to measure chromatin content (**Figure 4.3A**) (Davenne et al., 2020; Wing et al., 2021). We cultured cells in the desired conditions, and incubated with BrdU (10 μM for 60 minutes) to allow incorporation into newly synthesised DNA in actively proliferating cells (S phase). Total cellular DNA was visualised by PI

staining and cells have either 1 complement of chromosomes ($G_{0/1}$), or twice as many ($G_{2/M}$) immediately before their entry into mitosis (**Figure 4.3B**). The cells in S-phase are actively incorporating BrdU into their replicating DNA, and so are 488+, however they show a less well defined PI staining pattern than the 488- populations. This is likely reflective of unsynchronised cells that have entered mitosis at slightly different times, and therefore have more or less time to complete their DNA replication in the presence of BrdU.

To establish whether hypoxia arrested the cycling of HepG2-NTCP cells we cultured them in 18% or 1% oxygen for 72 hours, and included a control of 2.5% DMSO treatment as a known arresting agent. Hepatocytes *in vivo* are in deep quiescence or G_0 and it has been estimated that as few as 1 in 20,000 hepatocytes are in cell cycle in vivo (Furchtgott et al., 2009; Mangnall et al., 2003). However, our simple 2 colour FACs cannot discern between cells in G_0 or G_1, and as reviewed by Corlu et al. cell cycle arrest *in vitro* is at best a G_0-like stage, and represents a potent G_1 arrest (Corlu and Loyer, 2012; Mangnall et al., 2003). In our assay, both DMSO treatment and 1% oxygen caused an arrest in $G_{0/1}$, suggesting that hypoxic culture arrests cells in a more physiological manner (**Figure 4.3C**).

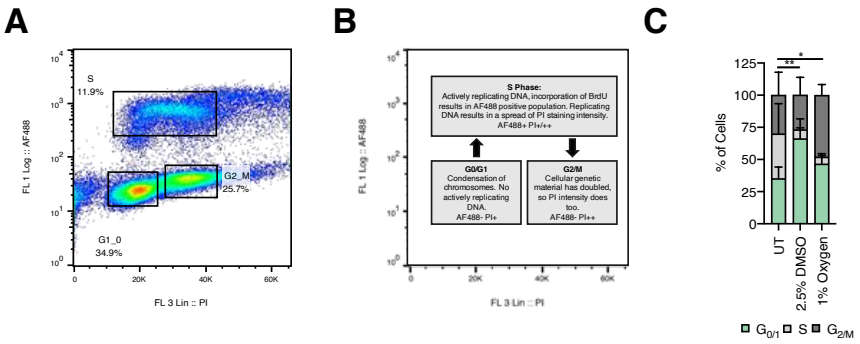


Figure 4.3: Hypoxia arrests hepatocyte cell cycle

(A) Cell cycle was determined by BrdU incorporation and Propidium Iodide staining by flow cytometry. Cells were treated with 10 μM BrdU for 60 minutes, before trypsinisation and fixation. A representative FACs plot to show gating strategy for each phase of the cell cycle (Davenne et al., 2020). **(B)** A schematic diagram highlighting the methodology used to determine phase based on BrdU incorporation, and DNA abundance by propidium iodide staining. **(C)** HepG2-NTCP cells were treated with 2.5% DMSO or cultured in 1% oxygen for 72 hours before cell cycle phases were determined. Both conditions resulted in modulation of cell cycle when compared with untreated samples (Wing et al., 2021). Data are representative of n=2 independent experiments, using Mann-Whitney tests to apply statistics to S-phase events.

4.5: Low oxygen potentiates HBV replication

Since HBV encodes 2 canonical HRE motifs (**Figure 4.1**), we were keen to understand the effect of low oxygen conditions on HBV replication. Preliminary data from Dr Peter Wing showed enhanced activity from a transiently transfected HBV BCP-luciferase construct in 1% O_2, peaking at 72 hours post hypoxic culture (Wing et al., 2021). With further support from Dr Peter Wing, we infected HepG2-NTCP cells for a 6 hour period, using a recently published protocol from Chakraborty et al. (Chakraborty et al., 2020), before culturing cells in either 18% or 1% oxygen for 72 hours. Given the evidence of cell cycle arrest in response to hypoxia, we initially assessed the levels of the viral cccDNA, the template for HBV replication. This was to ensure that any modulation in transcript levels were not simply a result of changes in cccDNA template, and we noted no variation in cccDNA levels in hypoxic cells (**Figure 4.4A**) (Wing et al., 2021).

Using our previously reported T1 primers, we quantified pC/pgRNA levels from the normoxic and hypoxic infected cultures (D'Arienzo et al., 2021b). We observed a 30-fold increase in pC/pgRNAs in response to hypoxia (**Figure 4.4B**). To assess the host cell response to hypoxia we quantified RNAs encoding Carbonic Anhydrase 9 (CA9), which was the most significantly upregulated HIF target gene presented in *Figure 3.2A.* CA9 is known as one of the most sensitive indicators of HIF transcriptional activity in many different cell types, and whilst we observe a significant increase in our hepatoma line, it is somewhat overshadowed by the increase in viral pC/pg RNA (**Figure 4.4C**) (Buffa et al., 2010; Giatromanolaki et al., 2001; Wing et al., 2021).

We sought to validate our findings in another model system, and employed a recently published reporter virus construct, which is a recombinant HBV that encodes a Gaussia Luciferase (GLuc) reporter in place of the viral polymerase coding region (Wing et al., 2019). As per the authentic HBV *de novo* infection model, we infected cells for 6 hours and cultured in 18% or 1% O_2 for 72 hours before harvesting intracellular RNAs and extracellular media containing secreted GLuc. We observed an oxygen dependent increase in the viral pC/pgRNA by qPCR, however when screening the GLuc activity, we noted that protein secretion was modestly, but significantly decreased (**Figure 4.4D**) (Wing et al., 2021). The GLuc reporter is under the control of a transthyretin promoter, rather than the endogenous HBV promoter and is repressed under low oxygen, thus highlighting the differential response driven by different gene promoters. This is a limitation of using reporter systems with artificial promoter constructs, rather than the endogenous viral promoter and enhancer regions. Whilst the most important message of these data is that HBV replication is potentiated by a low oxygen environment, it is worth noting the limitations of using virus genomes with heterologous reporters.

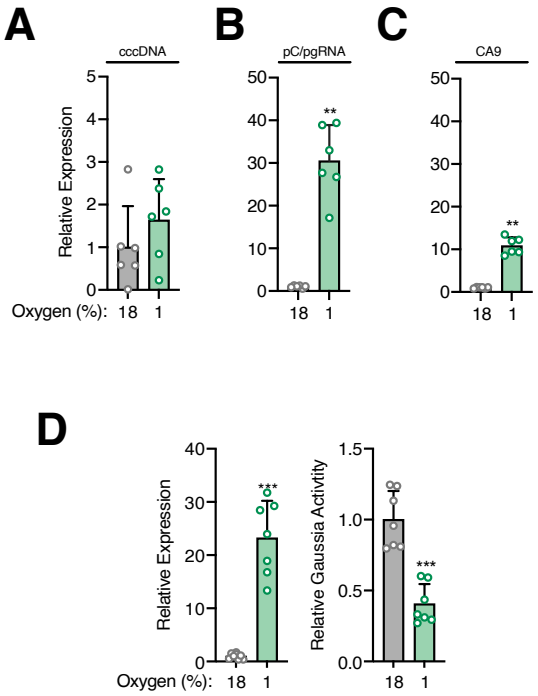


Figure 4.4: Low oxygen potentiates HBV replication

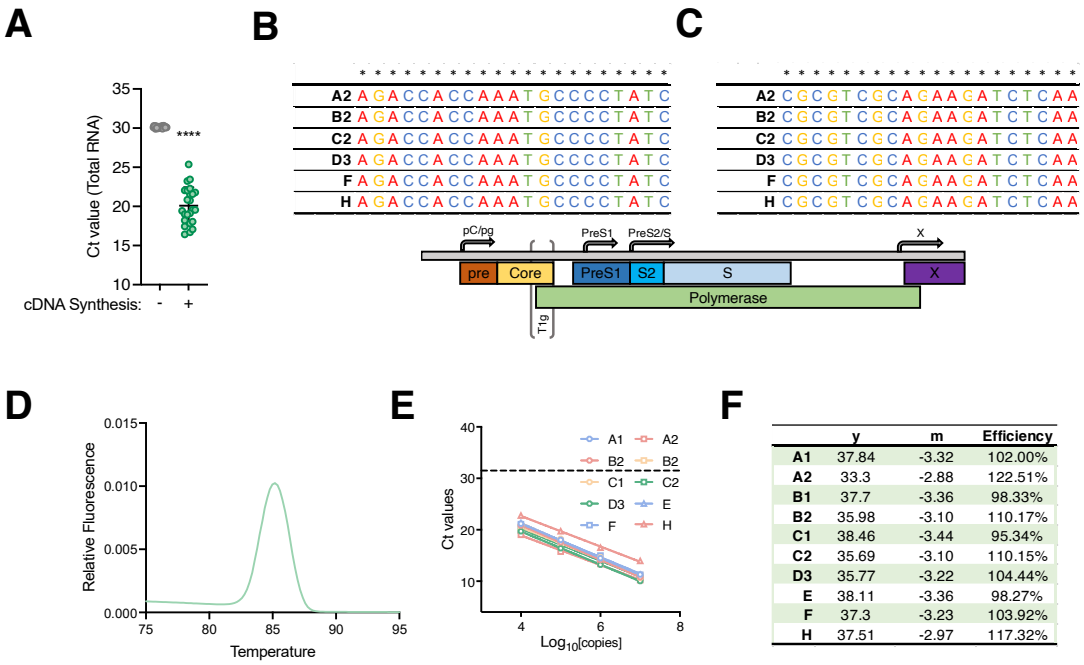
(A) HepG2-NTCP cells were infected with HBV for 6h, before extensive washing to remove unbound virus, and cultured in 18% or 1% oxygen for 72 hours. Total cellular DNA and RNA were harvested from the same well, to allow quantification of viral cccDNA and HBV RNAs. cccDNA copies were enumerated by qPCR and normalised to the single copy host gene PRP, then expressed relative to 18% levels. **(B)** From the same well HBV pC/pgRNA copies were enumerated by qPCR, adjusted to B2M housekeeper and normalised to 18% oxygen. **(C)** Host response to hypoxia was determined by quantifying CA9 mRNA levels, a HIF target gene (Wykoff et al., 2001). Fold change was calculated by a DDCt method and expressed relative to 18% oxygen. **(D)** HepG2-NTCP cells were infected with a HBV reporter virus encoding a Gaussia luciferase reporter, then cultured in 18% or 1% oxygen for 72 hours. Cells were lysed and HBV RNAs were enumerated by qPCR, simultaneously secreted Gaussia luciferase activity was quantified. **(A-D)** All data are derived from n=2 independent experiments and significance tested using Mann-Whitney U tests (Wing et al., 2021). *With thanks to Dr Peter Wing for providing samples for screening in Figure 4.4A,B,C and assistance with experiments in Figure 4.4D.*

4.6: Lipid transfection of overlength genomes

As reviewed in the *Chapter 1.2.6*, HBV can be classified into genotypes and sub-genotypes based on nucleotide sequence divergence, and the genotypes show distinct geographical distribution and differences in their molecular pathogenesis (Kramvis, 2014; Kramvis et al., 2005; Kramvis and Kew, 2005). One means of overcoming genotype specific differences in early infection events, such as entry or cccDNA genesis, is the delivery of HBV DNA by lipid transfection of overlength 1.3x genomes. Through a collaboration with Professor Peter Revill's laboratory at The University of Melbourne, Australia, we received HBV1.3 plasmids encoding the genomes of multiple diverse clones including genotypes and sub-genotypes: A1, A2, B1, B2, C1, C2, D3, E, F and H.

Due to perfect sequence homology between HBV DNA and RNA transcripts, we routinely perform DNAse digestion on RNAs derived from *de novo* infection systems. However, given that lipid transfection based delivery of DNA constructs operates at a much higher efficiency than *de novo* infection, we opted to use a more potent DNAse to destroy any residual plasmid DNA carryover from the extraction process. We extracted RNA from cells transfected with HBV1.3 GtD, and treated with TURBO DNAse. To evaluate the efficiency of DNAse digestion, we assessed total HBV RNA amplification in both RNA (-RT) and cDNA (+RT). We observed Ct values between 28 and 16 in the cDNA, whereas the -RT control resulted in Ct values greater than 30 (**Figure 4.5A**) (D'Arienzo et al., 2021b). This suggests that the TURBO DNAse digestion ablates the majority of residual plasmid DNA in the total cellular genomic material.

As described in *Chapter 3.4* our HBV transcript PCR is designed against a consensus sequence derived from HBV GtD and we designed a new primer pair, T1g, targetting a conserved region (between GtA, B, C, D, F and H) of the pC/pgRNA coding sequence with no overlap with PreS1 RNAs (**Figure 4.5B,C**) (D'Arienzo et al., 2021b). Using RNA derived from HepG2-NTCP cells transfected with representative clones of the aforementioned genotypes, we quantified pC/pgRNA using the T1g primer pair and observed a single clean melting peak, demonstrating primer specificity (**Figure 4.5D**). We tested the efficiency of our new T1g primers to amplify the different HBV genotypes on a dilution series of HBV1.3 DNA. The new primer pair showed comparable amplification efficiencies across the panel of diverse clones, with a similar detection limit of around 50 copies per reaction, amplifying in the same linear range as the T1-T4 primers (**Figure 4.5E,F**) (D'Arienzo et al., 2021b).



	y	m	Efficiency
A1	37.84	-3.32	102.00%
A2	33.3	-2.88	122.51%
B1	37.7	-3.36	98.33%
B2	35.98	-3.10	110.17%
C1	38.46	-3.44	95.34%
C2	35.69	-3.10	110.15%
D3	35.77	-3.22	104.44%
E	38.11	-3.36	98.27%
F	37.3	-3.23	103.92%
H	37.51	-2.97	117.32%

Figure 4.5: Lipid transfection of overlength genomes

(A) HepG2-NTCP cells were transfected with GtD HBV1.3 constructs, 72 hours later cells were lysed and HBV RNA quantified by qPCR, following TURBO DNAse digestion to remove plasmid DNA. The efficiency of DNAse digestion was determined by qPCR on material with or without reverse transcription. Significance was tested with a Mann-Whitney U test. **(B-C)** Alignment of HBV genomes from diverse genotypes showing the conserved binding sites of the T1g forward (B) and reverse (C) primers, with a schematic diagram of the viral genome to show primer pair binding location. **(D)** Dissociation curves of the PCR amplicon with the T1g primer set. **(E)** Specificity and sensitivity of the T1g primer pair was tested on a 10-fold dilution series of HBV1.3s of 6 different HBV genotypes, and standard curves generated. **(F)** Equations of standard curves and primer efficiencies were calculated from the points shown in E.

4.7: HBV-HRE mutant constructs

We previously used a bioinformatic motif scanning approach to identify HREs in the HBV genome, and identified that HBV GtH was the only human genotype which did not encode a HIF binding element in EnhI (**Figure 4.1**). Genome alignment and scanning revealed that the HBV1.3 clones were indeed representative, and our GtH construct did not encode a canonical HRE in EnhI (**Figure 4.6A**). We hypothesised this polymorphism would render GtH insensitive to hypoxic culture, and there would be no hypoxic-dependent increase in its replication. To test this hypothesis we delivered HBV DNA of GtD or GtH by lipid transfection into HepG2-NTCP cells and cultured in 18% or 1% oxygen for 72 hours before assessing viral RNAs by qPCR. As predicted, we observed a low oxygen dependent increase in the viral pC/pgRNA with GtD, and no significant modulation of RNAs in GtH. To assess whether any differences in transcription were masked by differential transfection efficiency, we quantified copies of intracellular HBV DNA and calculated transcriptional output, noting the same phenotype (**Figure 4.6B**). It would be tempting to speculate that the absence of the HRE in HBV GtH could be the driver of the less aggressive phenotype of this genotype *in vivo,* however this is speculative and would require comprehensive *in vivo* investigation to address (Sozzi et al., 2018).

We wanted to confirm that this phenotype was truly mediated by the HRE and not due to genotype specific differences in transcriptional activity. In collaboration with Professor Peter Revill, we obtained synthetic viral genomes with a mutated HRE-1 in GtD (GtD_{mut}), and a restored HRE-1 in GtH (GtH_{mut}). We profiled the hypoxic response of both mutated and wildtype constructs in HepG2-

NTCP cells and noted that GtD_{mut} was still responsive to the hypoxic stimulus, and observed modest upregulation of pC/pgRNA in both GtH and GtH_{mut}. However, these conclusions are limited as only HRE-1 was mutated in our constructs. Analysing secreted HBeAg levels revealed a modest increase with GtD, which was lost in the mutated construct, and a hypoxic reduction in GtH, although this was not reversed by restoration of the HRE in GtH_{mut} (**Figure 4.6C**).

We sought to rationalise our use of the HBV1.3 genomes, and compared authentic *de novo* infection of HepG2-NTCP cells with lipid transfected overlength DNA genomes. Using our 4 transcript PCR method, we investigated patterns of viral transcription in each model. We compared HBV RNAs derived from GtD genomes in *de novo* infected HepG2-NTCP and PHH cells, as well as HepG2-NTCP cells transfected with HBV1.3 GtD. 72 hours post-delivery, we observed little difference between patterns in both *de novo* infection models, with pC/pg and PreS1/2 RNAs representing the major transcripts. However the pattern in the HBV1.3 transfection was starkly different, with proportionally less pC/pgRNA (**Figure 4.6D**).

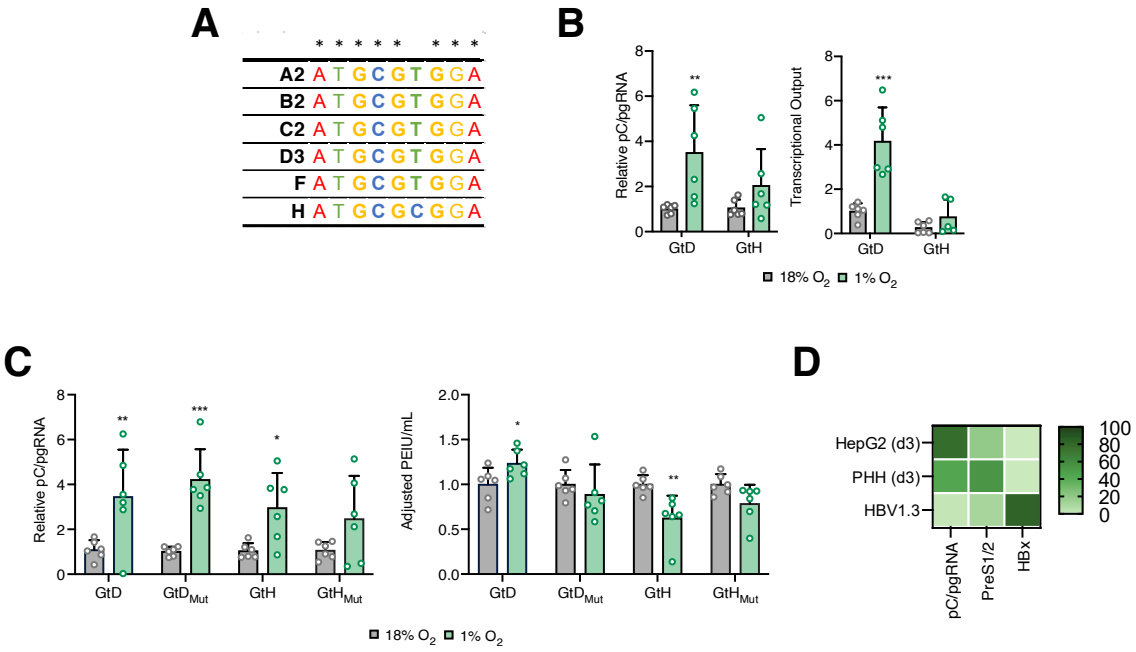


Figure 4.6: HBV-HRE mutant constructs

(A) Alignment of the HRE-1 motif in the BCP region of 6 diverse HBV clones. HRE-1 is conserved across all genotypes with the exception of GtH. **(B)** HepG2-NTCP cells were transfected with HBV1.3 GtD or GtH and cultured in 18% or 1% oxygen for 72 hours. Cells were lysed and HBV pC/pgRNA determined by qPCR, and expressed relative to 18% oxygen. HBV DNA copies were also enumerated as an internal control for transfection efficiency and expressing pC/pgRNA copies relative to HBV DNA shows transcriptional output. **(C)** Synthetic viral genomes were designed to restore HRE-1 in GtH (GtH_{mut}) and mutate HRE-1 in GtD (GtD_{mut}) constructs. Cells were transfected then cultured in low oxygen for 72 hours before pC/pgRNA was quantified using T1g primers (left), and secreted HBeAg was detected and expressed relative to HBV DNA (right). **(D)** Transcript pattern of HBV1.3 GtD was determined by qPCR and compared with viral RNAs extracted from *de novo* infection of HepG2-NTCP cells and PHHs. **(B-D)** Data are derived from n=2 independent experiments and statistics tested with Mann-Whitney U test. *With thanks to Professor Peter Revill for providing synthetic HRE mutant constructs.*

4.8: Shearing HBV DNA

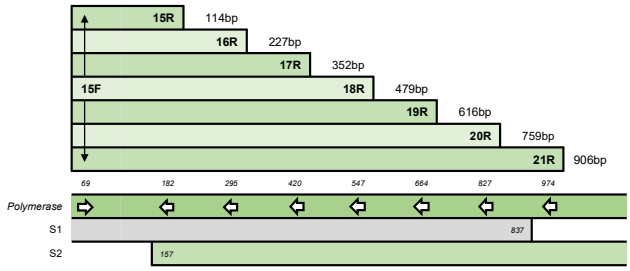
As previously discussed, HIFs regulate gene expression by directly binding the HRE motif in the promoter region of target genes, and we observed a hypoxic induction of HBV pC/pgRNA akin to a canonical HIF response gene. We therefore wanted to investigate whether this was through direct binding of HIF subunits to the HRE element in the viral BCP, and performed chromatin immunoprecipitation (ChIP) to assess transcription factor binding. To increase the signal to noise ratio in a ChIP-qPCR assay, it is important to shear and fragment the chromatin. Sonication typically breaks genomic DNA into fragments of around 250bp, and allows for a more sensitive detection of protein:DNA complexes (Steube et al., 2017). We are by no means the first group to perform ChIP assays on HBV DNA and many studies have applied ChIP-qPCR and ChIP-seq to study virus-host interactions (Belloni et al., 2012; Flecken et al., 2019; Tropberger et al., 2015). However, one report from Pollicino et al. stated that the viral mini-chromosome was resistant to sonication, however no data was provided to substantiate the claim (Pollicino et al., 2006).

Before investigating whether HIFs can bind HBV DNA, we initially sought to test whether viral DNA could be fragmented by sonication. We prepared whole cell lysates from HepG2-NTCP cells that had been infected with HBV for a period of 6 days, and pulse sonicated (15s ON; 15s OFF) half of the sample for 30 minutes at high intensity; this sonication protocol may seem severe but was recently used by collaborators in a published HIF ChIP-seq study (Smythies et al., 2019). We then extracted cellular DNA from the control or sonicated lysates by phenol:chloroform isolation. Using classical endpoint PCR we amplified HBV DNA of increasing

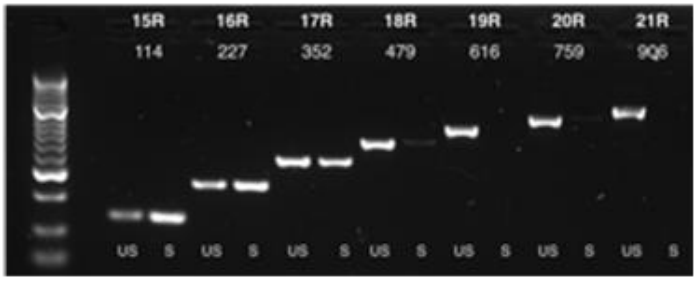
fragment lengths, whereby we used a universal forward primer (HepB15F) and walked the reverse primer across the genome at c100bp increments (**Figure 4.7A**). Using gel electrophoresis, we could detect HBV DNA products of up to 906 base pairs in the unsonicated samples, however sonication abrogated the amplification of products greater than 352 base pairs, demonstrating shearing of the HBV DNA (**Figure 4.7B**). This was also demonstrated in a recent publication where host factor CTCF binding was mapped to the HBV genome using the HepG2-pEpi model, and similar fragment sizes were observed (D'Arienzo et al., 2021a; Lucifora et al., 2014). As ChIP-qPCR is the gold standard method to assess transcription factor binding, we also assessed shearing by qPCR. We used the same samples and primer combinations as above, and reviewed the product dissociation curves to assess amplification. Both end-point and qPCR data sets showed excellent concordance, with clean melting peaks visible for the 114, 227 and 352 nucleotide products in the sonicated and unsonicated material. For the remaining primer combinations of increasing amplicon size, we observed clean melting peaks in the unsonicated samples, but spurious products producing double and unclean peaks in the sonicated DNA (**Figure 4.7C**). Taken together, these data show that HBV DNA can be sheared by sonication, and ChIP-qPCR could be used to provisionally map transcription factor binding sites in the viral genome.

A

Primer	Strand	Bindng Site Min	Bindng Site Max	Sequence	Amplicon Length
HepB15F	Forward	69	92	CTCCAGTTCAGGAACAGTAAACCC	
HepB15R	Reverse	159	182	AGGAATCCTGATGTGATGTTCTCC	114
HepB16R	Reverse	272	295	CGGTAGTTCCCCCTAGAAAATTGA	227
HepB17R	Reverse	397	420	CAGCAGGATGAAGAGGAAGATGAT	352
HepB18R	Reverse	525	547	TTCCTTGAGCAGTAGTCATGCAG	479
HepB19R	Reverse	661	684	TAGTAAACTGAGCCAGGAGAAACG	616
HepB20R	Reverse	804	827	ACCCAAAGACAAAAGAAAATTGGT	759
HepB21R	Reverse	951	974	AGGCCTGTTAATAGGAAGTTTTCT	906



B



C

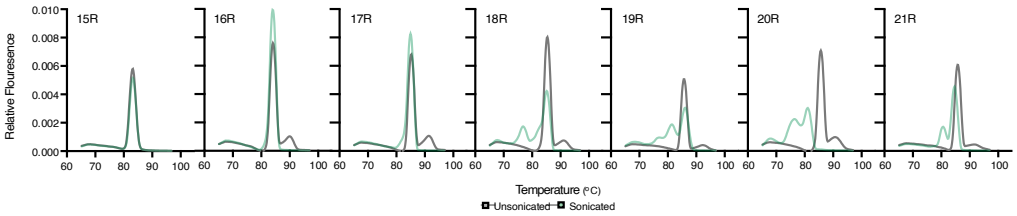


Figure 4.7: Shearing HBV DNA

(A) A table and schematic diagram depicting primer binding sites and amplicon lengths of a series of reverse primers when paired with a universal forward primer (15R). Each reverse primer extends the product length by an average of 128 base pairs. **(B)** Chromatin was extracted from a *de novo* infection of DMSO differentiated HepG2 cells, 6 days post infection. Cells were cross linked in formaldehyde, quenched in glycine, and lysed in SDS lysis buffer. Material was phenol:chloroform extracted +/- sonication. Sonication was performed in a water bath sonicator for 30 minutes, HIGH, 15s ON/15s OFF. Endpoint PCR was ran using each of the 8 reverse primers, with 15F forward primer on sonicated or unsonicated DNA. After 35 cycles, PCR products were resolved on a 1.8%

agarose gel. S denotes sonicated material, U denotes unsonicated. Headings show reverse primers, and amplicon length in bp. **(C)** Using the same strategy as in *B* sonicated or unsonicated chromatin was ran on qPCR using the eight primer combinations. After 50 cycles, melt peaks were analysed and show a loss of specificity in sonicated samples on products above 479bp (15F/18R).

4.9: Assessing HBV transcription factor interactions

Having demonstrated that HBV DNA could be sheared by sonication, we sought to optimise the conditions to retain high signal to noise ratios in the pull downs between our antibodies of interest, and the routinely used negative control IgG. As part of the optimisation experiment we opted to use HNF4α as a positive control; a host transcription factor that has previously been shown to bind the BCP and EnhI/II, and IgG as a specificity control (Cho et al., 2013; Long et al., 2009; Zheng et al., 2004). To assess transcription factor binding to episomal HBV DNA, we prepared chromatin from the HepG2-pEpi cells which support HBV replication from an overlength HBV genome encoded in an integration resistant vector, and thus mimic HBV cccDNA-like molecules (Lucifora et al., 2014). We sonicated samples in 5 minute intervals for up to 30 minutes, before immunoprecipitation with either anti-HNF4α antibody or IgG. We designed primers to amplify the HNF4α binding site in the BCP (HepB3), or an irrelevant site around 1500bp downstream (HepB16) (**Figure 4.8A**). Amplification of DNA from the immunoprecipitate revealed that we could detect HNF4α binding to HBV, with a greater signal at the HNF4α binding site (HepB3) compared to the irrelevant site (HepB16) (**Figure 4.8B**).

IgG is routinely used in ChIP as a control to demonstrate the specificity of the antibody directed against the factor of interest, however its use is frequently criticised as it can yield high background signal due to its affinity for ssDNA (Flensburg et al., 2014; Kidder et al., 2011). Despite this we compared %IP with both anti-HNF4α antibody and IgG at each time point, and the primers spanning the BCP returned a high signal compared with the background (**Figure 4.8C**).

However, this was not the case with the HepB16 primers which span the irrelevant genome site, where in most instances there was no signal above the negative control (**Figure 4.8C**). It is worth noting that even with the specific primers, when DNA was not sonicated there was no detectable signal, suggesting that the shearing stage is essential for this assay (**Figure 4.8C**). This became more obvious when we expressed the HNF4α signal relative to the IgG signal, and showed that sonication of at least 5 minutes improved the detection ratio. It also shows a difference in the fold enrichment between HepB3 and HepB16 primer sets, suggesting that a combination of sonication and selective primer design can increase the robustness of these assays (**Figure 4.8D**).

In short, these data provide an optimal protocol for ChIP-qPCR that relies on sonication and careful selection of primers to specifically target the region of interest, for example, including the cognate binding motif or binding site within the PCR amplicon. With these data in mind, we can study the interaction between HIFs and HBV DNA.

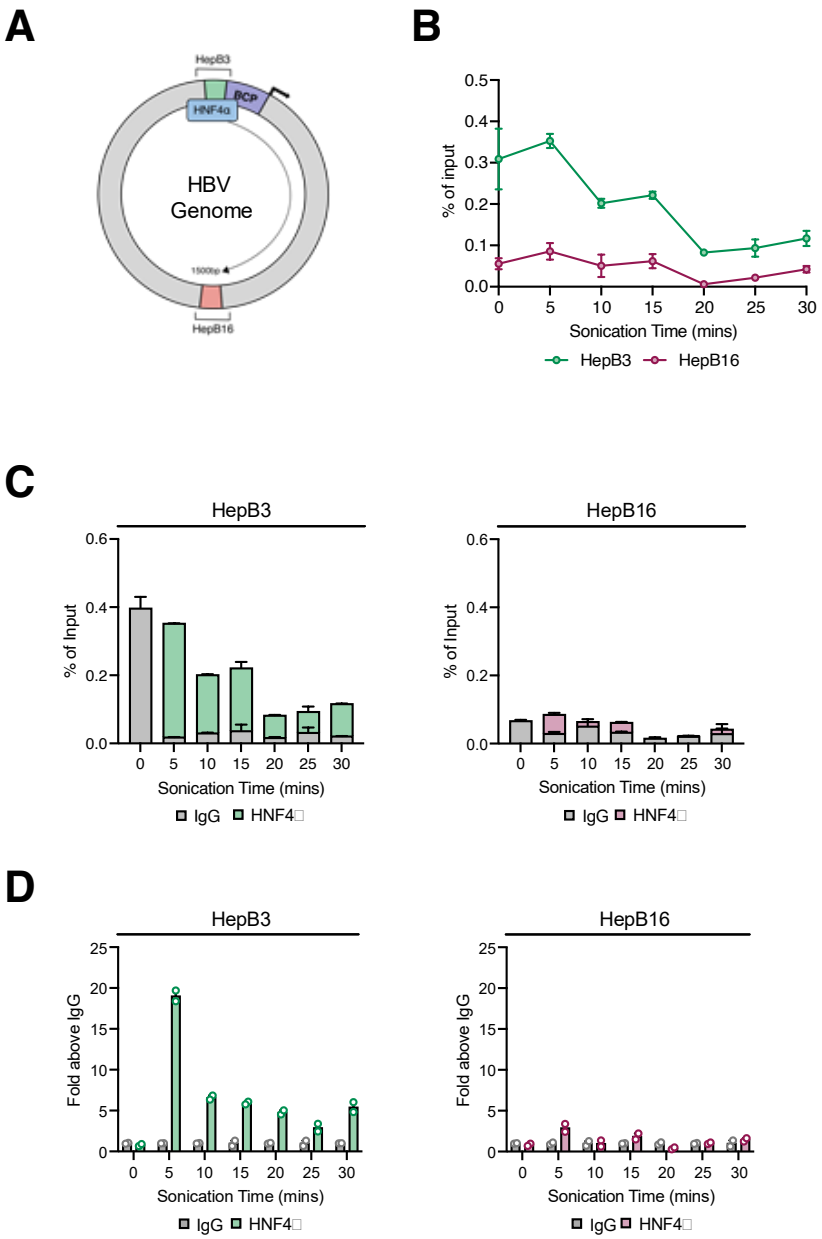


Figure 4.8: Assessing HBV and transcription factor interactions

(A) A cartoon to show primers specific for the HNF4α binding site in EnhI (HepB3) or an irrelevant site approximately 1500bp from the binding site (HepB16). **(B)** Chromatin was prepared from HepG2-pEpi cells, and sonicated for up to 30 minutes. Samples were immunoprecipitated with either anti-HNF4α or IgG and % input was calculated by qPCR using either HepB3 or HepB16 primer pairs. **(C)** %IP of both HNF4α and irrelevant IgG were compared across the binding site (left), and the irrelevant site (right). IgG and HNF4α IPs are overlayed to show signal to noise. **(D)** % IP values for HNF4α were expressed relative to IgG values to show the impact of sonication time on signal to noise

ratio. Data are representative of 2 independent biological replicates, and plotted as mean and range.

4.10: HIFs bind HBV DNA

We sought to investigate whether HIFs bound HBV DNA in response to hypoxia. We chose to pull down HIF-1β as this is the universal sub-unit in all HIF dimers, binding both HIF-1α and HIF-2α to activate transcription. Importantly, there are good commercially available antibodies to HIF-1β, which have been used in previous studies to perform ChIP assays (Smythies et al., 2019). Initially, we prepared chromatin from HepG2-pEpi cells that were untreated and cultured at 18% O_2, in these conditions HIF should be degraded and transcriptionally inactive. We were reassured that there was no specific signal of HIF-1β binding the viral genome in these conditions, nor was it bound to the promoter of the host HIF target gene CA9 (**Figure 4.9A**) (van den Beucken et al., 2009). As an internal reference and positive control for the immunoprecipitation, we utilised anti-HNF4α antibody based on our previous findings presented in *Figure 4.8*. We observed significant enrichment of HNF4α binding to the HBV genome and also to the promoter of APOB, a reported HNF4α regulated gene (**Figure 4.9B**) (Collins et al., 2012). Finally, we included a negative control factor: the retinoic acid receptor-related orphan receptor-α (RORα) which is an important circadian clock component and regulator of hepatic lipid metabolism, which has not been previously shown to directly bind HBV (Kim et al., 2017). RORα showed no evidence of binding HBV DNA, but bound the BMAL1 promoter, a known transcriptional target gene (**Figure 4.9C**) (Akashi and Takumi, 2005; Wing et al., 2021).

To advance these findings, we cultured HepG2-pEpi cells in 1% oxygen for 24 hours, a time point at which HIFs should be transcriptionally active (Smythies et

al., 2019). We also stabilised HIFs by using an inhibitor targeting the prolyl-hydroxylases, FG-4592, which inhibits HIF hydroxylation and their degradation. Importantly, we observed an enrichment of HIF-1β levels on the HBV genome in response to both 1% oxygen culture or FG-4592 treatment. We assessed the host response to hypoxia by evaluating HIF-1β binding to the promoter of CA9, and as expected both conditions resulted in accumulation of HIF-1β. Finally, the host control gene γ-globin does not encode an HRE in its promoter, nor was it seen to be differentially expressed in hypoxic transcriptomic data, and reassuringly we observed no enrichment in HIF-1β binding to its promoter (**Figure 4.9D**) (Wing et al., 2021).

In summary, the HBV BCP acts like the promoter of a host HIF regulated gene and binds HIF-1β in response to HIF stabilisation, either by pharmacological agents or hypoxic cell culture. Whilst HIF-1β does have alternative binding partners, such as the aryl hydrocarbon receptor (AhR), we believe this evidence is consistent with a role for canonical HIF-α/β dimers in the regulation of pC/pgRNA transcription (Hoffman et al., 1991; Wing et al., 2021).

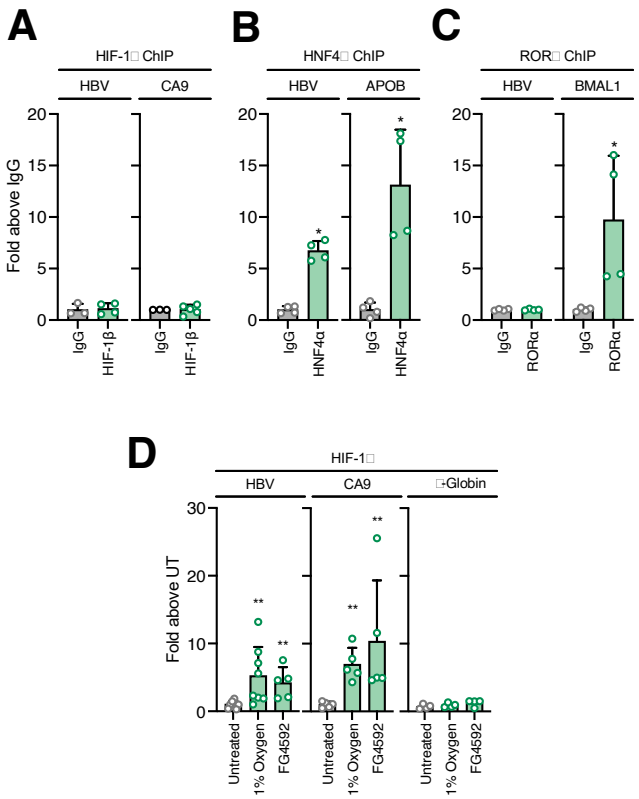


Figure 4.9: HIFs bind HBV DNA

(A) Chromatin was prepared from HepG2-pEpi cells, without any treatment or stimulus, and incubated and immunoprecipitated with an anti-HIF-1β antibody. qPCR was used to detect binding to HBV DNA or host target CA9 promoter, and % IP expressed as fold above IgG. **(B)** Chromatin was immunoprecipitated using HNF4α antibody and binding to HBV DNA and host target gene APOB was determined by qPCR. % Input was expressed as fold above IgG. **(C)** ChIP was performed using an anti-RORα antibody and binding analysed by qPCR using primers spanning a putative binding site on the HBV genome, and the RORα regulated host gene BMAL1. % IP is expressed relative to IgG control. **(D)** HepG2-pEpi cells were cultured in 1% oxygen or treated with FG-4592 for 24 hours, chromatin was prepared and immunoprecipitated with an anti-HIF-1β antibody. HIF-1β binding to HBV DNA, host HIF target gene CA9, and irrelevant house keeper γ-globin. % IP is expressed relative to untreated samples. **(A-D)** All data are derived from n=2 biological replicates, and Mann-Whitney U tests used to test significance. *With thanks to Dr Xiaodong Zhuang and Helene Borrmann for assistance with these assays.*

4.11: HBV-HIF complexes exist *in vivo*

To assess whether HIFs bind HBV DNA *in vivo* we selected liver samples from HBV infected human liver chimeric mice. As discussed in *Chapter 3*, the liver chimeric mouse model supports HBV infection and replication from authentic HBV cccDNA in human hepatocytes that are engrafted into the liver of immune deficient FNRG-NOD mice (Budker et al., 1996; Wilson et al., 2014a; Yang et al., 2002). These mice provide the ideal model to study HIF:HBV interactions, as only the human hepatocytes are susceptible to infection as murine hepatocytes lack a functional NTCP receptor. NTCP is essential for HBV entry, cccDNA formation and viral replication; and murine NTCP does not render cells permissive to either HBV or HDV entry (Yan et al., 2013; Yan et al., 2012)(reviewed in (Wei and Ploss, 2021b)). This enabled us to study the interactions between HBV DNA and host transcription factors *in vivo*. Through a collaboration with Professor Thomas Baumert's laboratory, animals were infected with HBV for 4 weeks, a short period to minimise the frequency of integration events, and at 7 day intervals post-infection peripheral HBV DNA was quantified. All animals showed an increase in HBV DNA over time, indicative of ongoing viral replication (**Figure 4.10A**). As well as monitoring the infection over time, the efficiency of the engraftment process was assessed by quantifying levels of human albumin (hALB) in the periphery, a liver factor that will not be expressed by the native murine hepatocytes. We observed a consistent level of hALB in the periphery for the duration of the experiment demonstrating viability of the human hepatocytes (**Figure 4.10B**).

Infection was maintained for 4 weeks and immediately before sacrifice, peripheral HBsAg and HBeAg were detected by ELISA (**Figure 4.10C**). Following

termination we disaggregated a small fragment of the liver tissue in trizol, and isolated RNAs for transcriptomic analysis and genomic quantification. As our qPCR primers are specific for human β-Actin and HBV RNAs, we can be sure the transcripts are derived from the engrafted human cells, and not from endogenous murine liver cells (D'Arienzo et al., 2021b). Reassuringly, our qPCR enumeration of pC/pgRNA and total RNA showed a good level of concordance with secreted antigen levels (**Figure 4.10D**). Finally, we quantified all major viral RNAs and despite differences in the absolute HBV RNA burden, we observed similar transcript patterns in 2 out of 3 mice, with 1081 showing a different distribution (**Figure 4.10E**).

We applied exactly the same ChIP strategy to the mice as we had to the *in vitro* HepG2-pEpi samples, discussed in *Figure 4.9*. We disaggregated liver tissue directly in the fixative buffer, and prepared chromatin, sonicated DNA and precipitated using antibodies specific for HIF-1α, HIF-2α, and HIF-1β as well as antibodies against control factors HNF4α, RORα and the IgG irrelevant control (Salama et al., 2015; Wiesener et al., 2003). Mouse 1083 was excluded from our analyses due to high % input from IgG controls, perhaps indicative of suboptimal extraction, sonication or immunoprecipitation. ChIP-qPCR using primers spanning the BCP showed significantly enriched HIF-1β and HIF-2α, and modest HIF-1α binding to viral genomes relative to the IgG control. As observed in the HepG2-pEpi model, we demonstrated HNF4α binding to both the HBV genome and APOB target gene, and no detectable association of RORα to the viral genome, but significant enrichment on the promoter of BMAL1 (**Figure 4.10F**) (Wing et al., 2021).

In conclusion, these data support a model whereby HIFs and HBV are natural binding partners in the hypoxic microenvironment of the liver. Our animal studies demonstrate that these HBV-HIF complexes exist without the addition of exogenous hypoxic stimuli, and highlight the suitability of tissue derived from humanised liver mice to study the interactions between host transcription factors and the viral genome.

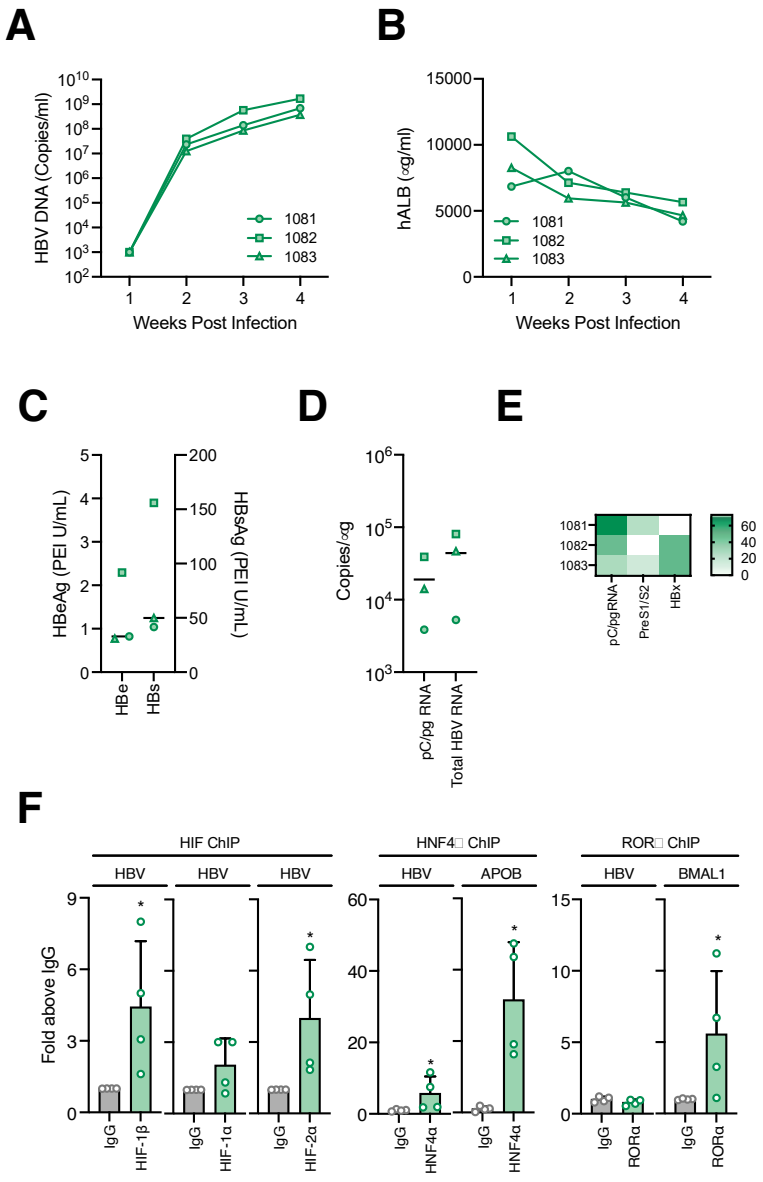


Figure 4.10: HBV-HIF complexes exist *in vivo*

(A) Humanised liver chimeric mice were infected with HBV for 4 weeks, before sacrifice. Viral parameters in the periphery were quantified to assess infection. **(B)** Human Albumin levels were quantified by ELISA to evaluate the hepatocyte viability. **(C)** 4 weeks post infection, viral antigens were quantified in the periphery by ELISA and HBe and HBs Ag were detectable in n=3 animals. **(D)** Mice were sacrificed 4 weeks post infection and livers snap frozen, before isolating RNA by trizol extraction. HBV RNAs were quantified by qPCR and expressed relative to β-Actin housekeeping gene. Transcript patterns plotted as percentage of viral RNAs. **(E)** Frozen liver samples were thawed and disaggregated in formaldehyde, then immunoprecipitated with antibodies against HIF-1α, -2α and -1β, before detecting TF binding to HBV DNA by qPCR.

(F) As an internal control, samples were also immunoprecipitated with antibodies against both HNF4α and RORα, and binding detected to both HBV DNA and host control genes APOB and BMAL1 respectively. Data are representative of 2 independent experiments, and statistics tested with Mann-Whitney U tests (Wing et al., 2021). *With thanks to Professor Thomas Baumert and colleagues for performing the animal studies and providing viral parameters on these samples, and Dr Xiaodong Zhuang for technical advice.*

4.12: Hypoxia selectively activates the BCP

HIFs can bind thousands of base pairs upstream of the transcription start site of a regulated gene, and we were interested to know whether HIFs could activate multiple HBV promoters (Arany et al., 1996; Benabdallah et al., 2019; Kindrick and Mole, 2020). We cultured HBV infected HepG2-NTCP cells at 18% or 1% oxygen for 72 hours, and harvested cellular RNAs to assess the quantity and pattern of viral RNAs. Our 4 transcript PCR method showed that pC/pgRNA constituted around 70% of all HBV RNAs, with detectable PreS1/2 and HBx encoding transcripts. However, when cells were cultured in hypoxia we observed a drastic change in the transcript pattern, with pC/pgRNA representing over 95% of all viral RNAs. Our previous data showed a 30-fold increase in pC/pgRNA levels (**Figure 4.4B**), however we did not see such a striking upregulation of any other viral transcript, suggesting that the hypoxic environment selectively potentiates pC/pgRNA levels in response to HIF binding the BCP (**Figure 4.11A**).

pgRNA is the template required for the synthesis of new progeny viral genomes, which is encapsidated and reverse transcribed to form rcDNA. We postulated that the increase in pC/pgRNA levels would promote the genesis and secretion of viral particles under hypoxic conditions. In a collaboration with Dr Peter Wing, we assessed this in 2 independent model systems, either through transduction of HepG2-NTCP cells with the HBV genome encoded in an adenoviral vector (Ad-HBV), or the routinely used HepG2.2.15 HBV-producer cell line (Sells et al., 1987; Wing et al., 2019). We detected secreted HBV DNA in these cultures and enumerated copies by qPCR, observing a marked increase in

the abundance of extracellular genomes in 1% oxygen in both model systems (**Figure 4.11B**) (Wing et al., 2021).

We have demonstrated, in *Chapter 3,* that during the HBeAg- negative phase of chronic disease HBV integrants are highly transcriptionally active, and most likely the major source of transcripts encoding HBsAg (Meier et al., 2021; Wooddell et al., 2017). Whilst the integrants lack the capacity to transcribe pC or pgRNA they do encode the PreS1, PreS2 and HBx promoters, and we sought to assess their sensitivity to hypoxia. We cultured hepatoma cell lines (PLC/PRF5, Huh1 and Hep3B cells) harbouring integrated copies in low oxygen for 72 hours, before quantifying the levels of PreS1/2 and HBx RNAs (Rivkina et al., 1988; Su et al., 1998). We noted a modest but significant decrease in PreS1/2 RNAs in PLC/PRF5 cells, and no change in either Huh1 or Hep3B cell lines. In PLC/PRF5 and Hep3B we detected fewer HBx RNAs than PreS1/2, and these showed no differential expression between normoxic and hypoxic conditions (**Figure 4.11C**). Finally, we assessed the hypoxic response of the integrant cells with respect to host HIF target gene expression, and in all cells we observed upregulation of both BNIP3 and CA9 RNAs, albeit with some variability in the magnitude of the induction (**Figure 4.11D**) (Wing et al., 2021).

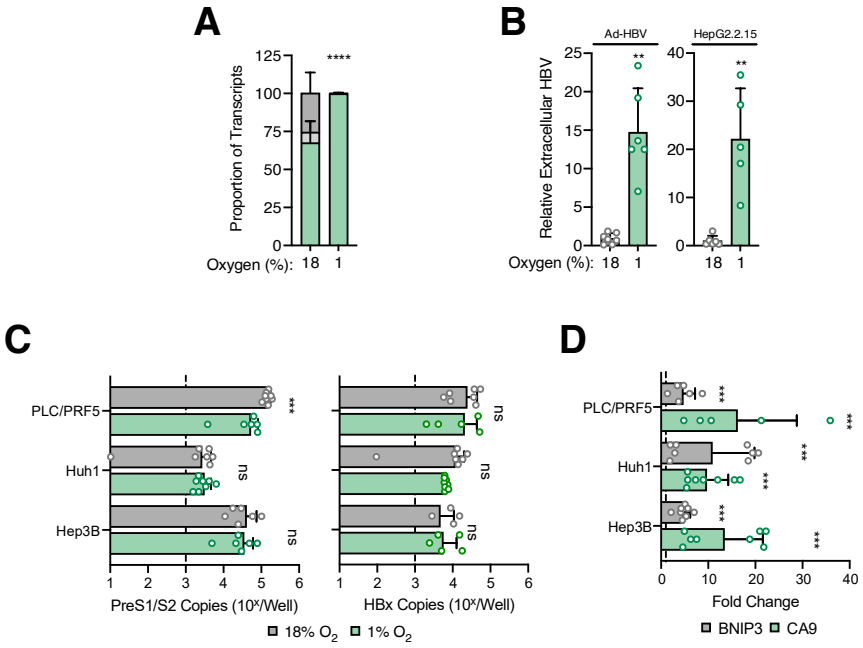


Figure 4.11: Hypoxia selectively activates the BCP

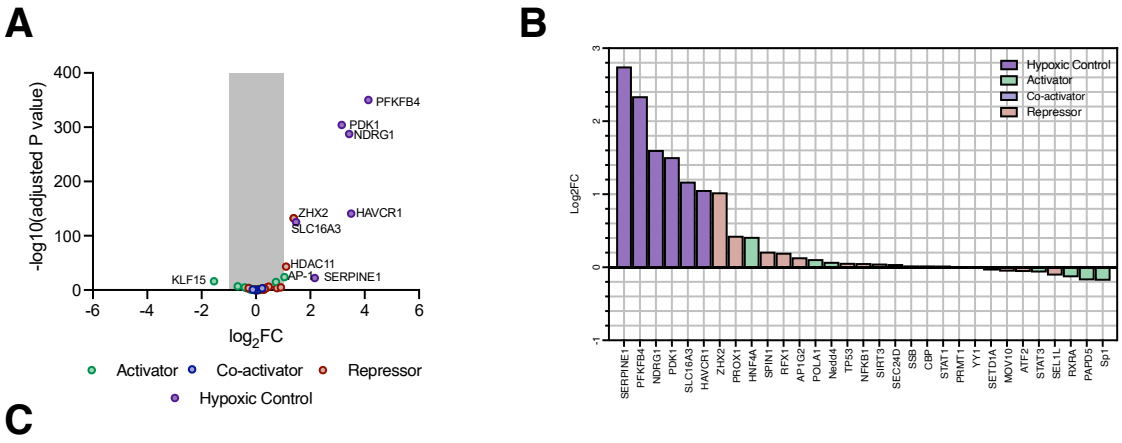
(A) HepG2-NTCP cells were infected with HBV and cultured in 18% or 1% oxygen for 72 hours. Cellular RNAs were extracted, viral transcript patterns were ascribed by qPCR, and copies of each transcript calculated as a percentage of total HBV RNA. Data are derived from n=2 independent experiments, and statistics tested by 2-way ANOVA to show the impact of oxygen on all transcripts. **(B)** HepG2-NTCP cells were transduced with Ad-HBV-GFP constructs (MOI 20), then challenged with 18% or 1% oxygen for 72 hours, before detecting secreted HBV DNA by qPCR. HepG2.2.15 cells were challenged with 18% or 1% oxygen for 72 hours, then extracellular HBV DNA was enumerated by qPCR. ETV was used as a control, and when experimental values were lower than ETV they were excluded from downstream analysis. Data are presented relative to 18% samples. **(C)** Hepatoma cell lines harbouring HBV integrants, PLC/PRF5, Huh1 and Hep3B were cultured in 18% or 1% oxygen for 72 hours. Cellular RNAs were extracted, and copies of HBV PreS1/2 (left) or HBx (right) enumerated by qPCR. **(D)** The host cell response to hypoxia was determined by qPCR detection of 2 canonical HIF target genes, BNIP3 and CA9. Dashed line represents expression in cells cultured in 18% oxygen. **(B-D)** All data are derived from 2 independent experiments and statistical significance tested with Mann-Whitney U tests (Wing et al., 2021). *With thanks to Dr Peter Wing for data presented in Figure 4.11B*

4.13: Hypoxic regulation of HBV host factors

As previously discussed hypoxic sensing and signalling pathways are complex, and HIFs are by no means the only oxygen dependent transcriptional regulators in the host cell. Low oxygen conditions inhibit the function of 2-OGDDs which have widespread roles in regulating gene expression (Dong et al., 2014; Islam et al., 2018; Kohli and Zhang, 2013). Inhibition of these factors can elicit large changes in the cellular transcriptome, and we were keen to explore this and investigate whether known modulators of HBV replication were differentially expressed in response to hypoxic signalling. In order to focus on HIF mediated transcriptional changes, we accessed transcriptomic data from HepG2 cells cultured at 0.5% oxygen for 16 hours, a sufficient time period to stabilise HIF, but functionality of other 2-OGDD members should be preserved (Smythies et al., 2019). We analysed these data for the expression of known transcriptional activators, co-activators and repressors reported to regulate HBV replication, as well as a panel of known HIF target genes (**Figure 4.12C**) (as reviewed in (Turton et al., 2020)). We noted upregulation of the transcripts encoding HIF response genes, but did not see any modulation in the expression of previously reported repressive factors, and only observed modest variation in the activatory factors (**Figure 4.12A**) (Wing et al., 2021).

As commented above, the cellular factors which orchestrate the host response to low oxygen can regulate gene expression at every level. To complement our transcriptomic analyses we obtained whole cell tandem mass tagged (TMT) proteomic data, from our collaborator Professor Mike Weekes (Weekes et al., 2014). Huh7 hepatoma cells were cultured in 1% oxygen for 24

hours, and intracellular protein levels assessed by NMR. Despite there often being differential responses between transcript and protein, in this instance we see a similar level of induction in both RNA-seq and proteomic datasets. We observed little change in the expression of activators and repressors of HBV, but a marked increase in the expression of many HIF response gene products (**Figure 4.12B**) (Wing et al., 2021).



C

Activators	
AP-1	Jun proto-oncogene
C/EBP	CCAAT enhancer binding protein beta
CREB	CAMP responsive element binding protein 1
FOXM1	Forkhead box m1
GTF2B	General transcription factor IIB
HNF4A	Hepatocyte nuclear factor 4 alpha
KLF15	Kruppel like factor 15
NEDD4	NEDD4 E3 ubiquitin protein. Ligase
NFYB	Nuclear transcription factor Y subunit beta
NR1H4	Nuclear receptor subfamily 1 group H member 4
NR5A2	Nuclear receptor subfamily 5 group A member 2
NRF1	Nuclear respiratory factor 1
PAPD5	Terminal nucleotidyltransferase 4B
PAPD7	Terminal nucleotidyltransferase 4A
POLA1	DNA polymerase alpha 1, catalytic subunit
POU2F1	POU class 2 homeobox 1
PPARA	Peroxisome proliferator activated receptor alpha
RXRA	Retinoid X receptor alpha
SP1	Sp1 transcription factor
STAT3	Signal transducer and activator of transcription 3
TBP	TATA-box binding protein

Co-activators	
CBP	CREB binding protein
PGC1A	PPARG coactivator 1 alpha
PRMT1	Protein arginine methyltransferase 1
SRC1	Nuclear receptor coactivator 1

Hypoxic Controls	
HAVCR1	Hepatitis A virus cellular receptor 1
SLC16A3	Monocarboxylic acid transporter 4
PDK1	Pyruvate deydrogenase kinase 1
NDRG1	N-myc downstream regulated 1
PFKFB4	6-phosphofructo-2-kinase/fructose-2,6-bisphosphatase 4
SERPINE1	Serpin family E member 1

Repressors	
AP1G2	Adaptor related protein complex 1 subunit gamma 2
APOBEC3G	Apolipoprotein B mrna editing enzyme catalytic subunit 3G
ATF2	Activating transcription factor 2
BCL6	BCL6 transcription repressor
DNASE1	Deoxyribonuclease 1
ESR1	Estrogen receptor 1
HDAC11	Histone deacetylase 11
HOXA10	Homeobox A10
ID1	Inhibitor of DNA binding 1, HLH protein
MAP3K1	Mitogen-activated protein kinase kinase kinase 1
MOV10	MOV10 risc complex RNA helicase
NFKB1	Nuclear factor kappa B subunit 1
NR0B2	Nuclear receptor subfamily 0 group B member 2
NR2F2	Nuclear receptor subfamily 2 group F member 2
OAS2	2'-5'-Oligoadenylate synthetase 2
ONECUT1	One cute homeobox 1
PDE4A	Phosphodiesterase 4A
PROX1	Prospero homeobox 1
RFX1	Regulatory factor X1
SEC24D	SEC24 Homolog D, COPII coat complex component
SEL1L	SEL1 adaptor subunit of ERAD E3 ubiquitin ligase
SETD1A	SET domain containing 1A, histone lysine methyltransferase
SIRT3	Sirtuin 1
SNAI2	Snail family transcriptional repressor 2
SOX7	SRY-Box transcription factor 7
SPIN1	Spindlin 1
SSB	Small RNA binding exonuclease protection factor la
STAT1	Signal transducer and activator of transcription 1
SUV39H1	Suppressor of variegation 3-9 homolog 1
TNFSF2	Tumour necrosis factor
TP53	Tumour protein P53
TP73	Tumour protein P73
TSPYL2	TSPY like 2
YY1	YY1 transcription factor
ZCCHC14	Zinc finger CCHC-type containing 14
ZHX2	Zinc finger and homeoboxes 2

Figure 4.12: Hypoxic regulation of HBV host factors

(A) HepG2 cells were cultured in 0.5% oxygen for 16 hours, and host gene expression determined by RNA sequencing, with differential expression analysis performed relative to cells cultured in 18% oxygen (Smythies et al., 2019). Data were interrogated for the expression of previously reported activators and repressors of HBV, with a panel of 6 host hypoxic genes included as an internal reference control. **(B)** TMT proteomic datasets from Huh7 cells cultured in 18% or 1% oxygen for 24 hours, were interrogated for the expression of previously reported activators or repressors of HBV, as well as host HIF target genes as a control. **(C)** A table listing the activators, co-activators, repressors and hypoxic

controls used for A-B (Wing et al., 2021). *With thanks to Professor Mike Weekes for the TMT proteomic datasets.*

4.14: Summary

The aim of this chapter was to understand the impact of hypoxia on HBV replication. We used a variety of model systems to investigate the contribution of HIFs at various stages in the HBV life cycle. Using a combination of bioinformatic analysis and molecular biology techniques we identified a role for HIFs in binding to and activating the BCP, promoting HBV replication and increasing particle genesis.

We began with a bioinformatic approach and conducted a motif scanning analysis of over 7,000 HBV genome sequences to search for the RCGTGC HRE motif. We identified 2 HREs in the viral genome both in enhancer regions, and these were present in all but one human genotype (GtH), and were conserved across avian, amphibian and primate viruses (**Figure 4.1**) (Wing et al., 2021). This led us to hypothesise that HBV cccDNA may respond to hypoxia in a manner similar to host HIF target genes, and so we profiled the hepatoma cell response to hypoxia. We utilised a qPCR microarray to study the hypoxic response of HepG2-NTCP cells with or without DMSO treatment. We observed that DMSO blunted the host cell response to hypoxia, by upregulating the basal expression of many HIF targets (**Figure 4.2A,B**) (Wing et al., 2021).

With this knowledge in mind, we performed the rest of our *in vitro* assays in a DMSO free system, and demonstrated that low oxygen culture arrested hepatocytes in $G_{0/1}$ phase of the cell cycle (**Figure 4.3C**). This is the natural state of hepatocytes in the liver, and suggests that hypoxic culture offers a more physiologically relevant method of arresting cell cycle. Given the arresting capability of hypoxia, we initially quantified copies of cccDNA in hypoxic infected

cells to assess the impact of cell cycle arrest on the cccDNA reservoir (**Figure 4.4A**). We observed no modulation of this viral template, but a significant increase in pC/pgRNA levels that outperformed a canonical HIF target gene (**Figure 4.4B,C**).

Having made these observations in systems supporting replication of HBV GtD, we sought to expand our findings to a panel of diverse HBV clones of varying genotype. These constructs were overlength HBV1.3 genomes, and we optimised techniques to work with these clones from rigorous DNAse treatment to remove plasmid contamination of RNAs, and designed genotype agnostic primers to quantify HBV pC/pgRNA (**Figure 4.5**). We also identified that HBV GtH was atypical, and encoded a polymorphism in the putative HRE motif (**Figure 4.6A**). When we challenged HepG2-NTCP cells transfected with GtD or GtH plasmids we observed that GtH was not responsive to low oxygen (**Figure 4.6B**). Synthetic viral genomes with a mutated HRE motif to restore HRE-1 in GtH and mutate HRE-1 in GtD were delivered, but did not significantly impact the hypoxic responses (**Figure 4.6C**).

It is well known that HIFs bind the HRE in the promoter of target genes to activate their transcription and so we sought to optimise a ChIP-qPCR assay to assess whether HIFs could bind HBV DNA. Since HBV cccDNA was previously reported to resist sonication, we used a simple PCR approach to amplify products of increasing length to assess whether the viral DNA was intact post-shearing. These experiments clearly showed that HBV DNA extracted from a *de novo* infection could be fragmented to lengths of approximately 400bp (**Figure 4.7**). Having optimised the sonication process, we focused on the ChIP assay and used HNF4α as a known binding factor to optimise the conditions for

immunoprecipitation. Our data suggested that a combination of sonication and selection of primers which span the transcription factor binding site increased the signal to noise ratio (**Figure 4.8**).

With confidence in our ChIP protocols, we performed experiments to assess HIF-1β binding to the HBV genome in HepG2-pEpi cells (Lucifora et al., 2014). When we stabilised HIFs either by low oxygen culture or treatment with the PHD-inhibitor FG-4592, we observed an enrichment of HIF-1β binding to the viral BCP and host CA9 promoter (**Figure 4.9D**) (Wing et al., 2021). Having showed that HIF-1β can bind HBV DNA in response to HIF stabilisation, we were keen to see whether these complexes exist *in vivo* in the naturally low oxygen environment of the liver. We performed ChIP assays against HIF-1α, -2α, -1β on DNA derived from the livers of HBV infected human liver chimeric mice. Importantly, we observed an enrichment of HIF-1β and HIF-2α to the viral genome without exogenous hypoxic stimulation, as well as a modest accumulation of HIF-1α (**Figure 4.10F**) (Wing et al., 2021). These data demonstrate that HBV-HIF complexes naturally exist *in vivo*, which is particularly interesting when one considers the natural oxygen gradient and zonation of the liver (Halpern et al., 2017; Kietzmann, 2017; Wilson et al., 2014b).

We observed that hypoxic culture exclusively potentiated pC/pgRNA levels and changed the viral transcript pattern, with the 3.5kb transcripts representing over 95% of all viral RNAs (**Figure 4.11A**). Furthermore, the increased abundance of pgRNA resulted in increased levels of secreted HBV DNA in hypoxia (**Figure 4.11B**). PreS1/2 RNAs derived from HBV integrants were insensitive to hypoxia, which is particularly pertinent when considering the role of HBsAg in chronic HBV, the progression to HCC, and the hypoxic nature of the tumour microenvironment

(**Figure 4.11C**) (Xiong et al., 2017). Finally, we interrogated hypoxic transcriptomic and proteomic datasets for expression of previously reported activators and repressors of HBV transcription (Turton et al., 2020; Wing et al., 2021). We only observed modest changes in the expression of these host factors, but cannot exclude the possibility of hypoxic regulation of pro-viral pathways such as immune responses and metabolism (**Figure 4.12**). For example, a recent study from Zhou et al. suggested that HBV modulates host cell metabolism in order to evade innate immune recognition (Zhou et al., 2021).

To summarise our findings in this chapter, for the first time we uncover a positive regulatory role for HIFs in the life cycle of HBV. HIFs bind to evolutionarily conserved HRE motifs in the viral BCP, and drive the transcription of pC/pgRNA. HIF-HBV complexes exist *in vivo* and BCP activation results in increased particle genesis. In standard laboratory conditions the role for HIFs would be overlooked, and this study highlights the importance of understanding the oxygen tension at the site of infection, and the host pathways that may be active or inhibited in these conditions. It is paramount to note that the host response to hypoxia is not exclusively regulated by HIFs, and that in our hypoxic culture systems we may also be inhibiting other 2-OGDD enzymes which in turn may be influencing viral replication.

Chapter 5: Histone lysine demethylase 4 as a HBV restriction factor

5.1: Introduction

Our work has uncovered a positive role for HIFs in regulating HBV transcription, however as previously discussed at length, the cellular response to hypoxia is regulated by a whole host of enzymes and HIFs are just one component of this complex pathway (Kindrick and Mole, 2020; Liu et al., 2020a; Wing et al., 2021). The 2-OGDDs are reliant on oxygen and the TCA cycle intermediate 2-OG for their function, thus they sit at the interface between oxygen sensing, metabolism and epigenetic modification (Kuiper and Vissers, 2014; Pineda Torra et al., 2003; Ploumakis and Coleman, 2015). Recent publications identified, for the first time, that KDM5 and 6 are cellular oxygen sensors (Batie et al., 2019; Chakraborty et al., 2019). Batie et al. cultured HeLa cells and human foreskin fibroblasts under hypoxic conditions (1% O_2) and showed hypermethylation of H3K4, the cognate mark of KDM5, within the first hour prior to HIF-1α expression. Additional experiments to pharmacologically inhibit VHL and silence HIF-1β demonstrated the HIF-independence of this pathway (Batie et al., 2019). Similarly, Chakraborty and colleagues used multiplexed mass spectrometry to assess the methylation status of histone lysine residues in hypoxia, and noted hypermethylation of H3K27me3. This lead them to discover that the enzymatic activity of KDM6 was directly modulated in hypoxia, independently of HIF-signalling and ROS activity (Chakraborty et al., 2019). In response to decreased oxygen levels KDMs can modulate chromatin structure and gene expression to allow the cell to adapt to subtle changes in the microenvironment (Batie et al., 2018). KDMs catalyse the removal of a methyl group on specific lysine residues of

histone 3 and 4, converting a tri-methyl group to a di-methyl group (Allis and Jenuwein, 2016; Kouzarides, 2007). Dependent on the specific lysine residue, methylation can activate or repress transcription by modifying the physical interaction between DNA and histone; regulating the accessibility to the transcription machinery (Beisel and Paro, 2011; Tropberger et al., 2015; Tropberger et al., 2013; Wang et al., 2008; Xin and Rohs, 2018). As widely reported, HBV cccDNA associates with histones and is chromatinised in a comparable manner to the host genome (Newbold et al., 1995; Raney et al., 1995). Given the role for KDM5 and KDM6 as cellular oxygen sensors we hypothesised that a KDM may regulate HBV transcription under hepatic low oxygen conditions.

In this chapter we identify a role for a HIF-independent oxygenase in regulating HBV replication. We employ qPCR and next generation sequencing approaches to study the effect of pharmacological inhibition of members of the KDM family on HBV replication in a range of model systems. We identify KDM4 as a new restriction factor for HBV and suggest that inhibition of KDM4 likely promotes viral replication through modifying the host cellular transcriptome, rather than through direct accumulation of H3K9me3 on the viral epigenome (Flecken et al., 2019; Klose et al., 2006; Tropberger et al., 2015). We assess the relationship between cellular oxygen levels and KDM4 activity using a combination of low oxygen culture conditions and pharmacological agents.

5.2: Host and viral transcriptional responses to low oxygen

The cellular response to low oxygen is dynamic, and a complex interplay between HIFs and non-HIF factors regulate gene expression to allow cells to adapt to changes in oxygen availability. As discussed in *Chapter 3*, the response to acute hypoxia is thought to be predominantly governed by HIF signalling, and a study from Smythies and colleagues showed that after 16 hours culture in 0.5% oxygen (acute hypoxia) there was little evidence of transcriptional repression, with the majority of responsive genes showing increased expression (**Figure 5.1A**). Our previous study demonstrated that HIFs promote HBV replication, and we observed an upregulation in pC/pgRNA levels after 72 hours of hypoxic culture, or treatment with the selective PHD-inhibitor FG-4592 (Wing et al., 2021). We sequenced the transcriptome of HBV infected HepG2-NTCP cells cultured in 1% O_2 (persistent hypoxia), or treated with 30 μM FG-4592 for 72 hours, and assessed the impact on host gene expression by differential expression analysis (**Figure 5.1B,C**). In contrast to the positive transcriptional response observed in *Figure 5.1A,* we noted an almost even distribution of up and downregulated genes in response to persistent hypoxia and FG-4592 treatment (**Figure 5.1A-C**). We assessed the expression of our previously identified hepatocyte specific hypoxic gene signature, as discussed in chapter 3, and sixty of the eighty genes were upregulated in both conditions (**Figure 5.1D**) (Liu et al., 2020b; Smythies et al., 2019). When comparing the differentially expressed genes, it was reassuring to see a 49% overlap between persistent hypoxia and FG-4592 treatment, as well as some genes unique to each condition. This is consistent with a role for both HIF and non-HIF factors in regulating the cellular response to low oxygen (**Figure 5.1D**). In contrast to the acute hypoxic response, we observe a large number of

genes downregulated in response to persistent hypoxia and FG-4592 treatment, with 46% of genes conserved between both groups perhaps suggesting indirect effects of HIF in supressing gene expression (**Figure 5.1E**).

We assessed the impact of persistent hypoxic culture and FG-4592 treatment on the viral transcriptome. We aligned the Illumina reads to the pgRNA ORF as previously reported, noting a greater depth of coverage in hypoxic cells compared to FG-4592 treatment (**Figure 5.1F**) (Lim et al., 2021). Analysing the read depth surrounding each of the transcriptional start sites (TSS) for the 6 major viral RNAs revealed that hypoxic conditions potentiated the activity at all TSS, whereas FG-4592 increased all with the exception of pC and HBx (**Figure 5.1G**) (Altinel et al., 2016). This suggests that another cellular oxygenase could be regulating HBV transcription independently of HIF.

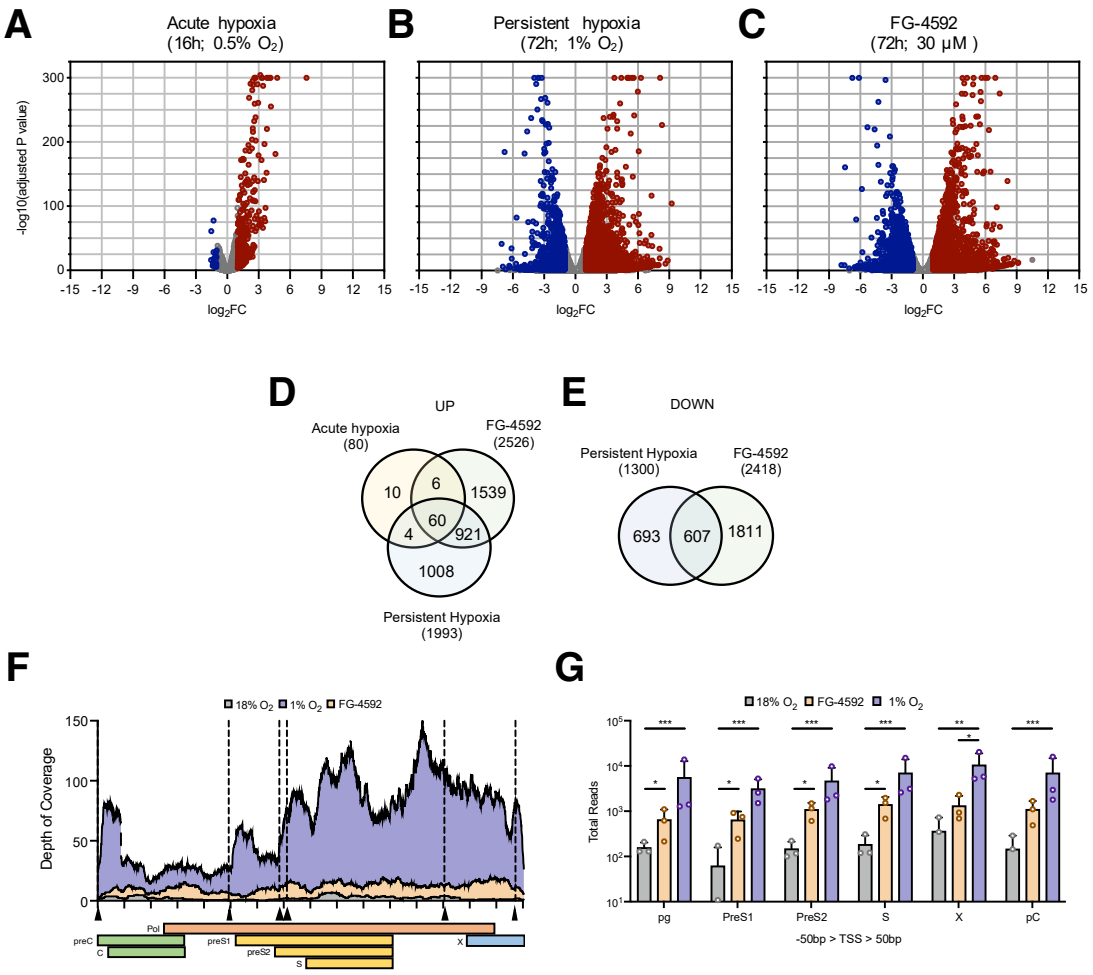


Figure 5.1: Host and viral transcriptional responses to low oxygen

(A-C) HepG2 cells were cultured in **(A)** acute hypoxia (16h; 0.5% O_2) (Smythies et al., 2019), **(B)** persistent hypoxia (72h; 1% O_2) or **(C)** treated with FG-4592 (30 µM) for 72 hours. DESeq2 analysis was performed between each group and matched untreated, normoxic controls. Significance was determined by a log_2FC of $\pm$ 1 and a FDR <0.05, with upregulated genes plotted in red, and downregulated genes in blue. **(D-E)** Venn diagrams depicting the overlap between significantly **(D)** upregulated genes in persistent hypoxia, FG-4592 treatment and a previously determined hypoxic gene signature (n=80 genes) from the acute hypoxia dataset (Liu et al., 2020b); and **(E)** the overlap of downregulated genes in persistent hypoxia and FG-4592 treated cells. **(F)** HepG2-NTCP cells were infected with HBV at a MOI of 300 and either cultured in 1% oxygen or treated with 30 µM FG-4592 for 72 hours. Samples were analysed by Illumina sequencing and the HBV reads mapped to the viral genome, with respect to the pgRNA ORF (Lim et al., 2021). Sequencing coverage (number of transcripts/million reads) was averaged from n=3 independent biological replicates. Schematic diagram shows HBV protein coding regions, dashed lines and arrows denote the TSS, and x-axis ticks denote 200 bp intervals. **(G)** Viral reads from C were quantified around (+/- 50bp) the TSS of each of the major viral RNAs (Altinel et al., 2016). The sum of the reads are plotted in each condition, and statistical significance determined using

a 2 way-ANOVA showing n=3 independent replicates. *With thanks to Dr Peter Balfe for assistance with aligning viral reads in Figure 5.1F*

5.3: A role for KDM4 in HBV transcription

We were intrigued when two independent studies reported histone lysine demethylase 5 and 6 (KDM5/6) as oxygen sensing factors (Batie et al., 2018; Chakraborty et al., 2019). Whilst it was commonly acknowledged that the 2-OGDD family are reliant on oxygen to function, for the first time these KDMs were labelled as regulators of the host hypoxic response, where they coordinate chromatin structure independently of HIF signalling (Batie et al., 2019; Chakraborty et al., 2019). These studies led us to hypothesise that one of the KDM family members could regulate HBV under low oxygen conditions. To investigate this, we obtained a panel of pharmacological agents to inhibit the enzymatic function of the KDMs. We screened inhibitors targeting KDM4 (QC6352), KDM5 (CPI-455) and KDM6 (GSK-J4), as well as the 2-OG analogue and pan-KDM inhibitor, JIB-04 (**Figure 5.2A**) (Chen et al., 2017; Heinemann et al., 2014; Vinogradova et al., 2016; Wang et al., 2013). Of note, all compounds were used at previously reported doses (Dobrynin et al., 2017; Heinemann et al., 2014; Vinogradova et al., 2016). As these agents inhibit the action of epigenetic modifiers, we hypothesised they would influence viral transcription, and we evaluated the effects of the drugs by treating cells following HBV infection. Having previously observed the hypoxic potentiation of pC/pgRNAs we assessed the impact of drug treatment on these transcripts and total HBV RNAs by qPCR. We noted a 12-fold upregulation of pC/pg and total HBV RNAs in response to QC6352 treatment, the specific inhibitor to KDM4, whereas the pan-KDM inhibitor JIB-04 resulted in a modest 3.1-fold increase in viral transcripts (**Figure 5.2B**). We confirmed that inhibiting KDM4 increased the susceptibility of cells to support HBV transcription using the previously reported HepG2-pEpi model, and whilst the magnitude of the induction

was modest, we observed a significant increase in pC/pg and total HBV RNAs (**Figure 5.2C**) (Lucifora et al., 2014). In both models neither CPI-455 nor GSK-J4 had any discernible effect on viral RNAs at the doses selected (**Figure 5.2B,C**).

To validate drug activity at the selected doses, we examined the histone methylation status of the cognate residue for KDM4 as listed in *Figure 5.2A*. In collaboration with Dr Peter Wing, we quantified H3K9me3 expression in HepG2-NTCP cells treated with either QC6352 or JIB-04, to assess their impact on KDM4 activity (Chen et al., 2006; Cloos et al., 2006; Klose et al., 2006). Treatment with both agents induced an accumulation of H3K9me3 consistent with reduced KDM4 activity, with the greatest reduction noted with QC6352 (5 μM) (**Figure 5.2D**). It is worth commenting that despite being abundant cellular proteins, histone mark western blots are technically challenging and published reports have used several different approaches and lysis buffers to evaluate expression (Chakraborty et al., 2019; Dobrynin et al., 2017; Hancock et al., 2017).

Having used a pharmacological agent to inhibit KDM4 activity, we sought to confirm the phenotype by transiently silencing KDM4 isoforms with siRNAs, in collaboration with Dr Peter Wing. We delivered a pool of siRNAs targeting KDM4A-D into HepG2-NTCP cells and infected with HBV, harvesting cellular RNA and protein 72 hours later (Duan et al., 2015). We observed a modest but significant increase in pC/pgRNA levels in response to silencing, and reduced KDM4A expression compared with the Scramble control (**Figure 5.2E**). As there are limited reagents available to other KDM4 isoforms we were only able to study KDM4A protein expression, however we confirmed silencing efficacy for KDM4A-D RNAs (**Figure 5.2F**). Taken together, these data suggest that either

pharmacological inhibition of KDM4 or genetic manipulation increases HBV RNAs, despite some variability in the absolute magnitude of the change.

A

KDM	Drug	Histone Mark	Histone Mark Function	Localisation
Pan-KDM	JIB-04	-	-	-
KDM4	QC6352	H3K9me3	Repressive	Heterochromatin
KDM5	CPI-455	H3K4me3	Active	TSS
KDM6	GSK-J4	H3K27me3	Repressive	TSS, Intergenic

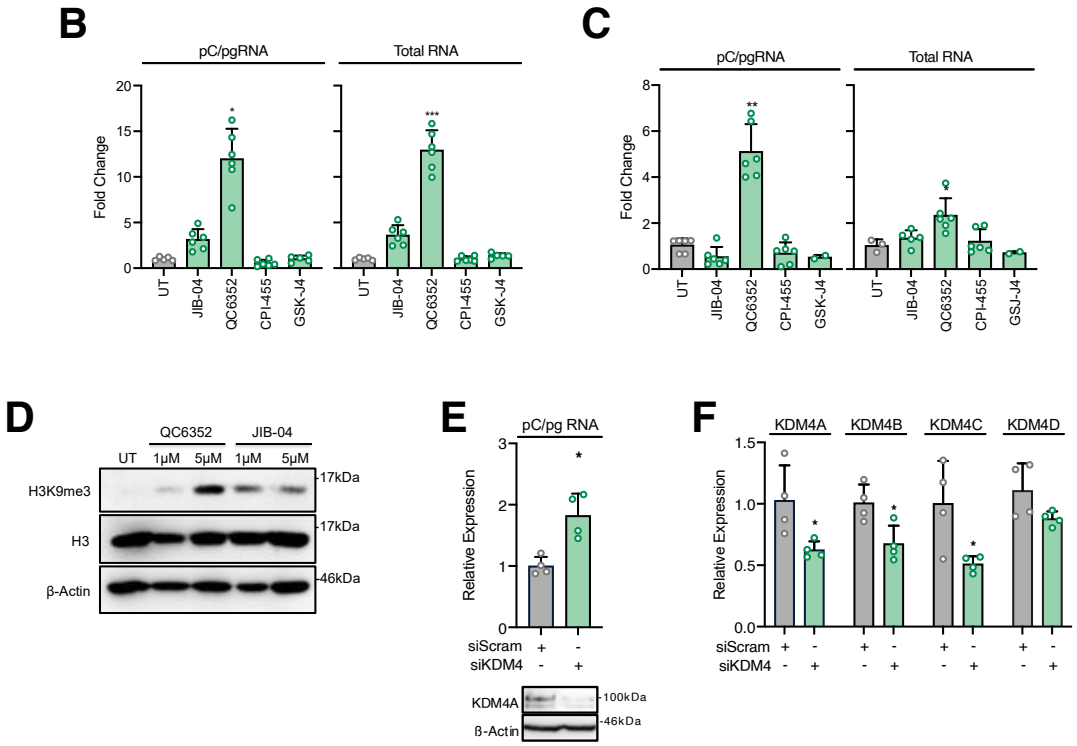


Figure 5.2: A role for KDM4 in HBV transcription

(A) A table to show the targets and epigenetic modifications targeted by a panel of selected KDM inhibitors. **(B)** HepG2-NTCP cells were infected with HBV, then treated with a panel of epigenetic modifiers as described in *A,* at doses of: JIB-04, 1 μM; QC6352, 5 μM; CPI-455, 1 μM; GSK-J4, 2 μM for 72 hours. HBV pC/pgRNA and total RNA copies were enumerated by qPCR and expressed relative to the untreated cells. **(C)** HepG2-pEpi cells were treated with a panel of epigenetic modifiers as above, for 72 hours. RNAs were treated with TURBO DNAse to remove plasmid DNA contaminant, then HBV pC/pg RNA and total RNA quantified by qPCR, and expressed relative to untreated cells. **(D)** To assess specificity of the KDM4 antagonist, HepG2-NTCP cells were treated with QC6352 or JIB-04 at 1 μM and 5 μM doses for 72 hours. Cells were lysed and H3K9me3 accumulation detected by western blot. **(E)** siRNAs to KDMA4A-D were transiently delivered to HepG2-NTCP cells before infection with HBV. 72 hours post infection, cellular RNAs and protein were extracted, and HBV pC/pgRNA quantified by qPCR. KDM4A protein levels were detected by western blot. **(F)** Transcript levels of KDM4A-D were quantified by qPCR in samples from

D, and expressed relative to siScr controls. **(B,C,E,F)** Data are derived from n=2 independent experiments and statistics tested with Mann-Whitney U test. *With thanks to Dr Peter Wing for assistance with 5.2D-F.*

5.4: The interplay between HIF signalling and KDM4 activity

The 60-80 enzymes of the 2-OGDD family are reliant on molecular oxygen to function, and KDM4 is no exception (Hancock et al., 2017; Ploumakis and Coleman, 2015). Having manipulated KDM4 activity by using either pharmacological agents or siRNA, we sought to perturb KDM4 function by reducing oxygen availability. We hypothesised that H3K9me3 levels and cell susceptibility to QC6352 activity would be dependent on the environmental oxygen tension, and used HIF-1α expression as an indicator of the cellular hypoxic response (Hancock et al., 2017). HepG2-NTCP cells were cultured under varying oxygen conditions of 18%, 3% or 1% for 72 hours, in the presence or absence of QC6352. KDM4 activity was assessed by analysing the abundance of H3K9me3 under the various conditions (Schneider et al., 2012). Densitometric analysis quantified H3K9me3 expression relative to total H3, and was adjusted to β-Actin levels as a loading control. In the absence of QC6352 treatment we noted a marked accumulation of H3K9me3 at 1%, but only a modest change at 3% oxygen (**Figure 5.3A**). At 18% and 3% oxygen we observed a notable accumulation of H3K9me3 in the presence of QC6352, however this increase was not apparent at 1% O_2 suggesting that KDM4 function is already inhibited at this oxygen tension (**Figure 5.3A**). HIF-1α expression showed a stepwise increase in cells cultured at 3% to 1% oxygen which is likely due to the oxygen dependency of the PHD enzymes. However in the presence of QC6352 there was minimal HIF-1α expression, consistent with a previously defined role for KDM4 to regulate HIF-1α transcription by catalysing the removal of repressive H3K9me3 marks from its promoter (Dobrynin et al., 2017). Finally, we were reassured to see that QC6352 treated HepG2 cells under 18% oxygen conditions did not stabilise HIF-1α, as a

previous study reported that treatment with the pan-KDM inhibitor JIB-04 stabilized HIF expression (**Figure 5.3A**) (Dobrynin et al., 2017; Thinnes et al., 2015). To further understand the pro-viral activity of QC6352 we quantified HIF target gene transcripts in drug treated cells and observed no changes in their expression, supporting our conclusion that QC6352 has a minimal effect on HIF signalling (**Figure 5.3B**).

As we saw oxygen dependent inhibition of KDM4, we hypothesised that viral RNAs would also increase proportionally to oxygen availability. We sought to understand the effects of differential oxygen tension on viral transcription, and infected HepG2-NTCP cells with HBV and cultured them as above. We saw that both 3% and 1% oxygen conditions significantly increased pC/pgRNA levels relative to 18% cultures as previously reported (**Figure 5.3C**) (Wing et al., 2021). However, we observed a 2-fold upregulation at 3% oxygen, compared with an 8.7-fold increase at 1% oxygen, which could result from either increased abundance of HIF-1α or reduced KDM4 activity (**Figure 5.3C**). In contrast we observed similar expression levels in a panel of canonical HIF target gene transcripts, where there was little difference between 3% and 1% oxygen conditions (**Figure 5.3D**). Collectively, our data suggest that both HIFs and KDM4 regulate HBV in low oxygen.

Having noted that KDM4 is inhibited at 1% oxygen, we proposed that QC6352 would have a minimal effect on viral replication when applied to hypoxic cultures. We infected HepG2-NTCP cells and cultured under 18% or 1% oxygen in the presence or absence of QC6352. As expected, we observed a significant induction in pC/pgRNA levels in response to both 1% oxygen culture or QC6352 treatment, however there was no additive effect of the drug when applied at 1%

oxygen (**Figure 5.3E**). These data suggest that local oxygen availability could be a major determinant of drug efficacy with agents targeting oxygen sensitive factors.

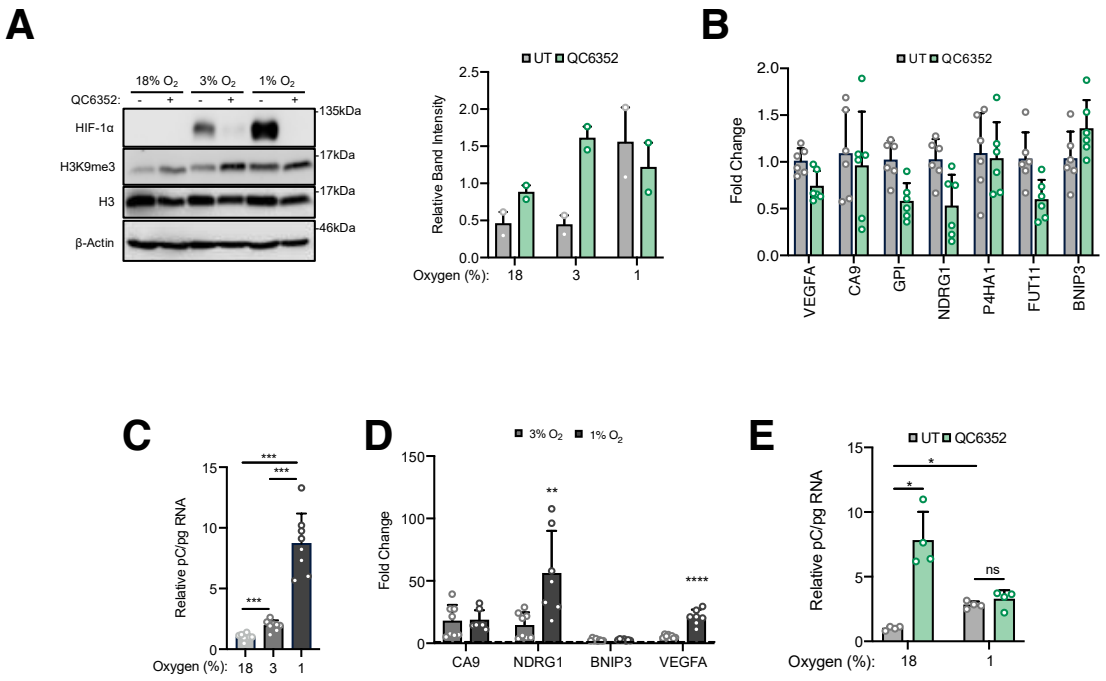


Figure 5.3: The interplay between HIF signalling and KDM4 activity

(A) HepG2-NTCP cells were treated with QC6352 and cultured under 18%, 3% or 1% oxygen for 72 hours. Cells were lysed, and levels of H3, H3K9me3 and HIF-1α analysed by western blot, with β-Actin as a housekeeper. Densitometry of H3K9me3 levels relative to H3, and adjusted to β-Actin expression from n=2 independent western blots, with data plotted as mean and range. **(B)** HepG2-NTCP cells were treated with QC6352, and host hypoxic regulated transcripts analysed to assess the overlap between KDM4 and HIF signalling. Fold change was calculated using DDCt and expressed relative to untreated cells. **(C)** HepG2-NTCP cells were infected with HBV, then cultured under 18%, 3% or 1% oxygen for 72 hours in the absence of QC6352. RNA was isolated and HBV pC/pgRNA copies enumerated by qPCR, and expressed relative to 18% samples. **(D)** Host HIF regulated gene transcripts were analysed by qPCR, from cells cultured in 3% or 1% oxygen. Data are expressed relative to 18% oxygen controls; dashed line represents 18% values **(E)** HepG2-NTCP cells were infected with HBV, and then cultured in 18% or 1% oxygen in the presence or absence of QC6352. 72 hours later, cellular RNAs were harvested and pC/pgRNA copies enumerated by qPCR. **(B-E)** Data are derived from n=2 independent experiments and statistics tested with Mann-Whitney U tests. *With thanks to Dr Peter Wing for assistance and providing samples for Figure 5.4A,C,E.*

5.5: Episomal and integrated genomes are sensitive to KDM4 inhibition

The cellular response to hypoxia is dynamic, and we sought to gain a better understanding of the kinetics underpinning the pro-viral phenotype of QC6352 treatment. HBV infected HepG2-NTCP cells were treated with QC6352 and samples harvested daily for up to 72 hours. We noted a modest but significant increase in HBV pC/pg RNAs 48 hours post treatment with the KDM4 inhibitor, but a more marked increase after 72 hours of treatment. To ascertain whether this was a product of increased transcription or due to effects on the cccDNA reservoir, we measured cccDNA copies and noted comparable levels at all time points (**Figure 5.4A**) (Dandri and Petersen, 2020). We calculated the viral transcriptional output ($\frac{pgRNA\ copies}{cccDNA\ copies}$) and detected secreted HBeAg 72 hours post infection, and noted significant increases in both parameters in response to KDM4 inhibition (**Figure 5.4B**) (Laras et al., 2006).

To assess the impact of QC352 treatment on antigen expression, we employed the HepG2-pEpi model, and noted an increase in pC/pg transcripts but no change in secreted HBeAg levels (**Figure 5.4C**) (Lucifora et al., 2014). To evaluate the impact of KDM4 inhibition in an independent model of chronic infection, we treated HepAD38 cells with QC6352 and measured pC/pgRNA levels and secreted HBeAg. HepAD38 cells support HBV replication from both cccDNA and integrants, and we observed an increase in pC/pgRNAs, but no variation in the abundance of extracellular HBeAg (**Figure 5.4C**). It is of interest to note that in both of these models we observe a pro-viral phenotype but the magnitude is modest compared to the *de novo* infection system.

Having assessed the impact of KDM4 inhibition on cccDNA, pC/pgRNA and HBeAg, we wanted to gain a fuller understanding of the impact on viral transcription. We analysed the RNA transcriptome of HBV infected HepG2-NTCP cells treated with QC6352 (5 µM), using an Illumina sequencing platform. Reads were mapped to the pgRNA ORF, and this showed some variability in the depth of the reads across each of the viral protein coding regions, suggesting modulation of other RNA transcripts (**Figure 5.4D**) (Lim et al., 2021). Analysing the RNA-seq data to assess the depth of coverage at the TSS of each of the major viral RNAs, showed a significant increase in the reads across all positions (**Figure 5.4E**) (Altinel et al., 2016). Of course, our interpretation of these data are limited due to the use of an Illumina sequencing platform, and other sequencing methods such as PacBio or MinION that provide long reads would help to identify specific viral transcripts (reviewed in (Alkan et al., 2011)).

However, to gain clarity on the regulation of other HBV RNAs, we studied the impact of QC6352 on hepatoma cell lines supporting HBV integrants. As discussed in *Chapters 3&4* HBV integrants are clinically relevant, and they provide the template for the majority of HBsAg which is implicated in immune evasion and carcinogenesis (Cornberg et al., 2017; Honer Zu Siederdissen and Cornberg, 2014; Iannacone and Guidotti, 2021; Meier et al., 2021; Ye et al., 2015; Zhao et al., 2016). We treated Huh1, PLC/PRF5 and Hep3B cells with QC6352 and harvested samples every 24 hours for 3 days (Rivkina et al., 1988; Su et al., 1998). qPCR enumeration of PreS1/2 RNA copies revealed that viral integrants were sensitive to KDM4 inhibition, with significant increases in viral transcripts visible at 48 hours in Huh1 and PLC/PRF5, and all 3 cell lines responded after 72 hours treatment (**Figure 5.4F**).

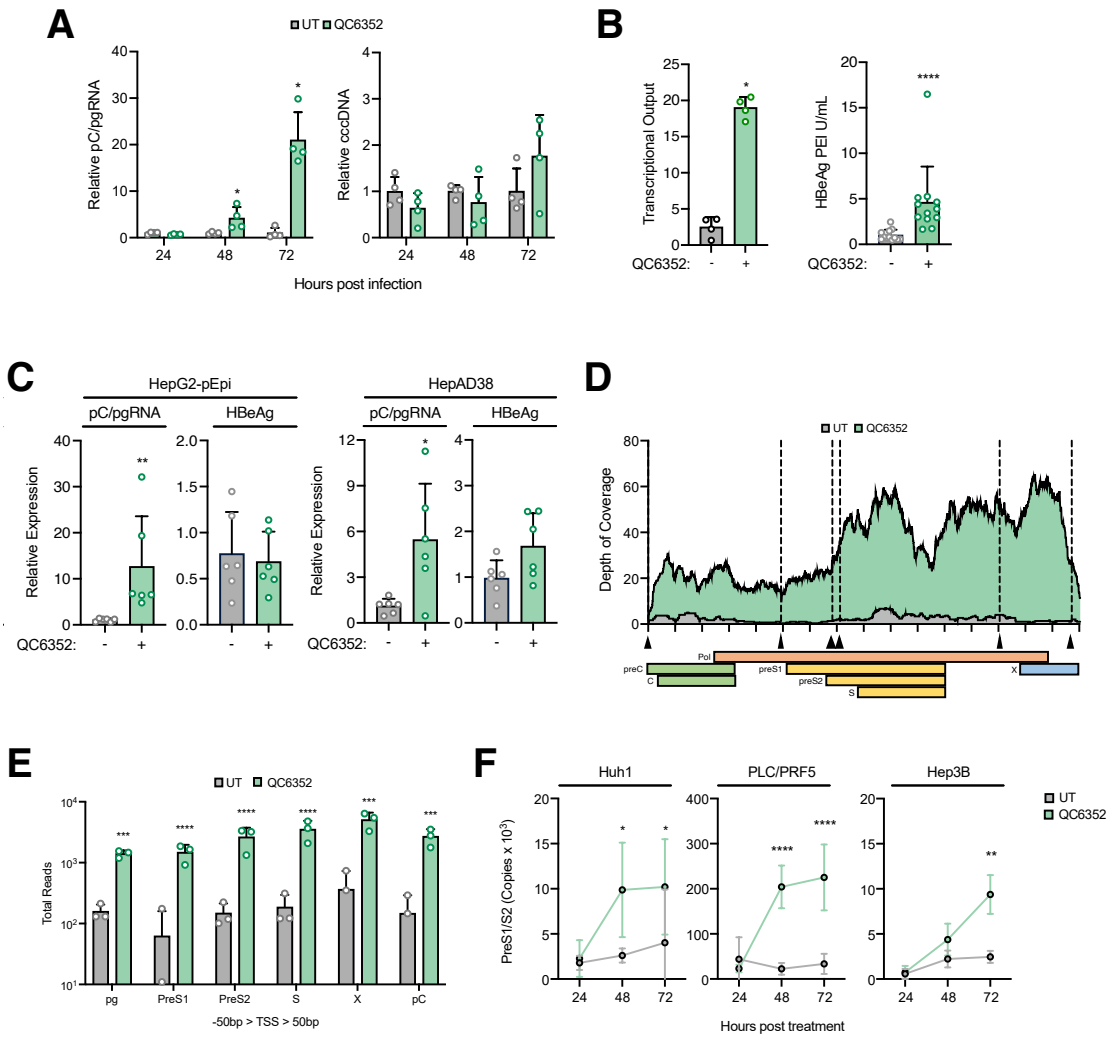


Figure 5.4: KDM4 regulation of integrated and episomal genomes

(A) HepG2-NTCP cells were infected with HBV, and then treated with QC6352 for up to 72 hours. Samples were taken at 24 hour timepoints, and cellular RNA and DNA extracted. HBV pC/pgRNA copies were enumerated by qPCR, adjusted to RPLP0, and expressed relative to untreated cells at each time point. HBV cccDNA was extracted from cellular DNA, and copies estimated by qPCR, adjusted to the host PRP transcript, then expressed relative to untreated cells at each time point. **(B)** By expressing copies of pC/pg RNA relative to cccDNA levels, transcriptional output was calculated from HepG2-NTCP cells infected with HBV at 3 days post infection. HepG2-NTCP cells were infected with HBV and treated with QC6352 for 6 days before HBeAg in the supernatant was detected by ELISA. **(C)** HepG2-pEpi and HepAD38 cells were treated with QC6352 for 72 hours, before intracellular RNAs and secreted proteins were analysed for viral parameters. pC/pgRNA levels were assessed by qPCR, and peripheral HBeAg quantified by ELISA. Data are plotted relative to untreated cells. **(D)** HepG2-NTCP cells were infected with HBV before being treated with

QC6352 for 72 hours. RNAs were harvested and transcriptomic analysis performed using Illumina RNA-sequencing. Reads were mapped and aligned to HBV with respect to the pgRNA coding sequence (Lim et al., 2021). Sequencing is derived from 3 independent biological replicates, schematic diagram shows the protein coding regions of the viral genome, with TSS depicted by dashed lines. x-axis ticks denote 200bp intervals. **(E)** Viral reads were assessed in the regions 50bp up- and down-stream of the TSS for each of the major viral RNAs. The total reads spanning the regions of interest were compared between UT and QC6352 treatment using a 2-way ANOVA. Symbols are representative of n=3 independent replicates. **(F)** 3 Human hepatoma cell lines harbouring transcriptionally active HBV integrated genomes, Huh1, PLC/PRF5, and Hep3B, were treated with QC6352 for up to 72 hours. Samples were extracted at 24 hour intervals, and PreS1/2 transcripts assessed by qPCR, and copies adjusted to host control RPLP0. Significance assessed with a 2-way ANOVA. **(A-C,E)** Data are representative of n=2 independent experiments, and statistics tested with Mann-Whitney U tests. *With thanks to Dr Peter Balfe for alignment of HBV RNA sequencing reads in Figure 5.6D.*

5.6: KDM4 inhibition promotes particle genesis

pgRNA is the template for progeny virus, which is reverse transcribed in the nucleocapsid to form rcDNA genomes. Our data show that KDM4 inhibition results in a marked increase of pgRNA transcripts, and we were interested to assess whether this resulted in a boost in secreted HBV DNA from infected cells. HepAD38 cells were treated with QC6352 for 3 days before quantifying extracellular HBV rcDNA by qPCR. Inhibiting KDM4 resulted in a 4-fold increase in secreted HBV DNA, whilst the nucleoside analogue entecavir (ETV) reduced particles by around 80% (**Figure 5.5A**). Having noted an increase in abundance of viral particles, we were interested to measure their infectivity. As such, we collected supernatants from HepAD38 cells treated with QC6352 for up to 6 days, and precipitated the viral particles using polyethylene glycol. We quantified the viral genomes by qPCR, and infected naïve HepG2-NTCP cells with an equal MOI of HBV (300) and assessed infectivity by measuring HBeAg expression after 14 days. We detected comparable levels of secreted HBeAg from cells infected with virus generated in the presence or absence of QC6352 (**Figure 5.5A**). This suggests that KDM4 inhibition only impacts the abundance of particles, and not their infectivity. As a result, QC6352 promotes the release of infectious particles from a HBV producer cell line.

We previously reported that culturing HepG2-NTCP cells in 1% oxygen for 72 hours was sufficient to arrest them in the $G_{0/1}$ phase of the cell cycle (**Figure 4.3B**) (Wing et al., 2021). As QC6352 was reported to have antiproliferative properties, we were keen to understand whether inhibiting KDM4 arrested HepG2-NTCP cell cycle (Black et al., 2010; Chen et al., 2017). We performed a time

course experiment and harvested cells every 24 hours for 3 days before measuring cell cycle phase by flow cytometry (Davenne et al., 2020). In the untreated samples we observed a modest change in the cell cycle distribution over time, suggesting that the cells were proliferating for the duration of the assay, and had not reached a state of over-confluence or contact-inhibition. In contrast, after 48 or 72 hours of QC6352 treatment there was an accumulation of cells in $G_{0/1}$ and a concomitant decrease of cells in S-Phase (**Figure 5.5B**). These data indicate that QC6352 treatment can arrest hepatoma cell cycle. To understand whether the pro-viral activity of KDM4 inhibition is dependent on its ability to arrest cells, we evaluated its activity in arrested and proliferating cultures. DMSO is routinely used *in vitro* to arrest cell cycle and we confirmed that in the presence or absence of DMSO, QC6352 still promoted pC/pgRNA, although the phenotype was modest compared to the non-arrested cells (**Figure 5.5C**) (Ko et al., 2018; Wing et al., 2021). This suggests that whilst cell cycle arrest may be a contributing factor, it does not fully explain the pro-viral phenotype of KDM4 inhibition.

SAM and HD Domain Containing Deoxynucleoside Triphosphate Triphosphohydrolase 1 (SAMHD1) is a dNTP tri-phosphohydrolase, with a major role in regulating the cellular dNTP pool. We and others have reported a dual role for SAMHD1 in regulating HBV replication by restricting the RT-dependent conversion of pgRNA to rcDNA, and promoting cccDNA genesis (Sommer et al., 2016; Wing et al., 2019). SAMHD1 function is defined by its phosphorylation status, which is determined by the cyclin dependent kinases that regulate host cell cycle progression (Goldstone et al., 2011; Powell et al., 2011). As such, SAMHD1 phosphorylation is linked to host cell cycle and since QC6352 arrests hepatocyte cell cycle we were keen to understand whether this treatment altered SAMHD1

phosphorylation (**Figure 5.5D**) (Schott et al., 2018). To that end, HepG2-NTCP cells were treated with QC6352 and SAMHD1 status assessed by western blot. We noticed that QC6352 treatment reduced phosphorylated SAMHD1 (pSAMHD1) that was accompanied by an increase in unphosphorylated SAMHD1, the form which can antagonise reverse transcription of pgRNA to rcDNA (**Figure 5.5E**). To understand the role of SAMHD1 in QC6352-dependent increase in HBV RNAs we used the HIV-2 Vpx protein to knockdown SAMHD1 (**Figure 5.5F**), transduced cells with an adenoviral vector containing the HBV genome, and studied the impact of QC6352 treatment (Hrecka et al., 2011; Jauregui et al., 2015; Laguette et al., 2011; Wing et al., 2019). After 7 days we quantified secreted rcDNA, and as expected ETV treatment reduced the abundance of particles 4-fold. Both Vpx transduction and QC6352 treatment alone significantly potentiated rcDNA levels, but combining the treatments resulted in a 50-fold increase in secreted HBV DNA (**Figure 5.5G**). This suggests that despite the marked effect of KDM4 inhibition on pC/pgRNA levels, SAMHD1 is a potent restriction factor able to supress the boost in viral replication.

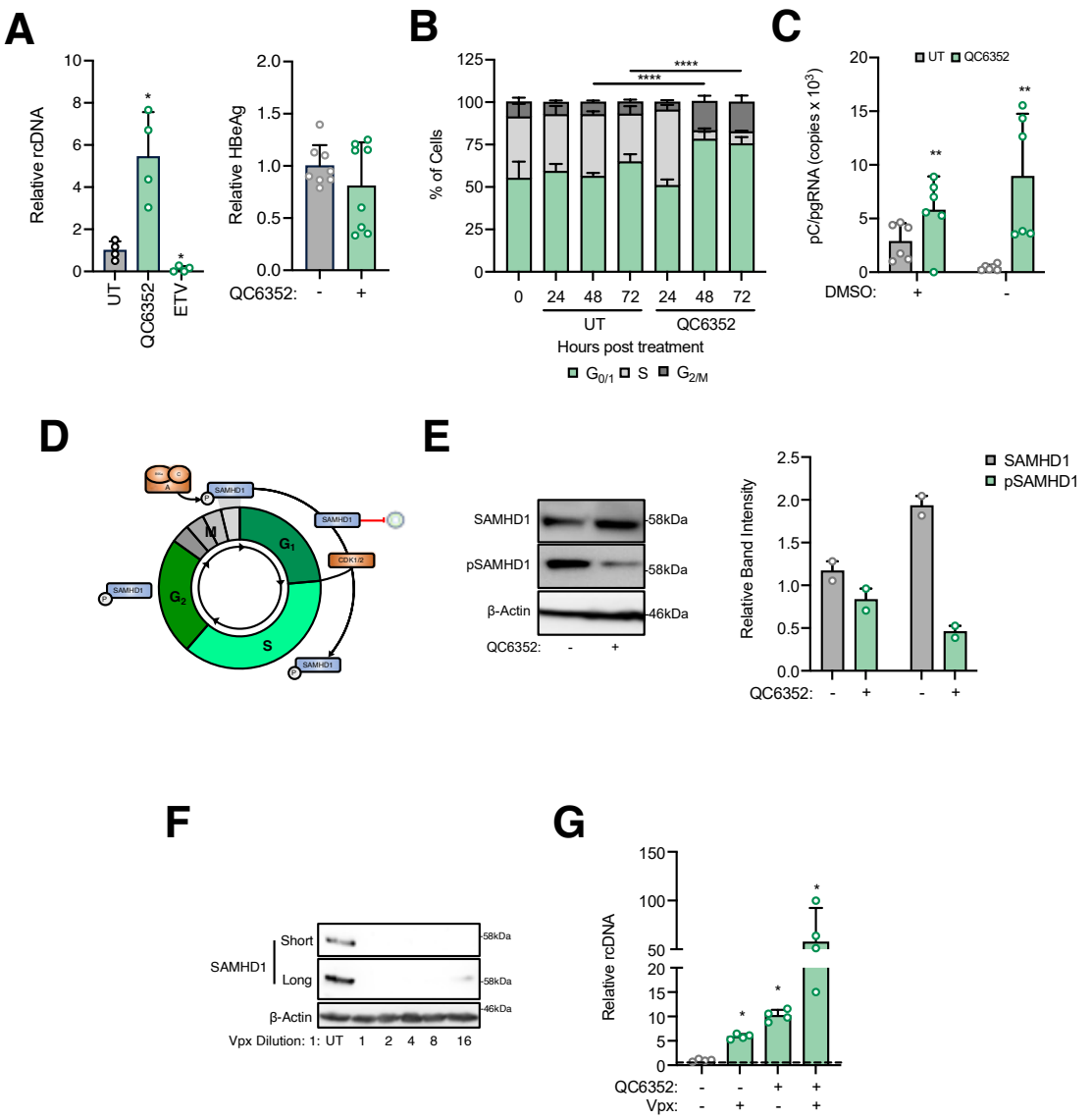


Figure 5.5: KDM4 inhibition promotes particle genesis

(A) HepAD38 cells were treated with QC6352 for up to 6 days. After 72 hours, HBV rcDNA was detected in the supernatant, using ETV as a control for signal:noise. rcDNA copies were expressed relative to untreated cells. Following 6 days of treatment, supernatants were PEG precipitated and used as inocula on naive HepG2-NTCP cells. 14 days post infection, HBeAg was detected in the supernatant, and quantified by ELISA. **(B)** HepG2-NTCP cells were treated with QC6352 for up to 72 hours, and the impact of treatment on cell cycle determined by flow cytometry at 24 hour intervals. Data are presented as a percentage of cells in each phase, and are representative of n=2 independent experiments with statistics tested using a 2-Way ANOVA. **(C)** HepG2-NTCP cells were treated with 2.5% DMSO for 72 hours before infection with HBV, and subsequent QC6352 treatment. Undifferentiated cells were included as a

comparator. 72 hours post infection, cellular RNAs were extracted and HBV pC/pg RNA copies enumerated by qPCR. **(D)** A schematic diagram showing the relationship between SAMHD1 phosphorylation status and host cell cycle progression. **(E)** HepG2-NTCP cells were treated with QC6352 for 3d after which, cells were lysed and protein levels analysed by western blot. Lysates were probed for expression of phospho- and unphosphorylated forms of SAMHD1, with β-Actin as a loading control. Densitometry was performed to look at SAMHD1 and pSAMHD1 levels relative to β-Actin. Data points are representative of 2 independent western blots, with mean and range plotted. **(F)** HepG2-NTCP cells were transduced with HIV-2 Vpx containing viral like particles (VLPs), in the presence of polybrene. VLPs were titrated onto cells, and efficiency of SAMHD1 knockdown was analysed by western blotting with both short and long exposures shown. **(G)** HepG2-NTCP cells were spinoculated with Vpx-VLPs before transduction with Ad-HBV-GFP. Cells were then treated with QC6352 or ETV for 6 days. 6 days post treatment, extracellular rcDNA was detected, copies enumerated by qPCR, and expressed relative to untreated cells. **(A,C,G)** Data are representative of n=2 independent experiments, and statistics were tested using Mann-Whitney U tests.

5.7: KDM4 and the hepatocellular transcriptome

In order to gain an insight into the host cell processes regulated by KDM4 we sequenced RNAs from HepG2-NTCP cells treated with QC6352 (5 μM) or cultured in 1% oxygen for 72 hours. We studied the host transcripts to look for pathways, processes or genes of interest that could explain the pro-viral activity of QC6352. Differential expression analysis using a DESeq2 package quantified the impact of QC6352 treatment or 1% oxygen culture on the host transcriptome (**Figure 5.6A**) (Love et al., 2014). As KDM4 is responsible for the removal of the inhibitory H3K9me3 mark from host histones, and its inhibition results in an accumulation of a transcriptional repressor we were surprised to see such a high frequency of upregulated genes (n=1,641) (**Figure 5.6A,B**) (Black et al., 2010; Hillringhaus et al., 2011). In contrast, the low oxygen cultured cells showed comparable numbers of up-regulated (n=2,429) and down-regulated (n=2,641) genes (**Figure 5.6B**). As discussed in *Figure 5.1* this is consistent with a model where the acute hypoxic transcriptional response is most likely attributable to the positive trans-activating potential of HIFs, whereas in this more persistent hypoxic state transcriptomic changes are likely influenced by indirect HIF effects or inhibition of other 2-OGDDs (Kindrick and Mole, 2020).

Our previous data shows that cellular oxygen availability restricts KDM4 function and comparing the transcriptomes of cells treated with QC6352 or cultured in 1% oxygen highlighted an overlap in upregulated (n=559) and downregulated genes (n=289) (**Figure 5.6B**). This is consistent with the reduced activity of KDM4 at 1% oxygen. Using GSEA and the hallmarks gene set, we compared the host cell processes that were regulated by QC6352 treatment or 1%

oxygen (Liberzon et al., 2015; Liberzon et al., 2011; Subramanian et al., 2005). We were reassured to see that KDM4 inhibition resulted in the upregulation of many pathways (n=29), compared with the downregulation of only seven (**Figure 5.6C**). In contrast, hypoxic culture repressed more pathways than it promoted (**Figure 5.6C**). Of note we saw that pathways involved in cell cycle regulation, such as genes associated with 'mitotic spindle' genesis and 'G2M checkpoint' were down-regulated in QC6352 treated and hypoxic cells respectively, providing a mechanism by which these conditions arrest hepatoma cell cycle (**Figure 5.5B, Figure 4.3C**). Furthermore, we observed an upregulation of genes associated with 'cholesterol homeostasis' that aligns with our recent report that Acyl CoA acyltransferase (ACAT), a major regulator of cholesterol esterification, positively influenced HBV particle genesis and HBV-specific CD8 T cell activity (Schmidt et al., 2021). Interestingly, along with other gene sets involved in immune regulation, we note that the IL6-JAK-STAT3 pathway was significantly upregulated in response to both hypoxic culture and QC6352 treatment; a pathway previously reported to positively regulate HBV cccDNA activation (Palumbo et al., 2015).

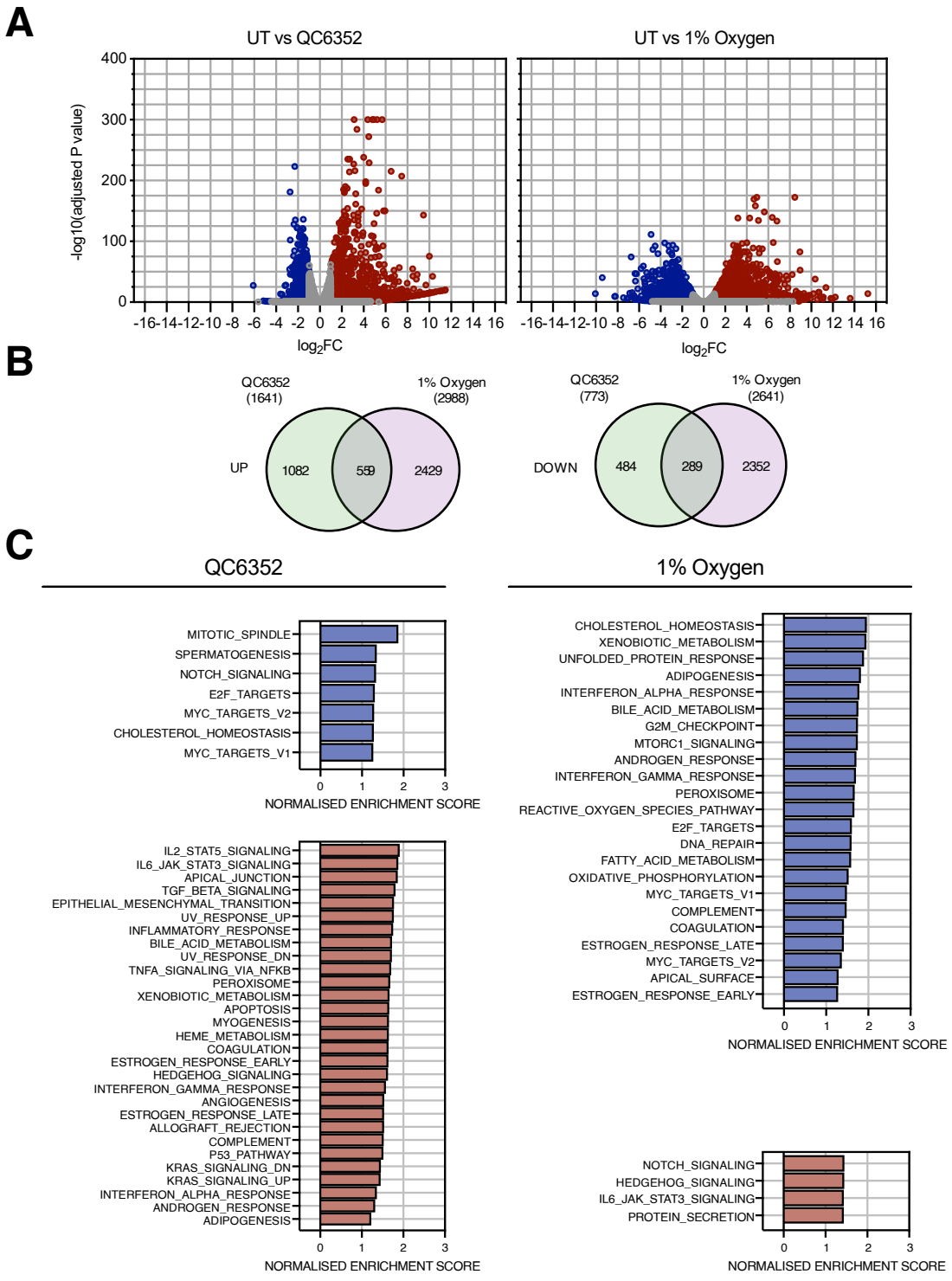


Figure 5.6: KDM4 regulation of host cell processes

(A) Differential expression analysis was performed between cells treated with QC6352 (5 μM), or cultured in 1% oxygen for 72 hours, against untreated cells using a DESeq2 package (Love et al., 2014). Statistical significance determined by a log_2FC +/-1 and FDR<0.05. **(B)** Venn diagrams to show the overlap of both

significantly up- or down- regulated genes between the two experimental conditions. **(C)** Using the Hallmarks gene sets from MSigDB, pathway analysis was performed to look at both up (red) and down (blue) regulated host pathways in both experimental conditions (Liberzon et al., 2015). In QC6352 treated cells we observe downregulation of 7 pathways, and upregulation of 29 gene sets. In hypoxic cultured cells, we noted significant downregulation of 23 pathways, compared with 4 upregulated. For pathway analysis FDR<0.25 was used as a cut-off for statistical significance. Sequencing results derive from n=3 independent biological replicates per condition.

5.8: KDM4 is inhibited in the CHB liver

As commented earlier, given that previous reports have not detected H3K9me3 on the HBV genome, we hypothesised that QC6352 increased viral replication by modulating essential host pathways (Flecken et al., 2019; Lebosse et al., 2020; Tropberger et al., 2015). To that end, we screened our transcriptomic data for expression of previously documented activators and repressors of HBV replication and noted a modest change in gene expression (Turton et al., 2020; Wing et al., 2021). However, hypoxia increased Janus Kinase (JUN), an activator of the JAK-STAT signalling pathway, as well as Terminal nucleotidyltransferase 4 (TENT4), a factor reported to influence HBV RNA stability (**Figure 5.7A**) (Turton et al., 2020; Wing et al., 2021).

The KDM4 family consists of 5 isoforms (A-E), although until the recent discovery of a functional protein KDM4E was believed to be a pseudogene (Hillringhaus et al., 2011). Similarly, it was speculated that KDM4F existed, however to date this isoform has not been detected at the protein level (Jack et al., 2013). To understand the hepatic expression of KDM4A-E we assessed transcript levels in published RNA-sequence data from PHHs and human hepatoma cell lines (Chakraborty et al., 2020; Hillringhaus et al., 2011; Labbe et al., 2013; Liu et al., 2020b; Niu et al., 2017). KDM4A was the dominant isoform expressed in cultured PHHs, with KDM4B and C as minor isoforms. Reassuringly, this was comparable with HepG2 and other human hepatoma cell lines, with KDM4A as the most highly expressed transcript (**Figure 5.7B**). It is worth noting that these data only show transcript levels and do not give any indication of protein expression or activity. These data go some way in supporting our use of

HepG2-NTCP cells as a model system, given similar KDM4 expression profiles between these and human hepatocytes.

We previously used a bioinformatic approach to study HIF transcriptional activity in the CHB liver using a cell culture derived gene signature (**Figure 3.3**) (Liu et al., 2020b). We applied a similar approach to determine whether there was evidence of a KDM4 transcriptional footprint in the CHB liver. We developed two putative gene signatures using the 100 most significantly differentially expressed genes in either QC6352 treated or hypoxic cells; these genes are represented by green symbols in the volcano plots (**Figure 5.7C**). Given the considerable overlap between these differentially expressed genes (**Figure 5.6**), we cross referenced the top 100 genes in each condition and only identified one gene in common (**Figure 5.7D**). Using GSEA, we assessed the expression of each gene signature in a CHB patient cohort where gene expression had been quantified by Affymetrix micro-array (Subramanian et al., 2007; Zhou et al., 2017). We observed increased expression of the KDM4 gene set in eighty two CHB patients above non-viral subjects (n=6), consistent with reduced KDM4 activity in the infected liver (**Figure 5.7E,** left). Similarly, GSEA revealed a significant enrichment in the expression of persistent hypoxia genes in the infected subjects, further highlighting the importance of hypoxic signalling in the diseased liver (**Figure 5.7E,** right) (Liu et al., 2020b; Zhou et al., 2017).

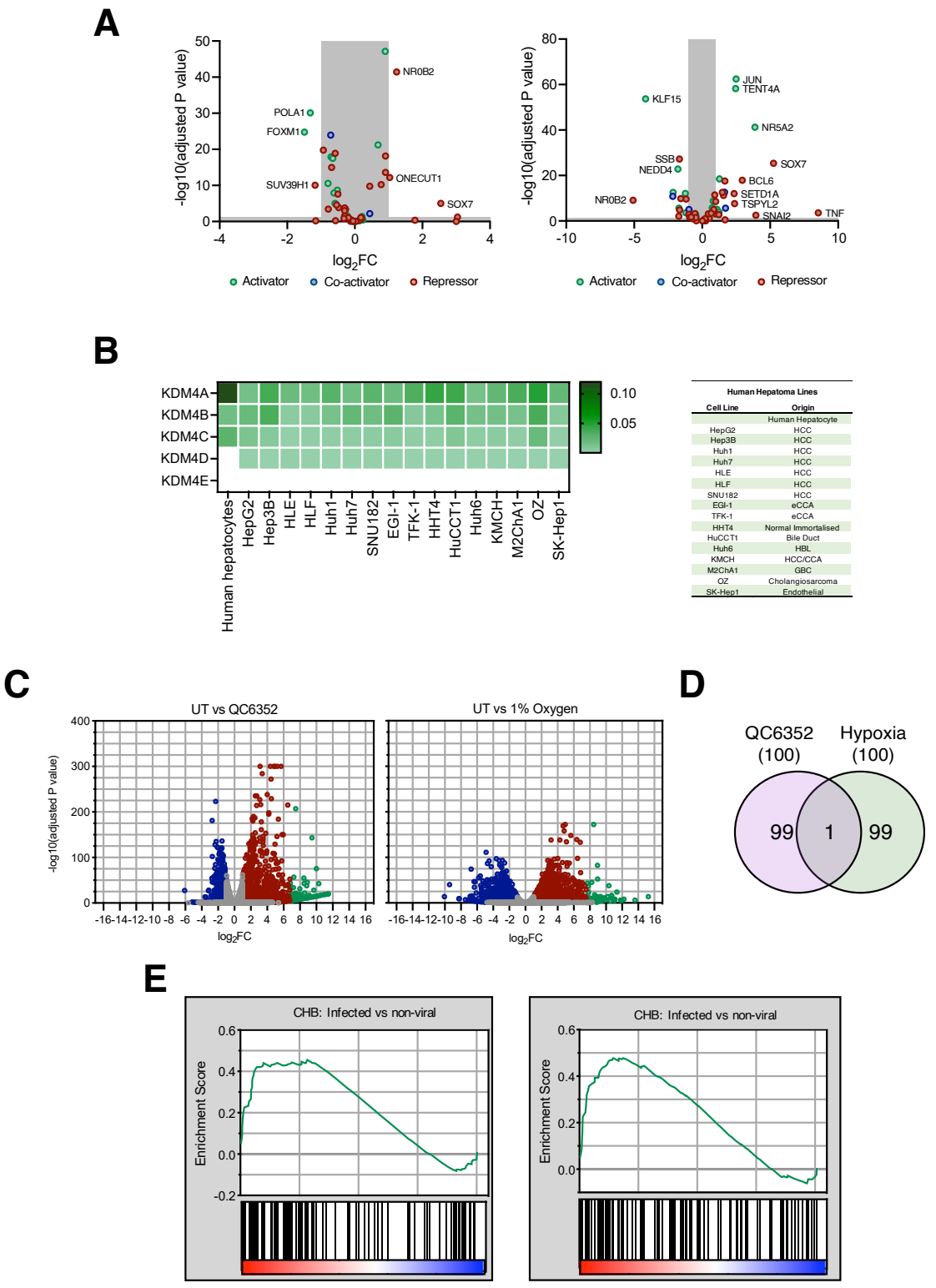


Figure 5.7: KDM4 is inhibited in the CHB liver

(A) Modulation of known activators, co-activators or repressors of HBV replication from the literature (Turton et al., 2020; Wing et al., 2021). Differential expression analysis shown above was interrogated for previously defined

factors. Statistical significance was determined by genes with a log_2FC of ± 1, and FDR<0.05. Transcriptomic analyses are derived from RNA sequencing of n=3 independent biological replicates. **(B)** Expression of KDM4 isoforms in a panel of human hepatoma cells and primary human hepatocytes from previously published RNA-sequencing datasets (Chakraborty et al., 2020; Niu et al., 2017). KDM4A-D normalised Taq-counts are expressed relative to the geometric mean of β-Actin and RPLP0 housekeeping genes. **(C)** Using the previously defined differential expression analysis, the 100 most significantly upregulated genes were selected as a putative signature for genes that were regulated by KDM4 or hypoxia. 100 genes are annotated in green on the volcano plots. **(D)** A Venn diagram to show the overlap of the 100 genes from *C* between both experimental conditions. **(E)** Gene set enrichment analysis was performed using genes defined in *C*, to look for evidence of KDM4 inhibition (left) or hypoxic gene expression (right) in the CHB liver. GSEA was carried out in a cohort of n=82 patients with CHB compared with n=6 non-viral subjects. Significant enrichment was observed in both groups, KDM4 genes (FDR = 0.151); hypoxic genes (FDR = 0.07).

5.9: Summary

The aim of this chapter was to explore the HIF independent hypoxic response and to identify new mechanisms that regulate HBV replication. We used a variety of molecular virology assays, next generation sequencing and transcriptomic analyses to identify a role for KDM4 as a restriction factor for HBV. KDM4 is an essential, oxygen sensitive chromatin modifier that is inhibited in the hypoxic environment of the liver. We suggest that under low oxygen conditions HBV is regulated by both HIFs and KDM4 (Wing et al., 2021).

We initially compared the host transcriptional response to acute or persistent hypoxia, or HIF stabilisation via FG-4592 treatment. We noted that the host response in these conditions was starkly different, and that HIF-signalling is not the only transcriptional regulator in hypoxia (**Figure 5.1A-E**). We then investigated the differential effects of persistent hypoxia and FG-4592 treatment on the HBV transcriptome. Comparison of Illumina sequencing of HBV RNAs revealed that hypoxia increased the abundance of viral reads at the TSS of all major viral RNAs, outperforming FG-4592 treatment (**Figure 5.1F,G**).

Given the discovery that KDM5 and 6 are novel oxygen sensors, we explored whether one of the KDMs could be responsible for the hypoxic regulation of HBV (**Figure 5.2A**) (Batie et al., 2019; Chakraborty et al., 2019). We screened a panel of inhibitors to KDM4, 5, and 6, or a generic pan-KDM inhibitor and this revealed that KDM4 inhibition potentiated HBV RNA levels, and phenocopied the hypoxic response (**Figure 5.2B,C**) (Chen et al., 2017; Heinemann et al., 2014; Vinogradova et al., 2016; Wang et al., 2013; Wing et al., 2021). Interestingly we noted a modest but non-significant increase in transcription with JIB-04 treatment.

This compound inhibits all KDMs and so both activatory and repressive histone marks will be modulated resulting in a null effect on HBV transcription. We then further validated the phenotype by boosting pC/pgRNA levels with transient siRNA silencing of KDM4-D (**Figure 5.2E**).

Our data suggest that KDM4 is inhibited at 1% oxygen, and QC6352 treatment has no additive effect on H3K9me3 levels in hypoxic cells (**Figure 5.3A**) (Chen et al., 2006; Hancock et al., 2015; Hancock et al., 2017; Ploumakis and Coleman, 2015). Further to this, we confirmed that QC6352 had no additional effect on viral RNAs when treatment was applied to hypoxic cultures (**Figure 5.3E**), and whilst we have only demonstrated this for QC6352 this suggests that cellular oxygen tension can mediate the sensitivity of cells to drugs targeting the epigenetic modifiers. We also showed that in a HepG2-NTCP cell KDM4 regulates H3K9me3 levels, which can in turn regulate the expression of HIF-1α, consistent with results of a previous study from Dobrynin et al. (**Figure 5.3A**) (Dobrynin et al., 2017). Importantly we demonstrated that QC6352 did not stabilise HIF expression or modify HIF function as assessed by measuring transcript levels of a panel of HIF-regulated genes (**Figure 5.3A,B**). This highlights the intricate interplay between oxygen availability and the host cell transcriptional response, and provided further evidence that KDM4 regulates HBV replication.

We investigated the kinetic properties of QC6352 and noted that the pro-viral phenotype was not apparent until 48 hours post treatment, and was even more significant by 72 hours (**Figure 5.4A**). We expected that if this compound was targeting the viral epigenome directly, it would be acting much quicker and suggests that KDM4 regulates a host cell process implicated in the viral life cycle rather than modulating the virus directly. Tropberger et al. and Flecken et al.

investigated the association of cccDNA with host histones using viral DNA derived from liver biopsy samples and *in vitro* model systems (Belloni et al., 2012; Flecken et al., 2019; Lebosse et al., 2020; Tropberger et al., 2015). Whilst they detected an abundance of activatory histone marks, such as H3K4me3 and H3K27ac, they detected little to no H3K9me3, or any other repressive marks associated with the viral genome (Flecken et al., 2019; Tropberger et al., 2015). We therefore believe that QC6352 elicits its pro-viral effects through modulation of host pathways, rather than causing an accumulation of the repressive H3K9me3 modification on the viral epigenome.

QC6352 had a minimal effect on cccDNA levels but maximised its transcriptional output and boosted HBeAg levels in *de novo* infected cells (**Figure 5.4A,B**). Analysis of sequencing reads at each of the viral TSS indicated a global increase in all viral RNA transcripts (**Figure 5.4D,E**). Furthermore, we found that integrant derived PreS1/2 RNAs were also sensitive to KDM4 inhibition (**Figure 5.4F**). These experiments demonstrated that KDM4 can restrict transcription from both HBV integrants and episomes, however it was clear that the *de novo* infection model showed the most striking phenotype. This could reflect the nature of the genomic material used, as the *de novo* infection is the only model which supports HBV replication exclusively from viral DNA. Integrants are randomly inserted into the host chromosome and will fall under the epigenetic regulation of surrounding genes. HepG2-pEpi cells support replication from HBV encoded in a plasmid vector backbone which may associate with histones differently, altering its sensitivity to epigenetic modification. In addition, there could be further roles of KDM4 in regulating cccDNA genesis or maintenance that were not apparent using the techniques employed here.

Studying extracellular rcDNA in QC6352 treated HepAD38 cells revealed an increase in particle genesis in response to KDM4 inhibition, with minimal changes in particle infectivity (**Figure 5.5A**). Consistent with previous reports, we confirmed that QC6352 treatment could arrest hepatoma cell cycle and suggest that the arrestive properties of the drug play some role in promoting viral replication, but do not fully explain the phenotype (**Figure 5.5B,C**) (Chen et al., 2017). We postulated that cell cycle arrest would modulate the phosphorylation status of SAMHD1 and perturb particle genesis (Sommer et al., 2016; Wing et al., 2019). We confirmed that in response to $G_{0/1}$ arrest SAMHD1 is present in its unphosphorylated state, where it can restrict particle release (**Figure 5.5D,E**). Our previous study suggested that pSAMHD1 also facilitates cccDNA genesis; promoting the conversion of rcDNA to cccDNA. We note that pSAMHD1 levels are reduced in QC6352 treated cells, but do not detect variation in cellular cccDNA levels following treatment (**Figure 5.4A**). Our data suggest that the magnitude of the increase in pC/pgRNA overwhelmed the cellular pool of SAMHD1 to restrict the conversion to rcDNA. To test this hypothesis we knocked down SAMHD1 using Vpx and observed a 50-fold increase in particle genesis with QC6352 treatment (**Figure 5.5F,G**). These data provide evidence for the role SAMHD1 plays in regulating the genesis of progeny viruses, and the impact of KDM4 inhibition would be more profound if SAMHD1 was not functionally active in this system.

Our transcriptomic analyses revealed a considerable overlap between QC6352 treatment and 1% oxygen culture, suggesting that in chronic hypoxia KDM4 regulates host gene expression (**Figure 5.6A,B**). It is of note that despite causing the accumulation of the repressive histone mark H3K9me3, KDM4

inhibition was associated with an upregulation of many host transcripts, which outnumber transcriptionally repressed genes (**Figure 5.6A,B**). However, it is unlikely that the accumulation of a repressive mark on the viral genome would result in such a striking upregulation of HBV transcripts (Flecken et al., 2019; Tropberger et al., 2015). Whilst we note accumulation of H3K9me3 on a whole cell level (**Figure 5.3A**), it would be surprising if H3K9me3 deposition on the viral genome potentiated replication so potently. As previously discussed, the viral genome is associated with activatory marks, but devoid of repressive histone modifications (Flecken et al., 2019; Tropberger et al., 2015). Finally, our *in vitro* transcriptomic data identified a 100 gene signature of host protein coding RNAs that are repressed by KDM4, and we used this signature to study CHB patient transcriptome data, finding evidence for KDM4 inhibition in the CHB liver (**Figure 5.7C,E**) (Zhou et al., 2017). This suggests that KDM4 inhibition by QC6352 may provide a more physiologically relevant microenvironment, applicable to the study of HBV in cell culture systems.

To conclude, we demonstrate a role for KDM4 to restrict HBV transcription from both integrated and episomal viral genomes. KDM4 is a major transcriptional regulator and orchestrates the host cell response to hypoxia, independent of the activity of HIFs. We also show that drug efficacy *in vitro* can be determined by local oxygen availability, which provides an interesting thought when considering the design of screening assays to discover and evaluate new anti-viral therapies. Collectively, we present the idea that KDM4 inhibition provides a physiologically relevant model system for arresting cell cycle, increasing HBV replication, and potentiating particle genesis.

Chapter 6: Discussion and Future Work

Across chapters 3-5 we have explored the contribution of hypoxia to the diseased hepatic transcriptome, and identified both HIF-dependent and independent mechanisms underpinning HBV replication. Throughout this study we employed a combination of bioinformatic analysis, molecular virology *in vitro* assays, and studied biopsy samples to further understand the interplay between hypoxia signalling and HBV replication.

The HRE motif is abundant in the host genome with as many as 1,000,000 occurrences, however only a fraction of these have been shown to bind HIFs (Kindrick and Mole, 2020; Mole et al., 2009). HIF-1α regulates a greater number of genes than HIF-2α, with a recent study identifying that at least 1,658 genes were regulated by HIF-1α and only 426 by HIF-2α in a hypoxic HepG2 cell (Smythies et al., 2019). The HBV genome encodes 2 HRE motifs, and our findings suggest they bind HIFs and this activates viral transcription. HBV is not unique and many human viruses encode at least one HRE, although their function and activity may not have been fully elucidated (reviewed in (Liu et al., 2020a)). During integration the HBV genome and associated HREs are incorporated into the host chromatin, providing new target genes for HIFs to regulate (Wing et al., 2021). Whilst the BCP and HRE motifs will be encoded in the dslDNA fragments, it is likely that the chromatinization is determined by the integration site, and both chromatin conformation and accessibility will regulate HIF binding (as reviewed in (Kindrick and Mole, 2020)). Integration of the HBV genome is associated with the onset of HCC and tumorigenesis, and dependent on the location of the integrant, the HREs could influence oncogene expression that could be activated in the hypoxic

tumour environment (Wilson et al., 2014b). In that respect, it is interesting that the PreS1/2 RNAs derived from HBV integrants were insensitive to hypoxia (**Figure 4.11C**), but were induced by KDM4 inhibition (**Figure 5.4F**) (Wing et al., 2021). Although hypoxia inhibits KDM4 activity (**Figure 5.3A**), it also perturbs the function of the whole 2-OGDD family and as such is likely to have wide reaching effects on the host epigenome (Hancock et al., 2015; Hancock et al., 2017). Whilst KDM4 inhibition may promote transcription, hypoxic regulation of an alternative host pathway or factor may dampen the effects of KDM4 inhibition.

Our pathway analyses and cell cycle assays revealed that hypoxic culture and KDM4 inhibition could arrest hepatic cell cycle, and as such we were keen to understand whether these conditions could influence cccDNA levels (**Figure 4.3**, **Figure 4.4**, **Figure 5.4-6**). A recent collaborative study with Chakraborty and colleagues revealed that cccDNA could be detected in the nuclei of cells as early as 6 hours post infection (Chakraborty et al., 2020). For our studies, we opted to treat cells or transfer to hypoxic conditions 6 hours post infection, to enable us to elucidate a role for these pathways in regulating HBV transcription, rather than viral entry or cccDNA genesis. In a collaboration with Dr Anindita Chakraborty, we demonstrated that hypoxia had little effect on HBV uptake or NTCP expression. In future it would be interesting to understand whether aspects of the hypoxic signalling cascade could regulate other stages in the viral life cycle such as nuclear import or cccDNA genesis, and as such whether hypoxia may influence a given cell's permissivity to infection (Ko et al., 2018; Tu et al., 2018; Yan et al., 2013; Yan et al., 2012). With both low oxygen culture and KDM4 inhibition we reassuringly observed no detectable changes in cccDNA levels and we attributed the oxygen mediated potentiation in transcripts to cccDNA activation, rather than

abundance (**Figure 4.4, Figure 5.4**). However, we must also acknowledge that hypoxia may modulate RNA half-life, either directly through alteration of the methylation status, or indirectly through modulation of the RNA processing machinery (Imam et al., 2018; Kim et al., 2021; Kim and Siddiqui, 2021). Previous studies have demonstrated that in hypoxia, total cellular RNA content decreased and the stability of host mRNAs was reduced to around 6 hours (Dolken et al., 2008; Schwanhausser et al., 2013; Tiana et al., 2020). Hypoxia can increase the ubiquitination and post-translational modification of RNA Pol II, which could explain the global reduction in RNA transcription (Ignacak et al., 2009). However despite the reduction in total cellular RNAs we observe a marked upregulation of HBV pC/pgRNAs in hypoxia. In our group, Dr Senko Tsukuda investigated the half-life of HBV RNAs using actinomycin D clamp assays, and showed a comparable half-life of pC/pgRNAs under low oxygen conditions (Imam et al., 2018). HBV RNAs are epigenetically modified, and as discussed in Chapter 1, the m6A epitranscriptomic modification in the 5' and 3' loops of the pC/pgRNA are essential in determining RNA fate (Kim et al., 2021; Kim and Siddiqui, 2021; Wang et al., 2014). RNA methylation is regulated by the oxygen sensitive 2-OGDDs, FTO and ALKBH5, and we are now working to understand their role in regulating HBV replication in physiological oxygen tensions (Thalhammer et al., 2011).

As well as regulating RNA fate through epitranscriptomic modifications, hypoxia has been reported to influence host cell RNA splicing (Farina et al., 2020; Han et al., 2017; Sena et al., 2014). As discussed previously, HBV RNAs undergo splicing and reports have identified spliced variants of all major viral RNAs, including eighteen spliced forms of pC/pgRNA (Duriez et al., 2017; Lim et al., 2021; Soussan et al., 2003), 4 PreS2 splices and several HBx truncates (Al-Anazi

et al., 2018; Candotti et al., 2012; Hass et al., 2005; Liu et al., 2008). The roles of each of the spliced RNAs are not fully understood, although SP1 the major spliced RNA is translated to form hepatitis B spliced protein (HBSP) (Soussan et al., 2003). In a HBVtg mouse model, HBSP reduced hepatic damage from chemically induced liver fibrosis, which was attributed to downregulation of C-C motif chemokine ligand 2 (CCL2). Interestingly, Duriez et al. also confirmed that HBSP can regulate CCL2 expression *in vitro,* and noted that in HBV chronic carriers Sp1 RNA levels are inversely proportional to CCL2 expression (Duriez et al., 2017). We recently identified a role for CTCF to restrict HBV replication, whereby both transient silencing and mutation of putative CTCF binding sites enhanced viral transcripts (D'Arienzo et al., 2021a). CTCF has been implicated in the regulation of RNA splicing by acting as a physical roadblock for RNA Pol II, resulting in polymerase jumping or stalling, and subsequent RNA splicing (Alharbi et al., 2021; Ferguson et al., 2021; Kornblihtt, 2012; Pentland et al., 2018). Currently, we are working to understand whether HIFs or KDM4 can regulate cellular CTCF levels, and whether low oxygen may impact HBV RNA splicing, perhaps through regulating CTCF activity or previously defined RNA processing pathways.

Despite the increased accessibility to sequencing services, qPCR measurement of viral DNA and RNAs is the most commonly used method to quantify HBV replication *in vitro*. The majority of studies quantify either pC/pgRNA or total viral RNA, as the overlapping nature of the viral genome makes primer design for each viral RNA technically challenging, and requires specific attention to detail with respect to amplicon size and primer efficiency (**Figure 3.4**, **Figure 3.5**) (Hallez et al., 2019; Meier et al., 2021; Suslov et al., 2021). Next generation sequencing based approaches and 5'RACE methods have been applied to clinical

samples, however these are relatively expensive, and sequencing approaches are limited in their reliance on polyA enrichment and short-reads of Illumina sequencing (Prakash et al., 2018; Stadelmayer et al., 2020). Our qPCR assay is able to ascribe relative transcript patterns to viral RNAs from both *in vitro* and *in vivo* sources, as well as discriminate between cccDNA and integrant derived RNAs. However, our technique will under-represent spliced RNAs and over-estimate the abundance of pC/pgRNAs.

A recent study from Ramirez et al. applied PACBIO sequencing to assess viral DNA and RNA in three integrant cell lines used in our study (Ramirez *et al.*, 2021). Interestingly they showed that none of the cell lines produced full length HBx RNAs, however our PCR approach detected X coding transcripts but we cannot comment on their length (Al-Anazi et al., 2018; Liu et al., 2008). A limitation of our sequencing data is that Illumina reads are fragmented and read as 300bp products. This means when they are aligned to the reference sequence it is not possible to determine the length of the original RNA. Future application of long-read sequencing would enable us to understand the impact of HIF signalling or KDM4 inhibition on each of the independent viral promoters. We observed a selective upregulation of pC/pgRNA levels in response to HIF activation of the BCP, which altered the pattern of viral transcripts to constitute over 95% of HBV RNAs. The genesis of viral capsids is reliant on the regulation of component parts, such as the ratio of HBc to genome, and formation of the outer lipoprotein envelope from HBsAg (Diab et al., 2018; Zhao et al., 2021; Zheng et al., 2019). This modulation in transcript pattern may have pleiotropic effects on other stages in the viral life cycle that we have not studied. However our observation that

hypoxia potentiates particle release suggests that the viral egress pathways remain uncompromised (**Figure 4.11**).

In a collaboration with Dr Thomas Michler and Professor Ulrike Protzer at the University of Munich, we transiently silenced HIF-1β in HBV transgenic mice (Guidotti et al., 1995; Wing et al., 2021). HBVtg support HBV replication from an integrated 1.3x overlength viral genome, and despite the lack of cccDNA they have been used extensively to study viral-host interactions and HBV replication (reviewed in (Oropeza et al., 2020; Ortega-Prieto *et al.*, 2019)). In the HBVtg model, there is clear evidence of pericentral HBcAg expression, and we noted an abundance of HBc-positive cells surrounding the central vein (Chisari, 1995; Guidotti et al., 1995). In the male mice, we noted a marked reduction in the frequency of HBc+ cells and reduced peripheral HBe and HBs Ag in response to HIF-1β silencing (Wing et al., 2021). It would be easy to speculate that the natural oxygen gradient of the liver is the driver of the pericentral localisation of HBcAg, and this would be supported by our observation that HIF-1β silencing abrogated the phenotype (Halpern et al., 2017; Kietzmann, 2017). However, this pericentral zonation is not as prominent in man, where the distribution of hepatocytes expressing HBcAg is less zonal. This could be reflective of a rare subset of hepatocytes that are permissive of HBV infection and can support cccDNA driven replication in the human liver, but may also be an artefact of studying mice supporting a single HBV integrant.

Our study was the first to identify interactions between HIFs and HBV DNA in response to hypoxic stimulation, but also naturally occurring in the infected liver of humanised liver chimeric mice (**Figure 4.9** and **Figure 4.10**). We demonstrated that HIF-1β bound the HBV genome *in vitro,* in response to either a PHD inhibitor

or 1% oxygen culture stabilisation of HIFs. As described in Chapter 1, there are alternative binding partners for HIF-1β other than HIF-α subunits, and we cannot state definitively that we were detecting HIF-α/β dimers. Furthermore, our data do not prove direct binding as ChIP cannot discriminate binding of individual transcription factors or large protein complexes that could be preserved during the crosslinking protocol. However, as the mechanism of HIF activation is well defined, we would be surprised if it was not a canonical HIF-α/β dimer that drives enhanced HBV transcription in hypoxia.

Our bioinformatic analysis provides evidence of HIF-signalling in the diseased liver (**Figure 3.3** and **Figure 5.7**) and we hypothesised that HIF-HBV complexes may exist in the inflamed liver. However, we were aware of the technical challenges of performing these ChIP assays on snap frozen tissue samples, such as variability in crosslinking, immunoprecipitation and the presence of other hepatic cell populations (Mukhopadhyay et al., 2008). Since our study, Pirosu et al. published a method for such assays, which is comparable to our protocol (Pirosu et al., 2021). Our experiments using HBV infected FNRG-NOD mice transplanted with human hepatocytes show an enrichment of HIF-1β and HIF-2α binding to the viral genome, with a more modest binding of HIF-1α (**Figure 4.10**). We were surprised to not observe a more striking result with HIF-1α pull-down, however it is difficult to compare the relative success of each immunoprecipitation, as the antibody is the biggest determinant of ChIP efficiency (Bao et al., 2013; Kidder et al., 2011). It is also worth noting that as these assays were performed on liver tissue samples, we were using a heterogenous mix of cells in contrast to our *in vitro* assays on hepatoma cell lines. Whilst we know that only engrafted human hepatocytes will support HBV replication, the presence of

murine parenchymal cells and the potential cross-reactivity of antibodies against human and mouse proteins should be considered. As mentioned above, our data from the HBVtg show distinct zonal staining of HBcAg, which suggests that HBV preferentially replicates in the hypoxic pericentral region. It would be easy to speculate that HIFs are stable in these cells, and perhaps our HIF-HBV complexes originate from cells adjacent to the central vein in the FNRG-NOD mice. It would be informative to perform immuno-histochemistry and look for colocalization of HIF-1α and HBcAg in human liver biopsy samples, although co-incidence of both factors would still not be sufficient to claim direct binding (Riedl et al., 2021).

To further understand the HIF-HBV interactions, ChIP assays could be performed on HBV genomes encoding mutant HREs. Our experiments using synthetic HBV1.3 genomes would require further optimisation to ensure mutation of both HRE-motifs (**Figure 4.6**). Our qPCR assay revealed that HBV1.3 genomes transcribe RNAs in different proportions to *de novo* infection systems, and caution should be taken when considering transcriptional regulation of these overlength constructs. In a similar strategy to our previous study on HBV and CTCF, we could mutagenize HRE motifs within HBV-mini circle genomes and generate material for HIF ChIPs (D'Arienzo et al., 2021a; Guo et al., 2016; Yan et al., 2017). In future, ChIP-seq could be used to study HIF binding and RNA Pol II enrichment on the HBV genome under hypoxic conditions (Ferguson et al., 2021; Flecken et al., 2019; Smythies et al., 2019; Tropberger et al., 2015). The application of techniques such as Capture C or ATAC-seq would enable us to understand the impact of hypoxia on DNA accessibility, and whether there is any variation across the other viral promoters. Previous studies have used these methods to study the accessibility of other DNA viral genomes, however there are limited publications to

indicate its application to HBV (Depledge et al., 2011; Johnston et al., 2021; Moreau et al., 2018). However, it would be challenging to predict the impact of hypoxia on cccDNA conformation, as it is thought that HIFs regulate ready primed genes with high H3K4me3 and RNA Pol II presence in their enhancers, rather than modulating chromatinization before binding (reviewed in (Hampsey and Reinberg, 2003; Hancock et al., 2015; Kindrick and Mole, 2020)).

Given that our ChIP assays were carried out on liver tissue samples, we cannot determine where in the liver lobule these complexes were found (**Figure 4.10**). Similarly, our inflammatory gene analysis using NanoString technology was performed on RNAs prepared from bulk liver biopsy material (**Figure 3.8**). As such, we cannot exclude the contribution of other cell types to the liver inflammasome, and bulk approaches give no indication of cell location. It would be interesting to study the spatial location of HBV DNA and RNAs, as well as HIFs and associated HIF target gene transcripts. *In situ* approaches such as RNA scope or smFISH could be applied to identify specific hepatocytes which appear capable of supporting cccDNA, and whether they show increased HIF signalling above neighbouring uninfected cells (Meier et al., 2021; Samuels et al., 2020; Zhang et al., 2016a). Whilst we do not observe such regular zonation of HBcAg in human livers, spatial transcriptomics could reveal co-localisation of HIF targets and viral RNA transcripts. Studies such as this would enhance understanding of the niche which renders hepatocytes permissive to HBV infection.

Recent ground breaking studies from Batie et al. and Chakraborty et al. identified that hypoxia can rapidly and directly modify the cellular epigenome through KDM5 and 6 (Batie et al., 2019; Chakraborty et al., 2019). Previous studies have investigated the HBV epigenome in clinical tissue and *in vitro* cell

culture models, and future work could probe cccDNA chromatin status under low-oxygen conditions (Flecken et al., 2019; Lebosse et al., 2020; Tropberger et al., 2015). We have demonstrated that HBV DNA can be sheared (**Figure 4.7**) which would allow putative mapping of TF binding or histone modification across key sites of the viral genome, however selecting appropriate model systems to reproduce the viral life cycle remains a challenge. Whilst *de novo* infection represents the gold standard and most physiologically relevant system, the routine treatment with DMSO is problematic as our data suggests that this process blunts the host HIF-response (**Figure 4.2**) (Wing et al., 2021). Equally, the use of producer cells such as the HepG2-pEpi cells allows for high levels of viral input, but the epigenetic status of the plasmid backbone may limit our interpretation. Technical challenges aside, studying the epigenetic status of cccDNA in physiological oxygen tensions would be highly informative and allow us to draw comparisons between the viral epigenome *in vivo*.

As well as looking at histone modification, studying nucleic acid modification in hypoxia would be of great interest. In collaboration with Professor Chunxiao Song's group we, for the first time, mapped the methylation status of HBV DNA at base-pair resolution using the novel TAPs sequencing approach (Liu et al., 2020c; Liu et al., 2019). Hypoxia can modulate the methylation status of DNA and RNA through perturbation of TET activity, and as such it would be interesting to learn whether oxygen changes the DNA methylation status of cccDNA or the HBV CpG islands (Guo et al., 2011; Kohli and Zhang, 2013; Tahiliani et al., 2009). Interestingly, we previously applied TAPs sequencing to HBV infected HepG2-NTCP cells, and showed that cccDNA was unmethylated in normoxic conditions 6 days post infection (Liu et al., 2019). Furthermore, this

approach could be applied to clinically derived tissues to study the HBV DNA methylome in the hypoxic, diseased liver. We are once again collaborating with Professor Song's group to study the methylation status of HBV DNA in our CHB patients (**Figure 3.5**). As well as studying methylation status, it would be interesting to investigate HBV sequence diversity in response to hypoxic culture. Reports have identified a role for APOBEC3 family members in the cytidine deamination of the viral genome, and others have noted that several APOBEC3 isoforms are either oxygen sensitive or HIF regulated (Kock and Blum, 2008; Lucifora et al., 2014; Nguyen and Hu, 2008; Vivekanandan et al., 2008a). As such sequencing both cccDNA and secreted HBV rcDNA genomes to look for changes in the transition to transversion ratio would inform us on the activity of these innate restriction factors in hypoxia.

In addition to direct HIF activation, our data suggest that there is HIF-independent regulation of HBV in low oxygen via KDM4 inhibition. We note that QC6352 treatment had wide reaching effects on host cell processes, many of which have the potential to influence multiple stages of the viral life cycle (**Figure 5.6**). For example, we demonstrate that both hypoxia and pharmacological inhibition of KDM4 arrests hepatoma cell cycle in $G_{0/1}$, which is the physiological state of hepatocytes *in vivo* (**Figure 4.3**, **Figure 5.5**). Cell cycle has been implicated in the life cycle of both DNA and RNA viruses, and as such culturing cells in physiologically relevant oxygen tensions may recapitulate key stages of the life cycle *in vitro* (Kannan et al., 2011; Phoolcharoen and Smith, 2004; Yin et al., 2019; Zack, 1995). In addition to cell cycle arrest, we and others have demonstrated modulation of the interferon response under low oxygen conditions (Miar et al., 2020). Whilst HBV does not elicit such a potent innate immune

response as HCV, interferon signalling and NF-κB activation have been shown to influence HBV replication (Duriez et al., 2017; Hosel et al., 2017; Liu and Zhang, 2015; Palumbo et al., 2015; Wieland and Chisari, 2005; Zhou et al., 2021). Hypoxic signalling is likely to impact many other host cell processes such as hepatocyte metabolism, and indeed glycolysis and gluconeogenesis are two pathways that demonstrate distinct zonation in the liver, which have been implicated in HBV infection (Teng et al., 2015). Our data suggest that the routinely used and rather crude DMSO differentiation blunts the cellular response to hypoxia, and as such the role of oxygen sensitive transcriptional regulators could have been overlooked (**Figure 4.2**).

We developed our HBV qPCR assay to study HBV transcript patterns and differential promoter usage in a CHB patient cohort, all of whom were infected with HBV GtD. We therefore designed primers based on the GtD consensus, which was also the genotype present in all of the *in vitro* systems we studied (**Figure 3.4**, **Figure 3.5**). Whilst our data show comparable amplification efficiency and sensitivity for T1-4 primer pairs, it must be acknowledged that primer redesign may well be needed to apply this approach to additional HBV genotypes. Given the high nucleotide divergence between HBV genotypes it would be surprising if the primers were to amplify all viruses with comparable efficiencies (D'Arienzo et al., 2021b). Lim et al. recently applied Illumina sequencing to study spliced viral RNAs in genotypes A, B, C and D, and reported notable differences between the genotypes (Lim et al., 2021). In order to perform these studies Lim and colleagues delivered overlength HBV genomes by lipid transfection into Huh7 cells. Our data presented and discussed in (**Figures 4.5** and **Figure 4.6**) demonstrate the importance of controlling for transfection efficiency to discern between assay

variability and genotype specific phenotypes. These data highlight the need for optimisation of cell culture models for *de novo* delivery of HBV to improve our understanding of virus-host interactions. It is without doubt that plasmid transfection provides a convenient tool, however there are important differences between the transfection and infection model systems. Overcoming these technical challenges will facilitate the establishment of reliable, robust and physiologically relevant models for studying diverse genotypes of HBV. However, we attempted to rationalise our use of the HBV1.3 constructs by comparing transcript patterns to a *de novo* infection and noticed plasmid transfections show a different pattern of viral RNAs (**Figure 4.6**). This could be reflective of differential promoter usage between models, total HBV DNA burden, or time dependent differences in transcription (D'Arienzo et al., 2021b; Doitsh and Shaul, 2004). These data suggest that whilst plasmid transfections are convenient and deliver a high level of DNA into the cell, there are model specific phenotypes that need to be considered.

We and others have reported a dual role for SAMHD1 in regulating HBV replication by acting as a restriction factor inhibiting the RT-dependent conversion of pgRNA to rcDNA, as well as promoting cccDNA genesis (Sommer et al., 2016; Wing et al., 2019). Our data suggest that through perturbation of host cell cycle, KDM4 inhibition modulates SAMHD1 phosphorylation status (**Figure 5.5**). Our previous study identified that SAMHD1 knockout significantly reduced cccDNA levels, and further identified that pSAMHD1 was the form regulating rcDNA repair (Wing et al., 2019). Whilst studies from Wei and Ploss did not identify SAMHD1 as an essential cccDNA repair factor, it is likely that additional host factors have roles in the maintenance of the cccDNA reservoir (Wei and Ploss, 2020; 2021a; b).

Despite the reduction in pSAMHD1 in response to KDM4 inhibition, we have data to suggest that treatment before infection does not abrogate cellular susceptibility to HBV. Additionally our RNA-seq analysis revealed that KDM4 inhibition does not alter the expression of the essential cccDNA repair factors (Hu et al., 2019; Wei and Ploss, 2020; 2021a; b), furthermore we demonstrated that in response to KDM4 inhibition there was no variation in cccDNA levels over time (**Figure 5.4**). However, given the effect of treatment on the SAMHD1:pSAMHD1 ratio, it would be interesting to explore the effect of QC6352 or hypoxia on the intracellular recycling pathway, and whether oxygen sensitive factors could affect capsid re-import or intracellular dNTP pools.

We demonstrate that we can discriminate between episomal or integrant derived transcripts and this simple qPCR approach can be applied to material derived from liver biopsy samples (**Figure 3.6**). Our PCR method is both cheap and readily accessible to most molecular virology laboratories, making it attractive over sequencing based approaches. It is important to note that measuring viral RNAs by qPCR also has limitations for example it is not as sensitive as sequencing methods, nor is it possible to discern between pC and pgRNAs. Additionally, variation in primer design and amplification efficiency can result in intra-assay variability. However, using this technique we identified a relationship between age and the transcriptional activity of the HBV integrants. It is important to remember that we did not detect integration events, but assessed their relative transcriptional activity. We also demonstrated that in CHB, it is possible to have active transcription and ongoing activity from both cccDNA and integrants, highlighting the chimerism of the diseased liver. This also prompted us to raise the question: what factors determine specific-cell tropism and permissivity *in vivo?*

Future experiments could investigate whether a cell is capable of supporting replication from both cccDNA and integrated genomes, or does the ‘replicative dead end’ of integration makes a cell refractory to incoming rcDNA, and can cccDNA repair occur in these cells?

To summarise, we suggest the following model (**Figure 6.1**). In the hypoxic environment of the diseased liver, HIF signalling is active and KDM4 is inhibited. We show evidence that when HIF is stable, it can bind HBV cccDNA and potentiate the transcription of pC/pgRNAs, which results in increased viral particle release. We also suggest that KDM4 is inhibited in low oxygen, and this results in perturbation of host cell gene expression that generates a pro-viral environment for HBV. We observe a potent increase in the abundance of pC/pgRNAs, but a more modest increase in particle release, which we attribute to the phosphorylation status of SAMHD1. Whilst HIF signalling has little impact on the output of the HBV iDNA, we show that KDM4 regulates the transcriptional activity of the integrants. We cannot comment on the zonation or cellular location of these pathways however we would suggest that both are occurring, perhaps simultaneously, in the context of the liver rather than in the same cell. On an organ level, hypoxia signalling is active and can regulate many pathways and processes that are essential for the virus, such as metabolism, cell cycle, immune signalling and RNA modification.

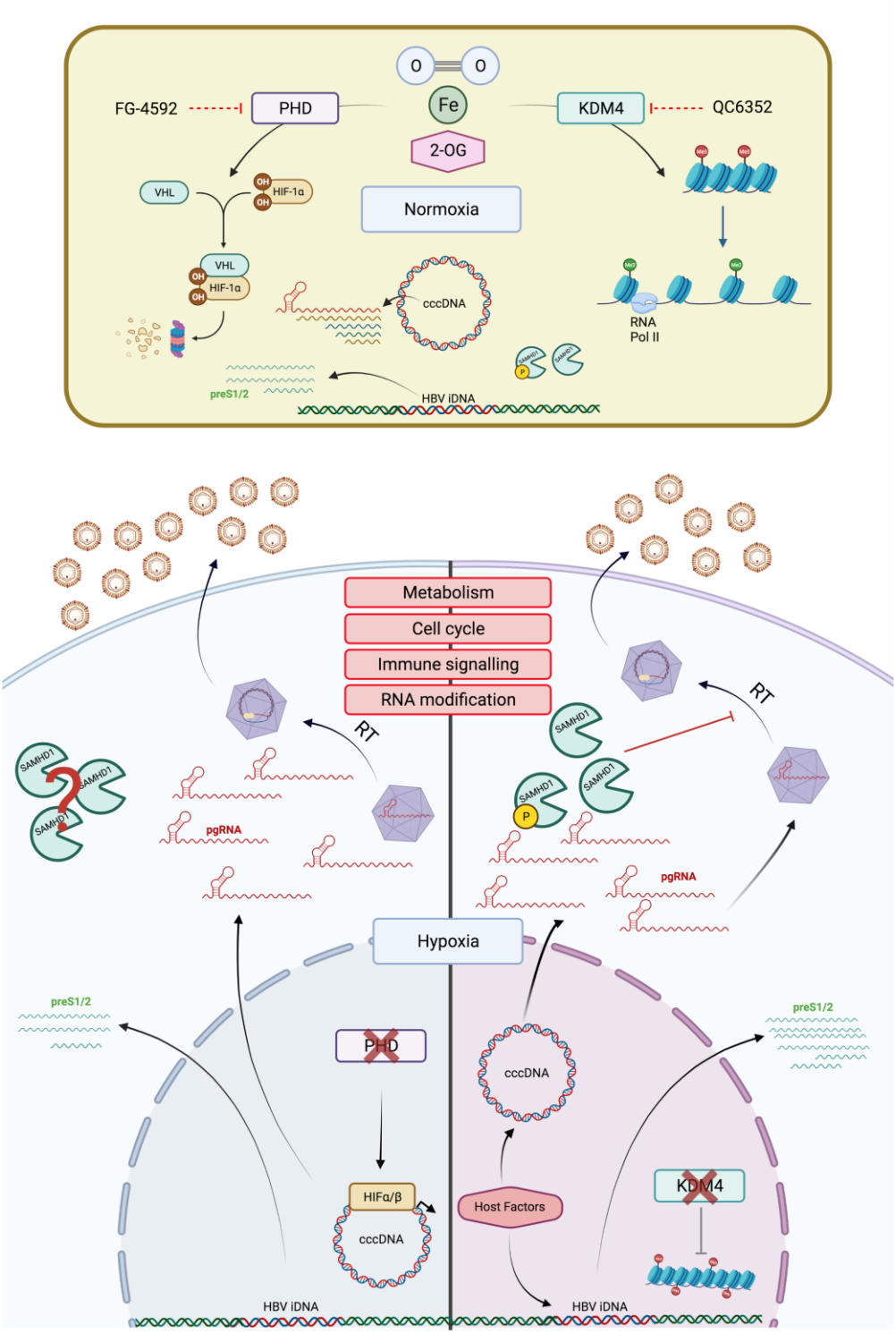


Figure 6.1: Suggested model

A cartoon to show the suggested model of the interplay between hypoxic signalling and hepatitis B virus replication. Figure made in BioRender.

In conclusion, this work demonstrates the importance of considering local oxygen tension in the context of HBV infection. As such, it may serve as an experimental paradigm for the study of other viruses, which may be activated or inhibited by aspects of the low oxygen signalling cascade in the tissues of interest. We highlight the importance of studying hypoxia, and the differential impact of HIF stabilisation and 2-OGDD inhibition on host cell processes and viral replication. Future work could aim to understand the hypoxic regulation of other stages in the HBV life cycle, and how oxygen sensitive host factors may be directly regulating the epigenetic landscape of cccDNA. Understanding viral-host interactions in physiologically relevant conditions *in vitro* will allow the future design of curative treatments and therapeutic agents to transcriptionally silence or eradicate cccDNA.

Chapter 7: Publications

Wing, PAC., Davenne, T., Wettengel, J., Lai, AG., Zhuang, X., Chakraborty, A., D'Arienzo, V., Kramer, C., Ko, C., Harris, JM., Schreiner, S., Higgs, M., Roessler, S., Parish, JL., McKeating, JA. 2019. A dual role for SAMHD1 in regulating HBV cccDNA and RT-dependent particle genesis. Life Science Alliance, 2 (2). PMID: 30918010

Liu, Y., Cheng, J., Siejka-Zielinska, P., Weldon, C., Roberts, H., Lopopolo, M., Magri, A., D'Arienzo, V., Harris, JM., McKeating, JA., Song, C. 2020. Accurate targeted long-read DNA methylation and hydroxymethylation sequencing with TAPS. Genome Biology. 21 (54). PMID: 32127008

Chakraborty, A., Ko, C., Henning, C., Lucko, A., Harris, JM., Chen, F., Zhuang, X., Wettengel, J., Roessler, S., Protzer, U., McKeating, JA. 2020. Synchronized infection identifies early rate-limiting steps in the hepatitis B virus life cycle. Cellular Microbiology. PMID: 32799415.

Liu, PJ.*, Harris, JM.*, Marchi, E., D'Arienzo, V., Michler, T., Wing, PAC., Magri, A., Ortega-Prieto, AM., van de Kulndert, M., Wettengel, J., Durantel, D., Dorner, M., Klenerman, P., Protzer, U., Giotis, ES., McKeating, JA. 2020. Hypoxic gene expression in chronic hepatitis B virus infected patients is not observed in state-of-the-art in vitro and mouse infection models. Scientific Reports. PMID: 33144758

D'Arienzo, V.*, Ferguson, J.*, Giraud, G., Chapus, F., Harris, JM., Wing, PAC., Claydon, A., Begum, S., Zhuang, X., Balfe, P., Testoni, B., McKeating, JA. ‡, Parish, JL. ‡ 2021. The CCCTC-binding factor CTCF represses hepatitis B virus Enhancer I and regulates viral transcription. Cellular Microbiology. PMID: 33006186

D'Arienzo, V., Magri, A., Harris, JM., Wing, PAC., Ko, C., Orbegozo-Rubio, C., Revill, PA., Protzer, U., Balfe, P and McKeating, JA. 2021. A PCR assay to quantify patterns of HBV transcription. Journal of General Virology. PMID: 31846416

Wing, PAC.*, Liu, PJ.*, Harris, JM.*, Magri, A., Michler, T., Zhuang, X., Borrmann, H., Minisini, R., Frampton, NR., Wettengel, JM., Mailly, L., D'Arienzo, V., Riedl, T., Nobre, L., Weekes, MP., Pirisi, M., Heikenwalder, M., Baumert, T., Hammond, EM., Mole, DR., Protzer, U., Balfe, P., McKeating, JA. 2021. Hypoxia inducible

factors regulate hepatitis B virus replication by activating the basal core promoter. Journal of Hepatology. PMID: 33516779.

Zhuang, X.*‡, Forde, D.*, Tsukuda, S., D'Arienzo, V., Mailly, L., Harris, JM., Wing, PAC., Borrmann, H., Schilling, M., Magri, A., Orbegozo-Rubio, C., Maidstone, RJ., Iqbal, M., Garzon, M., Minisini, R., Pirisi, M., Butterworth, S., Balfe, P., Ray, DW., Watashi, K., Baumert, TF., McKeating, JA‡. 2021. Circadian control of hepatitis B virus replication. Nature Communications. PMID: 33712578

Schmidt, NM., Wing, PAC., Diniz, MO., Pallett, LJ., Swadling, L., Harris, JM., Burton, AR., Jeffery-Smith, A., Zakeri, N., Amin, OE., Kucykowicz, S., Heemskerk, MH., Davidson, B., Meyer, T., Grove, J., Stauss, HJ., Pineda-Torra, I., Jolly, C., Jury, EC., McKeating, JA., Maini, MK. 2021. Targeting human Acyl-CoA: cholesterol acyltransferase as a dual viral and T-cell metabolic checkpoint. Nature Communications. PMID: 33990561

Zhuang, X.*, Tsukuda, S.*, Wrensch, F., Wing, PAC., Schilling, M., Harris, JM., Borrmann, H., Morgan, SB., Cane, JL., Mailly, L., Thakur, N., Conceicao, C., Sanghani, H., Heydmann, L., Bach, C., Ashton, A., Walsh, S., Tan, TK., Schimanski, L., Huang, K-YA., Schuster, C., Watashi, K., Hinks, TSC., Jagannath, A., Vausdevan, S., Bailey, D., Baumert, TF., McKeating, JA. 2021. The circadian clock component BMAL1 regulates SARS-CoV-2 entry and replication in lung epithelial cells. iScience. PMID: 34545347

Harris, JM., Magri, A., Balfe, P., Wing, PAC*., McKeating JA*. Intrinsic restriction of hepatitis B replication by the oxygen-dependent histone lysine demethylase 4. *Manuscript in preparation.*

Wing, PAC., Prange-Barczynska, M., Cross, A., Crotta, S., Orbegozo-Rubio, C., Cheng, X., Harris, JM., Zhuang, X., Johnson, RL., Ryan, KA., Hall, Y., Carroll, M., Issa, F., Balfe, P., Wack, A., Bishop., Salguero, FJ., McKeating, JA. Hypoxia inducible factors regulate infectious SARS-CoV-2, epithelial damage, and respiratory symptoms in a hamster COVID-19 model. *Manuscript in preparation.*

Magri, A., Harris, JM., D'Arienzo, V., Minisini, R., Jühling, F., Wing, PAC., Rapetti, R., Leutner, M., Testoni, B., Baumert, TF., Zoulim, F., Balfe, P., Pirisi, M., McKeating, JA. Identification of an inflammatory gene signature that associates with hepatitis B virus transcription. *Manuscript in preparation.*

Magri, A., Hill, M., Harris, JM., Rudge, S., Lopez, A., Probert, F., Wakelam, M., Zitzmann, N., McKeating JA. A hypoxic environment restricts HCV and related flavivirus replication and spread. *Manuscript in preparation.*

Barbaglia, MN., Harris, JM., Smirnov, A., Burlone, ME., Rigamonti, C., McKeating, JA., Pirisi, M., Minisini, R., Magri, A. 17β-Oestradiol protects from hepatitis C virus infection through induction of type I interferon. *Manuscript in preparation.*

Tsukuda, S., Wilson, TS., Lee, JY., Robertson, F., Harris, JM., Wing, PAC., Kim, GW., Siddiqui, A., Davis, I., McKeating, JA. A role for ALKBH5 in hypoxia-dependent potentiation of HBV transcription. *Manuscript in preparation.*

* and ‡ indicate equal contribution

Chapter 8: Bibliography

Abdel-Hady, M., and Kelly, D. (2013). Chronic hepatitis B in children and adolescents: epidemiology and management. Paediatr Drugs *15*, 311-317. 10.1007/s40272-013-0010-z.

Abdollahi, H., Harris, L.J., Zhang, P., McIlhenny, S., Srinivas, V., Tulenko, T., and DiMuzio, P.J. (2011). The role of hypoxia in stem cell differentiation and therapeutics. J Surg Res *165*, 112-117. 10.1016/j.jss.2009.09.057.

Adeva-Andany, M.M., Gonzalez-Lucan, M., Donapetry-Garcia, C., Fernandez-Fernandez, C., and Ameneiros-Rodriguez, E. (2016). Glycogen metabolism in humans. BBA Clin *5*, 85-100. 10.1016/j.bbacli.2016.02.001.

Aggarwal, B.B. (2004). Nuclear factor-kappaB: the enemy within. Cancer Cell *6*, 203-208. 10.1016/j.ccr.2004.09.003.

Aizarani, N., Saviano, A., Sagar, Mailly, L., Durand, S., Herman, J.S., Pessaux, P., Baumert, T.F., and Grun, D. (2019). A human liver cell atlas reveals heterogeneity and epithelial progenitors. Nature *572*, 199-204. 10.1038/s41586-019-1373-2.

Akashi, M., and Takumi, T. (2005). The orphan nuclear receptor RORalpha regulates circadian transcription of the mammalian core-clock Bmal1. Nat Struct Mol Biol *12*, 441-448. 10.1038/nsmb925.

Al-Anazi, M.R., Nazir, N., Colak, D., Al-Ahdal, M.N., and Al-Qahtani, A.A. (2018). Deletion and Functional Analysis of Hepatitis B Virus X Protein: Evidence for an Effect on Cell Cycle Regulators. Cell Physiol Biochem *49*, 1987-1998. 10.1159/000493670.

Alharbi, A.B., Schmitz, U., Bailey, C.G., and Rasko, J.E.J. (2021). CTCF as a regulator of alternative splicing: new tricks for an old player. Nucleic Acids Res *49*, 7825-7838. 10.1093/nar/gkab520.

Alkan, C., Sajjadian, S., and Eichler, E.E. (2011). Limitations of next-generation genome sequence assembly. Nat Methods *8*, 61-65. 10.1038/nmeth.1527.

Allis, C.D., and Jenuwein, T. (2016). The molecular hallmarks of epigenetic control. Nat Rev Genet *17*, 487-500. 10.1038/nrg.2016.59.

Allweiss, L., and Dandri, M. (2016). Experimental in vitro and in vivo models for the study of human hepatitis B virus infection. J Hepatol *64*, S17-S31. 10.1016/j.jhep.2016.02.012.

Allweiss, L., and Dandri, M. (2017). The Role of cccDNA in HBV Maintenance. Viruses *9*. 10.3390/v9060156.

Alter, M.J. (2003). Epidemiology of hepatitis B in Europe and worldwide. J Hepatol *39 Suppl 1*, S64-69. 10.1016/s0168-8278(03)00141-7.

Altinel, K., Hashimoto, K., Wei, Y., Neuveut, C., Gupta, I., Suzuki, A.M., Dos Santos, A., Moreau, P., Xia, T., Kojima, S., et al. (2016). Single-Nucleotide Resolution Mapping of Hepatitis B Virus Promoters in Infected Human Livers and Hepatocellular Carcinoma. J Virol *90*, 10811-10822. 10.1128/JVI.01625-16.

Antherieu, S., Chesne, C., Li, R., Camus, S., Lahoz, A., Picazo, L., Turpeinen, M., Tolonen, A., Uusitalo, J., Guguen-Guillouzo, C., and Guillouzo, A. (2010). Stable expression, activity, and inducibility of cytochromes P450 in differentiated HepaRG cells. Drug Metab Dispos *38*, 516-525. 10.1124/dmd.109.030197.

Anthony, P.P. (2001). Hepatocellular carcinoma: an overview. Histopathology *39*, 109-118. 10.1046/j.1365-2559.2001.01188.x.

Antunović, J., Lemieux, N., and Cromlish, J.A. (1993). The 17 kDa HBx protein encoded by hepatitis B virus interacts with the activation domains of Oct-1, and functions as a coactivator in the activation and repression of a human U6 promoter. Cell Mol Biol Res *39*, 463-482.

Arany, Z., Huang, L.E., Eckner, R., Bhattacharya, S., Jiang, C., Goldberg, M.A., Bunn, H.F., and Livingston, D.M. (1996). An essential role for p300/CBP in the cellular response to hypoxia. Proc Natl Acad Sci U S A *93*, 12969-12973. 10.1073/pnas.93.23.12969.

Araujo, N.M., Waizbort, R., and Kay, A. (2011). Hepatitis B virus infection from an evolutionary point of view: how viral, host, and environmental factors shape genotypes and subgenotypes. Infect Genet Evol *11*, 1199-1207. 10.1016/j.meegid.2011.04.017.

Arnold, P.R., Wells, A.D., and Li, X.C. (2019). Diversity and Emerging Roles of Enhancer RNA in Regulation of Gene Expression and Cell Fate. Front Cell Dev Biol *7*, 377. 10.3389/fcell.2019.00377.

Arzumanyan, A., Friedman, T., Ng, I.O., Clayton, M.M., Lian, Z., and Feitelson, M.A. (2011). Does the hepatitis B antigen HBx promote the appearance of liver cancer stem cells? Cancer Res *71*, 3701-3708. 10.1158/0008-5472.CAN-10-3951.

Ashburner, M., Ball, C.A., Blake, J.A., Botstein, D., Butler, H., Cherry, J.M., Davis, A.P., Dolinski, K., Dwight, S.S., Eppig, J.T., et al. (2000). Gene ontology: tool for the unification of biology. The Gene Ontology Consortium. Nat Genet *25*, 25-29. 10.1038/75556.

Audette, D.S., Anand, D., So, T., Rubenstein, T.B., Lachke, S.A., Lovicu, F.J., and Duncan, M.K. (2016). Prox1 and fibroblast growth factor receptors form a novel

regulatory loop controlling lens fiber differentiation and gene expression. Development *143*, 318-328. 10.1242/dev.127860.

Babeu, J.P., and Boudreau, F. (2014). Hepatocyte nuclear factor 4-alpha involvement in liver and intestinal inflammatory networks. World J Gastroenterol *20*, 22-30. 10.3748/wjg.v20.i1.22.

Bancroft, W.H., Snitbhan, R., Scott, R.M., Tingpalapong, M., Watson, W.T., Tanticharoenyos, P., Karwacki, J.J., and Srimarut, S. (1977). Transmission of hepatitis B virus to gibbons by exposure to human saliva containing hepatitis B surface antigen. J Infect Dis *135*, 79-85. 10.1093/infdis/135.1.79.

Bao, Y., Vinciotti, V., Wit, E., and t Hoen, P.A. (2013). Accounting for immunoprecipitation efficiencies in the statistical analysis of ChIP-seq data. BMC Bioinformatics *14*, 169. 10.1186/1471-2105-14-169.

Bar-Yishay, I., Shaul, Y., and Shlomai, A. (2011). Hepatocyte metabolic signalling pathways and regulation of hepatitis B virus expression. Liver Int *31*, 282-290. 10.1111/j.1478-3231.2010.02423.x.

Barrera, A., Guerra, B., Notvall, L., and Lanford, R.E. (2005). Mapping of the hepatitis B virus pre-S1 domain involved in receptor recognition. J Virol *79*, 9786-9798. 10.1128/JVI.79.15.9786-9798.2005.

Barski, A., Cuddapah, S., Cui, K., Roh, T.Y., Schones, D.E., Wang, Z., Wei, G., Chepelev, I., and Zhao, K. (2007). High-resolution profiling of histone methylations in the human genome. Cell *129*, 823-837. 10.1016/j.cell.2007.05.009.

Bartenschlager, R., and Schaller, H. (1992). Hepadnaviral assembly is initiated by polymerase binding to the encapsidation signal in the viral RNA genome. EMBO J *11*, 3413-3420.

Bartoszewski, R., Moszynska, A., Serocki, M., Cabaj, A., Polten, A., Ochocka, R., Dell'Italia, L., Bartoszewska, S., Kroliczewski, J., Dabrowski, M., and Collawn, J.F. (2019). Primary endothelial cell-specific regulation of hypoxia-inducible factor (HIF)-1 and HIF-2 and their target gene expression profiles during hypoxia. FASEB J *33*, 7929-7941. 10.1096/fj.201802650RR.

Batie, M., Del Peso, L., and Rocha, S. (2018). Hypoxia and Chromatin: A Focus on Transcriptional Repression Mechanisms. Biomedicines *6*. 10.3390/biomedicines6020047.

Batie, M., Frost, J., Frost, M., Wilson, J.W., Schofield, P., and Rocha, S. (2019). Hypoxia induces rapid changes to histone methylation and reprograms chromatin. Science *363*, 1222-1226. 10.1126/science.aau5870.

Batie, M., and Rocha, S. (2020). Gene transcription and chromatin regulation in hypoxia. Biochem Soc Trans *48*, 1121-1128. 10.1042/BST20191106.

Bayliss, J., Lim, L., Thompson, A.J., Desmond, P., Angus, P., Locarnini, S., and Revill, P.A. (2013). Hepatitis B virus splicing is enhanced prior to development of hepatocellular carcinoma. J Hepatol *59*, 1022-1028. 10.1016/j.jhep.2013.06.018.

Beisel, C., and Paro, R. (2011). Silencing chromatin: comparing modes and mechanisms. Nat Rev Genet *12*, 123-135. 10.1038/nrg2932.

Belloni, L., Allweiss, L., Guerrieri, F., Pediconi, N., Volz, T., Pollicino, T., Petersen, J., Raimondo, G., Dandri, M., and Levrero, M. (2012). IFN-alpha inhibits HBV transcription and replication in cell culture and in humanized mice by targeting the epigenetic regulation of the nuclear cccDNA minichromosome. J Clin Invest *122*, 529-537. 10.1172/JCI58847.

Belongia, E.A., Costa, J., Gareen, I.F., Grem, J.L., Inadomi, J.M., Kern, E.R., McHugh, J.A., Petersen, G.M., Rein, M.F., Sorrell, M.F., et al. (2008). NIH consensus development statement on management of hepatitis B. NIH Consens State Sci Statements *25*, 1-29.

Benabdallah, N.S., Williamson, I., Illingworth, R.S., Kane, L., Boyle, S., Sengupta, D., Grimes, G.R., Therizols, P., and Bickmore, W.A. (2019). Decreased Enhancer-Promoter Proximity Accompanying Enhancer Activation. Mol Cell *76*, 473-484 e477. 10.1016/j.molcel.2019.07.038.

Benatti, P., Dolfini, D., Vigano, A., Ravo, M., Weisz, A., and Imbriano, C. (2011). Specific inhibition of NF-Y subunits triggers different cell proliferation defects. Nucleic Acids Res *39*, 5356-5368. 10.1093/nar/gkr128.

Benveniste, D., Sonntag, H.J., Sanguinetti, G., and Sproul, D. (2014). Transcription factor binding predicts histone modifications in human cell lines. Proc Natl Acad Sci U S A *111*, 13367-13372. 10.1073/pnas.1412081111.

Berg, R.A., and Prockop, D.J. (1973). The thermal transition of a non-hydroxylated form of collagen. Evidence for a role for hydroxyproline in stabilizing the triple-helix of collagen. Biochem Biophys Res Commun *52*, 115-120. 10.1016/0006-291x(73)90961-3.

Bertoletti, A., and Ferrari, C. (2003). Kinetics of the immune response during HBV and HCV infection. Hepatology *38*, 4-13. 10.1053/jhep.2003.50310.

Bertoletti, A., and Ferrari, C. (2012). Innate and adaptive immune responses in chronic hepatitis B virus infections: towards restoration of immune control of viral infection. Gut *61*, 1754-1764. 10.1136/gutjnl-2011-301073.

Bertoletti, A., Maini, M.K., and Ferrari, C. (2010). The host-pathogen interaction during HBV infection: immunological controversies. Antivir Ther *15 Suppl 3*, 15-24. 10.3851/IMP1620.

Bertolino, P., Trescol-Biemont, M.C., and Rabourdin-Combe, C. (1998). Hepatocytes induce functional activation of naive CD8+ T lymphocytes but fail to promote survival. Eur J Immunol *28*, 221-236. 10.1002/(SICI)1521-4141(199801)28:01<221::AID-IMMU221>3.0.CO;2-F.

Bhoumik, A., Takahashi, S., Breitweiser, W., Shiloh, Y., Jones, N., and Ronai, Z. (2005). ATM-dependent phosphorylation of ATF2 is required for the DNA damage response. Mol Cell *18*, 577-587. 10.1016/j.molcel.2005.04.015.

Bilzer, M., Roggel, F., and Gerbes, A.L. (2006). Role of Kupffer cells in host defense and liver disease. Liver Int *26*, 1175-1186. 10.1111/j.1478-3231.2006.01342.x.

Bissig, K.D., Wieland, S.F., Tran, P., Isogawa, M., Le, T.T., Chisari, F.V., and Verma, I.M. (2010). Human liver chimeric mice provide a model for hepatitis B and C virus infection and treatment. J Clin Invest *120*, 924-930. 10.1172/JCI40094.

Black, J.C., Allen, A., Van Rechem, C., Forbes, E., Longworth, M., Tschop, K., Rinehart, C., Quiton, J., Walsh, R., Smallwood, A., et al. (2010). Conserved antagonism between JMJD2A/KDM4A and HP1gamma during cell cycle progression. Mol Cell *40*, 736-748. 10.1016/j.molcel.2010.11.008.

Block, T.M., Mehta, A.S., Fimmel, C.J., and Jordan, R. (2003). Molecular viral oncology of hepatocellular carcinoma. Oncogene *22*, 5093-5107. 10.1038/sj.onc.1206557.

Blum, H.E., and Moradpour, D. (2002). Viral pathogenesis of hepatocellular carcinoma. J Gastroenterol Hepatol *17 Suppl 3*, S413-420. 10.1046/j.1440-1746.17.s3.37.x.

Blumberg, B.S. (1977). Australia antigen and the biology of hepatitis B. Science *197*, 17-25. 10.1126/science.325649.

Bock, C.T., Kubicka, S., Manns, M.P., and Trautwein, C. (1999). Two control elements in the hepatitis B virus S-promoter are important for full promoter activity mediated by CCAAT-binding factor. Hepatology *29*, 1236-1247. 10.1002/hep.510290426.

Bock, C.T., Schranz, P., Schroder, C.H., and Zentgraf, H. (1994). Hepatitis B virus genome is organized into nucleosomes in the nucleus of the infected cell. Virus Genes *8*, 215-229. 10.1007/BF01703079.

Bock, C.T., Schwinn, S., Locarnini, S., Fyfe, J., Manns, M.P., Trautwein, C., and Zentgraf, H. (2001). Structural organization of the hepatitis B virus minichromosome. J Mol Biol *307*, 183-196. 10.1006/jmbi.2000.4481.

Boettler, T., Panther, E., Bengsch, B., Nazarova, N., Spangenberg, H.C., Blum, H.E., and Thimme, R. (2006). Expression of the interleukin-7 receptor alpha chain (CD127) on virus-specific CD8+ T cells identifies functionally and phenotypically defined memory T cells during acute resolving hepatitis B virus infection. J Virol *80*, 3532-3540. 10.1128/JVI.80.7.3532-3540.2006.

Bogomolski-Yahalom, V., Klein, A., Greenblat, I., Haviv, Y., and Tur-Kaspa, R. (1997). The TATA-less promoter of hepatitis B virus S gene contains a TBP binding site and an active initiator. Virus Res *49*, 1-7. 10.1016/s0168-1702(96)01429-3.

Boni, C., Fisicaro, P., Valdatta, C., Amadei, B., Di Vincenzo, P., Giuberti, T., Laccabue, D., Zerbini, A., Cavalli, A., Missale, G., et al. (2007). Characterization of hepatitis B virus (HBV)-specific T-cell dysfunction in chronic HBV infection. J Virol *81*, 4215-4225. 10.1128/JVI.02844-06.

Bowen, D.G., Zen, M., Holz, L., Davis, T., McCaughan, G.W., and Bertolino, P. (2004). The site of primary T cell activation is a determinant of the balance between intrahepatic tolerance and immunity. J Clin Invest *114*, 701-712. 10.1172/JCI21593.

Bray, F., Ferlay, J., Soerjomataram, I., Siegel, R.L., Torre, L.A., and Jemal, A. (2018). Global cancer statistics 2018: GLOBOCAN estimates of incidence and mortality worldwide for 36 cancers in 185 countries. CA Cancer J Clin *68*, 394-424. 10.3322/caac.21492.

Brechot, C., Pourcel, C., Louise, A., Rain, B., and Tiollais, P. (1980). Presence of integrated hepatitis B virus DNA sequences in cellular DNA of human hepatocellular carcinoma. Nature *286*, 533-535. 10.1038/286533a0.

Bruss, V. (1997). A short linear sequence in the pre-S domain of the large hepatitis B virus envelope protein required for virion formation. J Virol *71*, 9350-9357. 10.1128/JVI.71.12.9350-9357.1997.

Buckwold, V.E., Chen, M., and Ou, J.H. (1997). Interaction of transcription factors RFX1 and MIBP1 with the gamma motif of the negative regulatory element of the hepatitis B virus core promoter. Virology *227*, 515-518. 10.1006/viro.1996.8360.

Budker, V., Zhang, G., Knechtle, S., and Wolff, J.A. (1996). Naked DNA delivered intraportally expresses efficiently in hepatocytes. Gene Ther *3*, 593-598.

Buffa, F.M., Harris, A.L., West, C.M., and Miller, C.J. (2010). Large meta-analysis of multiple cancers reveals a common, compact and highly prognostic hypoxia metagene. Br J Cancer *102*, 428-435. 10.1038/sj.bjc.6605450.

Bultman, S., Gebuhr, T., Yee, D., La Mantia, C., Nicholson, J., Gilliam, A., Randazzo, F., Metzger, D., Chambon, P., Crabtree, G., and Magnuson, T. (2000). A Brg1 null mutation in the mouse reveals functional differences among mammalian SWI/SNF complexes. Mol Cell *6*, 1287-1295. 10.1016/s1097-2765(00)00127-1.

Butler, A.J., and Parker, M.G. (1995). COUP-TF II homodimers are formed in preference to heterodimers with RXR alpha or TR beta in intact cells. Nucleic Acids Res *23*, 4143-4150. 10.1093/nar/23.20.4143.

Cai, D., Mills, C., Yu, W., Yan, R., Aldrich, C.E., Saputelli, J.R., Mason, W.S., Xu, X., Guo, J.T., Block, T.M., et al. (2012). Identification of disubstituted sulfonamide compounds as specific inhibitors of hepatitis B virus covalently closed circular DNA formation. Antimicrob Agents Chemother *56*, 4277-4288. 10.1128/AAC.00473-12.

Cai, Y.N., Zhou, Q., Kong, Y.Y., Li, M., Viollet, B., Xie, Y.H., and Wang, Y. (2003). LRH-1/hB1F and HNF1 synergistically up-regulate hepatitis B virus gene transcription and DNA replication. Cell Res *13*, 451-458. 10.1038/sj.cr.7290187.

Caimi, G., Lo Presti, R., Montana, M., Contorno, A., Canino, B., Catania, A., Sarno, A., and Cerasola, G. (1995). Platelet membrane fluidity and platelet membrane lipid pattern in essential hypertension. Am J Hypertens *8*, 82-86. 10.1016/0895-7061(94)00183-C.

Calvisi, D.F., Ladu, S., Gorden, A., Farina, M., Lee, J.S., Conner, E.A., Schroeder, I., Factor, V.M., and Thorgeirsson, S.S. (2007). Mechanistic and prognostic significance of aberrant methylation in the molecular pathogenesis of human hepatocellular carcinoma. J Clin Invest *117*, 2713-2722. 10.1172/JCI31457.

Candotti, D., Lin, C.K., Belkhiri, D., Sakuldamrongpanich, T., Biswas, S., Lin, S., Teo, D., Ayob, Y., and Allain, J.P. (2012). Occult hepatitis B infection in blood donors from South East Asia: molecular characterisation and potential mechanisms of occurrence. Gut *61*, 1744-1753. 10.1136/gutjnl-2011-301281.

Carreau, A., El Hafny-Rahbi, B., Matejuk, A., Grillon, C., and Kieda, C. (2011). Why is the partial oxygen pressure of human tissues a crucial parameter? Small molecules and hypoxia. J Cell Mol Med *15*, 1239-1253. 10.1111/j.1582-4934.2011.01258.x.

Cento, V., Mirabelli, C., Dimonte, S., Salpini, R., Han, Y., Trimoulet, P., Bertoli, A., Micheli, V., Gubertini, G., Cappiello, G., et al. (2013). Overlapping structure of

hepatitis B virus (HBV) genome and immune selection pressure are critical forces modulating HBV evolution. J Gen Virol *94*, 143-149. 10.1099/vir.0.046524-0.

Chakraborty, A., Ko, C., Henning, C., Lucko, A., Harris, J.M., Chen, F., Zhuang, X., Wettengel, J.M., Roessler, S., Protzer, U., and McKeating, J.A. (2020). Synchronised infection identifies early rate-limiting steps in the hepatitis B virus life cycle. Cell Microbiol *22*, e13250. 10.1111/cmi.13250.

Chakraborty, A.A., Laukka, T., Myllykoski, M., Ringel, A.E., Booker, M.A., Tolstorukov, M.Y., Meng, Y.J., Meier, S.R., Jennings, R.B., Creech, A.L., et al. (2019). Histone demethylase KDM6A directly senses oxygen to control chromatin and cell fate. Science *363*, 1217-1222. 10.1126/science.aaw1026.

Chan, C., Thurnherr, T., Wang, J., Gallart-Palau, X., Sze, S.K., Rozen, S., and Lee, C.G. (2016). Global re-wiring of p53 transcription regulation by the hepatitis B virus X protein. Mol Oncol *10*, 1183-1195. 10.1016/j.molonc.2016.05.006.

Chandra, V., Huang, P., Hamuro, Y., Raghuram, S., Wang, Y., Burris, T.P., and Rastinejad, F. (2008). Structure of the intact PPAR-gamma-RXR- nuclear receptor complex on DNA. Nature *456*, 350-356. 10.1038/nature07413.

Chang, M.H., Chen, C.J., Lai, M.S., Hsu, H.M., Wu, T.C., Kong, M.S., Liang, D.C., Shau, W.Y., and Chen, D.S. (1997). Universal hepatitis B vaccination in Taiwan and the incidence of hepatocellular carcinoma in children. Taiwan Childhood Hepatoma Study Group. N Engl J Med *336*, 1855-1859. 10.1056/NEJM199706263362602.

Chang, M.H., You, S.L., Chen, C.J., Liu, C.J., Lee, C.M., Lin, S.M., Chu, H.C., Wu, T.C., Yang, S.S., Kuo, H.S., et al. (2009). Decreased incidence of hepatocellular carcinoma in hepatitis B vaccinees: a 20-year follow-up study. J Natl Cancer Inst *101*, 1348-1355. 10.1093/jnci/djp288.

Chang, M.L., and Liaw, Y.F. (2014). Hepatitis B flares in chronic hepatitis B: pathogenesis, natural course, and management. J Hepatol *61*, 1407-1417. 10.1016/j.jhep.2014.08.033.

Chantalat, S., Depaux, A., Hery, P., Barral, S., Thuret, J.Y., Dimitrov, S., and Gerard, M. (2011). Histone H3 trimethylation at lysine 36 is associated with constitutive and facultative heterochromatin. Genome Res *21*, 1426-1437. 10.1101/gr.118091.110.

Chen, B., Liu, H., Sun, X., and Yang, C.G. (2010). Mechanistic insight into the recognition of single-stranded and double-stranded DNA substrates by ABH2 and ABH3. Mol Biosyst *6*, 2143-2149. 10.1039/c005148a.

Chen, C., and Lou, T. (2017). Hypoxia inducible factors in hepatocellular carcinoma. Oncotarget *8*, 46691-46703. 10.18632/oncotarget.17358.

Chen, J., Wu, M., Wang, F., Zhang, W., Wang, W., Zhang, X., Zhang, J., Liu, Y., Liu, Y., Feng, Y., et al. (2015). Hepatitis B virus spliced variants are associated with an impaired response to interferon therapy. Sci Rep *5*, 16459. 10.1038/srep16459.

Chen, L., Vasoya, R.P., Toke, N.H., Parthasarathy, A., Luo, S., Chiles, E., Flores, J., Gao, N., Bonder, E.M., Su, X., and Verzi, M.P. (2020). HNF4 Regulates Fatty Acid Oxidation and Is Required for Renewal of Intestinal Stem Cells in Mice. Gastroenterology *158*, 985-999 e989. 10.1053/j.gastro.2019.11.031.

Chen, M., Hieng, S., Qian, X., Costa, R., and Ou, J.H. (1994). Regulation of hepatitis B virus ENI enhancer activity by hepatocyte-enriched transcription factor HNF3. Virology *205*, 127-132. 10.1006/viro.1994.1627.

Chen, M., Sallberg, M., Hughes, J., Jones, J., Guidotti, L.G., Chisari, F.V., Billaud, J.N., and Milich, D.R. (2005). Immune tolerance split between hepatitis B virus precore and core proteins. J Virol *79*, 3016-3027. 10.1128/JVI.79.5.3016-3027.2005.

Chen, Y., Maguire, T., Hileman, R.E., Fromm, J.R., Esko, J.D., Linhardt, R.J., and Marks, R.M. (1997). Dengue virus infectivity depends on envelope protein binding to target cell heparan sulfate. Nat Med *3*, 866-871. 10.1038/nm0897-866.

Chen, Y.K., Bonaldi, T., Cuomo, A., Del Rosario, J.R., Hosfield, D.J., Kanouni, T., Kao, S.C., Lai, C., Lobo, N.A., Matuszkiewicz, J., et al. (2017). Design of KDM4 Inhibitors with Antiproliferative Effects in Cancer Models. ACS Med Chem Lett *8*, 869-874. 10.1021/acsmedchemlett.7b00220.

Chen, Z., Zang, J., Whetstine, J., Hong, X., Davrazou, F., Kutateladze, T.G., Simpson, M., Mao, Q., Pan, C.H., Dai, S., et al. (2006). Structural insights into histone demethylation by JMJD2 family members. Cell *125*, 691-702. 10.1016/j.cell.2006.04.024.

Chiang, J.Y. (2013). Bile acid metabolism and signaling. Compr Physiol *3*, 1191-1212. 10.1002/cphy.c120023.

Chisari, F.V. (1995). Hepatitis B virus transgenic mice: insights into the virus and the disease. Hepatology *22*, 1316-1325. 10.1016/0270-9139(95)90645-2.

Chisari, F.V., Pinkert, C.A., Milich, D.R., Filippi, P., McLachlan, A., Palmiter, R.D., and Brinster, R.L. (1985). A transgenic mouse model of the chronic hepatitis B surface antigen carrier state. Science *230*, 1157-1160. 10.1126/science.3865369.

Cho, E.Y., Kim, H.J., Park, C., So, H.S., Park, R.K., and Kim, H.C. (2013). Impact of Nucleotide Mutations at the HNF3- and HNF4-Binding Sites in Enhancer 1 on Viral Replication in Patients with Chronic Hepatitis B Virus Infection. Gut Liver *7*, 569-575. 10.5009/gnl.2013.7.5.569.

Choi, C.Y., Choi, B.H., Park, G.T., and Rho, H.M. (1997). Activating transcription factor 2 (ATF2) down-regulates hepatitis B virus X promoter activity by the competition for the activating protein 1 binding site and the formation of the ATF2-Jun heterodimer. J Biol Chem *272*, 16934-16939. 10.1074/jbc.272.27.16934.

Chou, H.H., Chien, W.H., Wu, L.L., Cheng, C.H., Chung, C.H., Horng, J.H., Ni, Y.H., Tseng, H.T., Wu, D., Lu, X., et al. (2015). Age-related immune clearance of hepatitis B virus infection requires the establishment of gut microbiota. Proc Natl Acad Sci U S A *112*, 2175-2180. 10.1073/pnas.1424775112.

Chouaib, S., Noman, M.Z., Kosmatopoulos, K., and Curran, M.A. (2017). Hypoxic stress: obstacles and opportunities for innovative immunotherapy of cancer. Oncogene *36*, 439-445. 10.1038/onc.2016.225.

Choudhry, H., Schodel, J., Oikonomopoulos, S., Camps, C., Grampp, S., Harris, A.L., Ratcliffe, P.J., Ragoussis, J., and Mole, D.R. (2014). Extensive regulation of the non-coding transcriptome by hypoxia: role of HIF in releasing paused RNApol2. EMBO Rep *15*, 70-76. 10.1002/embr.201337642.

Christen, V., Duong, F., Bernsmeier, C., Sun, D., Nassal, M., and Heim, M.H. (2007). Inhibition of alpha interferon signaling by hepatitis B virus. J Virol *81*, 159-165. 10.1128/JVI.01292-06.

Cirillo, L.A., Lin, F.R., Cuesta, I., Friedman, D., Jarnik, M., and Zaret, K.S. (2002). Opening of compacted chromatin by early developmental transcription factors HNF3 (FoxA) and GATA-4. Mol Cell *9*, 279-289. 10.1016/s1097-2765(02)00459-8.

Claudel, T., Staels, B., and Kuipers, F. (2005). The Farnesoid X receptor: a molecular link between bile acid and lipid and glucose metabolism. Arterioscler Thromb Vasc Biol *25*, 2020-2030. 10.1161/01.ATV.0000178994.21828.a7.

Cloos, P.A., Christensen, J., Agger, K., Maiolica, A., Rappsilber, J., Antal, T., Hansen, K.H., and Helin, K. (2006). The putative oncogene GASC1 demethylates tri- and dimethylated lysine 9 on histone H3. Nature *442*, 307-311. 10.1038/nature04837.

Collins, I.M., Breathnach, O., and Felle, P. (2012). Electronic clinical decision support systems attitudes and barriers to use in the oncology setting. Ir J Med Sci *181*, 521-525. 10.1007/s11845-012-0809-6.

Colonno, R.J., Rose, R., Baldick, C.J., Levine, S., Pokornowski, K., Yu, C.F., Walsh, A., Fang, J., Hsu, M., Mazzucco, C., et al. (2006). Entecavir resistance is rare in nucleoside naive patients with hepatitis B. Hepatology *44*, 1656-1665. 10.1002/hep.21422.

Colson, P., Roquelaure, B., and Tamalet, C. (2009). Detection of a newly identified hepatitis B virus genotype in southeastern France. J Clin Virol *45*, 165-167. 10.1016/j.jcv.2009.03.007.

Corlu, A., and Loyer, P. (2012). Regulation of the g1/s transition in hepatocytes: involvement of the cyclin-dependent kinase cdk1 in the DNA replication. Int J Hepatol *2012*, 689324. 10.1155/2012/689324.

Cornberg, M., Wong, V.W., Locarnini, S., Brunetto, M., Janssen, H.L.A., and Chan, H.L. (2017). The role of quantitative hepatitis B surface antigen revisited. J Hepatol *66*, 398-411. 10.1016/j.jhep.2016.08.009.

Costa, M., Yan, Y., Zhao, D., and Salnikow, K. (2003). Molecular mechanisms of nickel carcinogenesis: gene silencing by nickel delivery to the nucleus and gene activation/inactivation by nickel-induced cell signaling. J Environ Monit *5*, 222-223. 10.1039/b210260a.

Cote, P.J., Korba, B.E., Miller, R.H., Jacob, J.R., Baldwin, B.H., Hornbuckle, W.E., Purcell, R.H., Tennant, B.C., and Gerin, J.L. (2000). Effects of age and viral determinants on chronicity as an outcome of experimental woodchuck hepatitis virus infection. Hepatology *31*, 190-200. 10.1002/hep.510310128.

Cramer, T., Yamanishi, Y., Clausen, B.E., Forster, I., Pawlinski, R., Mackman, N., Haase, V.H., Jaenisch, R., Corr, M., Nizet, V., et al. (2003). HIF-1alpha is essential for myeloid cell-mediated inflammation. Cell *112*, 645-657. 10.1016/s0092-8674(03)00154-5.

Crews, S.T., and Fan, C.M. (1999). Remembrance of things PAS: regulation of development by bHLH-PAS proteins. Curr Opin Genet Dev *9*, 580-587. 10.1016/s0959-437x(99)00003-9.

Creyghton, M.P., Cheng, A.W., Welstead, G.G., Kooistra, T., Carey, B.W., Steine, E.J., Hanna, J., Lodato, M.A., Frampton, G.M., Sharp, P.A., et al. (2010). Histone H3K27ac separates active from poised enhancers and predicts developmental state. Proc Natl Acad Sci U S A *107*, 21931-21936. 10.1073/pnas.1016071107.

Crispe, I.N. (2011). Liver antigen-presenting cells. J Hepatol *54*, 357-365. 10.1016/j.jhep.2010.10.005.

Crissien, A.M., and Frenette, C. (2014). Current management of hepatocellular carcinoma. Gastroenterol Hepatol (N Y) *10*, 153-161.

Crowder, S.W., Balikov, D.A., Hwang, Y.S., and Sung, H.J. (2014). Cancer Stem Cells under Hypoxia as a Chemoresistance Factor in Breast and Brain. Curr Pathobiol Rep *2*, 33-40. 10.1007/s40139-013-0035-6.

Cui, X., Guo, J.T., and Hu, J. (2015). Hepatitis B Virus Covalently Closed Circular DNA Formation in Immortalized Mouse Hepatocytes Associated with Nucleocapsid Destabilization. J Virol *89*, 9021-9028. 10.1128/JVI.01261-15.

Czermin, B., Melfi, R., McCabe, D., Seitz, V., Imhof, A., and Pirrotta, V. (2002). Drosophila enhancer of Zeste/ESC complexes have a histone H3 methyltransferase activity that marks chromosomal Polycomb sites. Cell *111*, 185-196. 10.1016/s0092-8674(02)00975-3.

D'Arienzo, V., Ferguson, J., Giraud, G., Chapus, F., Harris, J.M., Wing, P.A.C., Claydon, A., Begum, S., Zhuang, X., Balfe, P., et al. (2021a). The CCCTC-binding factor CTCF represses hepatitis B virus enhancer I and regulates viral transcription. Cell Microbiol *23*, e13274. 10.1111/cmi.13274.

D'Arienzo, V., Magri, A., Harris, J.M., Wing, P.A.C., Ko, C., Rubio, C.O., Revill, P.A., Protzer, U., Balfe, P., and McKeating, J.A. (2021b). A PCR assay to quantify patterns of HBV transcription. J Gen Virol *102*. 10.1099/jgv.0.001373.

Dahiya, P., Kamal, R., Sharma, V., and Kaur, S. (2015). "Hepatitis" - Prevention and management in dental practice. J Educ Health Promot *4*, 33. 10.4103/2277-9531.157188.

Dandri, M., Burda, M.R., Torok, E., Pollok, J.M., Iwanska, A., Sommer, G., Rogiers, X., Rogler, C.E., Gupta, S., Will, H., et al. (2001). Repopulation of mouse liver with human hepatocytes and in vivo infection with hepatitis B virus. Hepatology *33*, 981-988. 10.1053/jhep.2001.23314.

Dandri, M., and Petersen, J. (2020). cccDNA Maintenance in Chronic Hepatitis B - Targeting the Matrix of Viral Replication. Infect Drug Resist *13*, 3873-3886. 10.2147/IDR.S240472.

Das, A., Hoare, M., Davies, N., Lopes, A.R., Dunn, C., Kennedy, P.T., Alexander, G., Finney, H., Lawson, A., Plunkett, F.J., et al. (2008). Functional skewing of the global CD8 T cell population in chronic hepatitis B virus infection. J Exp Med *205*, 2111-2124. 10.1084/jem.20072076.

Das, S., Ramakrishnan, K., Behera, S.K., Ganesapandian, M., Xavier, A.S., and Selvarajan, S. (2019). Hepatitis B Vaccine and Immunoglobulin: Key Concepts. J Clin Transl Hepatol *7*, 165-171. 10.14218/JCTH.2018.00037.

Davenne, T., Klintman, J., Sharma, S., Rigby, R.E., Blest, H.T.W., Cursi, C., Bridgeman, A., Dadonaite, B., De Keersmaecker, K., Hillmen, P., et al. (2020). SAMHD1 Limits the Efficacy of Forodesine in Leukemia by Protecting Cells against the Cytotoxicity of dGTP. Cell Rep *31*, 107640. 10.1016/j.celrep.2020.107640.

de Martel, C., Maucort-Boulch, D., Plummer, M., and Franceschi, S. (2015). World-wide relative contribution of hepatitis B and C viruses in hepatocellular carcinoma. Hepatology *62*, 1190-1200. 10.1002/hep.27969.

del Mar Pena, L.M., and Laimins, L.A. (2001). Differentiation-dependent chromatin rearrangement coincides with activation of human papillomavirus type 31 late gene expression. J Virol *75*, 10005-10013. 10.1128/JVI.75.20.10005-10013.2001.

Depledge, D.P., Palser, A.L., Watson, S.J., Lai, I.Y., Gray, E.R., Grant, P., Kanda, R.K., Leproust, E., Kellam, P., and Breuer, J. (2011). Specific capture and whole-genome sequencing of viruses from clinical samples. PLoS One *6*, e27805. 10.1371/journal.pone.0027805.

Diab, A., Foca, A., Zoulim, F., Durantel, D., and Andrisani, O. (2018). The diverse functions of the hepatitis B core/capsid protein (HBc) in the viral life cycle: Implications for the development of HBc-targeting antivirals. Antiviral Res *149*, 211-220. 10.1016/j.antiviral.2017.11.015.

Ding, X.R., Yang, J., Sun, D.C., Lou, S.K., and Wang, S.Q. (2008). Whole genome expression profiling of hepatitis B virus-transfected cell line reveals the potential targets of anti-HBV drugs. Pharmacogenomics J *8*, 61-70. 10.1038/sj.tpj.6500459.

Disatham, J., Brennan, L., Chauss, D., Kantorow, J., Afzali, B., and Kantorow, M. (2021). A functional map of genomic HIF1alpha-DNA complexes in the eye lens revealed through multiomics analysis. BMC Genomics *22*, 497. 10.1186/s12864-021-07795-9.

Dixon, L.J., Barnes, M., Tang, H., Pritchard, M.T., and Nagy, L.E. (2013). Kupffer cells in the liver. Compr Physiol *3*, 785-797. 10.1002/cphy.c120026.

Dmitriev, R.I., and Papkovsky, D.B. (2015). In vitro ischemia decreases histone H4K16 acetylation in neural cells. FEBS Lett *589*, 138-144. 10.1016/j.febslet.2014.11.038.

Dobin, A., Davis, C.A., Schlesinger, F., Drenkow, J., Zaleski, C., Jha, S., Batut, P., Chaisson, M., and Gingeras, T.R. (2013). STAR: ultrafast universal RNA-seq aligner. Bioinformatics *29*, 15-21. 10.1093/bioinformatics/bts635.

Dobrynin, G., McAllister, T.E., Leszczynska, K.B., Ramachandran, S., Krieg, A.J., Kawamura, A., and Hammond, E.M. (2017). KDM4A regulates HIF-1 levels through H3K9me3. Sci Rep *7*, 11094. 10.1038/s41598-017-11658-3.

Dodd, K.M., Yang, J., Shen, M.H., Sampson, J.R., and Tee, A.R. (2015). mTORC1 drives HIF-1alpha and VEGF-A signalling via multiple mechanisms involving 4E-BP1, S6K1 and STAT3. Oncogene *34*, 2239-2250. 10.1038/onc.2014.164.

Doitsh, G., and Shaul, Y. (2004). Enhancer I predominance in hepatitis B virus gene expression. Mol Cell Biol *24*, 1799-1808. 10.1128/MCB.24.4.1799-1808.2004.

Dolken, L., Ruzsics, Z., Radle, B., Friedel, C.C., Zimmer, R., Mages, J., Hoffmann, R., Dickinson, P., Forster, T., Ghazal, P., and Koszinowski, U.H. (2008). High-resolution gene expression profiling for simultaneous kinetic parameter analysis of RNA synthesis and decay. RNA *14*, 1959-1972. 10.1261/rna.1136108.

Dong, C., Zhang, H., Xu, C., Arrowsmith, C.H., and Min, J. (2014). Structure and function of dioxygenases in histone demethylation and DNA/RNA demethylation. IUCrJ *1*, 540-549. 10.1107/S2052252514020922.

Dong, H., Zhang, L., Qian, Z., Zhu, X., Zhu, G., Chen, Y., Xie, X., Ye, Q., Zang, J., Ren, Z., and Ji, Q. (2015). Identification of HBV-MLL4 Integration and Its Molecular Basis in Chinese Hepatocellular Carcinoma. PLoS One *10*, e0123175. 10.1371/journal.pone.0123175.

Dratkiewicz, E., Simiczyjew, A., Mazurkiewicz, J., Zietek, M., Matkowski, R., and Nowak, D. (2021). Hypoxia and Extracellular Acidification as Drivers of Melanoma Progression and Drug Resistance. Cells *10*. 10.3390/cells10040862.

Du, J., Johnson, L.M., Jacobsen, S.E., and Patel, D.J. (2015). DNA methylation pathways and their crosstalk with histone methylation. Nat Rev Mol Cell Biol *16*, 519-532. 10.1038/nrm4043.

Duan, L., Rai, G., Roggero, C., Zhang, Q.J., Wei, Q., Ma, S.H., Zhou, Y., Santoyo, J., Martinez, E.D., Xiao, G., et al. (2015). KDM4/JMJD2 Histone Demethylase Inhibitors Block Prostate Tumor Growth by Suppressing the Expression of AR and BMYB-Regulated Genes. Chem Biol *22*, 1185-1196. 10.1016/j.chembiol.2015.08.007.

Dunn, C., Peppa, D., Khanna, P., Nebbia, G., Jones, M., Brendish, N., Lascar, R.M., Brown, D., Gilson, R.J., Tedder, R.J., et al. (2009). Temporal analysis of early immune responses in patients with acute hepatitis B virus infection. Gastroenterology *137*, 1289-1300. 10.1053/j.gastro.2009.06.054.

Duriez, M., Mandouri, Y., Lekbaby, B., Wang, H., Schnuriger, A., Redelsperger, F., Guerrera, C.I., Lefevre, M., Fauveau, V., Ahodantin, J., et al. (2017). Alternative splicing of hepatitis B virus: A novel virus/host interaction altering liver immunity. J Hepatol *67*, 687-699. 10.1016/j.jhep.2017.05.025.

Dutta, B., Ren, Y., Hao, P., Sim, K.H., Cheow, E., Adav, S., Tam, J.P., and Sze, S.K. (2014a). Profiling of the Chromatin-associated Proteome Identifies HP1BP3 as a Novel Regulator of Cell Cycle Progression. Mol Cell Proteomics *13*, 2183-2197. 10.1074/mcp.M113.034975.

Dutta, B., Yan, R., Lim, S.K., Tam, J.P., and Sze, S.K. (2014b). Quantitative profiling of chromatome dynamics reveals a novel role for HP1BP3 in hypoxia-induced oncogenesis. Mol Cell Proteomics *13*, 3236-3249. 10.1074/mcp.M114.038232.

Eales, K.L., Hollinshead, K.E., and Tennant, D.A. (2016). Hypoxia and metabolic adaptation of cancer cells. Oncogenesis *5*, e190. 10.1038/oncsis.2015.50.

EASL (2012). EASL clinical practice guidelines: Management of chronic hepatitis B virus infection. J Hepatol *57*, 167-185. 10.1016/j.jhep.2012.02.010.

EASL (2017). EASL 2017 Clinical Practice Guidelines on the management of hepatitis B virus infection. J Hepatol *67*, 370-398. 10.1016/j.jhep.2017.03.021.

Eastel, J.M., Lam, K.W., Lee, N.L., Lok, W.Y., Tsang, A.H.F., Pei, X.M., Chan, A.K.C., Cho, W.C.S., and Wong, S.C.C. (2019). Application of NanoString technologies in companion diagnostic development. Expert Rev Mol Diagn *19*, 591-598. 10.1080/14737159.2019.1623672.

Ebert, B.L., and Bunn, H.F. (1998). Regulation of transcription by hypoxia requires a multiprotein complex that includes hypoxia-inducible factor 1, an adjacent transcription factor, and p300/CREB binding protein. Mol Cell Biol *18*, 4089-4096. 10.1128/MCB.18.7.4089.

Ebert, G., Poeck, H., Lucifora, J., Baschuk, N., Esser, K., Esposito, I., Hartmann, G., and Protzer, U. (2011). 5' Triphosphorylated small interfering RNAs control replication of hepatitis B virus and induce an interferon response in human liver cells and mice. Gastroenterology *141*, 696-706, 706 e691-693. 10.1053/j.gastro.2011.05.001.

Eble, B.E., MacRae, D.R., Lingappa, V.R., and Ganem, D. (1987). Multiple topogenic sequences determine the transmembrane orientation of the hepatitis B surface antigen. Mol Cell Biol *7*, 3591-3601. 10.1128/mcb.7.10.3591-3601.1987.

Edgar, R., Domrachev, M., and Lash, A.E. (2002). Gene Expression Omnibus: NCBI gene expression and hybridization array data repository. Nucleic Acids Res *30*, 207-210. 10.1093/nar/30.1.207.

Edman, J.C., Gray, P., Valenzuela, P., Rall, L.B., and Rutter, W.J. (1980). Integration of hepatitis B virus sequences and their expression in a human hepatoma cell. Nature *286*, 535-538. 10.1038/286535a0.

Ehrismann, D., Flashman, E., Genn, D.N., Mathioudakis, N., Hewitson, K.S., Ratcliffe, P.J., and Schofield, C.J. (2007). Studies on the activity of the hypoxia-inducible-factor hydroxylases using an oxygen consumption assay. Biochem J *401*, 227-234. 10.1042/BJ20061151.

El-Serag, H.B. (2012). Epidemiology of viral hepatitis and hepatocellular carcinoma. Gastroenterology *142*, 1264-1273 e1261. 10.1053/j.gastro.2011.12.061.

Elaut, G., Henkens, T., Papeleu, P., Snykers, S., Vinken, M., Vanhaecke, T., and Rogiers, V. (2006). Molecular mechanisms underlying the dedifferentiation process of isolated hepatocytes and their cultures. Curr Drug Metab *7*, 629-660. 10.2174/138920006778017759.

Encode Project Consortium (2012). An integrated encyclopedia of DNA elements in the human genome. Nature *489*, 57-74. 10.1038/nature11247.

Epstein, A.C., Gleadle, J.M., McNeill, L.A., Hewitson, K.S., O'Rourke, J., Mole, D.R., Mukherji, M., Metzen, E., Wilson, M.I., Dhanda, A., et al. (2001). C. elegans EGL-9 and mammalian homologs define a family of dioxygenases that regulate HIF by prolyl hydroxylation. Cell *107*, 43-54. 10.1016/s0092-8674(01)00507-4.

Fabrizi, F., Messa, P., and Martin, P. (2008). Hepatitis B virus infection and the dialysis patient. Semin Dial *21*, 440-446. 10.1111/j.1525-139X.2008.00437.x.

Farina, A.R., Cappabianca, L., Sebastiano, M., Zelli, V., Guadagni, S., and Mackay, A.R. (2020). Hypoxia-induced alternative splicing: the 11th Hallmark of Cancer. J Exp Clin Cancer Res *39*, 110. 10.1186/s13046-020-01616-9.

Farshadi, E., van der Horst, G.T.J., and Chaves, I. (2020). Molecular Links between the Circadian Clock and the Cell Cycle. J Mol Biol *432*, 3515-3524. 10.1016/j.jmb.2020.04.003.

Fateen, A.A., Shahin, R.Y., Farres, M.N., Eldeeb, M.A., and Amer, H.A. (2012). Assessment of hepatic fibrosis and necroinflammation among inactive HBsAg carriers in Egypt. Ann Hepatol *11*, 464-470.

Favre, M., Breitburd, F., Croissant, O., and Orth, G. (1977). Chromatin-like structures obtained after alkaline disruption of bovine and human papillomaviruses. J Virol *21*, 1205-1209. 10.1128/JVI.21.3.1205-1209.1977.

Fedeles, B.I., Singh, V., Delaney, J.C., Li, D., and Essigmann, J.M. (2015). The AlkB Family of Fe(II)/alpha-Ketoglutarate-dependent Dioxygenases: Repairing Nucleic Acid Alkylation Damage and Beyond. J Biol Chem *290*, 20734-20742. 10.1074/jbc.R115.656462.

Ferguson, J., Campos-Leon, K., Pentland, I., Stockton, J.D., Gunther, T., Beggs, A., Grundhoff, A., Roberts, S., Noyvert, B., and Parish, J.L. (2021). The chromatin insulator CTCF regulates HPV18 transcript splicing and differentiation-dependent late gene expression. PLoS Pathog *17*, e1010032. 10.1371/journal.ppat.1010032.

Ferlay, J., Colombet, M., Soerjomataram, I., Mathers, C., Parkin, D.M., Pineros, M., Znaor, A., and Bray, F. (2019). Estimating the global cancer incidence and mortality in 2018: GLOBOCAN sources and methods. Int J Cancer *144*, 1941-1953. 10.1002/ijc.31937.

Fischer, S.F., Schmidt, K., Fiedler, N., Glebe, D., Schuttler, C., Sun, J., Gerlich, W.H., Repp, R., and Schaefer, S. (2006). Genotype-dependent activation or repression of HBV enhancer II by transcription factor COUP-TF1. World J Gastroenterol *12*, 6054-6058. 10.3748/wjg.v12.i37.6054.

Fisicaro, P., Valdatta, C., Boni, C., Massari, M., Mori, C., Zerbini, A., Orlandini, A., Sacchelli, L., Missale, G., and Ferrari, C. (2009). Early kinetics of innate and adaptive immune responses during hepatitis B virus infection. Gut *58*, 974-982. 10.1136/gut.2008.163600.

Fisicaro, P., Valdatta, C., Massari, M., Loggi, E., Biasini, E., Sacchelli, L., Cavallo, M.C., Silini, E.M., Andreone, P., Missale, G., and Ferrari, C. (2010). Antiviral intrahepatic T-cell responses can be restored by blocking programmed death-1 pathway in chronic hepatitis B. Gastroenterology *138*, 682-693, 693 e681-684. 10.1053/j.gastro.2009.09.052.

Flecken, T., Meier, M.A., Skewes-Cox, P., Barkan, D.T., Heim, M.H., Wieland, S.F., and Holdorf, M.M. (2019). Mapping the Heterogeneity of Histone Modifications on Hepatitis B Virus DNA Using Liver Needle Biopsies Obtained from Chronically Infected Patients. J Virol *93*. 10.1128/JVI.02036-18.

Flensburg, C., Kinkel, S.A., Keniry, A., Blewitt, M.E., and Oshlack, A. (2014). A comparison of control samples for ChIP-seq of histone modifications. Front Genet *5*, 329. 10.3389/fgene.2014.00329.

Flodell, S., Schleucher, J., Cromsigt, J., Ippel, H., Kidd-Ljunggren, K., and Wijmenga, S. (2002). The apical stem-loop of the hepatitis B virus encapsidation signal folds into a stable tri-loop with two underlying pyrimidine bulges. Nucleic Acids Res *30*, 4803-4811. 10.1093/nar/gkf603.

Frelin, L., Wahlstrom, T., Tucker, A.E., Jones, J., Hughes, J., Lee, B.O., Billaud, J.N., Peters, C., Whitacre, D., Peterson, D., and Milich, D.R. (2009). A mechanism to explain the selection of the hepatitis e antigen-negative mutant during chronic hepatitis B virus infection. J Virol *83*, 1379-1392. 10.1128/JVI.01902-08.

Fry, N.J., Law, B.A., Ilkayeva, O.R., Holley, C.L., and Mansfield, K.D. (2017). N(6)-methyladenosine is required for the hypoxic stabilization of specific mRNAs. RNA *23*, 1444-1455. 10.1261/rna.061044.117.

Fu, D., Jordan, J.J., and Samson, L.D. (2013). Human ALKBH7 is required for alkylation and oxidation-induced programmed necrosis. Genes Dev *27*, 1089-1100. 10.1101/gad.215533.113.

Fu, Y., Dai, Q., Zhang, W., Ren, J., Pan, T., and He, C. (2010). The AlkB domain of mammalian ABH8 catalyzes hydroxylation of 5-methoxycarbonylmethyluridine at the wobble position of tRNA. Angew Chem Int Ed Engl *49*, 8885-8888. 10.1002/anie.201001242.

Fuady, J.H., Gutsche, K., Santambrogio, S., Varga, Z., Hoogewijs, D., and Wenger, R.H. (2016). Estrogen-dependent downregulation of hypoxia-inducible factor (HIF)-2alpha in invasive breast cancer cells. Oncotarget *7*, 31153-31165. 10.18632/oncotarget.8866.

Fujimoto, A., Totoki, Y., Abe, T., Boroevich, K.A., Hosoda, F., Nguyen, H.H., Aoki, M., Hosono, N., Kubo, M., Miya, F., et al. (2012). Whole-genome sequencing of liver cancers identifies etiological influences on mutation patterns and recurrent mutations in chromatin regulators. Nat Genet *44*, 760-764. 10.1038/ng.2291.

Furchtgott, L.A., Chow, C.C., and Periwal, V. (2009). A model of liver regeneration. Biophys J *96*, 3926-3935. 10.1016/j.bpj.2009.01.061.

Galle, P.R., Hagelstein, J., Kommerell, B., Volkmann, M., Schranz, P., and Zentgraf, H. (1994). In vitro experimental infection of primary human hepatocytes with hepatitis B virus. Gastroenterology *106*, 664-673. 10.1016/0016-5085(94)90700-5.

Gan, E.S., and Ooi, E.E. (2020). Oxygen: viral friend or foe? Virol J *17*, 115. 10.1186/s12985-020-01374-2.

Gearhart, T.L., and Bouchard, M.J. (2011). The hepatitis B virus HBx protein modulates cell cycle regulatory proteins in cultured primary human hepatocytes. Virus Res *155*, 363-367. 10.1016/j.virusres.2010.09.023.

Gebhardt, R., Baldysiak-Figiel, A., Krugel, V., Ueberham, E., and Gaunitz, F. (2007). Hepatocellular expression of glutamine synthetase: an indicator of morphogen actions as master regulators of zonation in adult liver. Prog Histochem Cytochem *41*, 201-266. 10.1016/j.proghi.2006.12.001.

Gebhardt, R., and Matz-Soja, M. (2014). Liver zonation: Novel aspects of its regulation and its impact on homeostasis. World J Gastroenterol *20*, 8491-8504. 10.3748/wjg.v20.i26.8491.

Ghendon, Y. (1987). Perinatal transmission of hepatitis B virus in high-incidence countries. J Virol Methods *17*, 69-79. 10.1016/0166-0934(87)90070-x.

Giatromanolaki, A., Koukourakis, M.I., Sivridis, E., Pastorek, J., Wykoff, C.C., Gatter, K.C., and Harris, A.L. (2001). Expression of hypoxia-inducible carbonic anhydrase-9 relates to angiogenic pathways and independently to poor outcome in non-small cell lung cancer. Cancer Res *61*, 7992-7998.

Ginouves, A., Ilc, K., Macias, N., Pouyssegur, J., and Berra, E. (2008). PHDs overactivation during chronic hypoxia "desensitizes" HIFalpha and protects cells from necrosis. Proc Natl Acad Sci U S A *105*, 4745-4750. 10.1073/pnas.0705680105.

Glebe, D., Urban, S., Knoop, E.V., Cag, N., Krass, P., Grun, S., Bulavaite, A., Sasnauskas, K., and Gerlich, W.H. (2005). Mapping of the hepatitis B virus attachment site by use of infection-inhibiting preS1 lipopeptides and tupaia hepatocytes. Gastroenterology *129*, 234-245. 10.1053/j.gastro.2005.03.090.

Global Burden of Disease Liver Cancer, C., Akinyemiju, T., Abera, S., Ahmed, M., Alam, N., Alemayohu, M.A., Allen, C., Al-Raddadi, R., Alvis-Guzman, N., Amoako, Y., et al. (2017). The Burden of Primary Liver Cancer and Underlying Etiologies From 1990 to 2015 at the Global, Regional, and National Level: Results From the Global Burden of Disease Study 2015. JAMA Oncol *3*, 1683-1691. 10.1001/jamaoncol.2017.3055.

Goda, N., and Kanai, M. (2012). Hypoxia-inducible factors and their roles in energy metabolism. Int J Hematol *95*, 457-463. 10.1007/s12185-012-1069-y.

Goda, N., Ryan, H.E., Khadivi, B., McNulty, W., Rickert, R.C., and Johnson, R.S. (2003). Hypoxia-inducible factor 1alpha is essential for cell cycle arrest during hypoxia. Mol Cell Biol *23*, 359-369. 10.1128/MCB.23.1.359-369.2003.

Godoy, P., Hewitt, N.J., Albrecht, U., Andersen, M.E., Ansari, N., Bhattacharya, S., Bode, J.G., Bolleyn, J., Borner, C., Bottger, J., et al. (2013). Recent advances in 2D and 3D in vitro systems using primary hepatocytes, alternative hepatocyte sources and non-parenchymal liver cells and their use in investigating mechanisms of hepatotoxicity, cell signaling and ADME. Arch Toxicol *87*, 1315-1530. 10.1007/s00204-013-1078-5.

Goldstone, D.C., Ennis-Adeniran, V., Hedden, J.J., Groom, H.C., Rice, G.I., Christodoulou, E., Walker, P.A., Kelly, G., Haire, L.F., Yap, M.W., et al. (2011). HIV-1 restriction factor SAMHD1 is a deoxynucleoside triphosphate triphosphohydrolase. Nature *480*, 379-382. 10.1038/nature10623.

Gong, Q., Chen, S., Guo, J., Sun, H., Zheng, G., Liu, Q., Ren, H., and He, S. (2011). Chromosome remodeling related to hepatitis B virus replication in HepG2 cells. DNA Cell Biol *30*, 347-354. 10.1089/dna.2010.1172.

Gong, Y., Yao, E., and Tavis, J.E. (2001). Evidence that the RNAseH activity of the duck hepatitis B virus is unable to act on exogenous substrates. BMC Microbiol *1*, 12. 10.1186/1471-2180-1-12.

Grechez-Cassiau, A., Rayet, B., Guillaumond, F., Teboul, M., and Delaunay, F. (2008). The circadian clock component BMAL1 is a critical regulator of

p21WAF1/CIP1 expression and hepatocyte proliferation. J Biol Chem *283*, 4535-4542. 10.1074/jbc.M705576200.

Griffin, C.T., Brennan, J., and Magnuson, T. (2008). The chromatin-remodeling enzyme BRG1 plays an essential role in primitive erythropoiesis and vascular development. Development *135*, 493-500. 10.1242/dev.010090.

Grigoletto, A., Lestienne, P., and Rosenbaum, J. (2011). The multifaceted proteins Reptin and Pontin as major players in cancer. Biochim Biophys Acta *1815*, 147-157. 10.1016/j.bbcan.2010.11.002.

Grinstein, E., Jundt, F., Weinert, I., Wernet, P., and Royer, H.D. (2002). Sp1 as G1 cell cycle phase specific transcription factor in epithelial cells. Oncogene *21*, 1485-1492. 10.1038/sj.onc.1205211.

Gripon, P., Rumin, S., Urban, S., Le Seyec, J., Glaise, D., Cannie, I., Guyomard, C., Lucas, J., Trepo, C., and Guguen-Guillouzo, C. (2002). Infection of a human hepatoma cell line by hepatitis B virus. Proc Natl Acad Sci U S A *99*, 15655-15660. 10.1073/pnas.232137699.

Guerrieri, F., Belloni, L., D'Andrea, D., Pediconi, N., Le Pera, L., Testoni, B., Scisciani, C., Floriot, O., Zoulim, F., Tramontano, A., and Levrero, M. (2017). Genome-wide identification of direct HBx genomic targets. BMC Genomics *18*, 184. 10.1186/s12864-017-3561-5.

Guidotti, L.G., and Chisari, F.V. (2006). Immunobiology and pathogenesis of viral hepatitis. Annu Rev Pathol *1*, 23-61. 10.1146/annurev.pathol.1.110304.100230.

Guidotti, L.G., Martinez, V., Loh, Y.T., Rogler, C.E., and Chisari, F.V. (1994). Hepatitis B virus nucleocapsid particles do not cross the hepatocyte nuclear membrane in transgenic mice. J Virol *68*, 5469-5475. 10.1128/JVI.68.9.5469-5475.1994.

Guidotti, L.G., Matzke, B., Schaller, H., and Chisari, F.V. (1995). High-level hepatitis B virus replication in transgenic mice. J Virol *69*, 6158-6169. 10.1128/JVI.69.10.6158-6169.1995.

Guidotti, L.G., Rochford, R., Chung, J., Shapiro, M., Purcell, R., and Chisari, F.V. (1999). Viral clearance without destruction of infected cells during acute HBV infection. Science *284*, 825-829. 10.1126/science.284.5415.825.

Guo, H., Jiang, D., Zhou, T., Cuconati, A., Block, T.M., and Guo, J.T. (2007). Characterization of the intracellular deproteinized relaxed circular DNA of hepatitis B virus: an intermediate of covalently closed circular DNA formation. J Virol *81*, 12472-12484. 10.1128/JVI.01123-07.

Guo, W.N., Zhu, B., Ai, L., Yang, D.L., and Wang, B.J. (2018). Animal models for the study of hepatitis B virus infection. Zool Res *39*, 25-31. 10.24272/j.issn.2095-8137.2018.013.

Guo, X., Chen, P., Hou, X., Xu, W., Wang, D., Wang, T.Y., Zhang, L., Zheng, G., Gao, Z.L., He, C.Y., et al. (2016). The recombined cccDNA produced using minicircle technology mimicked HBV genome in structure and function closely. Sci Rep *6*, 25552. 10.1038/srep25552.

Guo, Y., Li, Y., Mu, S., Zhang, J., and Yan, Z. (2009). Evidence that methylation of hepatitis B virus covalently closed circular DNA in liver tissues of patients with chronic hepatitis B modulates HBV replication. J Med Virol *81*, 1177-1183. 10.1002/jmv.21525.

Guo, Y.H., Li, Y.N., Zhao, J.R., Zhang, J., and Yan, Z. (2011). HBc binds to the CpG islands of HBV cccDNA and promotes an epigenetic permissive state. Epigenetics *6*, 720-726. 10.4161/epi.6.6.15815.

Gusmao, E.G., Allhoff, M., Zenke, M., and Costa, I.G. (2016). Analysis of computational footprinting methods for DNase sequencing experiments. Nat Methods *13*, 303-309. 10.1038/nmeth.3772.

Haddad, J.J. (2002). Redox regulation of pro-inflammatory cytokines and IkappaB-alpha/NF-kappaB nuclear translocation and activation. Biochem Biophys Res Commun *296*, 847-856. 10.1016/s0006-291x(02)00947-6.

Hadziyannis, S.J., and Papatheodoridis, G.V. (2006). Hepatitis B e antigen-negative chronic hepatitis B: natural history and treatment. Semin Liver Dis *26*, 130-141. 10.1055/s-2006-939751.

Hadziyannis, S.J., and Vassilopoulos, D. (2001). Hepatitis B e antigen-negative chronic hepatitis B. Hepatology *34*, 617-624. 10.1053/jhep.2001.27834.

Haines, K.M., and Loeb, D.D. (2007). The sequence of the RNA primer and the DNA template influence the initiation of plus-strand DNA synthesis in hepatitis B virus. J Mol Biol *370*, 471-480. 10.1016/j.jmb.2007.04.057.

Halazonetis, T.D., Georgopoulos, K., Greenberg, M.E., and Leder, P. (1988). c-Jun dimerizes with itself and with c-Fos, forming complexes of different DNA binding affinities. Cell *55*, 917-924. 10.1016/0092-8674(88)90147-x.

Hallez, C., Li, X., Suspene, R., Thiers, V., Bouzidi, M.S., C, M.D., Lucansky, V., Wain-Hobson, S., Gaudin, R., and Vartanian, J.P. (2019). Hypoxia-induced human deoxyribonuclease I is a cellular restriction factor of hepatitis B virus. Nat Microbiol *4*, 1196-1207. 10.1038/s41564-019-0405-x.

Halpern, K.B., Shenhav, R., Matcovitch-Natan, O., Toth, B., Lemze, D., Golan, M., Massasa, E.E., Baydatch, S., Landen, S., Moor, A.E., et al. (2017). Single-cell spatial reconstruction reveals global division of labour in the mammalian liver. Nature *542*, 352-356. 10.1038/nature21065.

Hampsey, M., and Reinberg, D. (2003). Tails of intrigue: phosphorylation of RNA polymerase II mediates histone methylation. Cell *113*, 429-432. 10.1016/s0092-8674(03)00360-x.

Han, H.S., Kang, G., Kim, J.S., Choi, B.H., and Koo, S.H. (2016). Regulation of glucose metabolism from a liver-centric perspective. Exp Mol Med *48*, e218. 10.1038/emm.2015.122.

Han, J., Li, J., Ho, J.C., Chia, G.S., Kato, H., Jha, S., Yang, H., Poellinger, L., and Lee, K.L. (2017). Hypoxia is a Key Driver of Alternative Splicing in Human Breast Cancer Cells. Sci Rep *7*, 4108. 10.1038/s41598-017-04333-0.

Han, N.I., Chung, K.W., Ahn, B.M., Choi, S.W., Lee, Y.S., Lee, C.D., and Sun, H.S. (2001). Ultrastructural changes of hepatic stellate cells in the space of Disse in alcoholic fatty liver. Korean J Intern Med *16*, 160-166. 10.3904/kjim.2001.16.3.160.

Hancock, R.L., Dunne, K., Walport, L.J., Flashman, E., and Kawamura, A. (2015). Epigenetic regulation by histone demethylases in hypoxia. Epigenomics *7*, 791-811. 10.2217/epi.15.24.

Hancock, R.L., Masson, N., Dunne, K., Flashman, E., and Kawamura, A. (2017). The Activity of JmjC Histone Lysine Demethylase KDM4A is Highly Sensitive to Oxygen Concentrations. ACS Chem Biol *12*, 1011-1019. 10.1021/acschembio.6b00958.

Hangasky, J.A., Taabazuing, C.Y., Valliere, M.A., and Knapp, M.J. (2013). Imposing function down a (cupin)-barrel: secondary structure and metal stereochemistry in the alphaKG-dependent oxygenases. Metallomics *5*, 287-301. 10.1039/c3mt20153h.

Hao, D., Wang, Y., Li, L., Qian, G., Liu, J., Li, M., Zhang, Y., Zhou, R., and Yan, D. (2020). SHP-1 suppresses the antiviral innate immune response by targeting TRAF3. FASEB J *34*, 12392-12405. 10.1096/fj.202000600RR.

Hao, R., He, J., Liu, X., Gao, G., Liu, D., Cui, L., Yu, G., Yu, W., Chen, Y., and Guo, D. (2015). Inhibition of hepatitis B virus gene expression and replication by hepatocyte nuclear factor 6. J Virol *89*, 4345-4355. 10.1128/JVI.03094-14.

Hara, S., Hamada, J., Kobayashi, C., Kondo, Y., and Imura, N. (2001). Expression and characterization of hypoxia-inducible factor (HIF)-3alpha in human kidney:

suppression of HIF-mediated gene expression by HIF-3alpha. Biochem Biophys Res Commun *287*, 808-813. 10.1006/bbrc.2001.5659.

Harris, A.L. (2002). Hypoxia--a key regulatory factor in tumour growth. Nat Rev Cancer *2*, 38-47. 10.1038/nrc704.

Hass, M., Hannoun, C., Kalinina, T., Sommer, G., Manegold, C., and Gunther, S. (2005). Functional analysis of hepatitis B virus reactivating in hepatitis B surface antigen-negative individuals. Hepatology *42*, 93-103. 10.1002/hep.20748.

Hatanaka, M., Shimba, S., Sakaue, M., Kondo, Y., Kagechika, H., Kokame, K., Miyata, T., and Hara, S. (2009). Hypoxia-inducible factor-3alpha functions as an accelerator of 3T3-L1 adipose differentiation. Biol Pharm Bull *32*, 1166-1172. 10.1248/bpb.32.1166.

Haussinger, D., and Kordes, C. (2019). Space of Disse: a stem cell niche in the liver. Biol Chem *401*, 81-95. 10.1515/hsz-2019-0283.

Hawkins, K.E., Sharp, T.V., and McKay, T.R. (2013). The role of hypoxia in stem cell potency and differentiation. Regen Med *8*, 771-782. 10.2217/rme.13.71.

Hayden, M.S., West, A.P., and Ghosh, S. (2006). NF-kappaB and the immune response. Oncogene *25*, 6758-6780. 10.1038/sj.onc.1209943.

Hayer, J., Jadeau, F., Deleage, G., Kay, A., Zoulim, F., and Combet, C. (2013). HBVdb: a knowledge database for Hepatitis B Virus. Nucleic Acids Res *41*, D566-570. 10.1093/nar/gks1022.

He, F., Chen, E.Q., Liu, L., Zhou, T.Y., Liu, C., Cheng, X., Liu, F.J., and Tang, H. (2012). Inhibition of hepatitis B Virus replication by hepatocyte nuclear factor 4-alpha specific short hairpin RNA. Liver Int *32*, 742-751. 10.1111/j.1478-3231.2011.02748.x.

He, Q., Li, W., Ren, J., Huang, Y., Huang, Y., Hu, Q., Chen, J., and Chen, W. (2016). ZEB2 inhibits HBV transcription and replication by targeting its core promoter. Oncotarget *7*, 16003-16011. 10.18632/oncotarget.7435.

He, Y.F., Li, B.Z., Li, Z., Liu, P., Wang, Y., Tang, Q., Ding, J., Jia, Y., Chen, Z., Li, L., et al. (2011). Tet-mediated formation of 5-carboxylcytosine and its excision by TDG in mammalian DNA. Science *333*, 1303-1307. 10.1126/science.1210944.

Heermann, K.H., Goldmann, U., Schwartz, W., Seyffarth, T., Baumgarten, H., and Gerlich, W.H. (1984). Large surface proteins of hepatitis B virus containing the pre-s sequence. J Virol *52*, 396-402. 10.1128/JVI.52.2.396-402.1984.

Heidbreder, M., Qadri, F., Johren, O., Dendorfer, A., Depping, R., Frohlich, F., Wagner, K.F., and Dominiak, P. (2007). Non-hypoxic induction of HIF-3alpha by 2-deoxy-D-glucose and insulin. Biochem Biophys Res Commun *352*, 437-443. 10.1016/j.bbrc.2006.11.027.

Heinemann, B., Nielsen, J.M., Hudlebusch, H.R., Lees, M.J., Larsen, D.V., Boesen, T., Labelle, M., Gerlach, L.O., Birk, P., and Helin, K. (2014). Inhibition of demethylases by GSK-J1/J4. Nature *514*, E1-2. 10.1038/nature13688.

Hepatitis B Foundation. Hepatitis B Virus: Drug Watch. https://www.hepb.org/treatment-and-management/drug-watch/.

Herrscher, C., Pastor, F., Burlaud-Gaillard, J., Dumans, A., Seigneuret, F., Moreau, A., Patient, R., Eymieux, S., de Rocquigny, H., Hourioux, C., et al. (2020). Hepatitis B virus entry into HepG2-NTCP cells requires clathrin-mediated endocytosis. Cell Microbiol *22*, e13205. 10.1111/cmi.13205.

Heslop, J.A., Rowe, C., Walsh, J., Sison-Young, R., Jenkins, R., Kamalian, L., Kia, R., Hay, D., Jones, R.P., Malik, H.Z., et al. (2017). Mechanistic evaluation of primary human hepatocyte culture using global proteomic analysis reveals a selective dedifferentiation profile. Arch Toxicol *91*, 439-452. 10.1007/s00204-016-1694-y.

Hettiarachchi, G.K., Katneni, U.K., Hunt, R.C., Kames, J.M., Athey, J.C., Bar, H., Sauna, Z.E., McGill, J.R., Ibla, J.C., and Kimchi-Sarfaty, C. (2019). Translational and transcriptional responses in human primary hepatocytes under hypoxia. Am J Physiol Gastrointest Liver Physiol *316*, G720-G734. 10.1152/ajpgi.00331.2018.

Hillringhaus, L., Yue, W.W., Rose, N.R., Ng, S.S., Gileadi, C., Loenarz, C., Bello, S.H., Bray, J.E., Schofield, C.J., and Oppermann, U. (2011). Structural and evolutionary basis for the dual substrate selectivity of human KDM4 histone demethylase family. J Biol Chem *286*, 41616-41625. 10.1074/jbc.M111.283689.

Hinojosa-Laborde, C., and Mifflin, S.W. (2005). Sex differences in blood pressure response to intermittent hypoxia in rats. Hypertension *46*, 1016-1021. 10.1161/01.HYP.0000175477.33816.f3.

Hirsila, M., Koivunen, P., Gunzler, V., Kivirikko, K.I., and Myllyharju, J. (2003). Characterization of the human prolyl 4-hydroxylases that modify the hypoxia-inducible factor. J Biol Chem *278*, 30772-30780. 10.1074/jbc.M304982200.

Hoffman, E.C., Reyes, H., Chu, F.F., Sander, F., Conley, L.H., Brooks, B.A., and Hankinson, O. (1991). Cloning of a factor required for activity of the Ah (dioxin) receptor. Science *252*, 954-958. 10.1126/science.1852076.

Hogenesch, J.B., Gu, Y.Z., Moran, S.M., Shimomura, K., Radcliffe, L.A., Takahashi, J.S., and Bradfield, C.A. (2000). The basic helix-loop-helix-PAS protein

MOP9 is a brain-specific heterodimeric partner of circadian and hypoxia factors. J Neurosci *20*, RC83.

Holmes, J.A., Rutledge, S.M., and Chung, R.T. (2019). Direct-acting antiviral treatment for hepatitis C. Lancet *393*, 1392-1394. 10.1016/S0140-6736(18)32326-2.

Holmquist-Mengelbier, L., Fredlund, E., Lofstedt, T., Noguera, R., Navarro, S., Nilsson, H., Pietras, A., Vallon-Christersson, J., Borg, A., Gradin, K., et al. (2006). Recruitment of HIF-1alpha and HIF-2alpha to common target genes is differentially regulated in neuroblastoma: HIF-2alpha promotes an aggressive phenotype. Cancer Cell *10*, 413-423. 10.1016/j.ccr.2006.08.026.

Honer Zu Siederdissen, C., and Cornberg, M. (2014). The role of HBsAg levels in the current management of chronic HBV infection. Ann Gastroenterol *27*, 105-112.

Hong, X., Kim, E.S., and Guo, H. (2017). Epigenetic regulation of hepatitis B virus covalently closed circular DNA: Implications for epigenetic therapy against chronic hepatitis B. Hepatology *66*, 2066-2077. 10.1002/hep.29479.

Hopkinson, R.J., Tumber, A., Yapp, C., Chowdhury, R., Aik, W., Che, K.H., Li, X.S., Kristensen, J.B.L., King, O.N.F., Chan, M.C., et al. (2013). 5-Carboxy-8-hydroxyquinoline is a Broad Spectrum 2-Oxoglutarate Oxygenase Inhibitor which Causes Iron Translocation. Chem Sci *4*, 3110-3117. 10.1039/C3SC51122G.

Hosel, M., Quasdorff, M., Ringelhan, M., Kashkar, H., Debey-Pascher, S., Sprinzl, M.F., Bockmann, J.H., Arzberger, S., Webb, D., von Olshausen, G., et al. (2017). Hepatitis B Virus Activates Signal Transducer and Activator of Transcription 3 Supporting Hepatocyte Survival and Virus Replication. Cell Mol Gastroenterol Hepatol *4*, 339-363. 10.1016/j.jcmgh.2017.07.003.

Hossain, M.B., Ji, P., Anish, R., Jacobson, R.H., and Takada, S. (2009). Poly(ADP-ribose) Polymerase 1 Interacts with Nuclear Respiratory Factor 1 (NRF-1) and Plays a Role in NRF-1 Transcriptional Regulation. J Biol Chem *284*, 8621-8632. 10.1074/jbc.M807198200.

Hou, J., Liu, Z., and Gu, F. (2005). Epidemiology and Prevention of Hepatitis B Virus Infection. Int J Med Sci *2*, 50-57. 10.7150/ijms.2.50.

Houghton, M. (2009). Discovery of the hepatitis C virus. Liver Int *29 Suppl 1*, 82-88. 10.1111/j.1478-3231.2008.01925.x.

Howe, F.S., Fischl, H., Murray, S.C., and Mellor, J. (2017). Is H3K4me3 instructive for transcription activation? Bioessays *39*, 1-12. 10.1002/bies.201600095.

Hrecka, K., Hao, C., Gierszewska, M., Swanson, S.K., Kesik-Brodacka, M., Srivastava, S., Florens, L., Washburn, M.P., and Skowronski, J. (2011). Vpx

relieves inhibition of HIV-1 infection of macrophages mediated by the SAMHD1 protein. Nature *474*, 658-661. 10.1038/nature10195.

Hu, C.J., Wang, L.Y., Chodosh, L.A., Keith, B., and Simon, M.C. (2003). Differential roles of hypoxia-inducible factor 1alpha (HIF-1alpha) and HIF-2alpha in hypoxic gene regulation. Mol Cell Biol *23*, 9361-9374. 10.1128/MCB.23.24.9361-9374.2003.

Hu, J., Protzer, U., and Siddiqui, A. (2019). Revisiting Hepatitis B Virus: Challenges of Curative Therapies. J Virol *93*. 10.1128/JVI.01032-19.

Hu, J., and Seeger, C. (1996). Hsp90 is required for the activity of a hepatitis B virus reverse transcriptase. Proc Natl Acad Sci U S A *93*, 1060-1064. 10.1073/pnas.93.3.1060.

Hu, K.Q., and Siddiqui, A. (1991). Regulation of the hepatitis B virus gene expression by the enhancer element I. Virology *181*, 721-726. 10.1016/0042-6822(91)90906-r.

Huan, B., Kosovsky, M.J., and Siddiqui, A. (1995). Retinoid X receptor alpha transactivates the hepatitis B virus enhancer 1 element by forming a heterodimeric complex with the peroxisome proliferator-activated receptor. J Virol *69*, 547-551. 10.1128/JVI.69.1.547-551.1995.

Huang, H.C., Chen, C.C., Chang, W.C., Tao, M.H., and Huang, C. (2012a). Entry of hepatitis B virus into immortalized human primary hepatocytes by clathrin-dependent endocytosis. J Virol *86*, 9443-9453. 10.1128/JVI.00873-12.

Huang, L.R., Gabel, Y.A., Graf, S., Arzberger, S., Kurts, C., Heikenwalder, M., Knolle, P.A., and Protzer, U. (2012b). Transfer of HBV genomes using low doses of adenovirus vectors leads to persistent infection in immune competent mice. Gastroenterology *142*, 1447-1450 e1443. 10.1053/j.gastro.2012.03.006.

Huang, Z.M., Huang, Q.W., Qin, Y.Q., He, Y.Z., Qin, H.J., Zhou, Y.N., Xu, X., and Huang, M.J. (2005). YMDD mutations in patients with chronic hepatitis B untreated with antiviral medicines. World J Gastroenterol *11*, 867-870. 10.3748/wjg.v11.i6.867.

Hulo, C., de Castro, E., Masson, P., Bougueleret, L., Bairoch, A., Xenarios, I., and Le Mercier, P. (2011). ViralZone: a knowledge resource to understand virus diversity. Nucleic Acids Res *39*, D576-582. 10.1093/nar/gkq901.

Hyjek, M., Figiel, M., and Nowotny, M. (2019). RNases H: Structure and mechanism. DNA Repair (Amst) *84*, 102672. 10.1016/j.dnarep.2019.102672.

Iannacone, M., and Guidotti, L.G. (2021). Immunobiology and pathogenesis of hepatitis B virus infection. Nat Rev Immunol. 10.1038/s41577-021-00549-4.

Iannacone, M., Sitia, G., Isogawa, M., Marchese, P., Castro, M.G., Lowenstein, P.R., Chisari, F.V., Ruggeri, Z.M., and Guidotti, L.G. (2005). Platelets mediate cytotoxic T lymphocyte-induced liver damage. Nat Med *11*, 1167-1169. 10.1038/nm1317.

Iannacone, M., Sitia, G., Ruggeri, Z.M., and Guidotti, L.G. (2007). HBV pathogenesis in animal models: recent advances on the role of platelets. J Hepatol *46*, 719-726. 10.1016/j.jhep.2007.01.007.

Ignacak, M.L., Harbaugh, S.V., Dayyat, E., Row, B.W., Gozal, D., and Czyzyk-Krzeska, M.F. (2009). Intermittent hypoxia regulates RNA polymerase II in hippocampus and prefrontal cortex. Neuroscience *158*, 1436-1445. 10.1016/j.neuroscience.2008.11.025.

Imam, H., Khan, M., Gokhale, N.S., McIntyre, A.B.R., Kim, G.W., Jang, J.Y., Kim, S.J., Mason, C.E., Horner, S.M., and Siddiqui, A. (2018). N6-methyladenosine modification of hepatitis B virus RNA differentially regulates the viral life cycle. Proc Natl Acad Sci U S A *115*, 8829-8834. 10.1073/pnas.1808319115.

Imtiyaz, H.Z., and Simon, M.C. (2010). Hypoxia-inducible factors as essential regulators of inflammation. Curr Top Microbiol Immunol *345*, 105-120. 10.1007/82_2010_74.

Ishak, K., Baptista, A., Bianchi, L., Callea, F., De Groote, J., Gudat, F., Denk, H., Desmet, V., Korb, G., MacSween, R.N., and et al. (1995). Histological grading and staging of chronic hepatitis. J Hepatol *22*, 696-699. 10.1016/0168-8278(95)80226-6.

Islam, M.S., Leissing, T.M., Chowdhury, R., Hopkinson, R.J., and Schofield, C.J. (2018). 2-Oxoglutarate-Dependent Oxygenases. Annu Rev Biochem *87*, 585-620. 10.1146/annurev-biochem-061516-044724.

Islami, F., Miller, K.D., Siegel, R.L., Fedewa, S.A., Ward, E.M., and Jemal, A. (2017). Disparities in liver cancer occurrence in the United States by race/ethnicity and state. CA Cancer J Clin *67*, 273-289. 10.3322/caac.21402.

Ivan, M., Kondo, K., Yang, H., Kim, W., Valiando, J., Ohh, M., Salic, A., Asara, J.M., Lane, W.S., and Kaelin, W.G., Jr. (2001). HIFalpha targeted for VHL-mediated destruction by proline hydroxylation: implications for O2 sensing. Science *292*, 464-468. 10.1126/science.1059817.

Iwamoto, M., Saso, W., Nishioka, K., Ohashi, H., Sugiyama, R., Ryo, A., Ohki, M., Yun, J.H., Park, S.Y., Ohshima, T., et al. (2020). The machinery for endocytosis of epidermal growth factor receptor coordinates the transport of incoming hepatitis B virus to the endosomal network. J Biol Chem *295*, 800-807. 10.1074/jbc.AC119.010366.

Iwamoto, M., Saso, W., Sugiyama, R., Ishii, K., Ohki, M., Nagamori, S., Suzuki, R., Aizaki, H., Ryo, A., Yun, J.H., et al. (2019). Epidermal growth factor receptor is a host-entry cofactor triggering hepatitis B virus internalization. Proc Natl Acad Sci U S A *116*, 8487-8492. 10.1073/pnas.1811064116.

Iwamoto, M., Watashi, K., Tsukuda, S., Aly, H.H., Fukasawa, M., Fujimoto, A., Suzuki, R., Aizaki, H., Ito, T., Koiwai, O., et al. (2014). Evaluation and identification of hepatitis B virus entry inhibitors using HepG2 cells overexpressing a membrane transporter NTCP. Biochem Biophys Res Commun *443*, 808-813. 10.1016/j.bbrc.2013.12.052.

Jaakkola, P., Mole, D.R., Tian, Y.M., Wilson, M.I., Gielbert, J., Gaskell, S.J., von Kriegsheim, A., Hebestreit, H.F., Mukherji, M., Schofield, C.J., et al. (2001). Targeting of HIF-alpha to the von Hippel-Lindau ubiquitylation complex by O2-regulated prolyl hydroxylation. Science *292*, 468-472. 10.1126/science.1059796.

Jack, A.P., Bussemer, S., Hahn, M., Punzeler, S., Snyder, M., Wells, M., Csankovszki, G., Solovei, I., Schotta, G., and Hake, S.B. (2013). H3K56me3 is a novel, conserved heterochromatic mark that largely but not completely overlaps with H3K9me3 in both regulation and localization. PLoS One *8*, e51765. 10.1371/journal.pone.0051765.

Jafari, S., Buxton, J.A., Afshar, K., Copes, R., and Baharlou, S. (2012). Tattooing and risk of hepatitis B: a systematic review and meta-analysis. Can J Public Health *103*, 207-212.

Jain, R.K. (2005). Normalization of tumor vasculature: an emerging concept in antiangiogenic therapy. Science *307*, 58-62. 10.1126/science.1104819.

Jang, J.W., Kim, H.S., Kim, J.S., Lee, S.K., Han, J.W., Sung, P.S., Bae, S.H., Choi, J.Y., Yoon, S.K., Han, D.J., et al. (2021). Distinct Patterns of HBV Integration and TERT Alterations between in Tumor and Non-Tumor Tissue in Patients with Hepatocellular Carcinoma. Int J Mol Sci *22*. 10.3390/ijms22137056.

Jauregui, P., Logue, E.C., Schultz, M.L., Fung, S., and Landau, N.R. (2015). Degradation of SAMHD1 by Vpx Is Independent of Uncoating. J Virol *89*, 5701-5713. 10.1128/JVI.03575-14.

Jenkins, P.J., Binne, U.K., and Farrell, P.J. (2000). Histone acetylation and reactivation of Epstein-Barr virus from latency. J Virol *74*, 710-720. 10.1128/jvi.74.2.710-720.2000.

Jeong, J.H., Kwak, D.S., Rho, H.M., and Jung, G. (1996). The catalytic properties of human hepatitis B virus polymerase. Biochem Biophys Res Commun *223*, 264-271. 10.1006/bbrc.1996.0882.

Jiang, B., Himmelsbach, K., Ren, H., Boller, K., and Hildt, E. (2015). Subviral Hepatitis B Virus Filaments, like Infectious Viral Particles, Are Released via Multivesicular Bodies. J Virol *90*, 3330-3341. 10.1128/JVI.03109-15.

Jiang, H., Garcia, V., Yanum, J.A., Lee, J., and Dai, G. (2021). Circadian clock core component Bmal1 dictates cell cycle rhythm of proliferating hepatocytes during liver regeneration. Am J Physiol Gastrointest Liver Physiol *321*, G389-G399. 10.1152/ajpgi.00204.2021.

Jiang, J., and Tang, H. (2010). Mechanism of inhibiting type I interferon induction by hepatitis B virus X protein. Protein Cell *1*, 1106-1117. 10.1007/s13238-010-0141-8.

Johansson, C., Tumber, A., Che, K., Cain, P., Nowak, R., Gileadi, C., and Oppermann, U. (2014). The roles of Jumonji-type oxygenases in human disease. Epigenomics *6*, 89-120. 10.2217/epi.13.79.

Johnston, D., Kim, J., Taylor, J.F., Earley, B., McCabe, M.S., Lemon, K., Duffy, C., McMenamy, M., Cosby, S.L., and Waters, S.M. (2021). ATAC-Seq identifies regions of open chromatin in the bronchial lymph nodes of dairy calves experimentally challenged with bovine respiratory syncytial virus. BMC Genomics *22*, 14. 10.1186/s12864-020-07268-5.

Jones, S.A., Boregowda, R., Spratt, T.E., and Hu, J. (2012). In vitro epsilon RNA-dependent protein priming activity of human hepatitis B virus polymerase. J Virol *86*, 5134-5150. 10.1128/JVI.07137-11.

Juhling, F., Saviano, A., Ponsolles, C., Heydmann, L., Crouchet, E., Durand, S.C., El Saghire, H., Felli, E., Lindner, V., Pessaux, P., et al. (2021). Hepatitis B virus compartmentalization and single-cell differentiation in hepatocellular carcinoma. Life Sci Alliance *4*. 10.26508/lsa.202101036.

Jung, Y., Isaacs, J.S., Lee, S., Trepel, J., Liu, Z.G., and Neckers, L. (2003a). Hypoxia-inducible factor induction by tumour necrosis factor in normoxic cells requires receptor-interacting protein-dependent nuclear factor kappa B activation. Biochem J *370*, 1011-1017. 10.1042/BJ20021279.

Jung, Y.J., Isaacs, J.S., Lee, S., Trepel, J., and Neckers, L. (2003b). IL-1beta-mediated up-regulation of HIF-1alpha via an NFkappaB/COX-2 pathway identifies HIF-1 as a critical link between inflammation and oncogenesis. FASEB J *17*, 2115-2117. 10.1096/fj.03-0329fje.

Jungermann, K., and Kietzmann, T. (2000). Oxygen: modulator of metabolic zonation and disease of the liver. Hepatology *31*, 255-260. 10.1002/hep.510310201.

Junker, M., Galle, P., and Schaller, H. (1987). Expression and replication of the hepatitis B virus genome under foreign promoter control. Nucleic Acids Res *15*, 10117-10132. 10.1093/nar/15.24.10117.

Kadauke, S., and Blobel, G.A. (2009). Chromatin loops in gene regulation. Biochim Biophys Acta *1789*, 17-25. 10.1016/j.bbagrm.2008.07.002.

Kaelin, W.G., Jr., and Ratcliffe, P.J. (2008). Oxygen sensing by metazoans: the central role of the HIF hydroxylase pathway. Mol Cell *30*, 393-402. 10.1016/j.molcel.2008.04.009.

Kallio, P.J., Pongratz, I., Gradin, K., McGuire, J., and Poellinger, L. (1997). Activation of hypoxia-inducible factor 1alpha: posttranscriptional regulation and conformational change by recruitment of the Arnt transcription factor. Proc Natl Acad Sci U S A *94*, 5667-5672. 10.1073/pnas.94.11.5667.

Kamiya, H., Miyamoto, S., Goto, H., Kanda, G.N., Kobayashi, M., Matsuoka, I., and Harashima, H. (2013). Enhanced transgene expression from chromatinized plasmid DNA in mouse liver. Int J Pharm *441*, 146-150. 10.1016/j.ijpharm.2012.12.004.

Kane, M.A. (1996). Global status of hepatitis B immunisation. Lancet *348*, 696. 10.1016/S0140-6736(05)65598-5.

Kann, M., Sodeik, B., Vlachou, A., Gerlich, W.H., and Helenius, A. (1999). Phosphorylation-dependent binding of hepatitis B virus core particles to the nuclear pore complex. J Cell Biol *145*, 45-55. 10.1083/jcb.145.1.45.

Kannan, R.P., Hensley, L.L., Evers, L.E., Lemon, S.M., and McGivern, D.R. (2011). Hepatitis C virus infection causes cell cycle arrest at the level of initiation of mitosis. J Virol *85*, 7989-8001. 10.1128/JVI.00280-11.

Kao, J.H. (2002). Hepatitis B viral genotypes: clinical relevance and molecular characteristics. J Gastroenterol Hepatol *17*, 643-650. 10.1046/j.1440-1746.2002.02737.x.

Kasper, L.H., Boussouar, F., Boyd, K., Xu, W., Biesen, M., Rehg, J., Baudino, T.A., Cleveland, J.L., and Brindle, P.K. (2005). Two transactivation mechanisms cooperate for the bulk of HIF-1-responsive gene expression. EMBO J *24*, 3846-3858. 10.1038/sj.emboj.7600846.

Kawale, A.S., and Povirk, L.F. (2018). Tyrosyl-DNA phosphodiesterases: rescuing the genome from the risks of relaxation. Nucleic Acids Res *46*, 520-537. 10.1093/nar/gkx1219.

Kawata, H., Yamada, K., Shou, Z., Mizutani, T., Yazawa, T., Yoshino, M., Sekiguchi, T., Kajitani, T., and Miyamoto, K. (2003). Zinc-fingers and homeoboxes

(ZHX) 2, a novel member of the ZHX family, functions as a transcriptional repressor. Biochem J *373*, 747-757. 10.1042/BJ20030171.

Keeley, T.P., and Mann, G.E. (2019). Defining Physiological Normoxia for Improved Translation of Cell Physiology to Animal Models and Humans. Physiol Rev *99*, 161-234. 10.1152/physrev.00041.2017.

Kenneth, N.S., Mudie, S., van Uden, P., and Rocha, S. (2009). SWI/SNF regulates the cellular response to hypoxia. J Biol Chem *284*, 4123-4131. 10.1074/jbc.M808491200.

Kenneth, N.S., and Rocha, S. (2008). Regulation of gene expression by hypoxia. Biochem J *414*, 19-29. 10.1042/BJ20081055.

Kerur, N., Veettil, M.V., Sharma-Walia, N., Bottero, V., Sadagopan, S., Otageri, P., and Chandran, B. (2011). IFI16 acts as a nuclear pathogen sensor to induce the inflammasome in response to Kaposi Sarcoma-associated herpesvirus infection. Cell Host Microbe *9*, 363-375. 10.1016/j.chom.2011.04.008.

Kholodenko, I.V., and Yarygin, K.N. (2017). Cellular Mechanisms of Liver Regeneration and Cell-Based Therapies of Liver Diseases. Biomed Res Int *2017*, 8910821. 10.1155/2017/8910821.

Kidder, B.L., Hu, G., and Zhao, K. (2011). ChIP-Seq: technical considerations for obtaining high-quality data. Nat Immunol *12*, 918-922. 10.1038/ni.2117.

Kietzmann, T. (2017). Metabolic zonation of the liver: The oxygen gradient revisited. Redox Biol *11*, 622-630. 10.1016/j.redox.2017.01.012.

Kim, B.K., Lim, S.O., and Park, Y.G. (2008). Requirement of the cyclic adenosine monophosphate response element-binding protein for hepatitis B virus replication. Hepatology *48*, 361-373. 10.1002/hep.22359.

Kim, B.K., Revill, P.A., and Ahn, S.H. (2011a). HBV genotypes: relevance to natural history, pathogenesis and treatment of chronic hepatitis B. Antivir Ther *16*, 1169-1186. 10.3851/IMP1982.

Kim, C.M., Koike, K., Saito, I., Miyamura, T., and Jay, G. (1991). HBx gene of hepatitis B virus induces liver cancer in transgenic mice. Nature *351*, 317-320. 10.1038/351317a0.

Kim, G.W., Imam, H., and Siddiqui, A. (2021). The RNA Binding Proteins YTHDC1 and FMRP Regulate the Nuclear Export of N(6)-Methyladenosine-Modified Hepatitis B Virus Transcripts and Affect the Viral Life Cycle. J Virol *95*, e0009721. 10.1128/JVI.00097-21.

Kim, G.W., and Siddiqui, A. (2021). Hepatitis B virus X protein recruits methyltransferases to affect cotranscriptional N6-methyladenosine modification of viral/host RNAs. Proc Natl Acad Sci U S A *118*. 10.1073/pnas.2019455118.

Kim, J.W., Lee, S.H., Park, Y.S., Hwang, J.H., Jeong, S.H., Kim, N., and Lee, D.H. (2011b). Replicative activity of hepatitis B virus is negatively associated with methylation of covalently closed circular DNA in advanced hepatitis B virus infection. Intervirology *54*, 316-325. 10.1159/000321450.

Kim, K., Boo, K., Yu, Y.S., Oh, S.K., Kim, H., Jeon, Y., Bhin, J., Hwang, D., Kim, K.I., Lee, J.S., et al. (2017). RORalpha controls hepatic lipid homeostasis via negative regulation of PPARgamma transcriptional network. Nat Commun *8*, 162. 10.1038/s41467-017-00215-1.

Kim, M.S., Chung, N.G., Kang, M.R., Yoo, N.J., and Lee, S.H. (2011c). Genetic and expressional alterations of CHD genes in gastric and colorectal cancers. Histopathology *58*, 660-668. 10.1111/j.1365-2559.2011.03819.x.

Kindrick, J.D., and Mole, D.R. (2020). Hypoxic Regulation of Gene Transcription and Chromatin: Cause and Effect. Int J Mol Sci *21*. 10.3390/ijms21218320.

Kirmes, I., Szczurek, A., Prakash, K., Charapitsa, I., Heiser, C., Musheev, M., Schock, F., Fornalczyk, K., Ma, D., Birk, U., et al. (2015). A transient ischemic environment induces reversible compaction of chromatin. Genome Biol *16*, 246. 10.1186/s13059-015-0802-2.

Kitamura, K., Que, L., Shimadu, M., Koura, M., Ishihara, Y., Wakae, K., Nakamura, T., Watashi, K., Wakita, T., and Muramatsu, M. (2018). Flap endonuclease 1 is involved in cccDNA formation in the hepatitis B virus. PLoS Pathog *14*, e1007124. 10.1371/journal.ppat.1007124.

Kliewer, S.A., Umesono, K., Heyman, R.A., Mangelsdorf, D.J., Dyck, J.A., and Evans, R.M. (1992). Retinoid X receptor-COUP-TF interactions modulate retinoic acid signaling. Proc Natl Acad Sci U S A *89*, 1448-1452. 10.1073/pnas.89.4.1448.

Klose, R.J., Yamane, K., Bae, Y., Zhang, D., Erdjument-Bromage, H., Tempst, P., Wong, J., and Zhang, Y. (2006). The transcriptional repressor JHDM3A demethylates trimethyl histone H3 lysine 9 and lysine 36. Nature *442*, 312-316. 10.1038/nature04853.

Ko, C., Chakraborty, A., Chou, W.M., Hasreiter, J., Wettengel, J.M., Stadler, D., Bester, R., Asen, T., Zhang, K., Wisskirchen, K., et al. (2018). Hepatitis B virus genome recycling and de novo secondary infection events maintain stable cccDNA levels. J Hepatol *69*, 1231-1241. 10.1016/j.jhep.2018.08.012.

Kock, J., and Blum, H.E. (2008). Hypermutation of hepatitis B virus genomes by APOBEC3G, APOBEC3C and APOBEC3H. J Gen Virol *89*, 1184-1191. 10.1099/vir.0.83507-0.

Kock, J., Rosler, C., Zhang, J.J., Blum, H.E., Nassal, M., and Thoma, C. (2010). Generation of covalently closed circular DNA of hepatitis B viruses via intracellular recycling is regulated in a virus specific manner. PLoS Pathog *6*, e1001082. 10.1371/journal.ppat.1001082.

Kohli, R.M., and Zhang, Y. (2013). TET enzymes, TDG and the dynamics of DNA demethylation. Nature *502*, 472-479. 10.1038/nature12750.

Konig, A., Doring, B., Mohr, C., Geipel, A., Geyer, J., and Glebe, D. (2014). Kinetics of the bile acid transporter and hepatitis B virus receptor Na+/taurocholate cotransporting polypeptide (NTCP) in hepatocytes. J Hepatol *61*, 867-875. 10.1016/j.jhep.2014.05.018.

Koniger, C., Wingert, I., Marsmann, M., Rosler, C., Beck, J., and Nassal, M. (2014). Involvement of the host DNA-repair enzyme TDP2 in formation of the covalently closed circular DNA persistence reservoir of hepatitis B viruses. Proc Natl Acad Sci U S A *111*, E4244-4253. 10.1073/pnas.1409986111.

Kornberg, R.D. (1974). Chromatin structure: a repeating unit of histones and DNA. Science *184*, 868-871. 10.1126/science.184.4139.868.

Kornblihtt, A.R. (2012). CTCF: from insulators to alternative splicing regulation. Cell Res *22*, 450-452. 10.1038/cr.2012.22.

Koshy, R., Maupas, P., Muller, R., and Hofschneider, P.H. (1981). Detection of hepatitis B virus-specific DNA in the genomes of human hepatocellular carcinoma and liver cirrhosis tissues. J Gen Virol *57*, 95-102. 10.1099/0022-1317-57-1-95.

Kouzarides, T. (2007). Chromatin modifications and their function. Cell *128*, 693-705. 10.1016/j.cell.2007.02.005.

Kramvis, A. (2014). Genotypes and genetic variability of hepatitis B virus. Intervirology *57*, 141-150. 10.1159/000360947.

Kramvis, A., Kew, M., and Francois, G. (2005). Hepatitis B virus genotypes. Vaccine *23*, 2409-2423. 10.1016/j.vaccine.2004.10.045.

Kramvis, A., and Kew, M.C. (2005). Relationship of genotypes of hepatitis B virus to mutations, disease progression and response to antiviral therapy. J Viral Hepat *12*, 456-464. 10.1111/j.1365-2893.2005.00624.x.

Kramvis, A., and Paraskevis, D. (2013). Subgenotype A1 of HBV--tracing human migrations in and out of Africa. Antivir Ther *18*, 513-521. 10.3851/IMP2657.

Krebs, H.A., Freedland, R.A., Hems, R., and Stubbs, M. (1969). Inhibition of hepatic gluconeogenesis by ethanol. Biochem J *112*, 117-124. 10.1042/bj1120117.

Kriaucionis, S., and Heintz, N. (2009). The nuclear DNA base 5-hydroxymethylcytosine is present in Purkinje neurons and the brain. Science *324*, 929-930. 10.1126/science.1169786.

Krock, B.L., Skuli, N., and Simon, M.C. (2011). Hypoxia-induced angiogenesis: good and evil. Genes Cancer *2*, 1117-1133. 10.1177/1947601911423654.

Kubes, P., and Jenne, C. (2018). Immune Responses in the Liver. Annu Rev Immunol *36*, 247-277. 10.1146/annurev-immunol-051116-052415.

Kuiper, C., and Vissers, M.C. (2014). Ascorbate as a co-factor for fe- and 2-oxoglutarate dependent dioxygenases: physiological activity in tumor growth and progression. Front Oncol *4*, 359. 10.3389/fonc.2014.00359.

Kulik, L., and El-Serag, H.B. (2019). Epidemiology and Management of Hepatocellular Carcinoma. Gastroenterology *156*, 477-491 e471. 10.1053/j.gastro.2018.08.065.

Kumar, M., Jung, S.Y., Hodgson, A.J., Madden, C.R., Qin, J., and Slagle, B.L. (2011). Hepatitis B virus regulatory HBx protein binds to adaptor protein IPS-1 and inhibits the activation of beta interferon. J Virol *85*, 987-995. 10.1128/JVI.01825-10.

Kwon, S.Y., and Lee, C.H. (2011). Epidemiology and prevention of hepatitis B virus infection. Korean J Hepatol *17*, 87-95. 10.3350/kjhep.2011.17.2.87.

Labbe, R.M., Holowatyj, A., and Yang, Z.Q. (2013). Histone lysine demethylase (KDM) subfamily 4: structures, functions and therapeutic potential. Am J Transl Res *6*, 1-15.

Ladner, S.K., Otto, M.J., Barker, C.S., Zaifert, K., Wang, G.H., Guo, J.T., Seeger, C., and King, R.W. (1997). Inducible expression of human hepatitis B virus (HBV) in stably transfected hepatoblastoma cells: a novel system for screening potential inhibitors of HBV replication. Antimicrob Agents Chemother *41*, 1715-1720. 10.1128/AAC.41.8.1715.

Laguette, N., Sobhian, B., Casartelli, N., Ringeard, M., Chable-Bessia, C., Segeral, E., Yatim, A., Emiliani, S., Schwartz, O., and Benkirane, M. (2011). SAMHD1 is the dendritic- and myeloid-cell-specific HIV-1 restriction factor counteracted by Vpx. Nature *474*, 654-657. 10.1038/nature10117.

Lambert, C., Doring, T., and Prange, R. (2007). Hepatitis B virus maturation is sensitive to functional inhibition of ESCRT-III, Vps4, and gamma 2-adaptin. J Virol *81*, 9050-9060. 10.1128/JVI.00479-07.

Land, S.C., and Tee, A.R. (2007). Hypoxia-inducible factor 1alpha is regulated by the mammalian target of rapamycin (mTOR) via an mTOR signaling motif. J Biol Chem *282*, 20534-20543. 10.1074/jbc.M611782200.

Lane, D.P. (1992). Cancer. p53, guardian of the genome. Nature *358*, 15-16. 10.1038/358015a0.

Laras, A., Koskinas, J., Dimou, E., Kostamena, A., and Hadziyannis, S.J. (2006). Intrahepatic levels and replicative activity of covalently closed circular hepatitis B virus DNA in chronically infected patients. Hepatology *44*, 694-702. 10.1002/hep.21299.

Larsson, S.B., Tripodi, G., Raimondo, G., Saitta, C., Norkrans, G., Pollicino, T., and Lindh, M. (2018). Integration of hepatitis B virus DNA in chronically infected patients assessed by Alu-PCR. J Med Virol *90*, 1568-1575. 10.1002/jmv.25227.

Lauer, U., Weiss, L., Lipp, M., Hofschneider, P.H., and Kekule, A.S. (1994). The hepatitis B virus preS2/St transactivator utilizes AP-1 and other transcription factors for transactivation. Hepatology *19*, 23-31.

Laukka, T., Mariani, C.J., Ihantola, T., Cao, J.Z., Hokkanen, J., Kaelin, W.G., Jr., Godley, L.A., and Koivunen, P. (2016). Fumarate and Succinate Regulate Expression of Hypoxia-inducible Genes via TET Enzymes. J Biol Chem *291*, 4256-4265. 10.1074/jbc.M115.688762.

Lavanchy, D. (2004). Hepatitis B virus epidemiology, disease burden, treatment, and current and emerging prevention and control measures. J Viral Hepat *11*, 97-107. 10.1046/j.1365-2893.2003.00487.x.

Le, C., Sirajee, R., Steenbergen, R., Joyce, M.A., Addison, W.R., and Tyrrell, D.L. (2021). In Vitro Infection with Hepatitis B Virus Using Differentiated Human Serum Culture of Huh7.5-NTCP Cells without Requiring Dimethyl Sulfoxide. Viruses *13*. 10.3390/v13010097.

Lebosse, F., Inchauspe, A., Locatelli, M., Miaglia, C., Diederichs, A., Fresquet, J., Chapus, F., Hamed, K., Testoni, B., and Zoulim, F. (2020). Quantification and epigenetic evaluation of the residual pool of hepatitis B covalently closed circular DNA in long-term nucleoside analogue-treated patients. Sci Rep *10*, 21097. 10.1038/s41598-020-78001-1.

Lebosse, F., Testoni, B., Fresquet, J., Facchetti, F., Galmozzi, E., Fournier, M., Hervieu, V., Berthillon, P., Berby, F., Bordes, I., et al. (2017). Intrahepatic innate

immune response pathways are downregulated in untreated chronic hepatitis B. J Hepatol *66*, 897-909. 10.1016/j.jhep.2016.12.024.

Ledent, V., Paquet, O., and Vervoort, M. (2002). Phylogenetic analysis of the human basic helix-loop-helix proteins. Genome Biol *3*, RESEARCH0030. 10.1186/gb-2002-3-6-research0030.

Lee, H.Y., Choi, K., Oh, H., Park, Y.K., and Park, H. (2014). HIF-1-dependent induction of Jumonji domain-containing protein (JMJD) 3 under hypoxic conditions. Mol Cells *37*, 43-50. 10.14348/molcells.2014.2250.

Lee, I.C., Huang, Y.H., Su, C.W., Wang, Y.J., Huo, T.I., Lee, K.C., and Lin, H.C. (2013). CXCL9 associated with sustained virological response in chronic hepatitis B patients receiving peginterferon alfa-2a therapy: a pilot study. PLoS One *8*, e76798. 10.1371/journal.pone.0076798.

Lee, J., Shin, M.K., Lee, H.J., Yoon, G., and Ryu, W.S. (2004). Three novel cis-acting elements required for efficient plus-strand DNA synthesis of the hepatitis B virus genome. J Virol *78*, 7455-7464. 10.1128/JVI.78.14.7455-7464.2004.

Lee, J.H., Ku, J.L., Park, Y.J., Lee, K.U., Kim, W.H., and Park, J.G. (1999). Establishment and characterization of four human hepatocellular carcinoma cell lines containing hepatitis B virus DNA. World J Gastroenterol *5*, 289-295. 10.3748/wjg.v5.i4.289.

Lee, J.H., Tate, C.M., You, J.S., and Skalnik, D.G. (2007). Identification and characterization of the human Set1B histone H3-Lys4 methyltransferase complex. J Biol Chem *282*, 13419-13428. 10.1074/jbc.M609809200.

Lee, J.S., Kim, Y., Kim, I.S., Kim, B., Choi, H.J., Lee, J.M., Shin, H.J., Kim, J.H., Kim, J.Y., Seo, S.B., et al. (2010). Negative regulation of hypoxic responses via induced Reptin methylation. Mol Cell *39*, 71-85. 10.1016/j.molcel.2010.06.008.

Lee, W.M. (1997). Hepatitis B virus infection. N Engl J Med *337*, 1733-1745. 10.1056/NEJM199712113372406.

Leek, R.D., Landers, R.J., Harris, A.L., and Lewis, C.E. (1999). Necrosis correlates with high vascular density and focal macrophage infiltration in invasive carcinoma of the breast. Br J Cancer *79*, 991-995. 10.1038/sj.bjc.6690158.

Leistner, C.M., Gruen-Bernhard, S., and Glebe, D. (2008). Role of glycosaminoglycans for binding and infection of hepatitis B virus. Cell Microbiol *10*, 122-133. 10.1111/j.1462-5822.2007.01023.x.

Lempp, F.A., and Urban, S. (2014). Inhibitors of hepatitis B virus attachment and entry. Intervirology *57*, 151-157. 10.1159/000360948.

Leroux-Roels, G. (2015). Old and new adjuvants for hepatitis B vaccines. Med Microbiol Immunol *204*, 69-78. 10.1007/s00430-014-0375-9.

Leroux-Roels, G., Cao, T., De Knibber, A., Meuleman, P., Roobrouck, A., Farhoudi, A., Vanlandschoot, P., and Desombere, I. (2001). Prevention of hepatitis B infections: vaccination and its limitations. Acta Clin Belg *56*, 209-219. 10.1179/acb.2001.032.

Leung, I.K., Krojer, T.J., Kochan, G.T., Henry, L., von Delft, F., Claridge, T.D., Oppermann, U., McDonough, M.A., and Schofield, C.J. (2010). Structural and mechanistic studies on gamma-butyrobetaine hydroxylase. Chem Biol *17*, 1316-1324. 10.1016/j.chembiol.2010.09.016.

Levrero, M., and Zucman-Rossi, J. (2016). Mechanisms of HBV-induced hepatocellular carcinoma. J Hepatol *64*, S84-S101. 10.1016/j.jhep.2016.02.021.

Li, B., Carey, M., and Workman, J.L. (2007a). The role of chromatin during transcription. Cell *128*, 707-719. 10.1016/j.cell.2007.01.015.

Li, F., Cheng, L., Murphy, C.M., Reszka-Blanco, N.J., Wu, Y., Chi, L., Hu, J., and Su, L. (2016a). Minicircle HBV cccDNA with a Gaussia luciferase reporter for investigating HBV cccDNA biology and developing cccDNA-targeting drugs. Sci Rep *6*, 36483. 10.1038/srep36483.

Li, G.Q., Xu, W.Z., Wang, J.X., Deng, W.W., Li, D., and Gu, H.X. (2007b). Combination of small interfering RNA and lamivudine on inhibition of human B virus replication in HepG2.2.15 cells. World J Gastroenterol *13*, 2324-2327. 10.3748/wjg.v13.i16.2324.

Li, J., and Ou, J.H. (2001). Differential regulation of hepatitis B virus gene expression by the Sp1 transcription factor. J Virol *75*, 8400-8406. 10.1128/jvi.75.18.8400-8406.2001.

Li, J., Xu, Z., Zheng, Y., Johnson, D.L., and Ou, J.H. (2002). Regulation of hepatocyte nuclear factor 1 activity by wild-type and mutant hepatitis B virus X proteins. J Virol *76*, 5875-5881. 10.1128/jvi.76.12.5875-5881.2002.

Li, L., Lei, Q.S., Zhang, S.J., Kong, L.N., and Qin, B. (2016b). Suppression of USP18 Potentiates the Anti-HBV Activity of Interferon Alpha in HepG2.2.15 Cells via JAK/STAT Signaling. PLoS One *11*, e0156496. 10.1371/journal.pone.0156496.

Li, L., Shen, H., Li, A., Zhang, Z., Wang, B., Wang, J., Zheng, X., Wu, J., Yang, D., Lu, M., and Song, J. (2013a). Inhibition of hepatitis B virus (HBV) gene expression and replication by HBx gene silencing in a hydrodynamic injection mouse model with a new clone of HBV genotype B. Virol J *10*, 214. 10.1186/1743-422X-10-214.

Li, M., Xie, Y., Wu, X., Kong, Y., and Wang, Y. (1995). HNF3 binds and activates the second enhancer, ENII, of hepatitis B virus. Virology *214*, 371-378. 10.1006/viro.1995.0046.

Li, M.M., Nilsen, A., Shi, Y., Fusser, M., Ding, Y.H., Fu, Y., Liu, B., Niu, Y., Wu, Y.S., Huang, C.M., et al. (2013b). ALKBH4-dependent demethylation of actin regulates actomyosin dynamics. Nat Commun *4*, 1832. 10.1038/ncomms2863.

Li, M.W., Hou, W., Wo, J.E., and Liu, K.Z. (2005). Character of HBV (hepatitis B virus) polymerase gene rtM204V/I and rtL180M mutation in patients with lamivudine resistance. J Zhejiang Univ Sci B *6*, 664-667. 10.1631/jzus.2005.B0664.

Li, S., Wang, Z., Li, Y., and Ding, G. (2017). Adaptive evolution of proteins in hepatitis B virus during divergence of genotypes. Sci Rep *7*, 1990. 10.1038/s41598-017-02012-8.

Li, Y., Ito, M., Sun, S., Chida, T., Nakashima, K., and Suzuki, T. (2016c). LUC7L3/CROP inhibits replication of hepatitis B virus via suppressing enhancer II/basal core promoter activity. Sci Rep *6*, 36741. 10.1038/srep36741.

Li, Y., Que, L., Fukano, K., Koura, M., Kitamura, K., Zheng, X., Kato, T., Aly, H.H., Watashi, K., Tsukuda, S., et al. (2020). MCPIP1 reduces HBV-RNA by targeting its epsilon structure. Scientific Reports *10*, 20763. 10.1038/s41598-020-77166-z.

Liaw, Y.F. (2005). The current management of HBV drug resistance. J Clin Virol *34 Suppl 1*, S143-146. 10.1016/s1386-6532(05)80025-3.

Liaw, Y.F., Brunetto, M.R., and Hadziyannis, S. (2010). The natural history of chronic HBV infection and geographical differences. Antivir Ther *15 Suppl 3*, 25-33. 10.3851/IMP1621.

Liaw, Y.F., and Chu, C.M. (2009). Hepatitis B virus infection. Lancet *373*, 582-592. 10.1016/S0140-6736(09)60207-5.

Liaw, Y.F., Chu, C.M., Su, I.J., Huang, M.J., Lin, D.Y., and Chang-Chien, C.S. (1983). Clinical and histological events preceding hepatitis B e antigen seroconversion in chronic type B hepatitis. Gastroenterology *84*, 216-219.

Liaw, Y.F., Yang, S.S., Chen, T.J., and Chu, C.M. (1985). Acute exacerbation in hepatitis B e antigen positive chronic type B hepatitis. A clinicopathological study. J Hepatol *1*, 227-233. 10.1016/s0168-8278(85)80050-7.

Liberzon, A., Birger, C., Thorvaldsdottir, H., Ghandi, M., Mesirov, J.P., and Tamayo, P. (2015). The Molecular Signatures Database (MSigDB) hallmark gene set collection. Cell Syst *1*, 417-425. 10.1016/j.cels.2015.12.004.

Liberzon, A., Subramanian, A., Pinchback, R., Thorvaldsdottir, H., Tamayo, P., and Mesirov, J.P. (2011). Molecular signatures database (MSigDB) 3.0. Bioinformatics *27*, 1739-1740. 10.1093/bioinformatics/btr260.

Lim, C.S., Sozzi, V., Littlejohn, M., Yuen, L.K.W., Warner, N., Betz-Stablein, B., Luciani, F., Revill, P.A., and Brown, C.M. (2021). Quantitative analysis of the splice variants expressed by the major hepatitis B virus genotypes. Microb Genom *7*. 10.1099/mgen.0.000492.

Lim, K.H., Choi, H.S., Park, Y.K., Park, E.S., Shin, G.C., Kim, D.H., Ahn, S.H., and Kim, K.H. (2013). HBx-induced NF-kappaB signaling in liver cells is potentially mediated by the ternary complex of HBx with p22-FLIP and NEMO. PLoS One *8*, e57331. 10.1371/journal.pone.0057331.

Lin, J., Gu, C., Shen, Z., Liu, Y., Wang, W., Tao, S., Cui, X., Liu, J., and Xie, Y. (2017). Hepatocyte nuclear factor 1alpha downregulates HBV gene expression and replication by activating the NF-kappaB signaling pathway. PLoS One *12*, e0174017. 10.1371/journal.pone.0174017.

Lin, Y., Nomura, T., Cheong, J., Dorjsuren, D., Iida, K., and Murakami, S. (1997). Hepatitis B virus X protein is a transcriptional modulator that communicates with transcription factor IIB and the RNA polymerase II subunit 5. J Biol Chem *272*, 7132-7139. 10.1074/jbc.272.11.7132.

Lindenbach, B.D., Evans, M.J., Syder, A.J., Wolk, B., Tellinghuisen, T.L., Liu, C.C., Maruyama, T., Hynes, R.O., Burton, D.R., McKeating, J.A., and Rice, C.M. (2005). Complete replication of hepatitis C virus in cell culture. Science *309*, 623-626. 10.1126/science.1114016.

Liu, D., Wu, A., Cui, L., Hao, R., Wang, Y., He, J., and Guo, D. (2014). Hepatitis B virus polymerase suppresses NF-kappaB signaling by inhibiting the activity of IKKs via interaction with Hsp90beta. PLoS One *9*, e91658. 10.1371/journal.pone.0091658.

Liu, H.Y., and Zhang, X.Y. (2015). Innate immune recognition of hepatitis B virus. World J Hepatol *7*, 2319-2322. 10.4254/wjh.v7.i21.2319.

Liu, P.J., Balfe, P., McKeating, J.A., and Schilling, M. (2020a). Oxygen Sensing and Viral Replication: Implications for Tropism and Pathogenesis. Viruses *12*. 10.3390/v12111213.

Liu, P.J., Harris, J.M., Marchi, E., D'Arienzo, V., Michler, T., Wing, P.A.C., Magri, A., Ortega-Prieto, A.M., van de Klundert, M., Wettengel, J., et al. (2020b). Hypoxic gene expression in chronic hepatitis B virus infected patients is not observed in state-of-the-art in vitro and mouse infection models. Sci Rep *10*, 14101. 10.1038/s41598-020-70865-7.

Liu, T., Song, H.L., Zheng, W.P., and Shen, Z.Y. (2015). Inhibition of HBV Replication in HepG2.2.15 Cells by Human Peripheral Blood Mononuclear Cell-Derived Dendritic Cells. Ann Clin Lab Sci *45*, 495-501.

Liu, X.H., Lin, J., Zhang, S.H., Zhang, S.M., Feitelson, M.A., Gao, H.J., and Zhu, M.H. (2008). COOH-terminal deletion of HBx gene is a frequent event in HBV-associated hepatocellular carcinoma. World J Gastroenterol *14*, 1346-1352. 10.3748/wjg.14.1346.

Liu, Y., Cheng, J., Siejka-Zielinska, P., Weldon, C., Roberts, H., Lopopolo, M., Magri, A., D'Arienzo, V., Harris, J.M., McKeating, J.A., and Song, C.X. (2020c). Accurate targeted long-read DNA methylation and hydroxymethylation sequencing with TAPS. Genome Biol *21*, 54. 10.1186/s13059-020-01969-6.

Liu, Y., Siejka-Zielinska, P., Velikova, G., Bi, Y., Yuan, F., Tomkova, M., Bai, C., Chen, L., Schuster-Bockler, B., and Song, C.X. (2019). Bisulfite-free direct detection of 5-methylcytosine and 5-hydroxymethylcytosine at base resolution. Nat Biotechnol *37*, 424-429. 10.1038/s41587-019-0041-2.

Lok, A.S. (2002). Chronic hepatitis B. N Engl J Med *346*, 1682-1683. 10.1056/NEJM200205303462202.

Lok, A.S., Heathcote, E.J., and Hoofnagle, J.H. (2001a). Management of hepatitis B: 2000--summary of a workshop. Gastroenterology *120*, 1828-1853. 10.1053/gast.2001.24839.

Lok, A.S., and McMahon, B.J. (2009). Chronic hepatitis B: update 2009. Hepatology *50*, 661-662. 10.1002/hep.23190.

Lok, A.S., McMahon, B.J., and Practice Guidelines Committee, A.A.f.t.S.o.L.D. (2001b). Chronic hepatitis B. Hepatology *34*, 1225-1241. 10.1053/jhep.2001.29401.

Long, Y., Chen, E., Liu, C., Huang, F., Zhou, T., He, F., Liu, L., Liu, F., and Tang, H. (2009). The correlation of hepatocyte nuclear factor 4 alpha and 3 beta with hepatitis B virus replication in the liver of chronic hepatitis B patients. J Viral Hepat *16*, 537-546. 10.1111/j.1365-2893.2009.01089.x.

Lopez-Cabrera, M., Letovsky, J., Hu, K.Q., and Siddiqui, A. (1990). Multiple liver-specific factors bind to the hepatitis B virus core/pregenomic promoter: trans-activation and repression by CCAAT/enhancer binding protein. Proc Natl Acad Sci U S A *87*, 5069-5073. 10.1073/pnas.87.13.5069.

Lopez-Cabrera, M., Letovsky, J., Hu, K.Q., and Siddiqui, A. (1991). Transcriptional factor C/EBP binds to and transactivates the enhancer element II of the hepatitis B virus. Virology *183*, 825-829. 10.1016/0042-6822(91)91019-d.

Losman, J.A., Koivunen, P., and Kaelin, W.G., Jr. (2020). 2-Oxoglutarate-dependent dioxygenases in cancer. Nat Rev Cancer *20*, 710-726. 10.1038/s41568-020-00303-3.

Love, M.I., Huber, W., and Anders, S. (2014). Moderated estimation of fold change and dispersion for RNA-seq data with DESeq2. Genome Biol *15*, 550. 10.1186/s13059-014-0550-8.

Lozano, R., Naghavi, M., Foreman, K., Lim, S., Shibuya, K., Aboyans, V., Abraham, J., Adair, T., Aggarwal, R., Ahn, S.Y., et al. (2012). Global and regional mortality from 235 causes of death for 20 age groups in 1990 and 2010: a systematic analysis for the Global Burden of Disease Study 2010. Lancet *380*, 2095-2128. 10.1016/S0140-6736(12)61728-0.

Lu, C., and Thompson, C.B. (2012). Metabolic regulation of epigenetics. Cell Metab *16*, 9-17. 10.1016/j.cmet.2012.06.001.

Lu, C.C., and Yen, T.S. (1996). Activation of the hepatitis B virus S promoter by transcription factor NF-Y via a CCAAT element. Virology *225*, 387-394. 10.1006/viro.1996.0613.

Lucifora, J., Arzberger, S., Durantel, D., Belloni, L., Strubin, M., Levrero, M., Zoulim, F., Hantz, O., and Protzer, U. (2011). Hepatitis B virus X protein is essential to initiate and maintain virus replication after infection. J Hepatol *55*, 996-1003. 10.1016/j.jhep.2011.02.015.

Lucifora, J., Durantel, D., Testoni, B., Hantz, O., Levrero, M., and Zoulim, F. (2010). Control of hepatitis B virus replication by innate response of HepaRG cells. Hepatology *51*, 63-72. 10.1002/hep.23230.

Lucifora, J., Xia, Y., Reisinger, F., Zhang, K., Stadler, D., Cheng, X., Sprinzl, M.F., Koppensteiner, H., Makowska, Z., Volz, T., et al. (2014). Specific and nonhepatotoxic degradation of nuclear hepatitis B virus cccDNA. Science *343*, 1221-1228. 10.1126/science.1243462.

Luckenbaugh, L., Kitrinos, K.M., Delaney, W.E.t., and Hu, J. (2015). Genome-free hepatitis B virion levels in patient sera as a potential marker to monitor response to antiviral therapy. J Viral Hepat *22*, 561-570. 10.1111/jvh.12361.

Luger, K., Dechassa, M.L., and Tremethick, D.J. (2012). New insights into nucleosome and chromatin structure: an ordered state or a disordered affair? Nat Rev Mol Cell Biol *13*, 436-447. 10.1038/nrm3382.

Lum, J.J., Bui, T., Gruber, M., Gordan, J.D., DeBerardinis, R.J., Covello, K.L., Simon, M.C., and Thompson, C.B. (2007). The transcription factor HIF-1alpha plays a critical role in the growth factor-dependent regulation of both aerobic and anaerobic glycolysis. Genes Dev *21*, 1037-1049. 10.1101/gad.1529107.

Luo, C., Hajkova, P., and Ecker, J.R. (2018). Dynamic DNA methylation: In the right place at the right time. Science *361*, 1336-1340. 10.1126/science.aat6806.

Luo, J., Xi, J., Gao, L., and Hu, J. (2020). Role of Hepatitis B virus capsid phosphorylation in nucleocapsid disassembly and covalently closed circular DNA formation. PLoS Pathog *16*, e1008459. 10.1371/journal.ppat.1008459.

Lythgoe, K.A., Lumley, S.F., Pellis, L., McKeating, J.A., and Matthews, P.C. (2021). Estimating hepatitis B virus cccDNA persistence in chronic infection. Virus Evol *7*, veaa063. 10.1093/ve/veaa063.

Ma, Z., Cao, Q., Xiong, Y., Zhang, E., and Lu, M. (2018). Interaction between Hepatitis B Virus and Toll-Like Receptors: Current Status and Potential Therapeutic Use for Chronic Hepatitis B. Vaccines (Basel) *6*. 10.3390/vaccines6010006.

MacParland, S.A., Liu, J.C., Ma, X.Z., Innes, B.T., Bartczak, A.M., Gage, B.K., Manuel, J., Khuu, N., Echeverri, J., Linares, I., et al. (2018). Single cell RNA sequencing of human liver reveals distinct intrahepatic macrophage populations. Nat Commun *9*, 4383. 10.1038/s41467-018-06318-7.

Mahoney, F.J. (1999). Update on diagnosis, management, and prevention of hepatitis B virus infection. Clin Microbiol Rev *12*, 351-366. 10.1128/CMR.12.2.351.

Maini, M.K., Boni, C., Lee, C.K., Larrubia, J.R., Reignat, S., Ogg, G.S., King, A.S., Herberg, J., Gilson, R., Alisa, A., et al. (2000). The role of virus-specific CD8(+) cells in liver damage and viral control during persistent hepatitis B virus infection. J Exp Med *191*, 1269-1280. 10.1084/jem.191.8.1269.

Majka, J., and Burgers, P.M. (2004). The PCNA-RFC families of DNA clamps and clamp loaders. Prog Nucleic Acid Res Mol Biol *78*, 227-260. 10.1016/S0079-6603(04)78006-X.

Majmundar, A.J., Wong, W.J., and Simon, M.C. (2010). Hypoxia-inducible factors and the response to hypoxic stress. Mol Cell *40*, 294-309. 10.1016/j.molcel.2010.09.022.

Majoros, A., Platanitis, E., Kernbauer-Holzl, E., Rosebrock, F., Muller, M., and Decker, T. (2017). Canonical and Non-Canonical Aspects of JAK-STAT Signaling: Lessons from Interferons for Cytokine Responses. Front Immunol *8*, 29. 10.3389/fimmu.2017.00029.

Manco, R., and Itzkovitz, S. (2021). Liver zonation. J Hepatol *74*, 466-468. 10.1016/j.jhep.2020.09.003.

Mangnall, D., Bird, N.C., and Majeed, A.W. (2003). The molecular physiology of liver regeneration following partial hepatectomy. Liver Int *23*, 124-138. 10.1034/j.1600-0676.2003.00812.x.

Margolis, H.S., Alter, M.J., and Hadler, S.C. (1991). Hepatitis B: evolving epidemiology and implications for control. Semin Liver Dis *11*, 84-92. 10.1055/s-2008-1040427.

Markolovic, S., Leissing, T.M., Chowdhury, R., Wilkins, S.E., Lu, X., and Schofield, C.J. (2016). Structure-function relationships of human JmjC oxygenases-demethylases versus hydroxylases. Curr Opin Struct Biol *41*, 62-72. 10.1016/j.sbi.2016.05.013.

Mas, V.R., Maluf, D.G., Archer, K.J., Yanek, K., Kong, X., Kulik, L., Freise, C.E., Olthoff, K.M., Ghobrial, R.M., McIver, P., and Fisher, R. (2009). Genes involved in viral carcinogenesis and tumor initiation in hepatitis C virus-induced hepatocellular carcinoma. Mol Med *15*, 85-94. 10.2119/molmed.2008.00110.

Mason, W.S. (2015). Animal models and the molecular biology of hepadnavirus infection. Cold Spring Harb Perspect Med *5*. 10.1101/cshperspect.a021352.

Mason, W.S., Gill, U.S., Litwin, S., Zhou, Y., Peri, S., Pop, O., Hong, M.L., Naik, S., Quaglia, A., Bertoletti, A., and Kennedy, P.T. (2016). HBV DNA Integration and Clonal Hepatocyte Expansion in Chronic Hepatitis B Patients Considered Immune Tolerant. Gastroenterology *151*, 986-998 e984. 10.1053/j.gastro.2016.07.012.

Mason, W.S., Jilbert, A.R., and Litwin, S. (2021). Hepatitis B Virus DNA Integration and Clonal Expansion of Hepatocytes in the Chronically Infected Liver. Viruses *13*. 10.3390/v13020210.

Masson, N., Willam, C., Maxwell, P.H., Pugh, C.W., and Ratcliffe, P.J. (2001). Independent function of two destruction domains in hypoxia-inducible factor-alpha chains activated by prolyl hydroxylation. EMBO J *20*, 5197-5206. 10.1093/emboj/20.18.5197.

Matsuda, M., Suzuki, F., Suzuki, Y., Tsubota, A., Akuta, N., Hosaka, T., Someya, T., Kobayashi, M., Saitoh, S., Arase, Y., et al. (2004). Low rate of YMDD motif mutations in polymerase gene of hepatitis B virus in chronically infected patients not treated with lamivudine. J Gastroenterol *39*, 34-40. 10.1007/s00535-003-1242-4.

McCormack, P.L. (2013). DTaP-IPV-Hep B-Hib vaccine (Hexaxim(R)) : a review of its use in primary and booster vaccination. Paediatr Drugs *15*, 59-70. 10.1007/s40272-013-0007-7.

McDonough, M.A., Kavanagh, K.L., Butler, D., Searls, T., Oppermann, U., and Schofield, C.J. (2005). Structure of human phytanoyl-CoA 2-hydroxylase identifies

molecular mechanisms of Refsum disease. J Biol Chem *280*, 41101-41110. 10.1074/jbc.M507528200.

McGill, M.R. (2016). The past and present of serum aminotransferases and the future of liver injury biomarkers. EXCLI J *15*, 817-828. 10.17179/excli2016-800.

McMahon, B.J. (2009). The influence of hepatitis B virus genotype and subgenotype on the natural history of chronic hepatitis B. Hepatol Int *3*, 334-342. 10.1007/s12072-008-9112-z.

McMahon, S., Charbonneau, M., Grandmont, S., Richard, D.E., and Dubois, C.M. (2006). Transforming growth factor beta1 induces hypoxia-inducible factor-1 stabilization through selective inhibition of PHD2 expression. J Biol Chem *281*, 24171-24181. 10.1074/jbc.M604507200.

McNaughton, A.L., D'Arienzo, V., Ansari, M.A., Lumley, S.F., Littlejohn, M., Revill, P., McKeating, J.A., and Matthews, P.C. (2019). Insights From Deep Sequencing of the HBV Genome-Unique, Tiny, and Misunderstood. Gastroenterology *156*, 384-399. 10.1053/j.gastro.2018.07.058.

McQuillan, G.M., Townsend, T.R., Fields, H.A., Carroll, M., Leahy, M., and Polk, B.F. (1989). Seroepidemiology of hepatitis B virus infection in the United States. 1976 to 1980. Am J Med *87*, 5S-10S. 10.1016/0002-9343(89)90523-8.

Mehran Karimzadeh, M.M.H. (2021). Virtual ChIP-seq: predicting transcription factor binding by learning from the transcriptome. bioRxiv.

Meier, M.A., Calabrese, D., Suslov, A., Terracciano, L.M., Heim, M.H., and Wieland, S. (2021). Ubiquitous expression of HBsAg from integrated HBV DNA in patients with low viral load. J Hepatol. 10.1016/j.jhep.2021.04.051.

Melvin, A., and Rocha, S. (2012). Chromatin as an oxygen sensor and active player in the hypoxia response. Cell Signal *24*, 35-43. 10.1016/j.cellsig.2011.08.019.

Menne, S., and Cote, P.J. (2007). The woodchuck as an animal model for pathogenesis and therapy of chronic hepatitis B virus infection. World J Gastroenterol *13*, 104-124. 10.3748/wjg.v13.i1.104.

Mi, H., Ebert, D., Muruganujan, A., Mills, C., Albou, L.P., Mushayamaha, T., and Thomas, P.D. (2021). PANTHER version 16: a revised family classification, tree-based classification tool, enhancer regions and extensive API. Nucleic Acids Res *49*, D394-D403. 10.1093/nar/gkaa1106.

Miao, J., Xiao, Z., Kanamaluru, D., Min, G., Yau, P.M., Veenstra, T.D., Ellis, E., Strom, S., Suino-Powell, K., Xu, H.E., and Kemper, J.K. (2009). Bile acid signaling pathways increase stability of Small Heterodimer Partner (SHP) by inhibiting

ubiquitin-proteasomal degradation. Genes Dev *23*, 986-996. 10.1101/gad.1773909.

Miar, A., Arnaiz, E., Bridges, E., Beedie, S., Cribbs, A.P., Downes, D.J., Beagrie, R.A., Rehwinkel, J., and Harris, A.L. (2020). Hypoxia Induces Transcriptional and Translational Downregulation of the Type I IFN Pathway in Multiple Cancer Cell Types. Cancer Res *80*, 5245-5256. 10.1158/0008-5472.CAN-19-2306.

Milich, D.R., Jones, J.E., Hughes, J.L., Price, J., Raney, A.K., and McLachlan, A. (1990). Is a function of the secreted hepatitis B e antigen to induce immunologic tolerance in utero? Proc Natl Acad Sci U S A *87*, 6599-6603. 10.1073/pnas.87.17.6599.

Mizokami, M., Orito, E., Ohba, K., Ikeo, K., Lau, J.Y., and Gojobori, T. (1997). Constrained evolution with respect to gene overlap of hepatitis B virus. J Mol Evol *44 Suppl 1*, S83-90. 10.1007/pl00000061.

Mladenov, E., Magin, S., Soni, A., and Iliakis, G. (2016). DNA double-strand-break repair in higher eukaryotes and its role in genomic instability and cancer: Cell cycle and proliferation-dependent regulation. Semin Cancer Biol *37-38*, 51-64. 10.1016/j.semcancer.2016.03.003.

Mohrmann, L., and Verrijzer, C.P. (2005). Composition and functional specificity of SWI2/SNF2 class chromatin remodeling complexes. Biochim Biophys Acta *1681*, 59-73. 10.1016/j.bbaexp.2004.10.005.

Mole, D.R., Blancher, C., Copley, R.R., Pollard, P.J., Gleadle, J.M., Ragoussis, J., and Ratcliffe, P.J. (2009). Genome-wide association of hypoxia-inducible factor (HIF)-1alpha and HIF-2alpha DNA binding with expression profiling of hypoxia-inducible transcripts. J Biol Chem *284*, 16767-16775. 10.1074/jbc.M901790200.

Mootha, V.K., Lindgren, C.M., Eriksson, K.F., Subramanian, A., Sihag, S., Lehar, J., Puigserver, P., Carlsson, E., Ridderstrale, M., Laurila, E., et al. (2003). PGC-1alpha-responsive genes involved in oxidative phosphorylation are coordinately downregulated in human diabetes. Nat Genet *34*, 267-273. 10.1038/ng1180.

Mora, A., Sandve, G.K., Gabrielsen, O.S., and Eskeland, R. (2016). In the loop: promoter-enhancer interactions and bioinformatics. Brief Bioinform *17*, 980-995. 10.1093/bib/bbv097.

Moreau, P., Cournac, A., Palumbo, G.A., Marbouty, M., Mortaza, S., Thierry, A., Cairo, S., Lavigne, M., Koszul, R., and Neuveut, C. (2018). Tridimensional infiltration of DNA viruses into the host genome shows preferential contact with active chromatin. Nat Commun *9*, 4268. 10.1038/s41467-018-06739-4.

Moreira, R.K. (2007). Hepatic stellate cells and liver fibrosis. Arch Pathol Lab Med *131*, 1728-1734. 10.5858/2007-131-1728-HSCALF.

Mouzannar, K., Fusil, F., Lacombe, B., Ollivier, A., Menard, C., Lotteau, V., Cosset, F.L., Ramiere, C., and Andre, P. (2019). Farnesoid X receptor-alpha is a proviral host factor for hepatitis B virus that is inhibited by ligands in vitro and in vivo. FASEB J *33*, 2472-2483. 10.1096/fj.201801181R.

Movafagh, S., Crook, S., and Vo, K. (2015). Regulation of hypoxia-inducible factor-1a by reactive oxygen species: new developments in an old debate. J Cell Biochem *116*, 696-703. 10.1002/jcb.25074.

Movsisyan, A., Melendez-Torres, G.J., and Montgomery, P. (2016). A harmonized guidance is needed on how to "properly" frame review questions to make the best use of all available evidence in the assessment of effectiveness of complex interventions. J Clin Epidemiol *77*, 139-141. 10.1016/j.jclinepi.2016.04.003.

Muhlemann, B., Jones, T.C., Damgaard, P.B., Allentoft, M.E., Shevnina, I., Logvin, A., Usmanova, E., Panyushkina, I.P., Boldgiv, B., Bazartseren, T., et al. (2018). Ancient hepatitis B viruses from the Bronze Age to the Medieval period. Nature *557*, 418-423. 10.1038/s41586-018-0097-z.

Mukhopadhyay, A., Deplancke, B., Walhout, A.J., and Tissenbaum, H.A. (2008). Chromatin immunoprecipitation (ChIP) coupled to detection by quantitative real-time PCR to study transcription factor binding to DNA in Caenorhabditis elegans. Nat Protoc *3*, 698-709. 10.1038/nprot.2008.38.

Muller, S.F., Konig, A., Doring, B., Glebe, D., and Geyer, J. (2018). Characterisation of the hepatitis B virus cross-species transmission pattern via Na+/taurocholate co-transporting polypeptides from 11 New World and Old World primate species. PLoS One *13*, e0199200. 10.1371/journal.pone.0199200.

Murante, R.S., Rumbaugh, J.A., Barnes, C.J., Norton, J.R., and Bambara, R.A. (1996). Calf RTH-1 nuclease can remove the initiator RNAs of Okazaki fragments by endonuclease activity. J Biol Chem *271*, 25888-25897. 10.1074/jbc.271.42.25888.

Murphy, C.M., Xu, Y., Li, F., Nio, K., Reszka-Blanco, N., Li, X., Wu, Y., Yu, Y., Xiong, Y., and Su, L. (2016). Hepatitis B Virus X Protein Promotes Degradation of SMC5/6 to Enhance HBV Replication. Cell Rep *16*, 2846-2854. 10.1016/j.celrep.2016.08.026.

Nag, S., and Resnick, A. (2017). Stabilization of hypoxia inducible factor by cobalt chloride can alter renal epithelial transport. Physiol Rep *5*. 10.14814/phy2.13531.

Nakashima, Y., Brewitz, L., Tumber, A., Salah, E., and Schofield, C.J. (2021). 2-Oxoglutarate derivatives can selectively enhance or inhibit the activity of human oxygenases. Nat Commun *12*, 6478. 10.1038/s41467-021-26673-2.

Nanavaty, V., Abrash, E.W., Hong, C., Park, S., Fink, E.E., Li, Z., Sweet, T.J., Bhasin, J.M., Singuri, S., Lee, B.H., et al. (2020). DNA Methylation Regulates Alternative Polyadenylation via CTCF and the Cohesin Complex. Mol Cell *78*, 752-764 e756. 10.1016/j.molcel.2020.03.024.

Natsoulis, G., Pearson, C.I., Gollub, J., B, P.E., Ferng, J., Nair, R., Idury, R., Lee, M.D., Fielden, M.R., Brennan, R.J., et al. (2008). The liver pharmacological and xenobiotic gene response repertoire. Mol Syst Biol *4*, 175. 10.1038/msb.2008.9.

Negro, F. (2014). Hepatitis D virus coinfection and superinfection. Cold Spring Harb Perspect Med *4*, a021550. 10.1101/cshperspect.a021550.

Newbold, J.E., Xin, H., Tencza, M., Sherman, G., Dean, J., Bowden, S., and Locarnini, S. (1995). The covalently closed duplex form of the hepadnavirus genome exists in situ as a heterogeneous population of viral minichromosomes. J Virol *69*, 3350-3357. 10.1128/JVI.69.6.3350-3357.1995.

Ng, K.Y., Chai, S., Tong, M., Guan, X.Y., Lin, C.H., Ching, Y.P., Xie, D., Cheng, A.S., and Ma, S. (2016). C-terminal truncated hepatitis B virus X protein promotes hepatocellular carcinogenesis through induction of cancer and stem cell-like properties. Oncotarget *7*, 24005-24017. 10.18632/oncotarget.8209.

Nguyen, D.H., and Hu, J. (2008). Reverse transcriptase- and RNA packaging signal-dependent incorporation of APOBEC3G into hepatitis B virus nucleocapsids. J Virol *82*, 6852-6861. 10.1128/JVI.00465-08.

Nguyen, M.H., Wong, G., Gane, E., Kao, J.H., and Dusheiko, G. (2020). Hepatitis B Virus: Advances in Prevention, Diagnosis, and Therapy. Clin Microbiol Rev *33*. 10.1128/CMR.00046-19.

Ni, Y., Lempp, F.A., Mehrle, S., Nkongolo, S., Kaufman, C., Falth, M., Stindt, J., Koniger, C., Nassal, M., Kubitz, R., et al. (2014). Hepatitis B and D viruses exploit sodium taurocholate co-transporting polypeptide for species-specific entry into hepatocytes. Gastroenterology *146*, 1070-1083. 10.1053/j.gastro.2013.12.024.

Ni, Y., and Urban, S. (2017). Hepatitis B Virus Infection of HepaRG Cells, HepaRG-hNTCP Cells, and Primary Human Hepatocytes. Methods Mol Biol *1540*, 15-25. 10.1007/978-1-4939-6700-1_2.

Nijhara, R., Jana, S.S., Goswami, S.K., Rana, A., Majumdar, S.S., Kumar, V., and Sarkar, D.P. (2001). Sustained activation of mitogen-activated protein kinases and activator protein 1 by the hepatitis B virus X protein in mouse hepatocytes in vivo. J Virol *75*, 10348-10358. 10.1128/JVI.75.21.10348-10358.2001.

Nikolov, D.B., Chen, H., Halay, E.D., Hoffman, A., Roeder, R.G., and Burley, S.K. (1996). Crystal structure of a human TATA box-binding protein/TATA element complex. Proc Natl Acad Sci U S A *93*, 4862-4867. 10.1073/pnas.93.10.4862.

Ning, Q., Wu, D., Wang, G.Q., Ren, H., Gao, Z.L., Hu, P., Han, M.F., Wang, Y., Zhang, W.H., Lu, F.M., and Wang, F.S. (2019). Roadmap to functional cure of chronic hepatitis B: An expert consensus. J Viral Hepat *26*, 1146-1155. 10.1111/jvh.13126.

Ning, X., Nguyen, D., Mentzer, L., Adams, C., Lee, H., Ashley, R., Hafenstein, S., and Hu, J. (2011). Secretion of genome-free hepatitis B virus--single strand blocking model for virion morphogenesis of para-retrovirus. PLoS Pathog *7*, e1002255. 10.1371/journal.ppat.1002255.

Niu, C., Livingston, C.M., Li, L., Beran, R.K., Daffis, S., Ramakrishnan, D., Burdette, D., Peiser, L., Salas, E., Ramos, H., et al. (2017). The Smc5/6 Complex Restricts HBV when Localized to ND10 without Inducing an Innate Immune Response and Is Counteracted by the HBV X Protein Shortly after Infection. PLoS One *12*, e0169648. 10.1371/journal.pone.0169648.

Niu, X., Zhang, T., Liao, L., Zhou, L., Lindner, D.J., Zhou, M., Rini, B., Yan, Q., and Yang, H. (2012). The von Hippel-Lindau tumor suppressor protein regulates gene expression and tumor growth through histone demethylase JARID1C. Oncogene *31*, 776-786. 10.1038/onc.2011.266.

Odom, D.T., Zizlsperger, N., Gordon, D.B., Bell, G.W., Rinaldi, N.J., Murray, H.L., Volkert, T.L., Schreiber, J., Rolfe, P.A., Gifford, D.K., et al. (2004). Control of pancreas and liver gene expression by HNF transcription factors. Science *303*, 1378-1381. 10.1126/science.1089769.

Ooi, S.K., O'Donnell, A.H., and Bestor, T.H. (2009). Mammalian cytosine methylation at a glance. J Cell Sci *122*, 2787-2791. 10.1242/jcs.015123.

Oropeza, C.E., Li, L., and McLachlan, A. (2008). Differential inhibition of nuclear hormone receptor-dependent hepatitis B virus replication by the small heterodimer partner. J Virol *82*, 3814-3821. 10.1128/JVI.02507-07.

Oropeza, C.E., Tarnow, G., Sridhar, A., Taha, T.Y., Shalaby, R.E., and McLachlan, A. (2020). The Regulation of HBV Transcription and Replication. Adv Exp Med Biol *1179*, 39-69. 10.1007/978-981-13-9151-4_3.

Ortega-Prieto, A.M., Cherry, C., Gunn, H., and Dorner, M. (2019). In Vivo Model Systems for Hepatitis B Virus Research. ACS Infect Dis *5*, 688-702. 10.1021/acsinfecdis.8b00223.

Ortega-Prieto, A.M., Skelton, J.K., Wai, S.N., Large, E., Lussignol, M., Vizcay-Barrena, G., Hughes, D., Fleck, R.A., Thursz, M., Catanese, M.T., and Dorner, M. (2018). 3D microfluidic liver cultures as a physiological preclinical tool for hepatitis B virus infection. Nat Commun *9*, 682. 10.1038/s41467-018-02969-8.

Ortmann, B.M., Burrows, N., Lobb, I.T., Arnaiz, E., Wit, N., Bailey, P.S.J., Jordon, L.H., Lombardi, O., Penalver, A., McCaffrey, J., et al. (2021). The HIF complex recruits the histone methyltransferase SET1B to activate specific hypoxia-inducible genes. Nat Genet *53*, 1022-1035. 10.1038/s41588-021-00887-y.

Osiowy, C., Giles, E., Tanaka, Y., Mizokami, M., and Minuk, G.Y. (2006). Molecular evolution of hepatitis B virus over 25 years. J Virol *80*, 10307-10314. 10.1128/JVI.00996-06.

Osiowy, C., Kaita, K., Solar, K., and Mendoza, K. (2010). Molecular characterization of hepatitis B virus and a 9-year clinical profile in a patient infected with genotype I. J Med Virol *82*, 942-948. 10.1002/jmv.21758.

Oxygen Sensing: After the Nobel. (2020). Cell *180*, 7-8. 10.1016/j.cell.2019.12.008.

Palazon, A., Goldrath, A.W., Nizet, V., and Johnson, R.S. (2014). HIF transcription factors, inflammation, and immunity. Immunity *41*, 518-528. 10.1016/j.immuni.2014.09.008.

Palumbo, G.A., Scisciani, C., Pediconi, N., Lupacchini, L., Alfalate, D., Guerrieri, F., Calvo, L., Salerno, D., Di Cocco, S., Levrero, M., and Belloni, L. (2015). IL6 Inhibits HBV Transcription by Targeting the Epigenetic Control of the Nuclear cccDNA Minichromosome. PLoS One *10*, e0142599. 10.1371/journal.pone.0142599.

Pan, X., Cao, H., Lu, J., Shu, X., Xiong, X., Hong, X., Xu, Q., Zhu, H., Li, G., and Shen, G. (2011). Interleukin-32 expression induced by hepatitis B virus protein X is mediated through activation of NF-kappaB. Mol Immunol *48*, 1573-1577. 10.1016/j.molimm.2011.03.012.

Panduro, A., Maldonado-Gonzalez, M., Fierro, N.A., and Roman, S. (2013). Distribution of HBV genotypes F and H in Mexico and Central America. Antivir Ther *18*, 475-484. 10.3851/IMP2605.

Paran, N., Geiger, B., and Shaul, Y. (2001). HBV infection of cell culture: evidence for multivalent and cooperative attachment. EMBO J *20*, 4443-4453. 10.1093/emboj/20.16.4443.

Paris, C., Pentland, I., Groves, I., Roberts, D.C., Powis, S.J., Coleman, N., Roberts, S., and Parish, J.L. (2015). CCCTC-binding factor recruitment to the early region of the human papillomavirus 18 genome regulates viral oncogene expression. J Virol *89*, 4770-4785. 10.1128/JVI.00097-15.

Patel, N., White, S.J., Thompson, R.F., Bingham, R., Weiss, E.U., Maskell, D.P., Zlotnick, A., Dykeman, E., Tuma, R., Twarock, R., et al. (2017). HBV RNA pre-genome encodes specific motifs that mediate interactions with the viral core

protein that promote nucleocapsid assembly. Nat Microbiol *2*, 17098. 10.1038/nmicrobiol.2017.98.

Patient, R., Hourioux, C., and Roingeard, P. (2009). Morphogenesis of hepatitis B virus and its subviral envelope particles. Cell Microbiol *11*, 1561-1570. 10.1111/j.1462-5822.2009.01363.x.

Patient, R., Hourioux, C., Sizaret, P.Y., Trassard, S., Sureau, C., and Roingeard, P. (2007). Hepatitis B virus subviral envelope particle morphogenesis and intracellular trafficking. J Virol *81*, 3842-3851. 10.1128/JVI.02741-06.

Patro, R., Duggal, G., Love, M.I., Irizarry, R.A., and Kingsford, C. (2017). Salmon provides fast and bias-aware quantification of transcript expression. Nat Methods *14*, 417-419. 10.1038/nmeth.4197.

Pawlak, M., Lefebvre, P., and Staels, B. (2015). Molecular mechanism of PPARalpha action and its impact on lipid metabolism, inflammation and fibrosis in non-alcoholic fatty liver disease. J Hepatol *62*, 720-733. 10.1016/j.jhep.2014.10.039.

Peneau, C., Imbeaud, S., La Bella, T., Hirsch, T.Z., Caruso, S., Calderaro, J., Paradis, V., Blanc, J.F., Letouze, E., Nault, J.C., et al. (2021). Hepatitis B virus integrations promote local and distant oncogenic driver alterations in hepatocellular carcinoma. Gut. 10.1136/gutjnl-2020-323153.

Pentland, I., Campos-Leon, K., Cotic, M., Davies, K.J., Wood, C.D., Groves, I.J., Burley, M., Coleman, N., Stockton, J.D., Noyvert, B., et al. (2018). Disruption of CTCF-YY1-dependent looping of the human papillomavirus genome activates differentiation-induced viral oncogene transcription. PLoS Biol *16*, e2005752. 10.1371/journal.pbio.2005752.

Peppa, D., Micco, L., Javaid, A., Kennedy, P.T., Schurich, A., Dunn, C., Pallant, C., Ellis, G., Khanna, P., Dusheiko, G., et al. (2010). Blockade of immunosuppressive cytokines restores NK cell antiviral function in chronic hepatitis B virus infection. PLoS Pathog *6*, e1001227. 10.1371/journal.ppat.1001227.

Petersen, J., Thompson, A.J., and Levrero, M. (2016). Aiming for cure in HBV and HDV infection. J Hepatol *65*, 835-848. 10.1016/j.jhep.2016.05.043.

Petrick, J.L., and McGlynn, K.A. (2019). The changing epidemiology of primary liver cancer. Curr Epidemiol Rep *6*, 104-111. 10.1007/s40471-019-00188-3.

Petrova, M., and Kamburov, V. (2010). Breastfeeding and chronic HBV infection: clinical and social implications. World J Gastroenterol *16*, 5042-5046. 10.3748/wjg.v16.i40.5042.

Pfeifer, G.P., Kadam, S., and Jin, S.G. (2013). 5-hydroxymethylcytosine and its potential roles in development and cancer. Epigenetics Chromatin *6*, 10. 10.1186/1756-8935-6-10.

Phoolcharoen, W., and Smith, D.R. (2004). Internalization of the dengue virus is cell cycle modulated in HepG2, but not Vero cells. J Med Virol *74*, 434-441. 10.1002/jmv.20195.

Pineda Torra, I., Claudel, T., Duval, C., Kosykh, V., Fruchart, J.C., and Staels, B. (2003). Bile acids induce the expression of the human peroxisome proliferator-activated receptor alpha gene via activation of the farnesoid X receptor. Mol Endocrinol *17*, 259-272. 10.1210/me.2002-0120.

Pique-Regi, R., Degner, J.F., Pai, A.A., Gaffney, D.J., Gilad, Y., and Pritchard, J.K. (2011). Accurate inference of transcription factor binding from DNA sequence and chromatin accessibility data. Genome Res *21*, 447-455. 10.1101/gr.112623.110.

Pirosu, A., Allweiss, L., and Dandri, M. (2021). Chromatin Extraction from Frozen Chimeric Liver Tissue for Chromatin Immunoprecipitation Analysis. J Vis Exp. 10.3791/62179.

Ploumakis, A., and Coleman, M.L. (2015). OH, the Places You'll Go! Hydroxylation, Gene Expression, and Cancer. Mol Cell *58*, 729-741. 10.1016/j.molcel.2015.05.026.

Plymoth, A., Viviani, S., and Hainaut, P. (2009). Control of hepatocellular carcinoma through hepatitis B vaccination in areas of high endemicity: perspectives for global liver cancer prevention. Cancer Lett *286*, 15-21. 10.1016/j.canlet.2009.08.024.

Poisson, F., Severac, A., Hourioux, C., Goudeau, A., and Roingeard, P. (1997). Both pre-S1 and S domains of hepatitis B virus envelope proteins interact with the core particle. Virology *228*, 115-120. 10.1006/viro.1996.8367.

Polaris Observatory, C. (2018). Global prevalence, treatment, and prevention of hepatitis B virus infection in 2016: a modelling study. Lancet Gastroenterol Hepatol *3*, 383-403. 10.1016/S2468-1253(18)30056-6.

Pollard, P.J., Loenarz, C., Mole, D.R., McDonough, M.A., Gleadle, J.M., Schofield, C.J., and Ratcliffe, P.J. (2008). Regulation of Jumonji-domain-containing histone demethylases by hypoxia-inducible factor (HIF)-1alpha. Biochem J *416*, 387-394. 10.1042/BJ20081238.

Pollicino, T., Belloni, L., Raffa, G., Pediconi, N., Squadrito, G., Raimondo, G., and Levrero, M. (2006). Hepatitis B virus replication is regulated by the acetylation

status of hepatitis B virus cccDNA-bound H3 and H4 histones. Gastroenterology *130*, 823-837. 10.1053/j.gastro.2006.01.001.

Powell, R.D., Holland, P.J., Hollis, T., and Perrino, F.W. (2011). Aicardi-Goutieres syndrome gene and HIV-1 restriction factor SAMHD1 is a dGTP-regulated deoxynucleotide triphosphohydrolase. J Biol Chem *286*, 43596-43600. 10.1074/jbc.C111.317628.

Prakash, K., Rydell, G.E., Larsson, S.B., Andersson, M., Norkrans, G., Norder, H., and Lindh, M. (2018). High serum levels of pregenomic RNA reflect frequently failing reverse transcription in hepatitis B virus particles. Virol J *15*, 86. 10.1186/s12985-018-0994-7.

Prange, R., Werr, M., and Loffler-Mary, H. (1999). Chaperones involved in hepatitis B virus morphogenesis. Biol Chem *380*, 305-314. 10.1515/BC.1999.042.

Protzer, U., Nassal, M., Chiang, P.W., Kirschfink, M., and Schaller, H. (1999). Interferon gene transfer by a hepatitis B virus vector efficiently suppresses wild-type virus infection. Proc Natl Acad Sci U S A *96*, 10818-10823. 10.1073/pnas.96.19.10818.

Provenzano, R., Besarab, A., Sun, C.H., Diamond, S.A., Durham, J.H., Cangiano, J.L., Aiello, J.R., Novak, J.E., Lee, T., Leong, R., et al. (2016). Oral Hypoxia-Inducible Factor Prolyl Hydroxylase Inhibitor Roxadustat (FG-4592) for the Treatment of Anemia in Patients with CKD. Clin J Am Soc Nephrol *11*, 982-991. 10.2215/CJN.06890615.

Puche, J.E., Saiman, Y., and Friedman, S.L. (2013). Hepatic stellate cells and liver fibrosis. Compr Physiol *3*, 1473-1492. 10.1002/cphy.c120035.

Qin, J., Gao, D.M., Jiang, Q.F., Zhou, Q., Kong, Y.Y., Wang, Y., and Xie, Y.H. (2004). Prospero-related homeobox (Prox1) is a corepressor of human liver receptor homolog-1 and suppresses the transcription of the cholesterol 7-alpha-hydroxylase gene. Mol Endocrinol *18*, 2424-2439. 10.1210/me.2004-0009.

Quasdorff, M., and Protzer, U. (2010). Control of hepatitis B virus at the level of transcription. J Viral Hepat *17*, 527-536. 10.1111/j.1365-2893.2010.01315.x.

Quercia, R., Perno, C.F., Koteff, J., Moore, K., McCoig, C., St Clair, M., and Kuritzkes, D. (2018). Twenty-Five Years of Lamivudine: Current and Future Use for the Treatment of HIV-1 Infection. J Acquir Immune Defic Syndr *78*, 125-135. 10.1097/QAI.0000000000001660.

Rabe, B., Glebe, D., and Kann, M. (2006). Lipid-mediated introduction of hepatitis B virus capsids into nonsusceptible cells allows highly efficient replication and facilitates the study of early infection events. J Virol *80*, 5465-5473. 10.1128/JVI.02303-05.

Rabe, B., Vlachou, A., Pante, N., Helenius, A., and Kann, M. (2003). Nuclear import of hepatitis B virus capsids and release of the viral genome. Proc Natl Acad Sci U S A *100*, 9849-9854. 10.1073/pnas.1730940100.

Radziwill, G., Zentgraf, H., Schaller, H., and Bosch, V. (1988). The duck hepatitis B virus DNA polymerase is tightly associated with the viral core structure and unable to switch to an exogenous template. Virology *163*, 123-132. 10.1016/0042-6822(88)90239-5.

Rall, L.B., Standring, D.N., Laub, O., and Rutter, W.J. (1983). Transcription of hepatitis B virus by RNA polymerase II. Mol Cell Biol *3*, 1766-1773. 10.1128/mcb.3.10.1766-1773.1983.

Ramiere, C., Scholtes, C., Diaz, O., Icard, V., Perrin-Cocon, L., Trabaud, M.A., Lotteau, V., and Andre, P. (2008). Transactivation of the hepatitis B virus core promoter by the nuclear receptor FXRalpha. J Virol *82*, 10832-10840. 10.1128/JVI.00883-08.

Ramirez, R., van Buuren, N., Gamelin, L., Soulette, C., May, L., Han, D., Yu, M., Choy, R., Cheng, G., Bhardwaj, N., et al. (2021). Targeted Long-Read Sequencing Reveals Comprehensive Architecture, Burden, and Transcriptional Signatures from Hepatitis B Virus-Associated Integrations and Translocations in Hepatocellular Carcinoma Cell Lines. J Virol *95*, e0029921. 10.1128/JVI.00299-21.

Raney, A.K., Kline, E.F., Tang, H., and McLachlan, A. (2001). Transcription and replication of a natural hepatitis B virus nucleocapsid promoter variant is regulated in vivo by peroxisome proliferators. Virology *289*, 239-251. 10.1006/viro.2001.1169.

Raney, A.K., Le, H.B., and McLachlan, A. (1992). Regulation of transcription from the hepatitis B virus major surface antigen promoter by the Sp1 transcription factor. J Virol *66*, 6912-6921. 10.1128/JVI.66.12.6912-6921.1992.

Raney, A.K., Milich, D.R., Easton, A.J., and McLachlan, A. (1990). Differentiation-specific transcriptional regulation of the hepatitis B virus large surface antigen gene in human hepatoma cell lines. J Virol *64*, 2360-2368. 10.1128/JVI.64.5.2360-2368.1990.

Raney, A.K., Zhang, P., and McLachlan, A. (1995). Regulation of transcription from the hepatitis B virus large surface antigen promoter by hepatocyte nuclear factor 3. J Virol *69*, 3265-3272. 10.1128/JVI.69.6.3265-3272.1995.

Ratcliffe, P.J., Jones, R.W., Phillips, R.E., Nicholls, L.G., and Bell, J.I. (1990). Oxygen-dependent modulation of erythropoietin mRNA levels in isolated rat kidneys studied by RNase protection. J Exp Med *172*, 657-660. 10.1084/jem.172.2.657.

Ratcliffe, P.J., O'Rourke, J.F., Maxwell, P.H., and Pugh, C.W. (1998). Oxygen sensing, hypoxia-inducible factor-1 and the regulation of mammalian gene expression. J Exp Biol *201*, 1153-1162.

Raval, R.R., Lau, K.W., Tran, M.G., Sowter, H.M., Mandriota, S.J., Li, J.L., Pugh, C.W., Maxwell, P.H., Harris, A.L., and Ratcliffe, P.J. (2005). Contrasting properties of hypoxia-inducible factor 1 (HIF-1) and HIF-2 in von Hippel-Lindau-associated renal cell carcinoma. Mol Cell Biol *25*, 5675-5686. 10.1128/MCB.25.13.5675-5686.2005.

Reaiche, G.Y., Le Mire, M.F., Mason, W.S., and Jilbert, A.R. (2010). The persistence in the liver of residual duck hepatitis B virus covalently closed circular DNA is not dependent upon new viral DNA synthesis. Virology *406*, 286-292. 10.1016/j.virol.2010.07.013.

Rehermann, B., and Nascimbeni, M. (2005). Immunology of hepatitis B virus and hepatitis C virus infection. Nat Rev Immunol *5*, 215-229. 10.1038/nri1573.

Reith, W., Ucla, C., Barras, E., Gaud, A., Durand, B., Herrero-Sanchez, C., Kobr, M., and Mach, B. (1994). RFX1, a transactivator of hepatitis B virus enhancer I, belongs to a novel family of homodimeric and heterodimeric DNA-binding proteins. Mol Cell Biol *14*, 1230-1244. 10.1128/mcb.14.2.1230-1244.1994.

Riedl, T., Faure-Dupuy, S., Rolland, M., Schuehle, S., Hizir, Z., Calderazzo, S., Zhuang, X., Wettengel, J., Lopez, M.A., Barnault, R., et al. (2021). Hypoxia-Inducible Factor 1 Alpha-Mediated RelB/APOBEC3B Down-regulation Allows Hepatitis B Virus Persistence. Hepatology *74*, 1766-1781. 10.1002/hep.31902.

Ringelhan, M., McKeating, J.A., and Protzer, U. (2017). Viral hepatitis and liver cancer. Philos Trans R Soc Lond B Biol Sci *372*. 10.1098/rstb.2016.0274.

Riu, E., Chen, Z.Y., Xu, H., He, C.Y., and Kay, M.A. (2007). Histone modifications are associated with the persistence or silencing of vector-mediated transgene expression in vivo. Mol Ther *15*, 1348-1355. 10.1038/sj.mt.6300177.

Rivkina, M.B., Lunin, V.G., Mahov, A.M., Tikchonenko, T.I., and Kukain, R.A. (1988). Nucleotide sequence of integrated hepatitis B virus DNA and human flanking regions in the genome of the PLC/PRF/5 cell line. Gene *64*, 285-296. 10.1016/0378-1119(88)90343-5.

Rocha, S. (2007). Gene regulation under low oxygen: holding your breath for transcription. Trends Biochem Sci *32*, 389-397. 10.1016/j.tibs.2007.06.005.

Roche, O., Deguiz, M.L., Tiana, M., Galiana-Ribote, C., Martinez-Alcazar, D., Rey-Serra, C., Ranz-Ribeiro, B., Casitas, R., Galera, R., Fernandez-Navarro, I., et al. (2016). Identification of non-coding genetic variants in samples from hypoxemic

respiratory disease patients that affect the transcriptional response to hypoxia. Nucleic Acids Res *44*, 9315-9330. 10.1093/nar/gkw811.

Roggendorf, M., Schulte, I., Xu, Y., and Lu, M. (2007). Therapeutic vaccination in chronic hepatitis B: preclinical studies in the woodchuck model. J Viral Hepat *14 Suppl 1*, 51-57. 10.1111/j.1365-2893.2007.00914.x.

Roggendorf, M., and Tolle, T.K. (1995). The woodchuck: an animal model for hepatitis B virus infection in man. Intervirology *38*, 100-112. 10.1159/000150418.

Roingeard, P., and Sureau, C. (1998). Ultrastructural analysis of hepatitis B virus in HepG2-transfected cells with special emphasis on subviral filament morphogenesis. Hepatology *28*, 1128-1133. 10.1002/hep.510280431.

Rokuhara, A., Matsumoto, A., Tanaka, E., Umemura, T., Yoshizawa, K., Kimura, T., Maki, N., and Kiyosawa, K. (2006). Hepatitis B virus RNA is measurable in serum and can be a new marker for monitoring lamivudine therapy. J Gastroenterol *41*, 785-790. 10.1007/s00535-006-1856-4.

Rowley, M.J., and Corces, V.G. (2018). Organizational principles of 3D genome architecture. Nat Rev Genet *19*, 789-800. 10.1038/s41576-018-0060-8.

Rubin, B.R., Milner, T.A., Pickel, V.M., Coleman, C.G., Marques-Lopes, J., Van Kempen, T.A., Kazim, S.F., McEwen, B.S., Gray, J.D., and Pereira, A.C. (2020). Sex and age differentially affect GABAergic neurons in the mouse prefrontal cortex and hippocampus following chronic intermittent hypoxia. Exp Neurol *325*, 113075. 10.1016/j.expneurol.2019.113075.

Rusmintratip, V., and Sowers, L.C. (2000). An unexpectedly high excision capacity for mispaired 5-hydroxymethyluracil in human cell extracts. Proc Natl Acad Sci U S A *97*, 14183-14187. 10.1073/pnas.97.26.14183.

Ryan, T.T., Jr., and Aamoth, R.J. (1984). Hepatitis B: an occupational hazard for health care personnel. Health Matrix *2*, 3-12.

Ryu, D.K., Ahn, B.Y., and Ryu, W.S. (2010). Proximity between the cap and 5' epsilon stem-loop structure is critical for the suppression of pgRNA translation by the hepatitis B viral polymerase. Virology *406*, 56-64. 10.1016/j.virol.2010.07.005.

Ryu, D.K., Kim, S., and Ryu, W.S. (2008). Hepatitis B virus polymerase suppresses translation of pregenomic RNA via a mechanism involving its interaction with 5' stem-loop structure. Virology *373*, 112-123. 10.1016/j.virol.2007.11.010.

Sagnelli, C., Sagnelli, E., Russo, A., Pisaturo, M., Occhiello, L., and Coppola, N. (2021). HBV/HDV Co-Infection: Epidemiological and Clinical Changes, Recent Knowledge and Future Challenges. Life (Basel) *11*. 10.3390/life11020169.

Saitou, N., and Nei, M. (1987). The neighbor-joining method: a new method for reconstructing phylogenetic trees. Mol Biol Evol *4*, 406-425. 10.1093/oxfordjournals.molbev.a040454.

Saksouk, N., Simboeck, E., and Dejardin, J. (2015). Constitutive heterochromatin formation and transcription in mammals. Epigenetics Chromatin *8*, 3. 10.1186/1756-8935-8-3.

Salama, R., Masson, N., Simpson, P., Sciesielski, L.K., Sun, M., Tian, Y.M., Ratcliffe, P.J., and Mole, D.R. (2015). Heterogeneous Effects of Direct Hypoxia Pathway Activation in Kidney Cancer. PLoS One *10*, e0134645. 10.1371/journal.pone.0134645.

Salceda, S., and Caro, J. (1997). Hypoxia-inducible factor 1alpha (HIF-1alpha) protein is rapidly degraded by the ubiquitin-proteasome system under normoxic conditions. Its stabilization by hypoxia depends on redox-induced changes. J Biol Chem *272*, 22642-22647. 10.1074/jbc.272.36.22642.

Samuels, T.J., Jarvelin, A.I., Ish-Horowicz, D., and Davis, I. (2020). Imp/IGF2BP levels modulate individual neural stem cell growth and division through myc mRNA stability. Elife *9*. 10.7554/eLife.51529.

Sandalova, E., Laccabue, D., Boni, C., Tan, A.T., Fink, K., Ooi, E.E., Chua, R., Shafaeddin Schreve, B., Ferrari, C., and Bertoletti, A. (2010). Contribution of herpesvirus specific CD8 T cells to anti-viral T cell response in humans. PLoS Pathog *6*, e1001051. 10.1371/journal.ppat.1001051.

Santos-Rosa, H., Schneider, R., Bannister, A.J., Sherriff, J., Bernstein, B.E., Emre, N.C., Schreiber, S.L., Mellor, J., and Kouzarides, T. (2002). Active genes are tri-methylated at K4 of histone H3. Nature *419*, 407-411. 10.1038/nature01080.

Sarkar, M., Niranjan, N., and Banyal, P.K. (2017). Mechanisms of hypoxemia. Lung India *34*, 47-60. 10.4103/0970-2113.197116.

Sato, M., Yasumoto, H., and Arai, T. (2018). General anesthesia with propofol for ovarian teratoma excision associated with anti-N-methyl-D-aspartate receptor encephalitis. JA Clin Rep *4*, 14. 10.1186/s40981-018-0153-6.

Scheer, N., and Wilson, I.D. (2016). A comparison between genetically humanized and chimeric liver humanized mouse models for studies in drug metabolism and toxicity. Drug Discov Today *21*, 250-263. 10.1016/j.drudis.2015.09.002.

Schildberg, F.A., Wojtalla, A., Siegmund, S.V., Endl, E., Diehl, L., Abdullah, Z., Kurts, C., and Knolle, P.A. (2011). Murine hepatic stellate cells veto CD8 T cell activation by a CD54-dependent mechanism. Hepatology *54*, 262-272. 10.1002/hep.24352.

Schley, G., Klanke, B., Kalucka, J., Schatz, V., Daniel, C., Mayer, M., Goppelt-Struebe, M., Herrmann, M., Thorsteinsdottir, M., Palsson, R., et al. (2019). Mononuclear phagocytes orchestrate prolyl hydroxylase inhibition-mediated renoprotection in chronic tubulointerstitial nephritis. Kidney Int *96*, 378-396. 10.1016/j.kint.2019.02.016.

Schmidt, N.M., Wing, P.A.C., Diniz, M.O., Pallett, L.J., Swadling, L., Harris, J.M., Burton, A.R., Jeffery-Smith, A., Zakeri, N., Amin, O.E., et al. (2021). Targeting human Acyl-CoA:cholesterol acyltransferase as a dual viral and T cell metabolic checkpoint. Nat Commun *12*, 2814. 10.1038/s41467-021-22967-7.

Schneider, C.A., Rasband, W.S., and Eliceiri, K.W. (2012). NIH Image to ImageJ: 25 years of image analysis. Nat Methods *9*, 671-675. 10.1038/nmeth.2089.

Schodel, J., Oikonomopoulos, S., Ragoussis, J., Pugh, C.W., Ratcliffe, P.J., and Mole, D.R. (2011). High-resolution genome-wide mapping of HIF-binding sites by ChIP-seq. Blood *117*, e207-217. 10.1182/blood-2010-10-314427.

Schofield, C.J., and Ratcliffe, P.J. (2004). Oxygen sensing by HIF hydroxylases. Nat Rev Mol Cell Biol *5*, 343-354. 10.1038/nrm1366.

Schofield, C.J., and Zhang, Z. (1999). Structural and mechanistic studies on 2-oxoglutarate-dependent oxygenases and related enzymes. Curr Opin Struct Biol *9*, 722-731. 10.1016/s0959-440x(99)00036-6.

Scholz, C.C., Rodriguez, J., Pickel, C., Burr, S., Fabrizio, J.A., Nolan, K.A., Spielmann, P., Cavadas, M.A., Crifo, B., Halligan, D.N., et al. (2016). FIH Regulates Cellular Metabolism through Hydroxylation of the Deubiquitinase OTUB1. PLoS Biol *14*, e1002347. 10.1371/journal.pbio.1002347.

Schott, K., Fuchs, N.V., Derua, R., Mahboubi, B., Schnellbacher, E., Seifried, J., Tondera, C., Schmitz, H., Shepard, C., Brandariz-Nunez, A., et al. (2018). Dephosphorylation of the HIV-1 restriction factor SAMHD1 is mediated by PP2A-B55alpha holoenzymes during mitotic exit. Nat Commun *9*, 2227. 10.1038/s41467-018-04671-1.

Schreeder, M.T., Thompson, S.E., Hadler, S.C., Berquist, K.R., Zaidi, A., Maynard, J.E., Ostrow, D., Judson, F.N., Braff, E.H., Nylund, T., et al. (1982). Hepatitis B in homosexual men: prevalence of infection and factors related to transmission. J Infect Dis *146*, 7-15. 10.1093/infdis/146.1.7.

Schultz, U., Grgacic, E., and Nassal, M. (2004). Duck hepatitis B virus: an invaluable model system for HBV infection. Adv Virus Res *63*, 1-70. 10.1016/S0065-3527(04)63001-6.

Schulze, A., Gripon, P., and Urban, S. (2007). Hepatitis B virus infection initiates with a large surface protein-dependent binding to heparan sulfate proteoglycans. Hepatology *46*, 1759-1768. 10.1002/hep.21896.

Schulze-Bergkamen, H., Untergasser, A., Dax, A., Vogel, H., Buchler, P., Klar, E., Lehnert, T., Friess, H., Buchler, M.W., Kirschfink, M., et al. (2003). Primary human hepatocytes--a valuable tool for investigation of apoptosis and hepatitis B virus infection. J Hepatol *38*, 736-744. 10.1016/s0168-8278(03)00120-x.

Schwanhausser, B., Busse, D., Li, N., Dittmar, G., Schuchhardt, J., Wolf, J., Chen, W., and Selbach, M. (2013). Corrigendum: Global quantification of mammalian gene expression control. Nature *495*, 126-127. 10.1038/nature11848.

Schweitzer, A., Horn, J., Mikolajczyk, R.T., Krause, G., and Ott, J.J. (2015). Estimations of worldwide prevalence of chronic hepatitis B virus infection: a systematic review of data published between 1965 and 2013. Lancet *386*, 1546-1555. 10.1016/S0140-6736(15)61412-X.

Scott, R.M., Snitbhan, R., Bancroft, W.H., Alter, H.J., and Tingpalapong, M. (1980). Experimental transmission of hepatitis B virus by semen and saliva. J Infect Dis *142*, 67-71. 10.1093/infdis/142.1.67.

Scotto, J., Hadchouel, M., Hery, C., Alvarez, F., Yvart, J., Tiollais, P., Bernard, O., and Brechot, C. (1983). Hepatitis B virus DNA in children's liver diseases: detection by blot hybridisation in liver and serum. Gut *24*, 618-624. 10.1136/gut.24.7.618.

Seeger, C., and Mason, W.S. (2000). Hepatitis B virus biology. Microbiol Mol Biol Rev *64*, 51-68. 10.1128/MMBR.64.1.51-68.2000.

Seidel, S., Garvalov, B.K., Wirta, V., von Stechow, L., Schanzer, A., Meletis, K., Wolter, M., Sommerlad, D., Henze, A.T., Nister, M., et al. (2010). A hypoxic niche regulates glioblastoma stem cells through hypoxia inducible factor 2 alpha. Brain *133*, 983-995. 10.1093/brain/awq042.

Sells, M.A., Chen, M.L., and Acs, G. (1987). Production of hepatitis B virus particles in Hep G2 cells transfected with cloned hepatitis B virus DNA. Proc Natl Acad Sci U S A *84*, 1005-1009. 10.1073/pnas.84.4.1005.

Sells, M.A., Zelent, A.Z., Shvartsman, M., and Acs, G. (1988). Replicative intermediates of hepatitis B virus in HepG2 cells that produce infectious virions. J Virol *62*, 2836-2844. 10.1128/JVI.62.8.2836-2844.1988.

Semenza, G.L. (1998). Hypoxia-inducible factor 1: master regulator of O2 homeostasis. Curr Opin Genet Dev *8*, 588-594. 10.1016/s0959-437x(98)80016-6.

Semenza, G.L. (2000). HIF-1: mediator of physiological and pathophysiological responses to hypoxia. J Appl Physiol (1985) *88*, 1474-1480. 10.1152/jappl.2000.88.4.1474.

Semenza, G.L. (2001a). HIF-1 and mechanisms of hypoxia sensing. Curr Opin Cell Biol *13*, 167-171. 10.1016/s0955-0674(00)00194-0.

Semenza, G.L. (2001b). Hypoxia-inducible factor 1: oxygen homeostasis and disease pathophysiology. Trends Mol Med *7*, 345-350. 10.1016/s1471-4914(01)02090-1.

Semenza, G.L. (2012). Hypoxia-inducible factors in physiology and medicine. Cell *148*, 399-408. 10.1016/j.cell.2012.01.021.

Semenza, G.L., Jiang, B.H., Leung, S.W., Passantino, R., Concordet, J.P., Maire, P., and Giallongo, A. (1996). Hypoxia response elements in the aldolase A, enolase 1, and lactate dehydrogenase A gene promoters contain essential binding sites for hypoxia-inducible factor 1. J Biol Chem *271*, 32529-32537. 10.1074/jbc.271.51.32529.

Semenza, G.L., Nejfelt, M.K., Chi, S.M., and Antonarakis, S.E. (1991). Hypoxia-inducible nuclear factors bind to an enhancer element located 3' to the human erythropoietin gene. Proc Natl Acad Sci U S A *88*, 5680-5684. 10.1073/pnas.88.13.5680.

Sena, J.A., Wang, L., Heasley, L.E., and Hu, C.J. (2014). Hypoxia regulates alternative splicing of HIF and non-HIF target genes. Mol Cancer Res *12*, 1233-1243. 10.1158/1541-7786.MCR-14-0149.

Shang, J., Zheng, Y., Guo, X., Mo, J., Xie, X., Xiong, Y., Liu, Y., Wu, K., and Wu, J. (2015). Hepatitis B virus replication and sex-determining region Y box 4 production are tightly controlled by a novel positive feedback mechanism. Sci Rep *5*, 10066. 10.1038/srep10066.

Sharma, S.K., Saini, N., and Chwla, Y. (2005). Hepatitis B virus: inactive carriers. Virol J *2*, 82. 10.1186/1743-422X-2-82.

Sheehy, A.M., Gaddis, N.C., Choi, J.D., and Malim, M.H. (2002). Isolation of a human gene that inhibits HIV-1 infection and is suppressed by the viral Vif protein. Nature *418*, 646-650. 10.1038/nature00939.

Shieh, M.T., WuDunn, D., Montgomery, R.I., Esko, J.D., and Spear, P.G. (1992). Cell surface receptors for herpes simplex virus are heparan sulfate proteoglycans. J Cell Biol *116*, 1273-1281. 10.1083/jcb.116.5.1273.

Shin, H.J., DeCotiis, J., Giron, M., Palmeri, D., and Lukac, D.M. (2014). Histone deacetylase classes I and II regulate Kaposi's sarcoma-associated herpesvirus reactivation. J Virol *88*, 1281-1292. 10.1128/JVI.02665-13.

Shmakova, A., Batie, M., Druker, J., and Rocha, S. (2014). Chromatin and oxygen sensing in the context of JmjC histone demethylases. Biochem J *462*, 385-395. 10.1042/BJ20140754.

Shoulders, M.D., and Raines, R.T. (2009). Collagen structure and stability. Annu Rev Biochem *78*, 929-958. 10.1146/annurev.biochem.77.032207.120833.

Simone, C. (2006). SWI/SNF: the crossroads where extracellular signaling pathways meet chromatin. J Cell Physiol *207*, 309-314. 10.1002/jcp.20514.

Sitia, G., Isogawa, M., Iannacone, M., Campbell, I.L., Chisari, F.V., and Guidotti, L.G. (2004). MMPs are required for recruitment of antigen-nonspecific mononuclear cells into the liver by CTLs. J Clin Invest *113*, 1158-1167. 10.1172/JCI21087.

Slagle, B.L., Andrisani, O.M., Bouchard, M.J., Lee, C.G., Ou, J.H., and Siddiqui, A. (2015). Technical standards for hepatitis B virus X protein (HBx) research. Hepatology *61*, 1416-1424. 10.1002/hep.27360.

Smythies, J.A., Sun, M., Masson, N., Salama, R., Simpson, P.D., Murray, E., Neumann, V., Cockman, M.E., Choudhry, H., Ratcliffe, P.J., and Mole, D.R. (2019). Inherent DNA-binding specificities of the HIF-1alpha and HIF-2alpha transcription factors in chromatin. EMBO Rep *20*. 10.15252/embr.201846401.

Sommer, A.F., Riviere, L., Qu, B., Schott, K., Riess, M., Ni, Y., Shepard, C., Schnellbacher, E., Finkernagel, M., Himmelsbach, K., et al. (2016). Restrictive influence of SAMHD1 on Hepatitis B Virus life cycle. Sci Rep *6*, 26616. 10.1038/srep26616.

Soussan, P., Tuveri, R., Nalpas, B., Garreau, F., Zavala, F., Masson, A., Pol, S., Brechot, C., and Kremsdorf, D. (2003). The expression of hepatitis B spliced protein (HBSP) encoded by a spliced hepatitis B virus RNA is associated with viral replication and liver fibrosis. J Hepatol *38*, 343-348. 10.1016/s0168-8278(02)00422-1.

Sozzi, V., Shen, F., Chen, J., Colledge, D., Jackson, K., Locarnini, S., Yuan, Z., and Revill, P.A. (2018). In vitro studies identify a low replication phenotype for hepatitis B virus genotype H generally associated with occult HBV and less severe liver disease. Virology *519*, 190-196. 10.1016/j.virol.2018.04.015.

Sozzi, V., Walsh, R., Littlejohn, M., Colledge, D., Jackson, K., Warner, N., Yuen, L., Locarnini, S.A., and Revill, P.A. (2016). In Vitro Studies Show that Sequence Variability Contributes to Marked Variation in Hepatitis B Virus Replication, Protein

Expression, and Function Observed across Genotypes. J Virol *90*, 10054-10064. 10.1128/JVI.01293-16.

Sprinzl, M.F., Oberwinkler, H., Schaller, H., and Protzer, U. (2001). Transfer of hepatitis B virus genome by adenovirus vectors into cultured cells and mice: crossing the species barrier. J Virol *75*, 5108-5118. 10.1128/JVI.75.11.5108-5118.2001.

Stacey, A.R., Norris, P.J., Qin, L., Haygreen, E.A., Taylor, E., Heitman, J., Lebedeva, M., DeCamp, A., Li, D., Grove, D., et al. (2009). Induction of a striking systemic cytokine cascade prior to peak viremia in acute human immunodeficiency virus type 1 infection, in contrast to more modest and delayed responses in acute hepatitis B and C virus infections. J Virol *83*, 3719-3733. 10.1128/JVI.01844-08.

Stadelmayer, B., Diederichs, A., Chapus, F., Rivoire, M., Neveu, G., Alam, A., Fraisse, L., Carter, K., Testoni, B., and Zoulim, F. (2020). Full-length 5'RACE identifies all major HBV transcripts in HBV-infected hepatocytes and patient serum. J Hepatol *73*, 40-51. 10.1016/j.jhep.2020.01.028.

Stein, S.C., Hurst, R.W., and Sonnad, S.S. (2008). Meta-analysis of cranial CT scans in children. A mathematical model to predict radiation-induced tumors. Pediatr Neurosurg *44*, 448-457. 10.1159/000172967.

Steube, A., Schenk, T., Tretyakov, A., and Saluz, H.P. (2017). High-intensity UV laser ChIP-seq for the study of protein-DNA interactions in living cells. Nature Communications *8*, 1303. 10.1038/s41467-017-01251-7.

Stevens, C.E., Beasley, R.P., Tsui, J., and Lee, W.C. (1975). Vertical transmission of hepatitis B antigen in Taiwan. N Engl J Med *292*, 771-774. 10.1056/NEJM197504102921503.

Stiehl, D.P., Bordoli, M.R., Abreu-Rodriguez, I., Wollenick, K., Schraml, P., Gradin, K., Poellinger, L., Kristiansen, G., and Wenger, R.H. (2012). Non-canonical HIF-2alpha function drives autonomous breast cancer cell growth via an AREG-EGFR/ErbB4 autocrine loop. Oncogene *31*, 2283-2297. 10.1038/onc.2011.417.

Stieler, J.T., and Prange, R. (2014). Involvement of ESCRT-II in hepatitis B virus morphogenesis. PLoS One *9*, e91279. 10.1371/journal.pone.0091279.

Stroud, H., Feng, S., Morey Kinney, S., Pradhan, S., and Jacobsen, S.E. (2011). 5-Hydroxymethylcytosine is associated with enhancers and gene bodies in human embryonic stem cells. Genome Biol *12*, R54. 10.1186/gb-2011-12-6-r54.

Stunkel, W., and Bernard, H.U. (1999). The chromatin structure of the long control region of human papillomavirus type 16 represses viral oncoprotein expression. J Virol *73*, 1918-1930. 10.1128/JVI.73.3.1918-1930.1999.

Su, A.I., Pezacki, J.P., Wodicka, L., Brideau, A.D., Supekova, L., Thimme, R., Wieland, S., Bukh, J., Purcell, R.H., Schultz, P.G., and Chisari, F.V. (2002). Genomic analysis of the host response to hepatitis C virus infection. Proc Natl Acad Sci U S A *99*, 15669-15674. 10.1073/pnas.202608199.

Su, T.S., Hwang, W.L., and Yauk, Y.K. (1998). Characterization of hepatitis B virus integrant that results in chromosomal rearrangement. DNA Cell Biol *17*, 415-425. 10.1089/dna.1998.17.415.

Subramanian, A., Kuehn, H., Gould, J., Tamayo, P., and Mesirov, J.P. (2007). GSEA-P: a desktop application for Gene Set Enrichment Analysis. Bioinformatics *23*, 3251-3253. 10.1093/bioinformatics/btm369.

Subramanian, A., Tamayo, P., Mootha, V.K., Mukherjee, S., Ebert, B.L., Gillette, M.A., Paulovich, A., Pomeroy, S.L., Golub, T.R., Lander, E.S., and Mesirov, J.P. (2005). Gene set enrichment analysis: a knowledge-based approach for interpreting genome-wide expression profiles. Proc Natl Acad Sci U S A *102*, 15545-15550. 10.1073/pnas.0506580102.

Summers, J., Jilbert, A.R., Yang, W., Aldrich, C.E., Saputelli, J., Litwin, S., Toll, E., and Mason, W.S. (2003). Hepatocyte turnover during resolution of a transient hepadnaviral infection. Proc Natl Acad Sci U S A *100*, 11652-11659. 10.1073/pnas.1635109100.

Summers, J., Smolec, J.M., and Snyder, R. (1978). A virus similar to human hepatitis B virus associated with hepatitis and hepatoma in woodchucks. Proc Natl Acad Sci U S A *75*, 4533-4537. 10.1073/pnas.75.9.4533.

Sun, C.T., Lo, W.Y., Wang, I.H., Lo, Y.H., Shiou, S.R., Lai, C.K., and Ting, L.P. (2001). Transcription repression of human hepatitis B virus genes by negative regulatory element-binding protein/SON. J Biol Chem *276*, 24059-24067. 10.1074/jbc.M101330200.

Sun, D., and Nassal, M. (2006). Stable HepG2- and Huh7-based human hepatoma cell lines for efficient regulated expression of infectious hepatitis B virus. J Hepatol *45*, 636-645. 10.1016/j.jhep.2006.05.019.

Sun, Y., Yu, M., Qu, M., Ma, Y., Zheng, D., Yue, Y., Guo, S., Tang, L., Li, G., Zheng, W., et al. (2020). Hepatitis B virus-triggered PTEN/beta-catenin/c-Myc signaling enhances PD-L1 expression to promote immune evasion. Am J Physiol Gastrointest Liver Physiol *318*, G162-G173. 10.1152/ajpgi.00197.2019.

Sund, N.J., Ang, S.L., Sackett, S.D., Shen, W., Daigle, N., Magnuson, M.A., and Kaestner, K.H. (2000). Hepatocyte nuclear factor 3beta (Foxa2) is dispensable for maintaining the differentiated state of the adult hepatocyte. Mol Cell Biol *20*, 5175-5183. 10.1128/MCB.20.14.5175-5183.2000.

Sung, W.K., Zheng, H., Li, S., Chen, R., Liu, X., Li, Y., Lee, N.P., Lee, W.H., Ariyaratne, P.N., Tennakoon, C., et al. (2012). Genome-wide survey of recurrent HBV integration in hepatocellular carcinoma. Nat Genet *44*, 765-769. 10.1038/ng.2295.

Supek, F., Bosnjak, M., Skunca, N., and Smuc, T. (2011). REVIGO summarizes and visualizes long lists of gene ontology terms. PLoS One *6*, e21800. 10.1371/journal.pone.0021800.

Surviladze, Z., Sterkand, R.T., and Ozbun, M.A. (2015). Interaction of human papillomavirus type 16 particles with heparan sulfate and syndecan-1 molecules in the keratinocyte extracellular matrix plays an active role in infection. J Gen Virol *96*, 2232-2241. 10.1099/vir.0.000147.

Suslov, A., Meier, M.A., Ketterer, S., Wang, X., Wieland, S., and Heim, M.H. (2021). Transition to HBeAg-negative chronic hepatitis B virus infection is associated with reduced cccDNA transcriptional activity. J Hepatol *74*, 794-800. 10.1016/j.jhep.2020.11.003.

Sze, K.M., Chu, G.K., Lee, J.M., and Ng, I.O. (2013). C-terminal truncated hepatitis B virus x protein is associated with metastasis and enhances invasiveness by C-Jun/matrix metalloproteinase protein 10 activation in hepatocellular carcinoma. Hepatology *57*, 131-139. 10.1002/hep.25979.

Sze, K.M., Ho, D.W., Chiu, Y.T., Tsui, Y.M., Chan, L.K., Lee, J.M., Chok, K.S., Chan, A.C., Tang, C.N., Tang, V.W., et al. (2021). Hepatitis B Virus-Telomerase Reverse Transcriptase Promoter Integration Harnesses Host ELF4, Resulting in Telomerase Reverse Transcriptase Gene Transcription in Hepatocellular Carcinoma. Hepatology *73*, 23-40. 10.1002/hep.31231.

Tabibian, J.H., Masyuk, A.I., Masyuk, T.V., O'Hara, S.P., and LaRusso, N.F. (2013). Physiology of cholangiocytes. Compr Physiol *3*, 541-565. 10.1002/cphy.c120019.

Tahiliani, M., Koh, K.P., Shen, Y., Pastor, W.A., Bandukwala, H., Brudno, Y., Agarwal, S., Iyer, L.M., Liu, D.R., Aravind, L., and Rao, A. (2009). Conversion of 5-methylcytosine to 5-hydroxymethylcytosine in mammalian DNA by MLL partner TET1. Science *324*, 930-935. 10.1126/science.1170116.

Takeda, N., O'Dea, E.L., Doedens, A., Kim, J.W., Weidemann, A., Stockmann, C., Asagiri, M., Simon, M.C., Hoffmann, A., and Johnson, R.S. (2010). Differential activation and antagonistic function of HIF-{alpha} isoforms in macrophages are essential for NO homeostasis. Genes Dev *24*, 491-501. 10.1101/gad.1881410.

Takeuchi, Y., Yahagi, N., Aita, Y., Murayama, Y., Sawada, Y., Piao, X., Toya, N., Oya, Y., Shikama, A., Takarada, A., et al. (2016). KLF15 Enables Rapid Switching

between Lipogenesis and Gluconeogenesis during Fasting. Cell Rep *16*, 2373-2386. 10.1016/j.celrep.2016.07.069.

Takiguchi, M. (1998). The C/EBP family of transcription factors in the liver and other organs. Int J Exp Pathol *79*, 369-391. 10.1046/j.1365-2613.1998.00082.x.

Tan, A., Koh, S., and Bertoletti, A. (2015). Immune Response in Hepatitis B Virus Infection. Cold Spring Harb Perspect Med *5*, a021428. 10.1101/cshperspect.a021428.

Tan, A.T., Hoang, L.T., Chin, D., Rasmussen, E., Lopatin, U., Hart, S., Bitter, H., Chu, T., Gruenbaum, L., Ravindran, P., et al. (2014). Reduction of HBV replication prolongs the early immunological response to IFNalpha therapy. J Hepatol *60*, 54-61. 10.1016/j.jhep.2013.08.020.

Tang, H., and McLachlan, A. (2001). Transcriptional regulation of hepatitis B virus by nuclear hormone receptors is a critical determinant of viral tropism. Proc Natl Acad Sci U S A *98*, 1841-1846. 10.1073/pnas.041479698.

Tang, H.M., Gao, W.W., Chan, C.P., Cheng, Y., Chaudhary, V., Deng, J.J., Yuen, K.S., Wong, C.M., Ng, I.O., Kok, K.H., et al. (2014). Requirement of CRTC1 coactivator for hepatitis B virus transcription. Nucleic Acids Res *42*, 12455-12468. 10.1093/nar/gku925.

Tang, L., Sheraz, M., McGrane, M., Chang, J., and Guo, J.T. (2019). DNA Polymerase alpha is essential for intracellular amplification of hepatitis B virus covalently closed circular DNA. PLoS Pathog *15*, e1007742. 10.1371/journal.ppat.1007742.

Taniguchi, K., and Karin, M. (2018). NF-kappaB, inflammation, immunity and cancer: coming of age. Nat Rev Immunol *18*, 309-324. 10.1038/nri.2017.142.

Tarhonskaya, H., Hardy, A.P., Howe, E.A., Loik, N.D., Kramer, H.B., McCullagh, J.S., Schofield, C.J., and Flashman, E. (2015). Kinetic Investigations of the Role of Factor Inhibiting Hypoxia-inducible Factor (FIH) as an Oxygen Sensor. J Biol Chem *290*, 19726-19742. 10.1074/jbc.M115.653014.

Tarn, C., Lee, S., Hu, Y., Ashendel, C., and Andrisani, O.M. (2001). Hepatitis B virus X protein differentially activates RAS-RAF-MAPK and JNK pathways in X-transforming versus non-transforming AML12 hepatocytes. J Biol Chem *276*, 34671-34680. 10.1074/jbc.M104105200.

Tatematsu, K., Tanaka, Y., Kurbanov, F., Sugauchi, F., Mano, S., Maeshiro, T., Nakayoshi, T., Wakuta, M., Miyakawa, Y., and Mizokami, M. (2009). A genetic variant of hepatitis B virus divergent from known human and ape genotypes isolated from a Japanese patient and provisionally assigned to new genotype J. J Virol *83*, 10538-10547. 10.1128/JVI.00462-09.

Tavis, J.E., and Lomonosova, E. (2015). The hepatitis B virus ribonuclease H as a drug target. Antiviral Res *118*, 132-138. 10.1016/j.antiviral.2015.04.002.

Taylor, C.T., and Colgan, S.P. (2017). Regulation of immunity and inflammation by hypoxia in immunological niches. Nat Rev Immunol *17*, 774-785. 10.1038/nri.2017.103.

Teng, C.F., Hsieh, W.C., Wu, H.C., Lin, Y.J., Tsai, H.W., Huang, W., and Su, I.J. (2015). Hepatitis B Virus Pre-S2 Mutant Induces Aerobic Glycolysis through Mammalian Target of Rapamycin Signal Cascade. PLoS One *10*, e0122373. 10.1371/journal.pone.0122373.

Thalhammer, A., Bencokova, Z., Poole, R., Loenarz, C., Adam, J., O'Flaherty, L., Schodel, J., Mole, D., Giaslakiotis, K., Schofield, C.J., et al. (2011). Human AlkB homologue 5 is a nuclear 2-oxoglutarate dependent oxygenase and a direct target of hypoxia-inducible factor 1alpha (HIF-1alpha). PLoS One *6*, e16210. 10.1371/journal.pone.0016210.

Thienpont, B., Steinbacher, J., Zhao, H., D'Anna, F., Kuchnio, A., Ploumakis, A., Ghesquiere, B., Van Dyck, L., Boeckx, B., Schoonjans, L., et al. (2016). Tumour hypoxia causes DNA hypermethylation by reducing TET activity. Nature *537*, 63-68. 10.1038/nature19081.

Thinnes, C.C., England, K.S., Kawamura, A., Chowdhury, R., Schofield, C.J., and Hopkinson, R.J. (2014). Targeting histone lysine demethylases - progress, challenges, and the future. Biochim Biophys Acta *1839*, 1416-1432. 10.1016/j.bbagrm.2014.05.009.

Thinnes, C.C., Tumber, A., Yapp, C., Scozzafava, G., Yeh, T., Chan, M.C., Tran, T.A., Hsu, K., Tarhonskaya, H., Walport, L.J., et al. (2015). Betti reaction enables efficient synthesis of 8-hydroxyquinoline inhibitors of 2-oxoglutarate oxygenases. Chem Commun (Camb) *51*, 15458-15461. 10.1039/c5cc06095h.

Thomson, J.P., Skene, P.J., Selfridge, J., Clouaire, T., Guy, J., Webb, S., Kerr, A.R., Deaton, A., Andrews, R., James, K.D., et al. (2010). CpG islands influence chromatin structure via the CpG-binding protein Cfp1. Nature *464*, 1082-1086. 10.1038/nature08924.

Tian, H., McKnight, S.L., and Russell, D.W. (1997). Endothelial PAS domain protein 1 (EPAS1), a transcription factor selectively expressed in endothelial cells. Genes Dev *11*, 72-82. 10.1101/gad.11.1.72.

Tiana, M., Acosta-Iborra, B., Hernandez, R., Galiana, C., Fernandez-Moreno, M.A., Jimenez, B., and Del Peso, L. (2020). Metabolic labeling of RNA uncovers the contribution of transcription and decay rates on hypoxia-induced changes in RNA levels. RNA *26*, 1006-1022. 10.1261/rna.072611.119.

Tokusumi, Y., Zhou, S., and Takada, S. (2004). Nuclear respiratory factor 1 plays an essential role in transcriptional initiation from the hepatitis B virus x gene promoter. J Virol *78*, 10856-10864. 10.1128/JVI.78.20.10856-10864.2004.

Torrano, J., Al Emran, A., Hammerlindl, H., and Schaider, H. (2019). Emerging roles of H3K9me3, SETDB1 and SETDB2 in therapy-induced cellular reprogramming. Clin Epigenetics *11*, 43. 10.1186/s13148-019-0644-y.

Torres, C., Fernandez, M.D., Flichman, D.M., Campos, R.H., and Mbayed, V.A. (2013). Influence of overlapping genes on the evolution of human hepatitis B virus. Virology *441*, 40-48. 10.1016/j.virol.2013.02.027.

Toukan, A. (1990). Strategy for the control of hepatitis B virus infection in the Middle East and North Africa. The Middle East Regional Study Group. Vaccine *8 Suppl*, S117-121; discussion S134-118.

Trefts, E., Gannon, M., and Wasserman, D.H. (2017). The liver. Curr Biol *27*, R1147-R1151. 10.1016/j.cub.2017.09.019.

Treyer, A., and Musch, A. (2013). Hepatocyte polarity. Compr Physiol *3*, 243-287. 10.1002/cphy.c120009.

Triantafyllou, A., Liakos, P., Tsakalof, A., Georgatsou, E., Simos, G., and Bonanou, S. (2006). Cobalt induces hypoxia-inducible factor-1alpha (HIF-1alpha) in HeLa cells by an iron-independent, but ROS-, PI-3K- and MAPK-dependent mechanism. Free Radic Res *40*, 847-856. 10.1080/10715760600730810.

Tropberger, P., Mercier, A., Robinson, M., Zhong, W., Ganem, D.E., and Holdorf, M. (2015). Mapping of histone modifications in episomal HBV cccDNA uncovers an unusual chromatin organization amenable to epigenetic manipulation. Proc Natl Acad Sci U S A *112*, E5715-5724. 10.1073/pnas.1518090112.

Tropberger, P., Pott, S., Keller, C., Kamieniarz-Gdula, K., Caron, M., Richter, F., Li, G., Mittler, G., Liu, E.T., Buhler, M., et al. (2013). Regulation of transcription through acetylation of H3K122 on the lateral surface of the histone octamer. Cell *152*, 859-872. 10.1016/j.cell.2013.01.032.

Truant, R., Antunovic, J., Greenblatt, J., Prives, C., and Cromlish, J.A. (1995). Direct interaction of the hepatitis B virus HBx protein with p53 leads to inhibition by HBx of p53 response element-directed transactivation. J Virol *69*, 1851-1859. 10.1128/JVI.69.3.1851-1859.1995.

Tsukada, Y., Fang, J., Erdjument-Bromage, H., Warren, M.E., Borchers, C.H., Tempst, P., and Zhang, Y. (2006). Histone demethylation by a family of JmjC domain-containing proteins. Nature *439*, 811-816. 10.1038/nature04433.

Tsukuda, S., and Watashi, K. (2020). Hepatitis B virus biology and life cycle. Antiviral Res *182*, 104925. 10.1016/j.antiviral.2020.104925.

Tu, T., Budzinska, M.A., Shackel, N.A., and Urban, S. (2017). HBV DNA Integration: Molecular Mechanisms and Clinical Implications. Viruses *9*. 10.3390/v9040075.

Tu, T., Budzinska, M.A., Vondran, F.W.R., Shackel, N.A., and Urban, S. (2018). Hepatitis B Virus DNA Integration Occurs Early in the Viral Life Cycle in an In Vitro Infection Model via Sodium Taurocholate Cotransporting Polypeptide-Dependent Uptake of Enveloped Virus Particles. J Virol *92*. 10.1128/JVI.02007-17.

Tu, T., Mason, W.S., Clouston, A.D., Shackel, N.A., McCaughan, G.W., Yeh, M.M., Schiff, E.R., Ruszkiewicz, A.R., Chen, J.W., Harley, H.A., et al. (2015). Clonal expansion of hepatocytes with a selective advantage occurs during all stages of chronic hepatitis B virus infection. J Viral Hepat *22*, 737-753. 10.1111/jvh.12380.

Turton, K.L., Meier-Stephenson, V., Badmalia, M.D., Coffin, C.S., and Patel, T.R. (2020). Host Transcription Factors in Hepatitis B Virus RNA Synthesis. Viruses *12*. 10.3390/v12020160.

Twist, E.M., Clark, H.F., Aden, D.P., Knowles, B.B., and Plotkin, S.A. (1981). Integration pattern of hepatitis B virus DNA sequences in human hepatoma cell lines. J Virol *37*, 239-243. 10.1128/JVI.37.1.239-243.1981.

Tzlil, S., Kindt, J.T., Gelbart, W.M., and Ben-Shaul, A. (2003). Forces and pressures in DNA packaging and release from viral capsids. Biophys J *84*, 1616-1627. 10.1016/S0006-3495(03)74971-6.

Untergasser, A., Zedler, U., Langenkamp, A., Hosel, M., Quasdorff, M., Esser, K., Dienes, H.P., Tappertzhofen, B., Kolanus, W., and Protzer, U. (2006). Dendritic cells take up viral antigens but do not support the early steps of hepatitis B virus infection. Hepatology *43*, 539-547. 10.1002/hep.21048.

Urban, S., Neumann-Haefelin, C., and Lampertico, P. (2021). Hepatitis D virus in 2021: virology, immunology and new treatment approaches for a difficult-to-treat disease. Gut *70*, 1782-1794. 10.1136/gutjnl-2020-323888.

Urban, S., Schulze, A., Dandri, M., and Petersen, J. (2010). The replication cycle of hepatitis B virus. J Hepatol *52*, 282-284. 10.1016/j.jhep.2009.10.031.

Valenzuela, P. (1990). Hepatitis A, B, C, D and E viruses: structure of their genomes and general properties. Gastroenterol Jpn *25 Suppl 2*, 62-71. 10.1007/BF02779931.

Valinluck, V., Tsai, H.H., Rogstad, D.K., Burdzy, A., Bird, A., and Sowers, L.C. (2004). Oxidative damage to methyl-CpG sequences inhibits the binding of the methyl-CpG binding domain (MBD) of methyl-CpG binding protein 2 (MeCP2). Nucleic Acids Res *32*, 4100-4108. 10.1093/nar/gkh739.

van Bommel, F., Bartens, A., Mysickova, A., Hofmann, J., Kruger, D.H., Berg, T., and Edelmann, A. (2015). Serum hepatitis B virus RNA levels as an early predictor of hepatitis B envelope antigen seroconversion during treatment with polymerase inhibitors. Hepatology *61*, 66-76. 10.1002/hep.27381.

van den Beucken, T., Koritzinsky, M., Niessen, H., Dubois, L., Savelkouls, K., Mujcic, H., Jutten, B., Kopacek, J., Pastorekova, S., van der Kogel, A.J., et al. (2009). Hypoxia-induced expression of carbonic anhydrase 9 is dependent on the unfolded protein response. J Biol Chem *284*, 24204-24212. 10.1074/jbc.M109.006510.

van Steensel, B. (2011). Chromatin: constructing the big picture. EMBO J *30*, 1885-1895. 10.1038/emboj.2011.135.

Varbobitis, I., and Papatheodoridis, G.V. (2016). The assessment of hepatocellular carcinoma risk in patients with chronic hepatitis B under antiviral therapy. Clin Mol Hepatol *22*, 319-326. 10.3350/cmh.2016.0045.

Venkatakrishnan, B., and Zlotnick, A. (2016). The Structural Biology of Hepatitis B Virus: Form and Function. Annu Rev Virol *3*, 429-451. 10.1146/annurev-virology-110615-042238.

Verrier, E.R., Colpitts, C.C., Bach, C., Heydmann, L., Weiss, A., Renaud, M., Durand, S.C., Habersetzer, F., Durantel, D., Abou-Jaoude, G., et al. (2016). A targeted functional RNA interference screen uncovers glypican 5 as an entry factor for hepatitis B and D viruses. Hepatology *63*, 35-48. 10.1002/hep.28013.

Vieira, V.C., and Soares, M.A. (2013). The role of cytidine deaminases on innate immune responses against human viral infections. Biomed Res Int *2013*, 683095. 10.1155/2013/683095.

Villa, P., Arioli, P., and Guaitani, A. (1991). Mechanism of maintenance of liver-specific functions by DMSO in cultured rat hepatocytes. Exp Cell Res *194*, 157-160. 10.1016/0014-4827(91)90146-l.

Villagra, A., Sotomayor, E.M., and Seto, E. (2010). Histone deacetylases and the immunological network: implications in cancer and inflammation. Oncogene *29*, 157-173. 10.1038/onc.2009.334.

Vinogradova, M., Gehling, V.S., Gustafson, A., Arora, S., Tindell, C.A., Wilson, C., Williamson, K.E., Guler, G.D., Gangurde, P., Manieri, W., et al. (2016). An inhibitor

of KDM5 demethylases reduces survival of drug-tolerant cancer cells. Nat Chem Biol *12*, 531-538. 10.1038/nchembio.2085.

Visvanathan, K., Skinner, N.A., Thompson, A.J., Riordan, S.M., Sozzi, V., Edwards, R., Rodgers, S., Kurtovic, J., Chang, J., Lewin, S., et al. (2007). Regulation of Toll-like receptor-2 expression in chronic hepatitis B by the precore protein. Hepatology *45*, 102-110. 10.1002/hep.21482.

Vivekanandan, P., Kannangai, R., Ray, S.C., Thomas, D.L., and Torbenson, M. (2008a). Comprehensive genetic and epigenetic analysis of occult hepatitis B from liver tissue samples. Clin Infect Dis *46*, 1227-1236. 10.1086/529437.

Vivekanandan, P., Thomas, D., and Torbenson, M. (2008b). Hepatitis B viral DNA is methylated in liver tissues. J Viral Hepat *15*, 103-107. 10.1111/j.1365-2893.2007.00905.x.

Voigt, P., Tee, W.W., and Reinberg, D. (2013). A double take on bivalent promoters. Genes Dev *27*, 1318-1338. 10.1101/gad.219626.113.

Wake, K. (1971). "Sternzellen" in the liver: perisinusoidal cells with special reference to storage of vitamin A. Am J Anat *132*, 429-462. 10.1002/aja.1001320404.

Walmsley, S.R., Sheares, K.K., Sobolewski, A., Morrell, N.W., and Chilvers, E.R. (2004). New insights into oxygen sensing at a cellular level. Thorax *59*, 90-92. 10.1136/thorax.2003.017020.

Wang, B.J., Tian, Y.J., Meng, Z.J., Jiang, M., Wei, B.Q., Tao, Y.Q., Fan, W., Li, A.Y., Bao, J.J., Li, X.Y., et al. (2011). Establishing a new animal model for hepadnaviral infection: susceptibility of Chinese Marmota-species to woodchuck hepatitis virus infection. J Gen Virol *92*, 681-691. 10.1099/vir.0.025023-0.

Wang, F., Zhang, R., Beischlag, T.V., Muchardt, C., Yaniv, M., and Hankinson, O. (2004). Roles of Brahma and Brahma/SWI2-related gene 1 in hypoxic induction of the erythropoietin gene. J Biol Chem *279*, 46733-46741. 10.1074/jbc.M409002200.

Wang, H., Kim, S., and Ryu, W.S. (2009). DDX3 DEAD-Box RNA helicase inhibits hepatitis B virus reverse transcription by incorporation into nucleocapsids. J Virol *83*, 5815-5824. 10.1128/JVI.00011-09.

Wang, H., and Ryu, W.S. (2010). Hepatitis B virus polymerase blocks pattern recognition receptor signaling via interaction with DDX3: implications for immune evasion. PLoS Pathog *6*, e1000986. 10.1371/journal.ppat.1000986.

Wang, J., Shen, T., Huang, X., Kumar, G.R., Chen, X., Zeng, Z., Zhang, R., Chen, R., Li, T., Zhang, T., et al. (2016). Serum hepatitis B virus RNA is encapsidated

pregenome RNA that may be associated with persistence of viral infection and rebound. J Hepatol *65*, 700-710. 10.1016/j.jhep.2016.05.029.

Wang, J., Wang, Y., Duan, Z., and Hu, W. (2020). Hypoxia-induced alterations of transcriptome and chromatin accessibility in HL-1 cells. IUBMB Life *72*, 1737-1746. 10.1002/iub.2297.

Wang, L., Chang, J., Varghese, D., Dellinger, M., Kumar, S., Best, A.M., Ruiz, J., Bruick, R., Pena-Llopis, S., Xu, J., et al. (2013). A small molecule modulates Jumonji histone demethylase activity and selectively inhibits cancer growth. Nat Commun *4*, 2035. 10.1038/ncomms3035.

Wang, W.X., Li, M., Wu, X., Wang, Y., and Li, Z.P. (1998). HNF1 is critical for the liver-specific function of HBV enhancer II. Res Virol *149*, 99-108. 10.1016/s0923-2516(98)80085-x.

Wang, X., Li, Y., Mao, A., Li, C., Li, Y., and Tien, P. (2010). Hepatitis B virus X protein suppresses virus-triggered IRF3 activation and IFN-beta induction by disrupting the VISA-associated complex. Cell Mol Immunol *7*, 341-348. 10.1038/cmi.2010.36.

Wang, X., Lu, Z., Gomez, A., Hon, G.C., Yue, Y., Han, D., Fu, Y., Parisien, M., Dai, Q., Jia, G., et al. (2014). N6-methyladenosine-dependent regulation of messenger RNA stability. Nature *505*, 117-120. 10.1038/nature12730.

Wang, X.W., Forrester, K., Yeh, H., Feitelson, M.A., Gu, J.R., and Harris, C.C. (1994). Hepatitis B virus X protein inhibits p53 sequence-specific DNA binding, transcriptional activity, and association with transcription factor ERCC3. Proc Natl Acad Sci U S A *91*, 2230-2234. 10.1073/pnas.91.6.2230.

Wang, Z., Zang, C., Rosenfeld, J.A., Schones, D.E., Barski, A., Cuddapah, S., Cui, K., Roh, T.Y., Peng, W., Zhang, M.Q., and Zhao, K. (2008). Combinatorial patterns of histone acetylations and methylations in the human genome. Nat Genet *40*, 897-903. 10.1038/ng.154.

Watanabe, T., Sorensen, E.M., Naito, A., Schott, M., Kim, S., and Ahlquist, P. (2007). Involvement of host cellular multivesicular body functions in hepatitis B virus budding. Proc Natl Acad Sci U S A *104*, 10205-10210. 10.1073/pnas.0704000104.

Webster, G.J., Reignat, S., Brown, D., Ogg, G.S., Jones, L., Seneviratne, S.L., Williams, R., Dusheiko, G., and Bertoletti, A. (2004). Longitudinal analysis of CD8+ T cells specific for structural and nonstructural hepatitis B virus proteins in patients with chronic hepatitis B: implications for immunotherapy. J Virol *78*, 5707-5719. 10.1128/JVI.78.11.5707-5719.2004.

Webster, G.J., Reignat, S., Maini, M.K., Whalley, S.A., Ogg, G.S., King, A., Brown, D., Amlot, P.L., Williams, R., Vergani, D., et al. (2000). Incubation phase of acute hepatitis B in man: dynamic of cellular immune mechanisms. Hepatology *32*, 1117-1124. 10.1053/jhep.2000.19324.

Weekes, M.P., Tomasec, P., Huttlin, E.L., Fielding, C.A., Nusinow, D., Stanton, R.J., Wang, E.C.Y., Aicheler, R., Murrell, I., Wilkinson, G.W.G., et al. (2014). Quantitative temporal viromics: an approach to investigate host-pathogen interaction. Cell *157*, 1460-1472. 10.1016/j.cell.2014.04.028.

Wei, L., and Ploss, A. (2020). Core components of DNA lagging strand synthesis machinery are essential for hepatitis B virus cccDNA formation. Nat Microbiol *5*, 715-726. 10.1038/s41564-020-0678-0.

Wei, L., and Ploss, A. (2021a). Hepatitis B virus cccDNA is formed through distinct repair processes of each strand. Nat Commun *12*, 1591. 10.1038/s41467-021-21850-9.

Wei, L., and Ploss, A. (2021b). Mechanism of Hepatitis B Virus cccDNA Formation. Viruses *13*. 10.3390/v13081463.

Welch, J., Tilzey, A.J., Bertrand, J., Bott, E.C., and Banatvala, J.E. (1988). Risk to Metropolitan police officers from exposure to hepatitis B. BMJ *297*, 835-836. 10.1136/bmj.297.6652.835.

Wenger, R.H., Stiehl, D.P., and Camenisch, G. (2005). Integration of oxygen signaling at the consensus HRE. Sci STKE *2005*, re12. 10.1126/stke.3062005re12.

Westbye, M.P., Feyzi, E., Aas, P.A., Vagbo, C.B., Talstad, V.A., Kavli, B., Hagen, L., Sundheim, O., Akbari, M., Liabakk, N.B., et al. (2008). Human AlkB homolog 1 is a mitochondrial protein that demethylates 3-methylcytosine in DNA and RNA. J Biol Chem *283*, 25046-25056. 10.1074/jbc.M803776200.

Westra, J., Brouwer, E., Bos, R., Posthumus, M.D., Doornbos-van der Meer, B., Kallenberg, C.G., and Limburg, P.C. (2007). Regulation of cytokine-induced HIF-1alpha expression in rheumatoid synovial fibroblasts. Ann N Y Acad Sci *1108*, 340-348. 10.1196/annals.1422.035.

Wettengel, J.M., Linden, B., Esser, K., Laue, M., Burwitz, B.J., and Protzer, U. (2021). Rapid and Robust Continuous Purification of High-Titer Hepatitis B Virus for In Vitro and In Vivo Applications. Viruses *13*. 10.3390/v13081503.

Whalley, S.A., Murray, J.M., Brown, D., Webster, G.J., Emery, V.C., Dusheiko, G.M., and Perelson, A.S. (2001). Kinetics of acute hepatitis B virus infection in humans. J Exp Med *193*, 847-854. 10.1084/jem.193.7.847.

Wieland, S., Thimme, R., Purcell, R.H., and Chisari, F.V. (2004). Genomic analysis of the host response to hepatitis B virus infection. Proc Natl Acad Sci U S A *101*, 6669-6674. 10.1073/pnas.0401771101.

Wieland, S.F., and Chisari, F.V. (2005). Stealth and cunning: hepatitis B and hepatitis C viruses. J Virol *79*, 9369-9380. 10.1128/JVI.79.15.9369-9380.2005.

Wiesener, M.S., Jurgensen, J.S., Rosenberger, C., Scholze, C.K., Horstrup, J.H., Warnecke, C., Mandriota, S., Bechmann, I., Frei, U.A., Pugh, C.W., et al. (2003). Widespread hypoxia-inducible expression of HIF-2alpha in distinct cell populations of different organs. FASEB J *17*, 271-273. 10.1096/fj.02-0445fje.

Wilson, B.G., and Roberts, C.W. (2011). SWI/SNF nucleosome remodellers and cancer. Nat Rev Cancer *11*, 481-492. 10.1038/nrc3068.

Wilson, E.M., Bial, J., Tarlow, B., Bial, G., Jensen, B., Greiner, D.L., Brehm, M.A., and Grompe, M. (2014a). Extensive double humanization of both liver and hematopoiesis in FRGN mice. Stem Cell Res *13*, 404-412. 10.1016/j.scr.2014.08.006.

Wilson, G.K., Tennant, D.A., and McKeating, J.A. (2014b). Hypoxia inducible factors in liver disease and hepatocellular carcinoma: current understanding and future directions. J Hepatol *61*, 1397-1406. 10.1016/j.jhep.2014.08.025.

Wilson, R., Warner, N., Ryan, K., Selleck, L., Colledge, D., Rodgers, S., Li, K., Revill, P., and Locarnini, S. (2011). The hepatitis B e antigen suppresses IL-1beta-mediated NF-kappaB activation in hepatocytes. J Viral Hepat *18*, e499-507. 10.1111/j.1365-2893.2011.01484.x.

Winer, B.Y., Huang, T.S., Pludwinski, E., Heller, B., Wojcik, F., Lipkowitz, G.E., Parekh, A., Cho, C., Shrirao, A., Muir, T.W., et al. (2017). Long-term hepatitis B infection in a scalable hepatic co-culture system. Nat Commun *8*, 125. 10.1038/s41467-017-00200-8.

Wing, P.A., Davenne, T., Wettengel, J., Lai, A.G., Zhuang, X., Chakraborty, A., D'Arienzo, V., Kramer, C., Ko, C., Harris, J.M., et al. (2019). A dual role for SAMHD1 in regulating HBV cccDNA and RT-dependent particle genesis. Life Sci Alliance *2*. 10.26508/lsa.201900355.

Wing, P.A.C., Liu, P.J., Harris, J.M., Magri, A., Michler, T., Zhuang, X., Borrmann, H., Minisini, R., Frampton, N.R., Wettengel, J.M., et al. (2021). Hypoxia inducible factors regulate hepatitis B virus replication by activating the basal core promoter. J Hepatol *75*, 64-73. 10.1016/j.jhep.2020.12.034.

Witt-Kehati, D., Bitton Alaluf, M., and Shlomai, A. (2016). Advances and Challenges in Studying Hepatitis B Virus In Vitro. Viruses *8*. 10.3390/v8010021.

Wolff, J.A. (1997). Naked DNA transport and expression in mammalian cells. Neuromuscul Disord *7*, 314-318. 10.1016/s0960-8966(97)00055-2.

Wolfrum, C., and Stoffel, M. (2006). Coactivation of Foxa2 through Pgc-1beta promotes liver fatty acid oxidation and triglyceride/VLDL secretion. Cell Metab *3*, 99-110. 10.1016/j.cmet.2006.01.001.

Wong, G.L., Chan, H.L., Mak, C.W., Lee, S.K., Ip, Z.M., Lam, A.T., Iu, H.W., Leung, J.M., Lai, J.W., Lo, A.O., et al. (2013). Entecavir treatment reduces hepatic events and deaths in chronic hepatitis B patients with liver cirrhosis. Hepatology *58*, 1537-1547. 10.1002/hep.26301.

Woodcock, C.L., and Ghosh, R.P. (2010). Chromatin higher-order structure and dynamics. Cold Spring Harb Perspect Biol *2*, a000596. 10.1101/cshperspect.a000596.

Wooddell, C.I., Yuen, M.F., Chan, H.L., Gish, R.G., Locarnini, S.A., Chavez, D., Ferrari, C., Given, B.D., Hamilton, J., Kanner, S.B., et al. (2017). RNAi-based treatment of chronically infected patients and chimpanzees reveals that integrated hepatitis B virus DNA is a source of HBsAg. Sci Transl Med *9*. 10.1126/scitranslmed.aan0241.

Wooldridge, T.R., and Laimins, L.A. (2008). Regulation of human papillomavirus type 31 gene expression during the differentiation-dependent life cycle through histone modifications and transcription factor binding. Virology *374*, 371-380. 10.1016/j.virol.2007.12.011.

World Health Organisation, W. (2021). Hepatitis B. Fact Sheet *https://www.who.int/en/news-room/fact-sheets/detail/hepatitis-b*.

Wounderlich, G., and Bruss, V. (1996). Characterization of early hepatitis B virus surface protein oligomers. Arch Virol *141*, 1191-1205. 10.1007/BF01718824.

Wouters, B.G., and Koritzinsky, M. (2008). Hypoxia signalling through mTOR and the unfolded protein response in cancer. Nat Rev Cancer *8*, 851-864. 10.1038/nrc2501.

Wu, J., Meng, Z., Jiang, M., Pei, R., Trippler, M., Broering, R., Bucchi, A., Sowa, J.P., Dittmer, U., Yang, D., et al. (2009). Hepatitis B virus suppresses toll-like receptor-mediated innate immune responses in murine parenchymal and nonparenchymal liver cells. Hepatology *49*, 1132-1140. 10.1002/hep.22751.

Wu, T.T., Coates, L., Aldrich, C.E., Summers, J., and Mason, W.S. (1990). In hepatocytes infected with duck hepatitis B virus, the template for viral RNA synthesis is amplified by an intracellular pathway. Virology *175*, 255-261. 10.1016/0042-6822(90)90206-7.

Wykoff, C.C., Beasley, N., Watson, P.H., Campo, L., Chia, S.K., English, R., Pastorek, J., Sly, W.S., Ratcliffe, P., and Harris, A.L. (2001). Expression of the hypoxia-inducible and tumor-associated carbonic anhydrases in ductal carcinoma in situ of the breast. Am J Pathol *158*, 1011-1019. 10.1016/S0002-9440(10)64048-5.

Xia, Y., Cheng, X., Li, Y., Valdez, K., Chen, W., and Liang, T.J. (2018). Hepatitis B Virus Deregulates the Cell Cycle To Promote Viral Replication and a Premalignant Phenotype. J Virol *92*. 10.1128/JVI.00722-18.

Xiao, C., and Ghosh, S. (2005). NF-kappaB, an evolutionarily conserved mediator of immune and inflammatory responses. Adv Exp Med Biol *560*, 41-45. 10.1007/0-387-24180-9_5.

Xin, B., and Rohs, R. (2018). Relationship between histone modifications and transcription factor binding is protein family specific. Genome Res. 10.1101/gr.220079.116.

Xiong, X.X., Qiu, X.Y., Hu, D.X., and Chen, X.Q. (2017). Advances in Hypoxia-Mediated Mechanisms in Hepatocellular Carcinoma. Mol Pharmacol *92*, 246-255. 10.1124/mol.116.107706.

Xu, L., Wu, Z., Tan, S., Wang, Z., Lin, Q., Li, X., Song, X., Liu, Y., Song, Y., Zhang, J., et al. (2018). Tumor suppressor ZHX2 restricts hepatitis B virus replication via epigenetic and non-epigenetic manners. Antiviral Res *153*, 114-123. 10.1016/j.antiviral.2018.03.008.

Xu, P.L., Liu, Y.Q., Shan, S.F., Kong, Y.Y., Zhou, Q., Li, M., Ding, J.P., Xie, Y.H., and Wang, Y. (2004). Molecular mechanism for the potentiation of the transcriptional activity of human liver receptor homolog 1 by steroid receptor coactivator-1. Mol Endocrinol *18*, 1887-1905. 10.1210/me.2003-0334.

Xu, R., Hu, P., Li, Y., Tian, A., Li, J., and Zhu, C. (2021). Advances in HBV infection and replication systems in vitro. Virol J *18*, 105. 10.1186/s12985-021-01580-6.

Yaginuma, K., Kobayashi, H., Kobayashi, M., Morishima, T., Matsuyama, K., and Koike, K. (1987). Multiple integration site of hepatitis B virus DNA in hepatocellular carcinoma and chronic active hepatitis tissues from children. J Virol *61*, 1808-1813. 10.1128/JVI.61.6.1808-1813.1987.

Yan, H., Peng, B., He, W., Zhong, G., Qi, Y., Ren, B., Gao, Z., Jing, Z., Song, M., Xu, G., et al. (2013). Molecular determinants of hepatitis B and D virus entry restriction in mouse sodium taurocholate cotransporting polypeptide. J Virol *87*, 7977-7991. 10.1128/JVI.03540-12.

Yan, H., Zhong, G., Xu, G., He, W., Jing, Z., Gao, Z., Huang, Y., Qi, Y., Peng, B., Wang, H., et al. (2012). Sodium taurocholate cotransporting polypeptide is a functional receptor for human hepatitis B and D virus. Elife *1*, e00049. 10.7554/eLife.00049.

Yan, Z., Zeng, J., Yu, Y., Xiang, K., Hu, H., Zhou, X., Gu, L., Wang, L., Zhao, J., Young, J.A.T., and Gao, L. (2017). HBVcircle: A novel tool to investigate hepatitis B virus covalently closed circular DNA. J Hepatol *66*, 1149-1157. 10.1016/j.jhep.2017.02.004.

Yang, D., Hanna, D.L., Usher, J., LoCoco, J., Chaudhari, P., Lenz, H.J., Setiawan, V.W., and El-Khoueiry, A. (2014). Impact of sex on the survival of patients with hepatocellular carcinoma: a Surveillance, Epidemiology, and End Results analysis. Cancer *120*, 3707-3716. 10.1002/cncr.28912.

Yang, J., AlTahan, A., Jones, D.T., Buffa, F.M., Bridges, E., Interiano, R.B., Qu, C., Vogt, N., Li, J.L., Baban, D., et al. (2015). Estrogen receptor-alpha directly regulates the hypoxia-inducible factor 1 pathway associated with antiestrogen response in breast cancer. Proc Natl Acad Sci U S A *112*, 15172-15177. 10.1073/pnas.1422015112.

Yang, J.D., Kim, W.R., Coelho, R., Mettler, T.A., Benson, J.T., Sanderson, S.O., Therneau, T.M., Kim, B., and Roberts, L.R. (2011). Cirrhosis is present in most patients with hepatitis B and hepatocellular carcinoma. Clin Gastroenterol Hepatol *9*, 64-70. 10.1016/j.cgh.2010.08.019.

Yang, P.L., Althage, A., Chung, J., and Chisari, F.V. (2002). Hydrodynamic injection of viral DNA: a mouse model of acute hepatitis B virus infection. Proc Natl Acad Sci U S A *99*, 13825-13830. 10.1073/pnas.202398599.

Yang, P.L., Althage, A., Chung, J., Maier, H., Wieland, S., Isogawa, M., and Chisari, F.V. (2010). Immune effectors required for hepatitis B virus clearance. Proc Natl Acad Sci U S A *107*, 798-802. 10.1073/pnas.0913498107.

Yang, Q., Zhang, Q., Zhang, X., You, L., Wang, W., Liu, W., Han, Y., Ma, C., Xu, W., Chen, J., et al. (2019). HoxA10 Facilitates SHP-1-Catalyzed Dephosphorylation of p38 MAPK/STAT3 To Repress Hepatitis B Virus Replication by a Feedback Regulatory Mechanism. J Virol *93*. 10.1128/JVI.01607-18.

Yang, W., Mason, W.S., and Summers, J. (1996). Covalently closed circular viral DNA formed from two types of linear DNA in woodchuck hepatitis virus-infected liver. J Virol *70*, 4567-4575. 10.1128/JVI.70.7.4567-4575.1996.

Yang, W., and Summers, J. (1998). Infection of ducklings with virus particles containing linear double-stranded duck hepatitis B virus DNA: illegitimate replication and reversion. J Virol *72*, 8710-8717. 10.1128/JVI.72.11.8710-8717.1998.

Yang, W., and Summers, J. (1999). Integration of hepadnavirus DNA in infected liver: evidence for a linear precursor. J Virol *73*, 9710-9717. 10.1128/JVI.73.12.9710-9717.1999.

Yang, X., Cai, W., Sun, X., Bi, Y., Zeng, C., Zhao, X., Zhou, Q., Xu, T., Xie, Q., Sun, P., and Zhou, X. (2020). Defined host factors support HBV infection in non-hepatic 293T cells. J Cell Mol Med *24*, 2507-2518. 10.1111/jcmm.14944.

Yang, Y., Zheng, B., Han, Q., Zhang, C., Tian, Z., and Zhang, J. (2016). Targeting blockage of STAT3 inhibits hepatitis B virus-related hepatocellular carcinoma. Cancer Biol Ther *17*, 449-456. 10.1080/15384047.2016.1156257.

Yao, N.Y., and O'Donnell, M. (2012). The RFC clamp loader: structure and function. Subcell Biochem *62*, 259-279. 10.1007/978-94-007-4572-8_14.

Yap, K.L., and Zhou, M.M. (2011). Structure and mechanisms of lysine methylation recognition by the chromodomain in gene transcription. Biochemistry *50*, 1966-1980. 10.1021/bi101885m.

Ye, B., Liu, X., Li, X., Kong, H., Tian, L., and Chen, Y. (2015). T-cell exhaustion in chronic hepatitis B infection: current knowledge and clinical significance. Cell Death Dis *6*, e1694. 10.1038/cddis.2015.42.

Yin, H., Qu, J., Peng, Q., and Gan, R. (2019). Molecular mechanisms of EBV-driven cell cycle progression and oncogenesis. Med Microbiol Immunol *208*, 573-583. 10.1007/s00430-018-0570-1.

Yoo, Y.G., Cho, S., Park, S., and Lee, M.O. (2004). The carboxy-terminus of the hepatitis B virus X protein is necessary and sufficient for the activation of hypoxia-inducible factor-1alpha. FEBS Lett *577*, 121-126. 10.1016/j.febslet.2004.10.004.

Yoo, Y.G., Na, T.Y., Seo, H.W., Seong, J.K., Park, C.K., Shin, Y.K., and Lee, M.O. (2008). Hepatitis B virus X protein induces the expression of MTA1 and HDAC1, which enhances hypoxia signaling in hepatocellular carcinoma cells. Oncogene *27*, 3405-3413. 10.1038/sj.onc.1211000.

Yoo, Y.G., Oh, S.H., Park, E.S., Cho, H., Lee, N., Park, H., Kim, D.K., Yu, D.Y., Seong, J.K., and Lee, M.O. (2003). Hepatitis B virus X protein enhances transcriptional activity of hypoxia-inducible factor-1alpha through activation of mitogen-activated protein kinase pathway. J Biol Chem *278*, 39076-39084. 10.1074/jbc.M305101200.

Yoshida, H., Okada, T., Haze, K., Yanagi, H., Yura, T., Negishi, M., and Mori, K. (2000). ATF6 activated by proteolysis binds in the presence of NF-Y (CBF) directly to the cis-acting element responsible for the mammalian unfolded protein response. Mol Cell Biol *20*, 6755-6767. 10.1128/MCB.20.18.6755-6767.2000.

Yousif, M., Mudawi, H., Bakhiet, S., Glebe, D., and Kramvis, A. (2013). Molecular characterization of hepatitis B virus in liver disease patients and asymptomatic carriers of the virus in Sudan. BMC Infect Dis *13*, 328. 10.1186/1471-2334-13-328.

Yu, H., Yuan, Q., Ge, S.X., Wang, H.Y., Zhang, Y.L., Chen, Q.R., Zhang, J., Chen, P.J., and Xia, N.S. (2010a). Molecular and phylogenetic analyses suggest an additional hepatitis B virus genotype "I". PLoS One *5*, e9297. 10.1371/journal.pone.0009297.

Yu, S., Chen, J., Wu, M., Chen, H., Kato, N., and Yuan, Z. (2010b). Hepatitis B virus polymerase inhibits RIG-I- and Toll-like receptor 3-mediated beta interferon induction in human hepatocytes through interference with interferon regulatory factor 3 activation and dampening of the interaction between TBK1/IKKepsilon and DDX3. J Gen Virol *91*, 2080-2090. 10.1099/vir.0.020552-0.

Yuen, M.F., Chen, D.S., Dusheiko, G.M., Janssen, H.L.A., Lau, D.T.Y., Locarnini, S.A., Peters, M.G., and Lai, C.L. (2018). Hepatitis B virus infection. Nat Rev Dis Primers *4*, 18035. 10.1038/nrdp.2018.35.

Yuh, C.H., and Ting, L.P. (1990). The genome of hepatitis B virus contains a second enhancer: cooperation of two elements within this enhancer is required for its function. J Virol *64*, 4281-4287. 10.1128/JVI.64.9.4281-4287.1990.

Zack, J.A. (1995). The role of the cell cycle in HIV-1 infection. Adv Exp Med Biol *374*, 27-31. 10.1007/978-1-4615-1995-9_3.

Zannolli, R., and Morgese, G. (1997). Hepatitis B vaccine: current issues. Ann Pharmacother *31*, 1059-1067. 10.1177/106002809703100916.

Zeilinger, K., Freyer, N., Damm, G., Seehofer, D., and Knospel, F. (2016). Cell sources for in vitro human liver cell culture models. Exp Biol Med (Maywood) *241*, 1684-1698. 10.1177/1535370216657448.

Zhang, N., Fu, Z., Linke, S., Chicher, J., Gorman, J.J., Visk, D., Haddad, G.G., Poellinger, L., Peet, D.J., Powell, F., and Johnson, R.S. (2010). The asparaginyl hydroxylase factor inhibiting HIF-1alpha is an essential regulator of metabolism. Cell Metab *11*, 364-378. 10.1016/j.cmet.2010.03.001.

Zhang, W., Zhang, D., Dou, X., Xie, Q., Jiang, J., Chen, X., and Ren, H. (2018). Consensus on Pegylated Interferon Alpha in Treatment of Chronic Hepatitis B. J Clin Transl Hepatol *6*, 1-10. 10.14218/JCTH.2017.00073.

Zhang, X., Bernatavichute, Y.V., Cokus, S., Pellegrini, M., and Jacobsen, S.E. (2009). Genome-wide analysis of mono-, di- and trimethylation of histone H3 lysine 4 in Arabidopsis thaliana. Genome Biol *10*, R62. 10.1186/gb-2009-10-6-r62.

Zhang, X., Lu, W., Zheng, Y., Wang, W., Bai, L., Chen, L., Feng, Y., Zhang, Z., and Yuan, Z. (2016a). In situ analysis of intrahepatic virological events in chronic hepatitis B virus infection. J Clin Invest *126*, 1079-1092. 10.1172/JCI83339.

Zhang, Y., Li, C., Zhang, Y., Zhu, H., Kang, Y., Liu, H., Wang, J., Qin, Y., Mao, R., Xie, Y., et al. (2013). Comparative analysis of CpG islands among HBV genotypes. PLoS One *8*, e56711. 10.1371/journal.pone.0056711.

Zhang, Y., Yan, Q., Gong, L., Xu, H., Liu, B., Fang, X., Yu, D., Li, L., Wei, T., Wang, Y., et al. (2021). C-terminal truncated HBx initiates hepatocarcinogenesis by downregulating TXNIP and reprogramming glucose metabolism. Oncogene *40*, 1147-1161. 10.1038/s41388-020-01593-5.

Zhang, Z., Zehnder, B., Damrau, C., and Urban, S. (2016b). Visualization of hepatitis B virus entry - novel tools and approaches to directly follow virus entry into hepatocytes. FEBS Lett *590*, 1915-1926. 10.1002/1873-3468.12202.

Zhang, Z.Q., Wang, Y.B., Lu, W., Liu, D.P., Shi, B.S., Zhang, X.N., Huang, D., Li, X.F., Zhou, X.L., and Ding, R.R. (2019). Performance of Hepatitis B Core-Related Antigen Versus Hepatitis B Surface Antigen and Hepatitis B Virus DNA in Predicting HBeAg-positive and HBeAg-negative Chronic Hepatitis. Ann Lab Med *39*, 67-75. 10.3343/alm.2019.39.1.67.

Zhao, F., Xie, X., Tan, X., Yu, H., Tian, M., Lv, H., Qin, C., Qi, J., and Zhu, Q. (2021). The Functions of Hepatitis B Virus Encoding Proteins: Viral Persistence and Liver Pathogenesis. Front Immunol *12*, 691766. 10.3389/fimmu.2021.691766.

Zhao, L.H., Liu, X., Yan, H.X., Li, W.Y., Zeng, X., Yang, Y., Zhao, J., Liu, S.P., Zhuang, X.H., Lin, C., et al. (2016). Genomic and oncogenic preference of HBV integration in hepatocellular carcinoma. Nat Commun *7*, 12992. 10.1038/ncomms12992.

Zheng, C.L., Fu, Y.M., Xu, Z.X., Zou, Y., and Deng, K. (2019). Hepatitis B virus core protein dimerdimer interface is critical for viral replication. Mol Med Rep *19*, 262-270. 10.3892/mmr.2018.9620.

Zheng, Y., Li, J., and Ou, J.H. (2004). Regulation of hepatitis B virus core promoter by transcription factors HNF1 and HNF4 and the viral X protein. J Virol *78*, 6908-6914. 10.1128/JVI.78.13.6908-6914.2004.

Zhou, C.H., Zhang, X.P., Liu, F., and Wang, W. (2015). Modeling the interplay between the HIF-1 and p53 pathways in hypoxia. Sci Rep *5*, 13834. 10.1038/srep13834.

Zhou, D.X., and Yen, T.S. (1991). The ubiquitous transcription factor Oct-1 and the liver-specific factor HNF-1 are both required to activate transcription of a

hepatitis B virus promoter. Mol Cell Biol *11*, 1353-1359. 10.1128/mcb.11.3.1353-1359.1991.

Zhou, J., Schmid, T., and Brune, B. (2003). Tumor necrosis factor-alpha causes accumulation of a ubiquitinated form of hypoxia inducible factor-1alpha through a nuclear factor-kappaB-dependent pathway. Mol Biol Cell *14*, 2216-2225. 10.1091/mbc.e02-09-0598.

Zhou, L., He, R., Fang, P., Li, M., Yu, H., Wang, Q., Yu, Y., Wang, F., Zhang, Y., Chen, A., et al. (2021). Hepatitis B virus rigs the cellular metabolome to avoid innate immune recognition. Nat Commun *12*, 98. 10.1038/s41467-020-20316-8.

Zhou, W., Ma, Y., Zhang, J., Hu, J., Zhang, M., Wang, Y., Li, Y., Wu, L., Pan, Y., Zhang, Y., et al. (2017). Predictive model for inflammation grades of chronic hepatitis B: Large-scale analysis of clinical parameters and gene expressions. Liver Int *37*, 1632-1641. 10.1111/liv.13427.

Zhuang, X., Forde, D., Tsukuda, S., D'Arienzo, V., Mailly, L., Harris, J.M., Wing, P.A.C., Borrmann, H., Schilling, M., Magri, A., et al. (2021). Circadian control of hepatitis B virus replication. Nat Commun *12*, 1658. 10.1038/s41467-021-21821-0.

Zilfou, J.T., and Lowe, S.W. (2009). Tumor suppressive functions of p53. Cold Spring Harb Perspect Biol *1*, a001883. 10.1101/cshperspect.a001883.

Zoulim, F., and Durantel, D. (2015). Antiviral therapies and prospects for a cure of chronic hepatitis B. Cold Spring Harb Perspect Med *5*. 10.1101/cshperspect.a021501.